The University of Nottingham

Institute of Engineering Surveying and

Space Geodesy

POSITION ESTIMATION USING THE DIGITAL AUDIO BROADCAST (DAB) SIGNAL

Duncan Palmer

BSc (Hons), MSc

Thesis submitted to the University of Nottingham for the degree

of Doctor of Philosophy

August 2010

ABSTRACT

Over the past decades, there have been a number of trends that have driven the desire to improve the ability to navigate in all environments. While the Global Positioning System has been the driving factor behind most of these trends, there are limitations to this system that have become more evident over time as the world has increasingly come to rely on navigation. These limitations are mostly due to the low transmission power of the satellites, where navigation signals broadcast from space are comparatively weak, especially by the time they have travelled to receivers on the ground. This makes the signals particularly vulnerable to fading in difficult environments such as "urban jungles" and other built up areas. The low signal-to-noise ratio (SNR) also means, that the signals are susceptible to jamming, both hostile and accidental.

This motivates the need for alternatives technologies to satellite navigation and consider terrestrial based alternatives such as LORAN-C and eLORAN, but there is also significant interest in the exploitation of other non-navigation signals for positioning and navigation purposes. These so-called *'Signals of Opportunity'* do not generally require any alterations to existing communications transmission infrastructure and utilise alternative multi-carrier modulation techniques to those used by navigation systems.

This project examines the use of such a signal, the Digital Audio Broadcast (DAB) signal, as a positioning source. This thesis contains complete research from initial coverage simulations in the UK, through to extensive static testing, and the use of the signal in a dynamic environment and it has been shown that the Digital Audio Broadcast signal has potential as a terrestrial based positioning signal.

ACKNOWLEDGEMENTS

The work undertaken in this thesis commenced in February 2007 and took place primarily at the Institute of Engineering Surveying and Space Geodesy (IESSG) at the University of Nottingham, with a six month secondment spent working at the Geospatial Research Centre (NZ) Ltd at the University of Canterbury, Christchurch, New Zealand from March to September 2008.

I would like to thank my supervisors in Nottingham, Professor Terry Moore and Dr. Chris Hill, and my supervisors in Christchurch, Dr. Marcus Andreotti and Dr. David Park, for their invaluable help and guidance throughout the duration of this project.

Thanks also to Mike Ellis at the BBC for his help in understanding how the UK DAB network operates.

I would also like to thank my parents for their support during all my years of study, and Eleanor who has valiantly endured me while I have been writing up this year.

CONTENTS

List of Figures

List of Tables

1 INTRODUCTION

1.1 BACKGROUND

As Global Navigation Satellite Systems (GNSS) receivers have become almost standard in devices such as mobile phones and vehicle navigation systems, the threat of the signals becoming unavailable, particularly in critical safety-of-life applications is a concern. It is well documented that GNSS signals arrive at the Earth's surface with a very low signal-to-noise ratio (SNR), due to the relatively low power of transmission from the satellites themselves and the degrading effects of the atmosphere on the signals. The threat from jamming, intentional or otherwise, is increasing with jammer schematics posted on the internet giving users freely available knowledge to build such a device, and with this technical expertise, in addition to the low power of the received signals, interference to GNSS signals is a modern concern.

1.2 MOTIVATION

The original outline of this project was the mitigation of the effects of jamming on a GPS signal; however, it soon became clear that due to constraints on broadcasting signals on the L1 band, testing of such an approach would be unfeasible. Jamming exercises are conducted by the UK and other governments, but naturally due to the extensive problems this has the potential to cause, these tests have to be performed remotely and with widespread public consultation.

Therefore, the project took an alternative approach with an examination into terrestrial based signals, both for navigation and communication. The use of non-navigation signals, or so-called *Signals of Opportunity,* for navigation is a relatively recent field of study and one that could offer a terrestrial-based solution to the well-documented issues that GNSS suffer. A number of these signals have been investigated for this purpose during recent years, and an intensive literature review was undertaken at an early stage to establish potential directions for this project.

It was from this review that the Digital Audio Broadcast (DAB) signal emerged as a particularly good candidate for positioning potential in the UK, reasons which are discussed thoroughly later in this document. The UK has one of the highest Digital Audio Broadcast coverage rates in the world, and with the announcement during this project that radio stations would be switched from the Frequency Modulation (FM) band to DAB merely added to the case for this technology.

1.3 Aims and Objectives

Following this process, a broad aim and more defined objectives were established. The general aims of the project being:

- To undertake research into the use of the Digital Audio Broadcast signal as an alternative positioning source to satellite navigation.
- To develop software capable of calculating the location of a Digital Audio Broadcast receiver without assistance from other positioning systems.

These aims were then broken down into the following key objectives:

- To develop a system capable of standalone positioning without the requirement for additional infrastructure.
- To adopt a "Software Defined Radio" approach to demodulate the data and ultimately position the receiver.

- To develop a system using off the shelf components with the aim of proving the potential behind freely available components.
- To test such a system in a variety of environments and conditions.

1.4 Overview & Methodology

This project used the following research methodology in order to achieve the aims and objectives highlighted previously. This consisted of:

- Performing a review of the navigation signals currently in use and examining the vulnerabilities that are present in each system.
- Performing a review of the various jamming methods and the state of the technologies used to counter this.
- Performing a case-study of non-navigation signals in the UK.
- Using data simulations to examine the coverage of DAB networks in the UK, and establishing the minimum number of transmitters required to locate a receiver.
- Construct a software based receiver to capture/decode and extract timing information from a DAB signal for positioning purposes.
- Thoroughly test the platform in a wide variety of environments.

Chapter 2 contains the review carried out on the current state of dedicated navigation signals, from the most widely used Global Positioning System (GPS) to lesser known terrestrial based systems such as Datatrak. The chapter then continues to examine a range of jamming methods and contains a review of the mitigation techniques developed to counteract jamming. The chapter concludes discussing the fact that no one mitigation solution is suitable for all environments.

Chapter 3 examines a variety of signals not designed for navigation and presents a review of the signals used previously for such a purpose. A review of the different signal propagation techniques is then examined with the purpose of highlighting the benefits and drawbacks of each and to coincide with the general non-navigation signals discussion. The chapter then concludes with the decision to attempt using the Digital Audio Broadcast signal as the chosen signal for the remainder of this project.

The Digital Audio Broadcasting signal is discussed in detail during Chapter 4, examining the signal structure and highlighting the required portions of the signal which would be useful for location purposes. This chapter also reviews the coverage of DAB within the UK and further afield.

Chapter 5 examines the various positioning techniques that might be exploitable from the information available in the DAB signal, concluding that a Time Difference of Arrival approach be adopted.

The complete start to end processing of the DAB signal is broken down and presented in Chapter 6, commencing with the capture of the raw signal and introduction of the Universal Software Radio Peripheral as the only major hardware component required during this project. This is followed by a breakdown of the signal processing blocks, culminating in the solving of the observation equations using the Least Squares process.

Chapter 7 contains the various simulations based on actual DAB transmitter locations in the UK, and discusses the regions where signal penetration will be at its greatest. These regions are shown to be in large built up areas as would be expected, but also the areas where satellite navigation would suffer from the effects of large scale structures.

The complete testing undertaken is then presented in Chapter 8. This is broken down into key areas starting with the system testing in a known location and altering factors

such as the antenna and its height. This then continues with the system being taken out in to regions of the Midlands to test how the system copes with data received in rural, suburban and dense urban areas. Finally, a modified version of the processing software is tested using captures taken from a moving vehicle over a period of time. The outcome of these tests shows that the system developed has the ability to position a receiver when static to a degree of accuracy determined by the layout of the received transmitters.

The final chapter then examines the project as a whole, summarising the results and presenting potential future directions that may be taken on the back of this research.

2 NAVIGATION SIGNALS

This chapter contains an overview of the current status of dedicated navigation signals, both from satellite and terrestrial transmitters. Each system will be examined in turn followed by an examination of the weaknesses of both satellite and terrestrial based positioning systems.

2.1 GLOBAL NAVIGATION SATELLITE SYSTEMS (GNSS)

This section provides a brief overview of the currently available and upcoming GNSS. Each GNSS provide a means of acquiring direct position and speed estimates using passive ranging measurements from a constellation of satellites. The various systems will be examined in turn, followed by a summary of the error sources and weaknesses of GNSS which helped to inspire this project.

2.1.1 The Global Positioning System (GPS)

The *NAVSTAR Global Positioning System* (GPS) was the first fully operational GNSS and is the most widely used at the current time, being owned and operated by the United States government. The system broadcasts ranging signals on two primary frequencies, L1 (1.57542 GHz) and L2 (1.22760 GHz) and also on the forthcoming L5 (1.17645 GHz) which will not be examined further here. The GPS constellation consists of up to 32 satellites orbiting in three circular Medium Earth Orbit (MEO)

planes. The mean orbital altitude of the constellations is roughly 20,200km, meaning each satellite completes two orbits each sidereal day.

GPS uses a Time of Arrival (TOA) ranging method (see section 5.1), meaning that each satellite in the constellation must broadcast its position and time of signal transmission in order for a receiver to be able to calculate its position. This places the receiver at the intersection point between a minimum of three ranging spheres. The clock inside a GPS receiver is of relative poor quality when compared to the precise atomic clocks housed inside each satellite. This means that a fourth measurement (and therefore satellite) is required to correct for this time offset and allow the receiver to calculate its position. When a receiver is initially switched on in, it has no information as to its location or the precise time and has to attempt to search through each satellites code until it finds one. Having found one code, the receiver downloads the *almanac* – a database of the current constellation status and the position of each satellite at the current time. This allows the receiver to find further satellites and compute its current position.

Each GPS satellite broadcasts a Coarse Acquisition Code (C/A Code) on the L1 frequency (Hofmann-Wellenhof et al., 2001). This code is composed of a Pseudo-Random Noise (PRN) 1023-bit Gold code (a code providing excellent auto-correlation properties) which has a repetition rate of once every 1×10^{-3} seconds. The code is modulated using a Binary Phase Shift Keying (BPSK) approach. Each satellite in the constellation has an individual code, which are all broadcast on the same frequency. This means that the system adopts a Code Division Multiple Access (CDMA) modulation, allowing the signals to arrive at the receiver without causing any Inter-Symbol Interference (ISI). L1 will also carry a further code in the future known as the L1C code.

The L2 frequency broadcasts the encrypted Precision Code (P code) along with the new L2C code, a second civilian code. The P code consists of a master sequence of ≈ 2.35×10^{14} bits in length, with each satellite assigned a segment (6.1871×10^{12} bits) of this code to repeat at weekly intervals. The code is broadcast at ten times the rate of the C/A code at 10.23 MHz. In order to use the P code, a receiver must first position itself using the C/A code. This is due to the length of the P code, which gives it very good correlation properties, but makes it difficult to lock on to without knowing the current location and time. In order to prevent *Spoofing* (a type of jamming signal used to inject bogus information to a GPS receiver by emulating a satellite/s code) the P code is encrypted by the W code in order to create the Y code, or as it is generally referred, the P(Y) code.

GPS uses a timing system identical to Coordinated Universal Time (UTC) with one key difference in that GPS time does not take into account leap seconds. Leap seconds are used occasionally by UTC in order to correct for the non-uniform nature of the Earth's rotation.

GPS uses the World Geodetic System 1984 (WGS84) coordinate system.

2.1.2 GLONASS

The *GLObal NAvigation Satellite System* (GLONASS) is a Russian system adopting a similar approach to GPS, albeit with some key differences. The system finally reached full operational capacity by late 1995, many years behind schedule following the break-up of the Soviet Union in the early 1990's.

GLONASS was originally designed to uses a constellation of 24 satellites orbiting in three MEO orbital planes at a mean altitude of 19,100 km. The system broadcasts using a Frequency Division Multiple Access approach, as opposed to CDMA used by GPS. This means that each satellite broadcasts the same codes on different frequencies rather than different codes on the same frequency. The central frequency

of the L1 broadcast is at 1.602 GHz, with each of the fifteen channels broadcast at a multiple of 0.5625 MHz (± 7) either side of the central frequency, based on the assigned number of the channel. As there are more satellites than channels, satellites on opposite sides of the Earth broadcast on the same frequencies. The Earth lies between satellites on opposite sides of the constellation thus preventing a user receiving signals from two satellites broadcasting on the same frequency simultaneously. The central frequency (f_c) of the L2 broadcast is situated at 1.246 GHz with the broadcasts at multiples of 0.4375 MHz either side of f_c. Each satellite broadcasts two signals, the Standard Precision (SP) and High Precision (HP) signals. These are similar to the C/A and P(Y) codes in GPS, with the SP code acting as the civilian code and the HP code the encrypted military code.

As with GPS, GLONASS also uses a TOA positioning approach, with a minimum of four satellites required to find a receiver's location, three for the 3D coordinates and a fourth to correct the receiver clock offset. Unlike GPS, GLONASS uses the PZ-90 coordinate system as opposed to WGS 84.

2.1.3 Future GNSS

Galileo is the positioning system currently under construction by the European Union and due to be fully-operational by 2013. The system design is fairly similar to that of GPS and will use a constellation of 28 satellites in three orbital MEO planes. The mean orbital altitude of the satellites will be slightly higher than GPS at 23,200 km (GSA, 2010).

The system will be broken down into a number of services. The Open Service (OS) will be the equivalent of the civilian signals in GPS and GLONASS. This will broadcast over two frequency ranges, 1.563 to 1.591 GHz and 1.164 to 1.214 GHz using Multiplexed Binary Offset Carrier (MBOC) modulation (Rodriguez et al., 2010). The estimated positioning accuracy of the civilian system will be better than

15 metres horizontally and 35 metres vertically. A second unencrypted service to be provided by the system is the Safety of Life (SOL) service, for use by systems where the safety of human life is paramount, such as aircraft navigation and emergency services. This will provide users with a guaranteed accuracy and the integration of integrity messages into the signal.

As with GPS and GLONASS, Galileo will feature two additional encrypted codes. The first, the Commercial Service (CS), will be a premium service and charge users for the ability to decode the signals. The signal will be broadcast on the same frequencies as the OS and include a third range operating from 1.260 to 1.3 GHz. A receiver with the ability to decode this signal should achieve an accuracy of better than one metre. Galileo will also feature the encrypted Public Regulated Service (PRS), which will be a robust signal to help mitigate against jamming and spoofing and thus be used for safety of life applications.

Compass is the second major GNSS currently under construction by China. The system features a number of similar features to the previously examined GNSS, although there are likely to be a few key differences. Firstly, while 30 of the 35 satellites will orbit at MEO altitude, 5 will remain in a Geostationary orbit (GEO).

In addition to these global systems, two regional systems are also currently under development in India and Japan. The Indian Regional Navigational Satellite System (IRNSS) is a government run system and will be composed of seven satellites, three of which will be in geostationary orbit (Inside GNSS, 2008). Similar to IRNSS is the Quasi-Zenith Satellite System (QZSS) being developed by Japan. QZSS will use only three satellites which whilst broadcasting GPS-type signals, will also be used as part of a communications network. Development of both systems was inspired to counter the well-documented vulnerabilities of GPS by having the ability to be used as a standalone system should GPS fail for any reason.

2.2 ISSUES AFFECTING GNSS SIGNALS

2.2.1 Multipath

Multipath of a signal occurs when an antenna receives multiple copies of the same signal, the multiple copies having been reflected off of objects in or close to the propagation path of the signal.

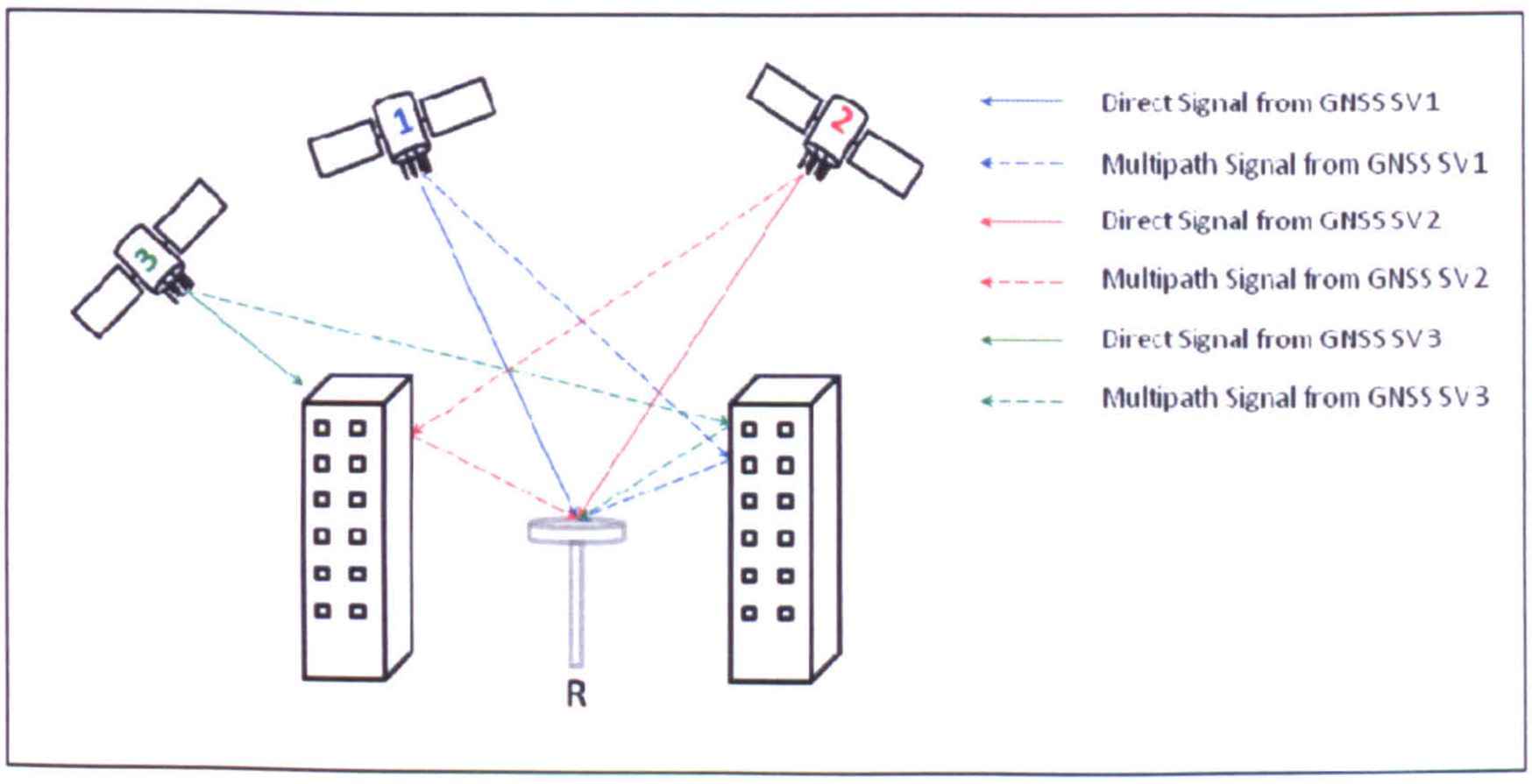

Figure 2-1: GNSS Multipath

This effect has been well documented in the use of GNSS and some examples of attempts to mitigate it can be seen in (Julg, 1996), (van den Brekel and van Dee, 1992). Due to the low transmission power used by GNSS satellites, signals can be completely obscured by objects yet still receive the same signal reflected off of nearby buildings. Figure 2-1 shows a simple example of multipath signals arriving from three GNSS satellites to a receiver R. The receiver has line-of-sight to satellites 1 and 2 and due to its location between high-rise buildings, also sees multipath signals reflected off of these. The signal from satellite 3 is obscured completely for a line-of-sight path but the signal does arrive at the receiver via a multipath route. As the reflected signals take longer to travel between the satellite and receiver, this adds an error when calculating the range to each satellite.

2.2.2 Atmospheric Effects

The effects of a GNSS signal travelling through the various layers of the Earth's atmosphere has long been known as an error source, and the effect can be mitigated to some extent. These effects can be segmented into two portions of the atmosphere which can cause delaying effects on GNSS signals (see Figure 2-2).

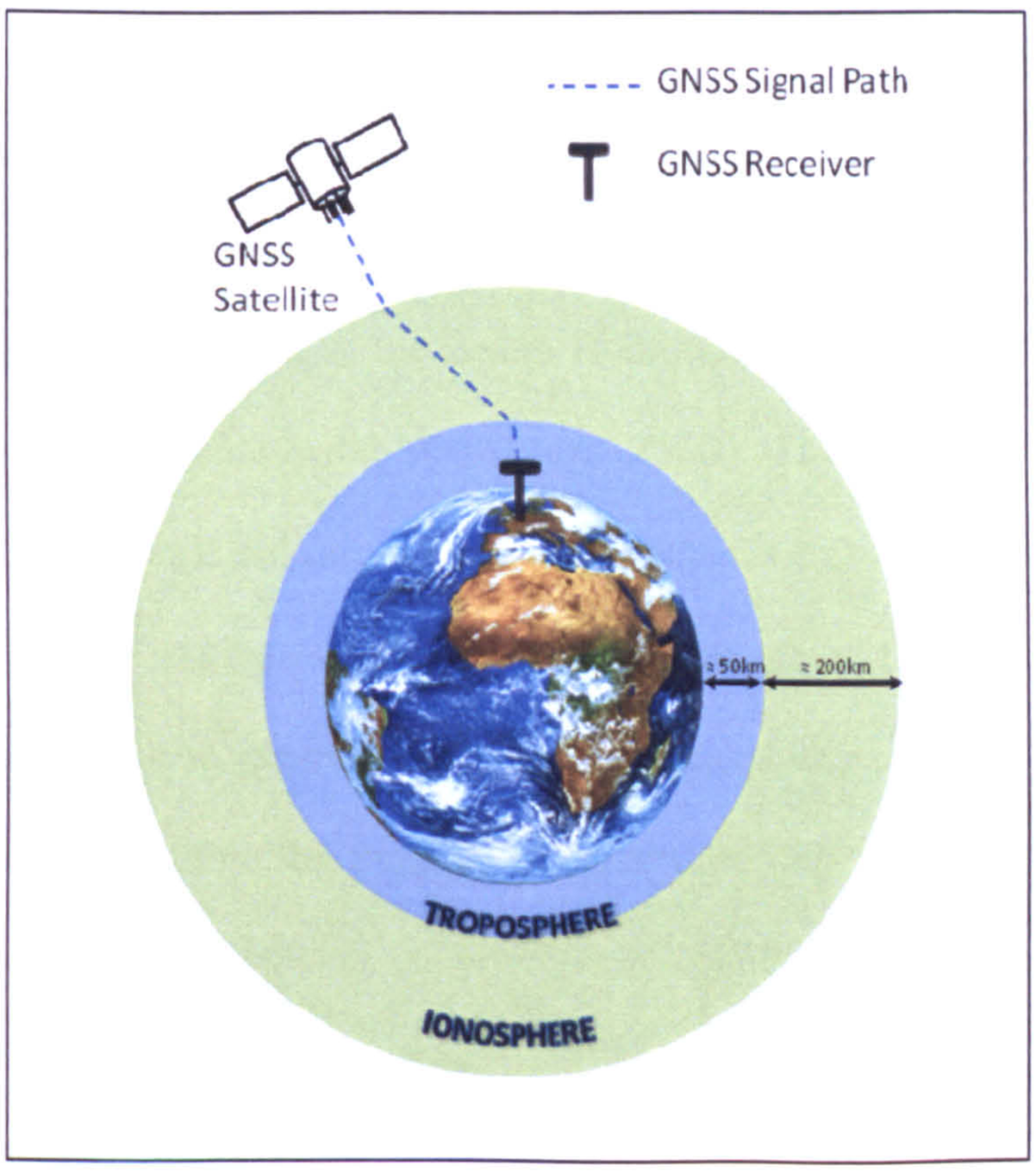

Figure 2-2: Atmospheric effects on GNSS signals

- **The Ionosphere –** The upper part of the atmosphere that GNSS signals travel through following broadcast (between 50 and 250km above the Earth's surface). There are two distinct effects this has on the signal as it enters the Ionosphere; firstly the Pseudo-ranges are delayed as the signal is refracted and secondly, the carrier phase is advanced. The magnitude of the Pseudo-range delay is dependent on the Total Electron Content (TEC) along the ionospheric

portion of the signal path. This content varies with the sun-spot cycle, with the worst effects occurring during the Solar Maximum of that cycle. As the magnitude of both effects is broadcast frequency dependent, the L1 and L2 pseudo-range signals used by GPS are slowed at slightly different rates. This effect is beneficial at the receiver as it helps to mitigate and cancel out the ionospheric effect using L1 and L2 dual-frequency observations.

- **The Troposphere –** The lower part of the atmosphere that GNSS signals travel through following broadcast (up to 50km above the Earth's surface). As with the Ionosphere, the Troposphere also affects GNSS signals in two ways. There are two delaying factors present in this part of the atmosphere, the dry delay (known as the Zenith Hydrostatic Delay – ZHD) and the wet delay (known as the Zenith Wet Delay – ZWD). The Troposphere delays both the pseudo-range and carrier phase measurements and whilst the dry delay can be removed relatively easily by modelling the effect, the wet delay is much more difficult to remove due to the unpredictability of water vapour levels present. Therefore the tropospheric errors are only mitigated in standalone positioning by applying a generalised model or by using differential positioning over a short baseline.

2.2.3 Doppler Effects

GNSS satellites orbiting on a MEO travel at a speed of roughly 3900 ms^{-1} relative to the Earth. This effect, in addition to the rotation of the Earth ($\approx$ 400 ms^{-1}) and the movement of a GNSS receiver relative to the surface (Zhang et al., 2006), means that Doppler effects are generated as the signal is in transit between the satellites and the receiver.

2.2.4 Satellite Geometry

Geometry of observable satellites at a receiver affects the accuracy of GNSS observations. Figure 2-3 shows two two-dimensional scenarios *A* and *B*, each

indicating the position of two satellites (*1* and *2*) relative to each other and to a receiver on the ground.

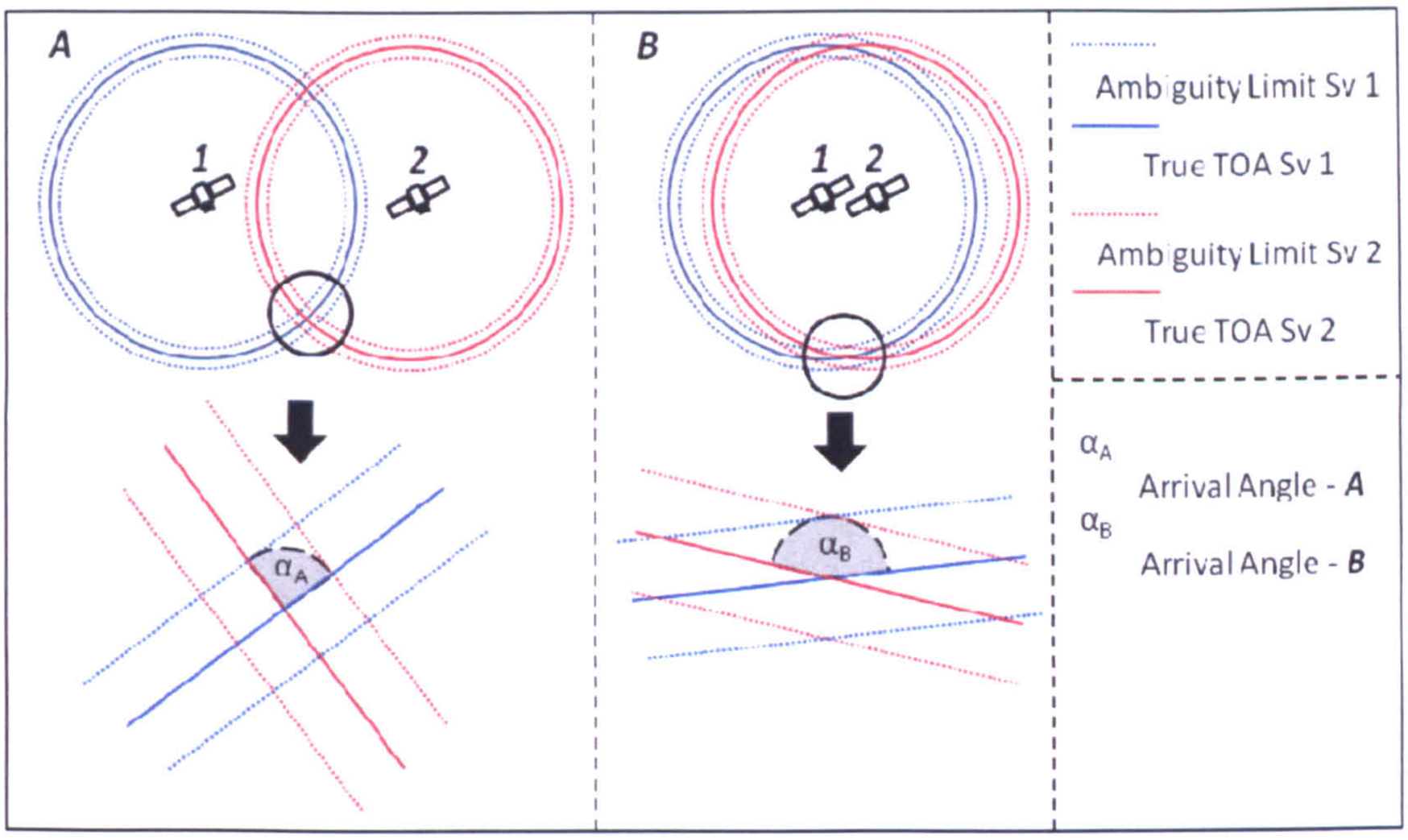

Figure 2-3: GNSS Satellite Geometry

In scenario *A*, the intersection of the arriving signals at the receiver gives an arrival angle of α_A, at roughly 90°. This gives the smallest area of uncertainty possible around the receiver's true location. Compare this to scenario ***B*** where the two satellites are closer to each other in orbit. This gives a much wider signal arrival angle intersection (α_B), and therefore a wider area of ambiguity around the receiver. The ambiguity limit lines on the diagrams are caused by the other error sources present in the system discussed in this chapter.

As will be seen later in this document, the problem of transmitter geometry is present with all signals transmitting positioning signals.

2.2.5 Jamming

Jamming of civilian GNSS signals is a topic of importance due to the large-scale rollout of GPS satellite navigation units and other safety of life applications in recent years. The dependency on the coverage and integrity of the signals is going to be paramount and jamming of the signals either intentionally or accidentally could potentially have catastrophic consequences. This section will briefly examine some jamming techniques and how they could affect a GPS receiver.

The objective of an intentional jammer is to interfere with a radio transmission by broadcasting electromagnetic energy in the form of spurious signals to cause disruption or complete denial of a radio communication system. Figure 2-4 shows the jammer-to-signal (JSR) ratio levels at which the GPS signals tracking and signal acquisition is affected. It shows a jammers ability to jam both the C/A and P code signals dependent upon the jammers transmission power and its distance from the receiver.

A jamming signal (intentional or otherwise) is present in addition to the background noise present on all frequencies. Background noise can fluctuate naturally due to factors such as the time of day and the solar flare cycle. This section will examine the types of jamming signals that can be produced.

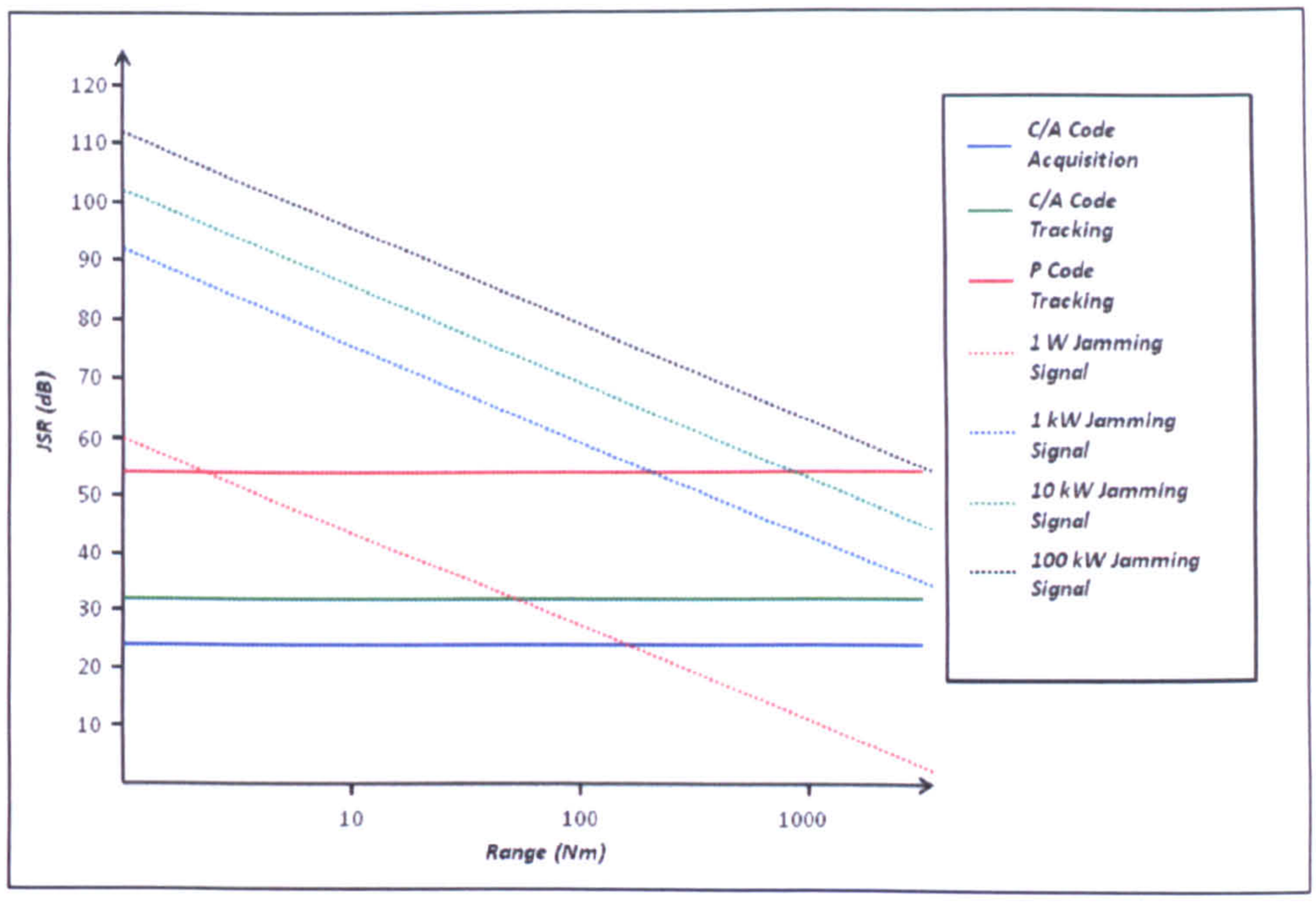

Figure 2-4: Jammer Effect on GPS Code Acquisition/Tracking

(recreated from (Abbott, 2002))

2.2.5.1 Narrow-band & Wide-band Jamming

Jammers can be set to target complete or only parts of signal frequencies so as to cause disruption. Naturally, the wider the bandwidth in which the jammer operates, the more power is required. This means that narrow-band jammers can operate at higher output power levels when using the equivalent input power of a wide-band jammer. Figure 2-5 indicates how broad and narrow-band jammers might swamp the GPS L1 signal. The wide-band jammer engulfs a bandwidth of 20.46MHz, covering both the P and C/A code.

By comparison, the narrow-band jammer shown is focused only on the C/A code bandwidth (2.046MHz), leaving other segments of the signal less or completely unaffected (P code). However, the narrow-band jammer has a higher output power resulting in a lower signal-to-noise ratio over the C/A code than with the wide-band example.

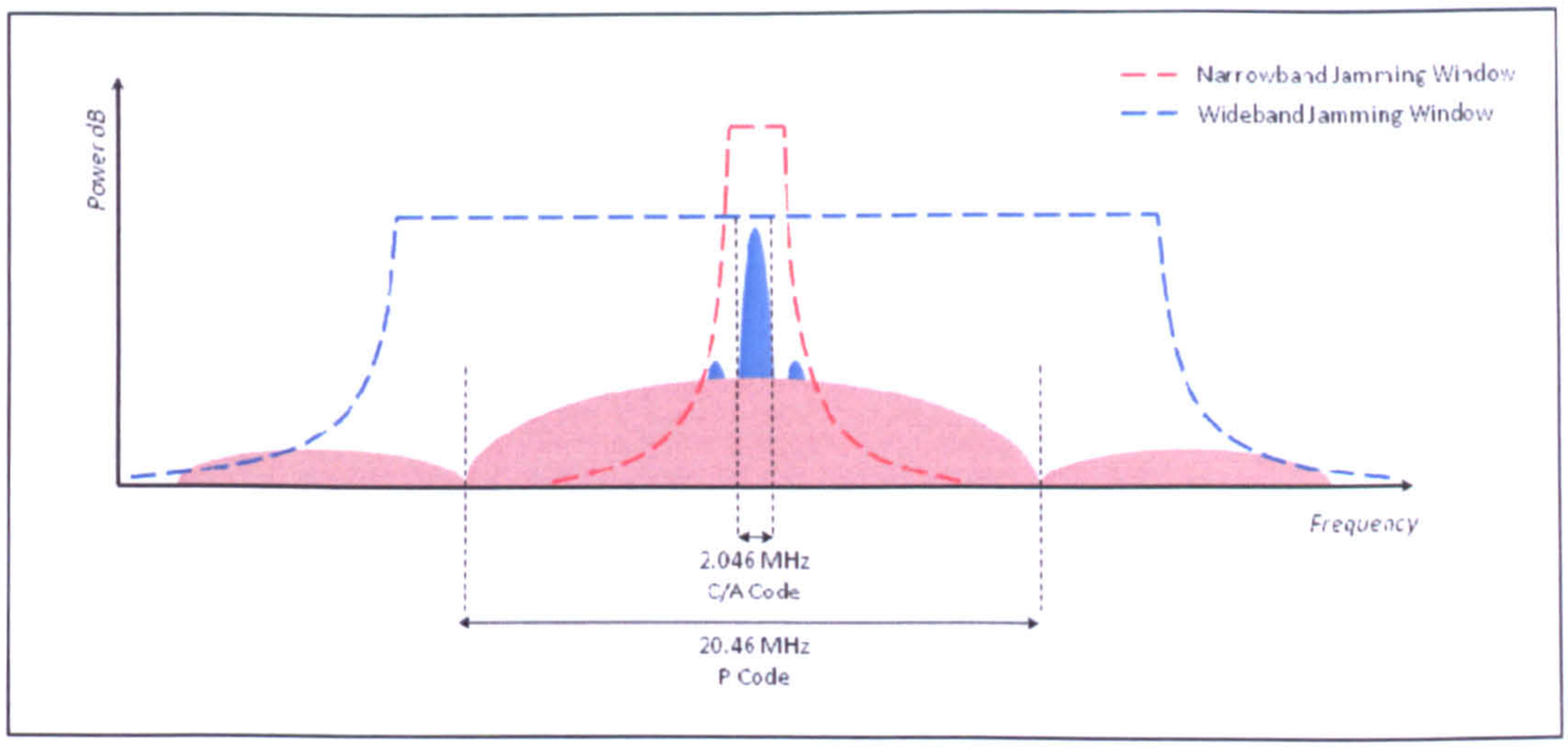

Figure 2-5: Narrow and Wideband jamming of GPS L1 Signals

2.2.5.2 Continuous Wave Jamming

Continuous Wave (CW) Jamming involves an even simpler system than wide-band or narrow-band jammers. The CW jammer transmits an un-modulated continuous sine wave signal at a critical frequency of the source, usually the central transmission frequency, so that the receiver cannot attain lock on the signal of interest. Due to its very narrow band frequency, this jammer type requires less power than narrow band jamming. Multiple CW jamming waves can be produced simultaneously to produce what is known as a *Multi-tone Jammer* (Rash, 1997).

2.2.5.3 Brute Force Jamming

The simplest jamming technique is called Brute Force or barrage jamming, and involves the broadcast of additional white (Gaussian) noise over the targeted region of the spectrum. The jamming signal does not require any knowledge of the broadcast signal other than the frequency over which it has to be effective. It can be used in

both broad and narrow-band jamming techniques. The spectral density *Nj* of the wide-band brute force jamming can be expressed by 2.1, where *J* is the total power and *W* is the bandwidth of the jamming signal:

$$N_j = \frac{J}{W} \qquad 2.1$$

$$N_j = \frac{J}{W_j} \qquad 2.2$$

Additionally, the narrow-band version is expressed by 2.2, where *Wj* is the jamming signal bandwidth as a portion of the original signal bandwidth *W* (*Wj* < *W*). The narrow-band signal can be used to sweep the entire signal bandwidth *W* in portions of width *Wj*. The usage of this technique is known as "Sweep-Spot Noise" (Pinker and Smith, 1999).

2.2.5.4 Pulse Jamming

Pulse Jamming involves the continuous switching on and off of a jamming signal. This conserves power at the transmission end whilst also allowing a narrow-band or CW jammer to switch frequencies. Whilst a wide-band brute force jammer will continuously broadcast a jamming signal over the spectrum of interest W, a wide-band pulse jammer would broadcast its pulsed signal over the spectrum width W for a predetermined time t. This allows the pulse jammer to use a fraction of the energy required from the continuous brute-force jammer.

2.2.5.5 Chirp Jamming

Chirp jamming involves the alteration in frequency modulation (FM) with respect to time to produce sinusoidal interference. Because of the frequency modulation over time, this causes a Doppler Shift Effect. Figure 2-6 shows an example of an

increasing chirp signal represented in the time domain, a reverse of the process may also be used (decrease in frequency over time).

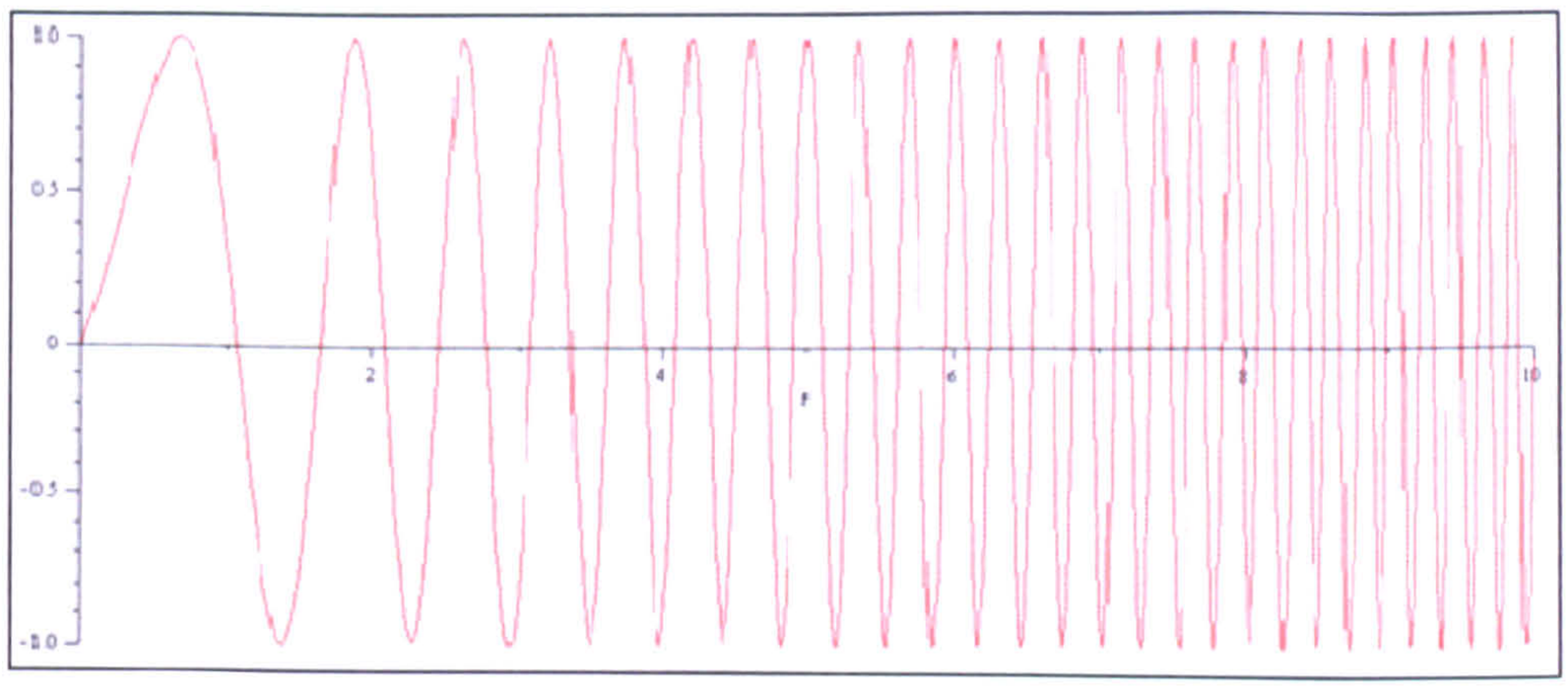

Figure 2-6: Example of a Chirp Signal in the temporal domain

This technique would be used to target a spread spectrum signal such as GPS, due to its wide bandwidth. The frequency spread of the jamming signal would cover the entire useful bandwidth of the target signal; therefore this information would have to be known in order to deploy this jamming technique successfully.

2.2.6 Unintentional Jamming

Whilst cases of unintentional GNSS jamming are rare, a well-documented case occurred in Moss Landing harbour in California, USA (Vincent et al., 2003). A small television antenna pre-amplifier on board a boat malfunctioned in this case, preventing GPS signals from being received in much of the harbour and up to a kilometre out to sea.

2.3 JAMMING MITIGATION TECHNIQUES

There are a number of anti-jam techniques that may be employed to mitigate GPS interference. The choice of technique to be used is dependent on a variety of constraints, primarily size, cost and power.

2.3.1 Adaptive Filtering

A digital filter can be thought of as a 'black box' system whereby a signal is sampled, passed through the system and outputs a filtered signal. The black-box is usually run on a CPU. This is in contrast to an analogue filter, which can perform the same task using a combination of electrical components. The following sections will be examining a variety of digital filters used to mitigate jamming.

Adaptive filtering involves the adjustment of a digital filter used in the processing of a signal depending on the signals input characteristics. It is an iterative process, with the simplest approach using an estimation algorithm, such as the Least Mean Squares (Steinbuch and Widrow, 1965) and Kalman Filters (Kalman, 1960) with a feedback loop so the output of the filter is involved with the adjustment of the next iteration. A major disadvantage of this technique is that the interfering signal structure must be known in order to filter out the expected jamming signal. The use of adaptive filtering is most effective when used to combat narrowband jammers.

2.3.2 Time-Frequency Domain Filtering

As GPS signals arrive at receivers at very low power levels, the jammers tend to be of much higher power and can therefore be distinguished from the GPS signal in the frequency domain. The Time-Frequency distribution can be used to describe the power of a signal as a two-dimensional function of time and frequency. There are a number of Time-Frequency distributions which can be used to signify the signal in the frequency domain. Slow-changing, less-dynamic signals can obtain time-frequency distributions by calculating the spectrogram, whilst more dynamic signals requiring

higher frequency resolutions would use the Wigner-Ville (Guanghua et al., 2006) or Choi-Williams (Choi and Williams, 1989) distributions. Once the combined GPS and jamming signal are represented in the frequency domain, the two signals must be separated before converting back to the time domain. Time-Frequency techniques are only effective against narrowband and CW interference, not against wideband jamming signals. A brief summary of these techniques, including their advantages and disadvantages follow.

2.3.2.1 Short-time Fourier Transform (STFT)

The Short-time Fourier Transform uses a window moving through the signal in the frequency domain in order to take the Fast Fourier Transform of the highlighted selection in the window (Durak and Arikan, 2003). This removes the jamming portion of the signal in the frequency domain which can then be transformed back to the time domain. The windowing technique used in the STFT can distort the signal; a narrow window provides good time resolution but poor frequency resolution, whilst a wide window provides good frequency resolution but poor time resolution. However, the technique can be deployed using relatively low power and may be fitted in discretely in small devices.

2.3.2.2 Filter Banks

Filter banks are structures composed of low-pass, band-pass and high-pass filters constructed specifically for the spectral decomposing and recomposing of signals (Mertins, 1996). Once decomposed into its various sub-bands by the analysis filter bank within the frequency domain, a spectral modification function is applied to each band in order to remove the jamming/interference. Finally, the sub-band signals are

recomposed by the synthesis filter bank in order to reconstruct the original signal with the interference removed.

In (Jones and Jones, 1992), the technique was successfully used to remove a narrowband pulse jamming source from a Direct Sequence Spread Spectrum system. This technique allows the efficient extraction of jamming/interference spectral components, and has the same advantages as the Short-time Fourier Transform method without the disadvantage of window signal distortion.

2.3.2.3 IIR and FIR Filtering

Infinite Impulse Response (IIR) and Finite Impulse Response (FIR) Filters are digital filters which may be used to mitigate narrow-band or multiple narrow-band jamming signals in the time domain. The technique may be implemented in real-time as a front-end to the GPS processing, or as a post-processing tool.

A certain type of IIR/FIR filter used by (Kukrer and Hocanin, 2006) and (Choi and Cho, 2001) is the notch filter – a narrow-band band-stop filter. The notch of the filter was placed at the frequency of a CW jammer transmitting additional noise in order to mitigate it. In the case of (Kukrer and Hocanin, 2006), the FIR filter was used rather than an IIR filter due to its stability. However, in the case of (Choi and Cho, 2001) the IIR filter is used in preference to the FIR Filter as the former can provide frequency responses closer to an ideal notch filter than the latter of the same order, thus being more computationally efficient. In both cases, a frequency estimator is required in order to determine the Instantaneous Frequency (IF) of the jamming signal. The band-stop notch of the filter is then placed at this frequency to block the interference.

The main advantage of this technique is that it is small and cheap to implement, therefore suitable for use in civilian receivers. However, it is limited in that it cannot mitigate wideband jamming signals without substantially more costly and power demanding analogue-to-digital converters.

2.3.2.4 Wavelet Transforms

Wavelet Transforms are closely related to the STFT discussed in section 2.3.2.1, although the technique is often defined as a time-scale analysis rather than a time-frequency analysis (Daubechies, 1990). The Discrete Wavelet Transform (DWT) and Continuous Wavelet Transform (CWT) are two of the more widely used wavelet transforms and are alternatives to the Fast Fourier Transform used by the STFT technique. Rather than using a fixed window like the STFT, wavelet transforms use a window which varies in size as it passes over the signal. This provides a flexible resolution in both the time and frequency domain which compares much more favourably to the STFT, which has a fixed frequency resolution for the duration of the window.

2.3.2.5 Subspace Processing

Subspace processing or projection is a pre-correlation technique requiring the estimation of the Instantaneous Frequency of the jammer. This is provided by implementing one of the time-frequency distributions mentioned in 2.3.2. The Instantaneous Frequency defines the temporal signature of an orthogonal signal space in which the jamming signal occupies one dimension (Zhao et al., 2000). The definition quality of the Instantaneous Frequency is critical in this case, as the better the accuracy, the better the anti-jamming performance of the system will be.

This technique was used successfully to mitigate an FM signal attempting to jam the C/A code by (Zhao et al., 2002). Once the signal is decomposed, both original signal and jamming signal can be represented as two distinct vectors. The dimension occupied by the jamming signal can then be removed from the original signal and reconstructed in the time domain without interference.

A second technique involving subspace projection involves the implementation of a time-varying notch filter, the placement of which is also defined by the Instantaneous Frequency quality of the jamming source. However, this technique can cause distortions in the signal.

2.3.2.6 The De-chirp Method

The de-chirp technique is used to identify a chirp jamming signal (discussed in 2.2.5.5), then reconstruct this signal locally in the receiver in order to subtract it from the signal of interest (Zaka et al., 2005). The instantaneous frequency (IF) of the signal is attained using an appropriate time-frequency distribution technique as described in 2.3.2. This allows the calculation of the instantaneous phase and with the assistance of a low-pass filter, an estimate of the instantaneous amplitude of the chirp. With these three pieces of information (frequency, phase, amplitude) and using an iterative process, the chirp signal may be reconstructed and subsequently subtracted from the signal.

2.3.3 Adaptive Antennas

2.3.3.1 Beam Forming

Beam forming involves the control of the radiation pattern (or the physical direction) of an antenna. The antenna is controlled so as to give high gain in the direction of the desired signal, whilst limiting or eliminating any incoming interference. In the case of GPS signals, the beam would be directed towards signals coming in from overhead and nulls in the direction of any jamming sources that may be being broadcast from the ground. This technique works well when the signal of interest and the jamming source are well spaced apart, but its weakness occurs when both signals arrive from the same direction. For example, GPS satellites that are broadcasting from lower on

the horizon may be transmitting on the same line of sight as a source of interference (Brown and Gerein, 2001). Whilst this is a successful technique, the physical size and cost of the equipment makes is unfeasible for use on anything other than a fixed receiver on land or a large sea vessel.

2.3.3.2 Null Steering

Null Steering (also known as a Controlled Radiation Pattern Antenna – CRPA) is a technique that may be employed in addition to Beam Forming (Zoltowski and Green, 1995) or as a standalone mitigation technique. The method employs a circular array of slot elements in order to produce a pattern of nulls which can be directed towards interference sources. This is a very robust method to eliminate interference, and can tackle both wideband and narrowband jamming signals (Casabona and Rosen, 1999). On the negative side, the number of nulls produced by the slot elements can limit the number of satellites in view at any one time, whilst the physical equipment size and cost make it nonviable for compact civilian receivers. As mentioned, this technique can work alongside beam forming, the beam being pointed skywards to receive GPS signals whilst the nulls are steered towards the sources of interference on the ground plane.

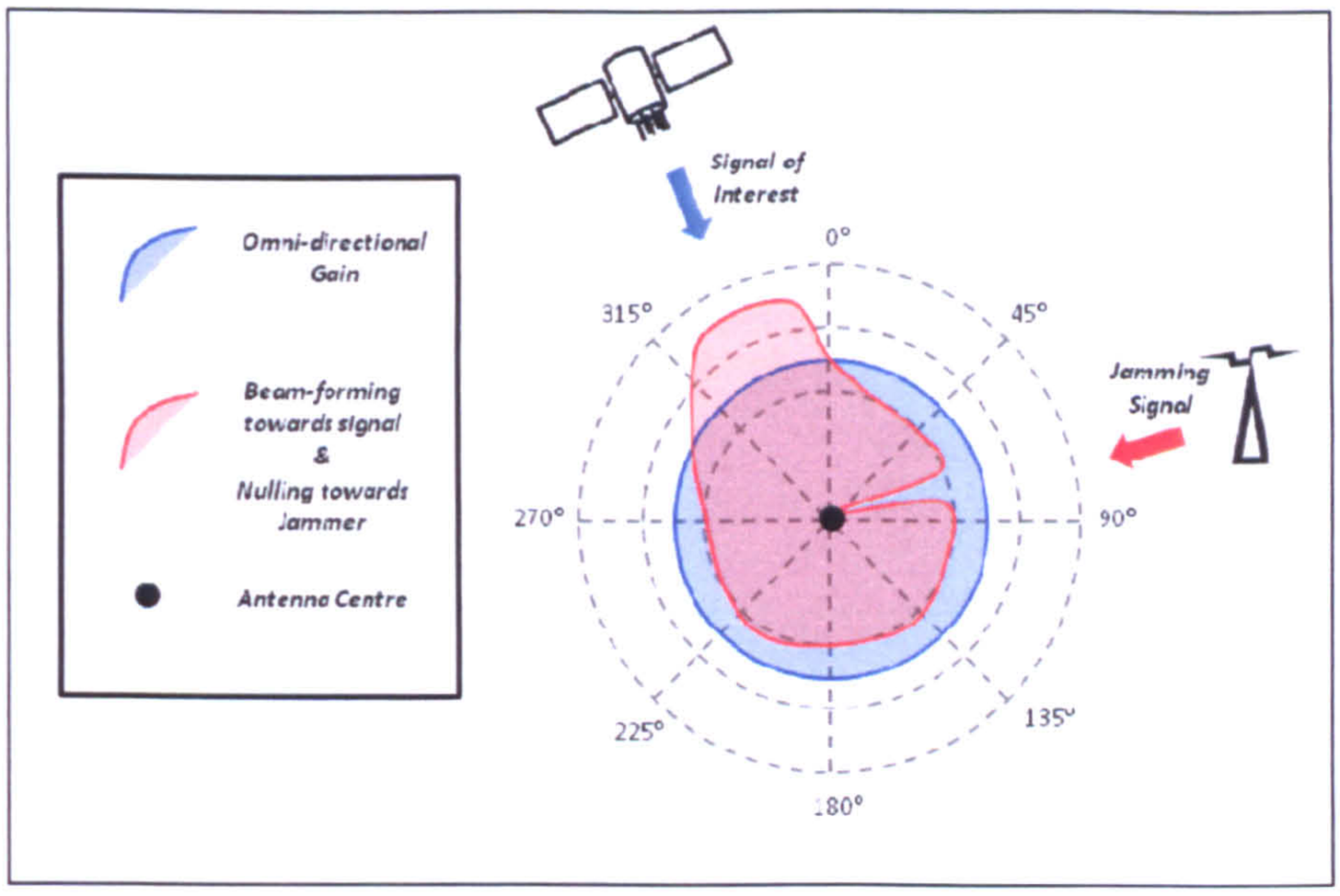

Figure 2-7: Simple example showing Beamforming and Nulling

Axial Nulling is a simplified variation of Null Steering commonly employed with GPS guided weapons. The null is produced along the axis of the projectile, mitigating jamming signals incoming from the direction of travel only. This technique could be used to guide a GPS guided missile to destroy an enemy jammer.

2.3.4 Inertial Measurement Unit Integration

The integration of GPS with Inertial Measurement Units (IMU) allows either technology to assist the other. An IMU consists of an accelerometer and a gyro fixed along each dimension measurements are to be taken. In the case of a three-dimensional environment, three such pairs are installed orthogonally to each other so as to measure the linear acceleration (from the accelerometer) and orientation (from the gyro) in each plane.

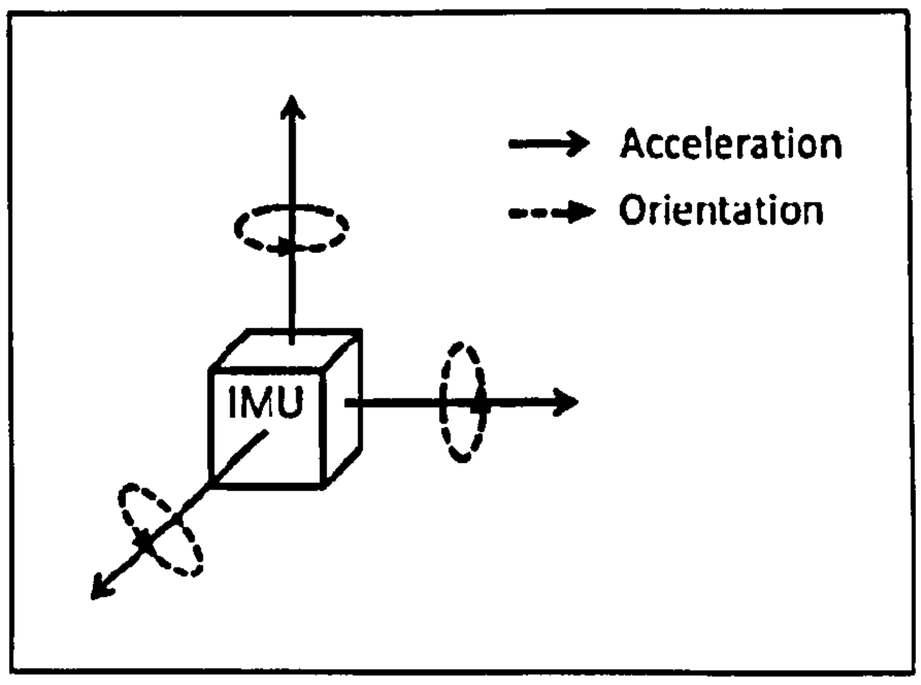

Figure 2-8: IMU operating in three dimensions

When used as a standalone unit an IMU suffers from several error sources which can cause the sensors to drift. IMU's are available in different grades and sizes, generally the more expensive and bulky units have a much lower rate of drift than Micro-Electro-Mechanical Systems (MEMS) devices which can easily fit onto a printed circuit-board (Hide, 2003). The purpose of integrating the IMU with a GPS receiver is their ability to assist each other when implemented via a Kalman Filter (Kalman, 1960). The inertial measurement improves the GPS receivers tracking ability, assisting it to counter interference/jamming for short periods of time depending on the grade of the IMU. At the same time, the GPS measurement helps to bound the errors of the IMU, without which would continually drift (rate of which also dependent on the IMU grade).

Therefore this technique can only overcome jamming for pre-determined periods of time, after which the position estimate becomes unusable due to the IMU drift.

2.3.5 Summary of Jamming Mitigation Techniques

Although there are many methods available to mitigate the effect of a jamming signal on GPS, they each have their own advantages and weaknesses.

Adaptive filtering, whilst being cheap to implement and small in size requires knowledge of the interference signal structure and is also unable to mitigate wideband jamming.

The Time-Frequency Domain Filtering techniques provide a range of different tools to remove most sorts of narrowband interference. They are low cost, require nominal power and can be implemented in the full range of receivers. This makes them particularly useful for highly dynamic receivers which will be changing direction constantly (e.g. hand-held, in-car satellite navigation). The major disadvantage of this is, like adaptive filtering, they cannot be used to mitigate wideband jamming.

The inertial measurement integration technique can aid GPS tracking for short periods, the duration of which depends on the quality (and hence increase in size, cost and power) of the IMU. This means during periods of prolonged jamming or GPS unavailability, the position estimate would decay at an exponential rate over time.

The adaptive antenna techniques such as beam-forming and null steering are capable of removing all types of interference at a pre-correlation stage, but due to the nature of the antenna arrays, the cost, power and space requirements are much higher than internal processing techniques. These are also incapable of successfully removing interference in dynamic situations and are limited to static or slow-moving platforms.

To summarise, there is not currently one solution discussed which can fulfil all criteria and successfully mitigate all known types of jamming within size, cost and power constraints. This leads on to consider terrestrial positioning systems such as LORAN (section 2.4.1), and the so called Signals of Opportunity (section 3) – certain communications signals which whilst not designed for positioning, have elements which may be used for this purpose.

2.4 TERRESTRIAL NAVIGATION

This section will examine the currently available terrestrial navigation systems and compare their positional accuracies and vulnerabilities with the GNSS described in 2.1.

2.4.1 LORAN/LORAN-C

LORAN is a terrestrial radio navigation system and has been maintained by the United States Coast Guard for over 40 years (Lo et al., 2004) with LORAN-C being the currently adopted universal standard. While GPS coverage is essentially global, LORAN is limited to certain areas, see Figure 2-9 for coverage details. As this map shows, the coverage is limited to the northern hemisphere leaving large parts of the landmass without any coverage.

Figure 2-9: Global LORAN Coverage

(http://www.locusinc.com)

2.4.1.1 Positioning Technique

The LORAN system is divided into a number of 'chains'. A chain contains three or more stations (one master transmitter and two or more slave transmitters), each

transmitting a highly accurate atomic timing pulse from a known location. The basis of the positioning system is as follows.

- The master transmitter transmits a series of nine timing pulses – these are received by each slave transmitter in the chain and any LORAN receiver within range of the master transmitter.
- On receipt of the master pulse group, each slave transmitter waits a highly accurate, predefined length of time before transmitting a series of eight pulses back (each slave transmitter has a different delay time which allows chain identification). The extra ninth pulse from the master station allows identification of the master signal.
- A LORAN roving receiver compares the difference in the timing signals received from the master and slave transmitters. This places the user at some point along a hyperbola between the master and slave transmitters.
- A second chain (using a second slave transmitter) produces a second hyperbola – hence the point where the two hyperbolas intersect is the position of the user.

The time interval between two subsequent master pulses is called the Group Repetition Interval (GRI). Each chain has a different GRI and these vary from 40 – 100 milliseconds.

LORAN-C signals are broadcast in the LF band using a carrier wave centred at 100 kHz (giving an approximate wavelength of 3km). Figure 3-1 shows an example of a generated LORAN pulse.

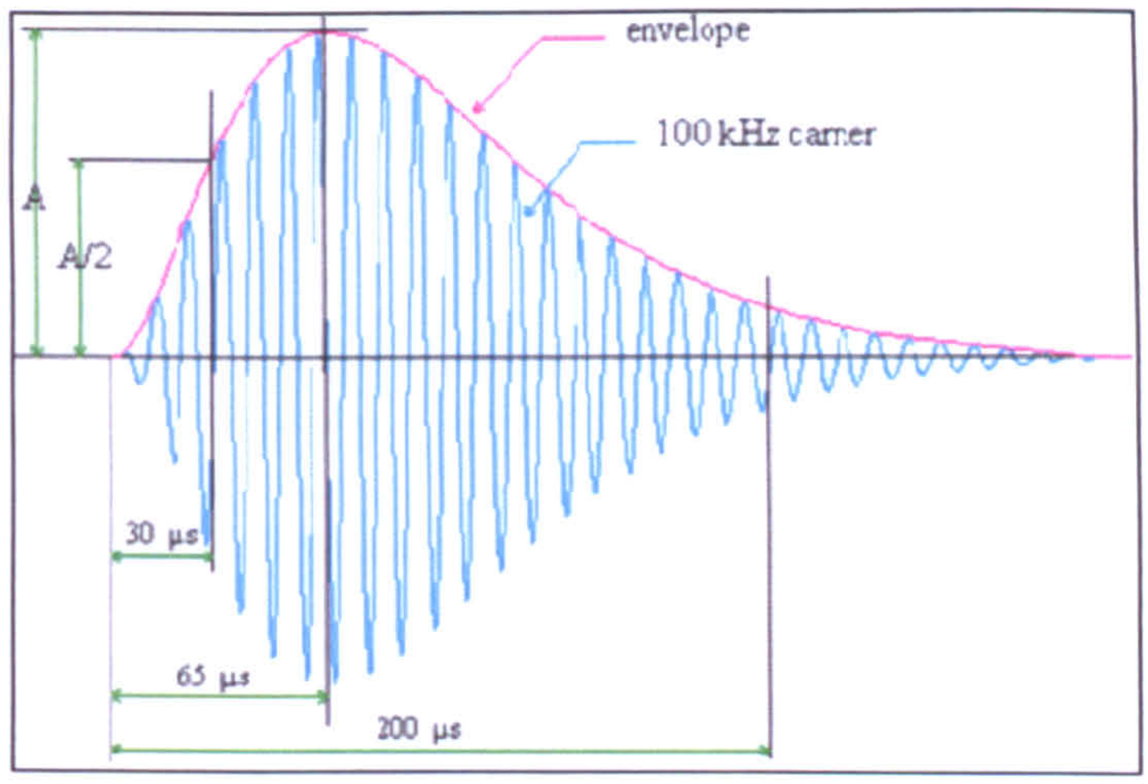

Figure 2-10: LORAN Pulse

Each transmitted pulse has an approximate (useful) length of 200µs before decaying exponentially up to 300µs. The time difference between the first and subsequent pulses in each group is 1000µs. The exception to this is the last two pulses from the master transmitter (pulse's eight and nine), which have a gap of 2000µs.

This frequency allows the signal to propagate along what is known as the ground-wave. Ground-wave propagation refracts the signal around the earth so that it may be received below the horizon of the transmitter; this allows the signal to travel over longer distances than line-of-sight transmissions (100's km). Most signals in the LF band and the lower end of the MF band can travel via this method. The refraction reduces the power of the signal the further it travels as the energy is absorbed by the earth's surface. The rate that the energy is absorbed depends on the ground itself, for example, the signal will travel further over open water (due to higher conductivity) than it will through a built-up city environment.

The signal can also be affected by sky-wave propagation as the signal is distorted by the differing refractive index of the ionosphere and can vary depending on solar conditions. Sky-wave propagation distorts the carrier phase and shape of the pulse.

This causes two versions of the same pulse arriving at the receiver, the direct Ground-wave signal arriving fractionally before the Sky-wave signal.

2.4.1.2 eLORAN

eLORAN is an updated system to LORAN-C to be used to complement or back-up a GPS receiver. The theoretical accuracy of eLORAN is between 8 – 20 m (Basker, 2006) which is comparable to the accuracy of standalone GPS. In addition to this, the new signal has the ability to broadcast differential GPS corrections.

2.4.1.3 Limitations

The LORAN system is limited by several factors due to the ground-wave propagation of the signal and the large distance between stations. The speed of signal transition differs depending on the ground over which it is travelling, for example, the speed of the signal slows slightly over salt-water compared to that over land. This means a receiver based on the land has to apply what are known as Additional Secondary Factor (ASF) corrections to the measurements made in order to mitigate the error. As these ASFs are location dependant, a model of values has to be maintained to apply the necessary correction factors. It has also been shown that the presence of power-lines near a receiver can cause problems with the LORAN signal (Lachapelle et al., 1993).

Limitations also exist with the hardware component of a LORAN receiver. As the signals are broadcast at low-frequency, a relatively large antenna is required to receive the signals (Lorenzo et al., 2009). Judging the state of LORAN antennas available currently, it is unlikely that a sufficiently miniaturised LORAN antenna of adequate quality will appear in a market that requires one, such as the mobile phone market.

2.4.2 Datatrak

Datatrak is a commercial system broadcast in the LF band and primarily used to track and locate vehicles, often integrated with GPS as the Datatrak transmitters additionally

broadcast differential GPS corrections. The system operates in a way similar to LORAN in that it is a hyperbolic system. Transmitters are located in a network with a range of roughly 160km between each and broadcast the signals on 133 and 145 kHz. In addition to the positioning network, a receiver has the ability to report its position (to an accuracy of 50 metres) back via a dedicated data network (Banks, 1991). Little has been published about Datatrak since its inception, mainly due to the closed-source commercial nature of the system. The signals cannot be used by third-party receivers.

2.4.3 Summary

The current status of ground based radio navigation systems is currently limited to LORAN (in its various states) and Datatrak. Neither system operates globally, with LORAN limited to the northern hemisphere and Datatrak limited to certain European countries. As Datatrak is a private system, the signal cannot be realistically used as a potential solution to GPS non-availability. Land-based LORAN, whilst having a far greater signal-to-noise ratio than GPS, has issues due to the Additional Secondary Factor "errors", the effect of power-lines on signals broadcast at that frequency and the physical size of the equipment required to calculate position. This means that LORAN is a viable back-up to a GNSS when the receiver is based upon an oceanic vessel, with plenty of space for the necessary equipment, but not to a mobile phone or vehicular satellite navigation user who does not have the space requirements for the hardware.

This leaves one to consider the use of other, non-navigation signals currently being broadcast for potential positioning purposes, which the next chapter will examine.

3 SIGNALS OF OPPORTUNITY

3.1 INTRODUCTION

A "Signal of Opportunity" (referred to as a *SoOp* from here onwards) can be loosely defined as any communications signal which can be used for positioning purposes. These signals are not designed to be used as positioning systems; however, they have certain properties which make them usable as such. A number of attempts have been made over the years to take advantage of these SoOp's, some more successful than others. The signals are used to either fill gaps from designated positioning systems which may suffer certain weaknesses, or act as a standalone positioning system. These SoOp's however do have particular advantages and disadvantages depending on the signal examined. The following summary of SoOp strengths and weaknesses was published by (Raquet et al., 2007), and these highlight a good high-level overview of the use of non-navigation signals for positioning purposes.

3.2 ADVANTAGES

- *Availability* – there are a multitude of different signals available, transmitted from different directions and at different frequencies. Urban areas will receive a greater quantity of signals than less populated areas.
- *Power* – compared to GNSS, terrestrial signals are transmitted at much higher powers, giving them the ability to reach users where GNSS cannot penetrate.

GNSS signals are transmitted with a power of approx 300W at a distance of at least 20,000km from the Earth. By comparison, the television and radio transmitter at Sutton Coldfield transmits at 250kW and is approximately 60km from Nottingham. Signals also do not suffer the ionospheric and Doppler errors experienced by GNSS.

- *Infrastructure* – no additional infrastructure is required to transmit the signals and as they are being transmitted for other purposes, there is no additional cost to the user.
- *Technology Advances* – with the advent of Software Defined Radios, it is now possible to capture and process large swathes of the radio spectrum in order to monitor more than one incoming signal source.

3.3 DISADVANTAGES

- *System Design* – signals of opportunity are not designed for the purpose of navigation/positioning. For Time of Arrival (TOA) and Time Difference of Arrival (TDOA) positioning, precise network synchronisation is required (in the region of a few nanoseconds) to create a position fix without the need for a second reference receiver.
- *Availability* – there are numerous signals available (dependent on location), but the standards can differ greatly by continent/country leaving no one global standard for many signals of interest. This causes further receiver design problems if the device was to be used globally. For example, the different digital terrestrial television standards adopted by Europe (DVB-T) and the USA (ATSC). Whilst the data itself is not as important, it is the different modulation techniques used that could cause complications.
- *Transmitters* – the location of all transmitters used for positioning must be precisely known.

- *Receiver Design* – examining wider regions of the spectrum requires more powerful processors, faster analogue-digital converters, and more complex antennas and filters. Additionally, more recent digital signals use wideband channels in preference to narrow-band channels. For example, the digital television (DVB-T) channels in the UK are delivered in 8MHz channels spanning the region 470 – 862 MHz.

- *Multipath* – probably the main problem facing all signals in urban environments. When used solely for communications purposes, multipath signals can be mitigated at the receiver and even used advantageously to boost performance in some systems. However, to be used as a positioning system, the direct signal transition time from transmitter to receiver is of utmost importance.

3.4 SIGNALS USED FOR POSITIONING

There have been some successful attempts to utilise various signals of opportunity for navigation/positioning purposes.

3.4.1 Medium Wave (Amplitude Modulation)

In the Medium Wave (MW) region, (Hall, 2002) created a carrier-phase positioning system utilising a software defined receiver to digitise the entire band (520 – 1710 kHz) transmitted from approximately 30 stations broadcasting around Boston, USA. The results were promising, indicating errors of less than 15 metres on non-urban open land. However, results in the urban environment were subject to large errors. Further complications involved the signal propagation. Medium Wave signals are affected by sky-wave propagation at night which means that signals can "bounce" between the bottom layer of the Ionosphere (known as the D-layer) and the ground, hence travelling further and along a non-direct path. To counter this, some MW stations do

not transmit at night, or do so at a reduced power level. However, for positioning using the carrier phase, this adds large errors to the integer ambiguity.

A subsequent paper by the author (Hall, 2004) discusses these signal propagation problems faced and the modelling techniques involved to mitigate these as much as possible.

Also in the MW radio band, (McEllroy, 2004) used the Universal Software Radio Peripheral (USRP) to measure TDOA transmissions using one receiver as a reference base station and a second as a rover. McEllroy encountered difficulties in the data link between the two USRP receivers due to clock synchronisation issues (one example of which involved a 17 second straight line movement travelling 13 metres, whilst the measurements indicated a distance of 16000km!). This was mainly due to the limitations of the RF front end used with the USRP which was not able to capture and digitise the entire band, unlike Hall's experiments.

3.4.2 Analogue/Digital Television

Digital and analogue US television sources (ATSC & NTSC respectively) were used for both an outdoor and indoor positioning system by (Rabinowitz and Spilker, 2005). These signals use a single frequency network, therefore the synchronisation block of the signal was used to obtain a position estimate using a TOA approach. Another advantage of ATSC is that it is a wideband signal (6MHz or greater), allowing for much improved propagation in urban environments and mitigation of multipath.

3.4.3 Digital Audio Broadcasting (DAB)

The use of Digital Audio Broadcasting (DAB) for positioning was investigated by (Layer et al., 1998) to provide rough position estimates in DAB Single Frequency Networks (SFNs) in Germany. The German DAB system operates in the L-band portion of the spectrum as opposed to the Band III portion used in the UK. Two approaches were used for position determination. The phase shift between pairs of

carrier waves (spaced by 1kHz), and the evaluation of the channel impulse response. These pieces of information allowed the inter-arrival times of signals from each transmitter to be found and hence the estimated position of the receiver.

An integrated positioning system using DAB and the Global System for Mobile Communications (GSM) was modelled by (Rooney et al., 2000). As DAB and GSM systems are not synchronised as an integrated system, a TDOA approach was used with the synchronised DAB network. GSM positioning works better in urban areas due to the number of transmitters; however it suffers in low-population areas because of fewer transmitters. The objective was that DAB positioning could fill in the gaps where GSM positioning was unavailable.

Due to the completely different technologies involved (GSM – Narrowband and non-synchronised and DAB – Wideband and synchronised), the two technologies were seen to mitigate each other's weaknesses to a certain degree, DAB to work in more remote areas, GSM in the urban environment. As the GSM network is not synchronised, this portion of the system involved a data link to local transmitters using the SMS service.

3.4.4 Global System for Mobile Communications (GSM)

In 2006, (Varshavsky et al., 2005) discussed that GSM phones can be used as an adequate positioning system to within an accuracy of 5 to 75 metres in both indoor and outdoor environments. The authors claim this by testing two different algorithms (FingerPrinting and Centroid) with GSM and Wi-Fi localization systems to capture the signature of RF frequencies around an environment during a 'training phase'. These signatures then form the basis of a model by which to navigate. Problems naturally occur with this technique due to the change of infrastructure and more importantly, the dynamic environment within an urban landscape. Limitations also arise as the receiver is unable to navigate in an environment in which it has not been before.

3.4.5 Other Signals

Other signals of interest which have been examined for positioning purposes include Wi-Fi (Akiyama et al., 2009), WiMax (Jiao et al., 2008), Bluetooth (Hallberg et al., 2003) and Ultra-wideband (Schroeder et al., 2005). However, due to the high frequency of these and similar signals (>2.4GHz), their range is strictly limited. Using Wi-Fi as an example, a wireless router has a maximum range of 100's of metres. Whilst within the urban environment, Wi-Fi 'hotspots' overlap to a certain degree, these cannot always be guaranteed. Additionally, the exact locations of Wi-Fi hotspots are not generally publicly known, making it extremely difficult to create any sort of timing positioning system by hopping from network to network.

Bluetooth is another two-way communications device designed for even shorter range than Wi-Fi, therefore this makes the signal an unfeasible choice for this project. A more wide-scale approach is taken with a more recent technology called WiMax - a long range system designed to operate over 10's of kilometres. There is also a South Korean equivalent system called WiBro. Due to the current lack of WiMax/WiBro systems in operation, particularly in the UK, this system would be better examined in future work.

Ultra-wideband (UWB) is another short-range communications technology. UWB devices work in the region 3.1 to 10.6 GHz. A small number of UWB positioning systems currently exist. UbiSense (Ward, 2007) and Thales (Ingram et al., 2004) have both developed UWB positioning systems for use indoors or for deployment at emergency scenarios. These systems have been developed for short-range positioning, and require the presence of additional infrastructure.

Finally, Radio-frequency identification (RFID) positioning (Wang and Shen, 2002) involves the use of a transponder located on a person or object which can then be tracked using a series of detectors. However, the object to be tracked must be within

several metres of the detectors with the added complexity of the infrastructure involved making this technology also unfeasible.

3.5 SUMMARY OF SIGNALS

Table 1 shows an overview of both the navigation and non-navigation radio signals discussed in this chapter.

Signal/System	*Propagation Method*	*Approximate Range (km)*	*Synchronised Network?*	*Additional Infrastructure Required?*	*Passive/Active Receiver*
LORAN	Groundwave	2000	Yes	No	Passive
Datatrak	Groundwave	150	Unknown but likely	Commercial receiver required	Passive + optional data link
AM - Longwave	Groundwave	2000	No	No	Passive
AM - Mediumwave	Groundwave (Skywave – night)	500 1000+	No	No	Passive
AM - Shortwave	Skywave	1000+	No	No	Passive
FM/RDS	Line of sight	See note*	No	No	Passive
DAB	Line of sight	See note*	Yes	No	Passive
DVB-T	Line of sight	See note*	Yes	No	Passive
GSM & equivalent	Line of sight	See note*	No	No	Active
Wi-Fi	Line of sight	See note*	Either	Dependent on coverage	Active
Bluetooth	Line of sight	See note*	No	Yes	Active
WiMax/WiBro	Line of sight	See note*	Yes	Yes	Active
Ultra-wideband	Line of sight	See note*	Yes	Yes	Active
RFID	Line of sight	See note*	System dependent	Yes	Either

** Line-of-sight range depends on height of transmitting antenna + output power*

Table 1: Summary of Signals

Whilst a range of non-navigation signals have been examined, only two of these signals fulfil the criteria required for this investigation:

- No additional infrastructure required
- Synchronised transmitters, for standalone positioning
- Signal propagates on a line-of-sight basis to avoid sky-wave/ground-wave issues (discussed in section 3.6)

These two signals as highlighted in Table 1 are the DVB-T and DAB signals. As DVB-T had already been investigated to the point of a commercial system being available, the choice was made to investigate DAB further as a potential positioning source.

3.6 SIGNAL PROPAGATION

Radio signals propagate in different ways depending on the frequency they are broadcast in. There are three main ways in which signals can propagate from transmitter to receiver (Rohan, 1991):

3.6.1 Ground-wave

Ground-wave propagation affects signals broadcast below 2MHz, such as Long Wave and Medium Wave AM radio and eLORAN. In this case, the signal path from the transmitter to receiver is distorted such that it follows the curvature of the Earth's surface (Connor, 1972) (Anderson, 1986).

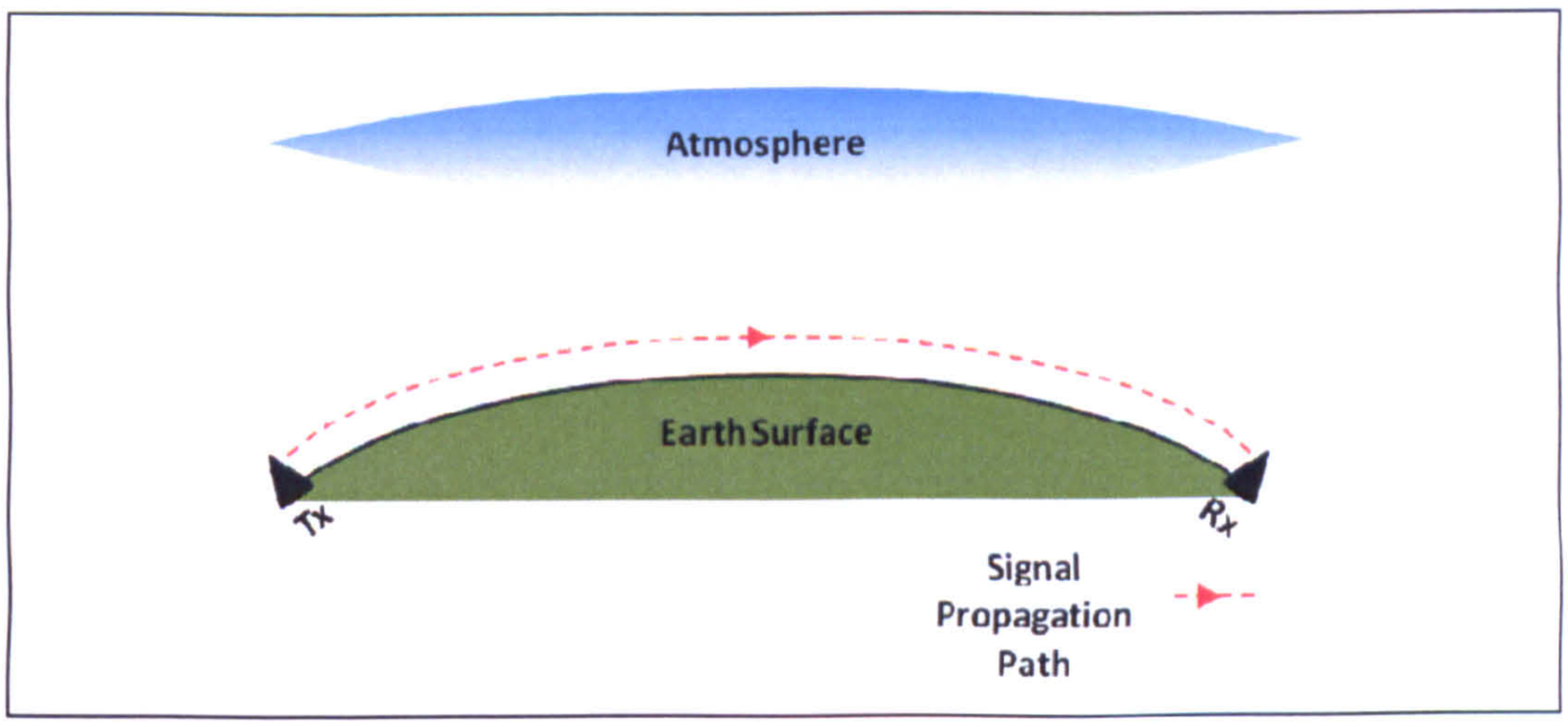

Figure 3-1: Ground-wave Propagation

3.6.2 Sky-wave

Sky-wave propagation affects signals in the High Frequency band (between 3 – 30MHz), which includes the Shortwave AM radio band. The signal is affected by refracting off of the ionosphere and thus creates a delaying effect between the true signal and the secondary signal being slowed and refracted by the atmosphere. This kind of propagation means that signals can be received from much further afield than intended and this can cause problems with inter-symbol interference (ISI) and interference with stations broadcast on the same frequency in different countries (Wang, 1995) (Connor, 1973).

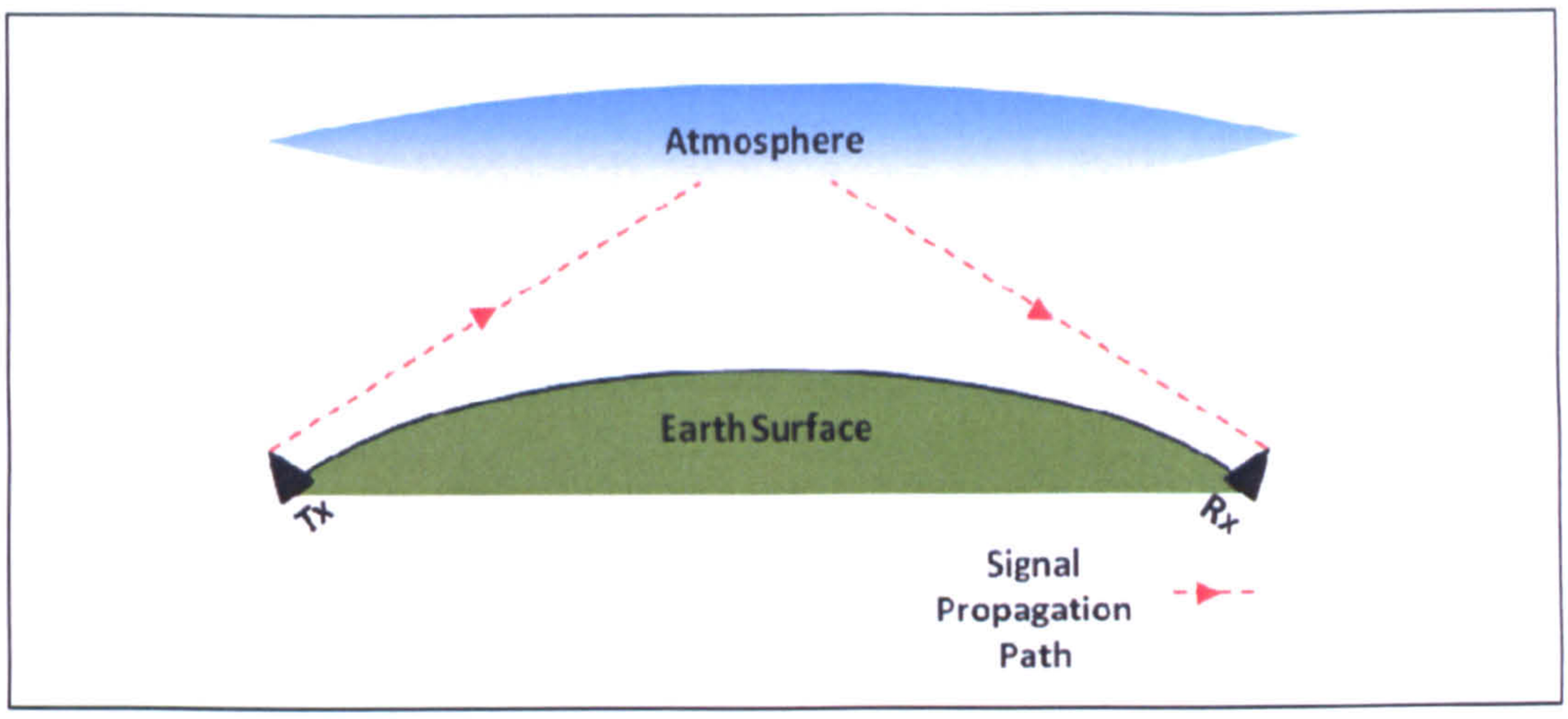

Figure 3-2: Sky-wave Propagation

3.6.3 Line-of-Sight (Spacewave)

Line-of-sight or Spacewave propagation affects signals transmitted above 30MHz (including VHF/UHF bands, FM radio broadcasts, DAB, DVB etc). This means that a receiver antenna must be 'visible' to the transmitter in that the transmitting antenna must not be below the horizon. This transition line between the two antennas is the maximum distance that the signal may travel.

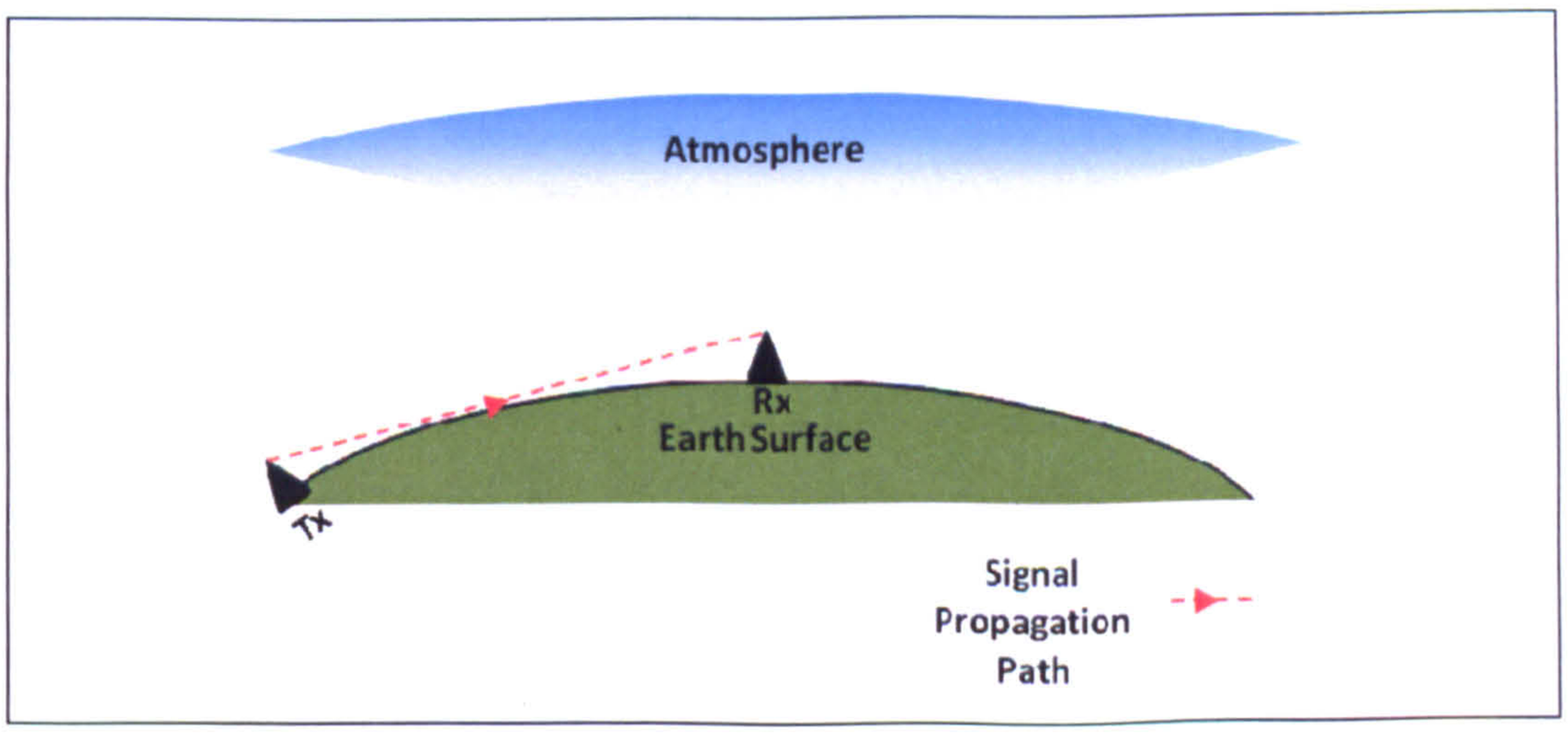

Figure 3-3: Line-of-Sight Propagation

3.6.4 Fresnel Zone

The Fresnel Zone is a hypothetical region which lies between a transmitter and a receiver when examining a signal propagating by Line-of-Sight (Anderson, 1964).

This region is described by a series of ellipsoids, the foci of which are situated at the transmitter and receiver. The region was examined during the early roll-out of the Eureka-147 system (European DAB standard) (Grosskopf, 1995) to establish the signal strength at locations where large obstacles may obstruct the direct Line-of-Sight line between transmitter and a receiver. The diagram in Figure 3-4 shows the basic concept of the Fresnel Zone.

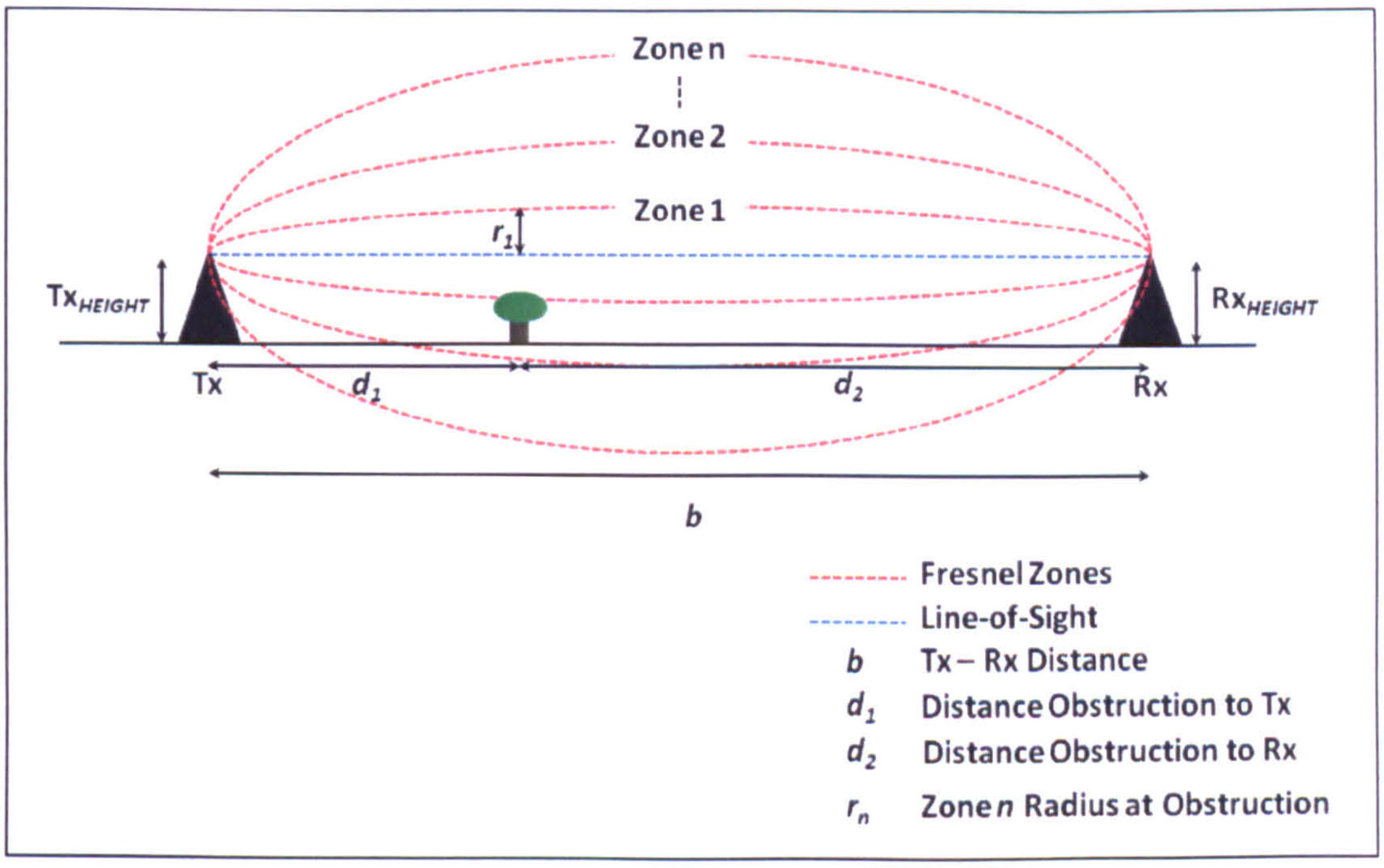

Figure 3-4: Fresnel Zones

The n^{th} Fresnel Zone radius (r_n) may be found from equation 3.1:

$$r_n = \sqrt{\frac{n\lambda d_1 d_2}{d_1 + d_2}} \qquad 3.1$$

Where λ is the wavelength of the signal of interest.

3.6.5 Path-Loss Models

Any signal in transit will, over distance, lose an amount of power depending on the density of the landscape over which it travels. In (Abhayawardhana et al., 2005), the authors compare three models in order to be able to predict this path loss based on a

number of factors. The models used in this case were the ECC-33 Model, the Stanford University Interim Model and the COST-231 Hata Model.

The Hata Path-Loss Model was originally devised by (Hata, 1980) and then improved upon to become the COST Hata Model as a result of the COST 231 meeting (Damosso and Correia, 1999). This showed that the signal propagation was based upon:

- the frequency of the broadcast
- the distance from transmitter to receiver
- the height above sea level of both transmitter and receiver
- the density of the landscape the signal travels through

Using these parameters, the following formula was devised to calculate the median path loss (dB) for an urban environment:

$$L_{URB} = 69.55 + 26.16\log f - 13.82\log h_B - C_H + [44.9 - 6.55\log h_B]\log d \qquad 3.2$$

Where the receiver antenna height correction factor C_H is defined as:

$$C_H = 3.2(\log(11.75h_R))^2 - 4.97 \qquad 3.3$$

- f = frequency of the transmission (MHz) – (where $200 < f \leq 1500$)
- h_B = height of the transmitter (metres)
- h_R = height of the receiver (metres)
- d = distance between transmitter and receiver (kilometres)

Equations 3.2 and 3.3 differ depending on the environment the signal is travelling through. Using the same definitions as for urban environments, the path-loss for suburban areas (L_{SUR}) is defined as:

$$L_{SUR} = L_{URB} - 2\left(\log\frac{f}{28}\right)^2 - 5.4 \qquad 3.4$$

Where L_{URB} represents the average value of the calculated path loss in 3.2.

Finally, the equation developed in the same report for open/rural areas (L_{RUR}) is defined as follows:

$$L_{RUR} = L_{URB} - 4.78(\log f)^2 + 18.33\log f - 40.94 \qquad 3.5$$

These path loss equations allow the calculation of the distance a signal travels over the Earth's surface.

3.6.6 Gaussian Noise

Gaussian noise (or White noise) is a statistical noise measurement, being simply noise on the communication channel between the transmitter and a receiver, the frequency distribution of which follows a normal (Gaussian) distribution. Such noise can be caused by any number of natural sources, such as solar radiation.

3.6.7 Summary

This section has shown the different types of signal propagation and the effects they can have on signals broadcast at certain wavelengths. The most important effects which affect this project are the Hata Path-Loss Models and the Fresnel Zone effect, due to the wavelengths at which the DAB signal is broadcast. The Hata models will be shown in use later in this thesis when the coverage of the DAB networks in the UK is examined, and the areas of the country where insufficient transmitters are present can be found.

4 THE DAB SIGNAL

This chapter will introduce the basic elements of the DAB signal, where it has been deployed as a transmission system worldwide and identify the parts of the signal which have the potential to be used for positioning purposes.

4.1 INTRODUCTION

The Digital Audio Broadcast (DAB hereafter) standard was developed in Europe in the 1980's as part of the Eureka-147 project, in order to combat the variety of problems associated with FM broadcasts (fading, interference, multipath etc), particularly when a receiver is mobile (Hallier et al., 1994) (Rau, 1995). The system was designed to be far more spectrally efficient than the FM standard, as numerous stations could be broadcast simultaneously on a single frequency without the need to retune the receiver (European Broadcasting Union, 1997). The signal could also carry a certain amount of multimedia content, greater than the RDS system used by FM transmissions. The audio quality was designed to be near CD quality at the time, although this came under criticism in more recent years, and paved the way for a more robust so-called DAB^{+} system design (European Broadcasting Union, 2007).

Figure 4-1: The DAB Logo

(The 'DAB Digital Radio' logo and the stylised 'r' mark ® and © Digital One Limited.)

4.2 DAB COVERAGE

The UK has one of the most widely deployed DAB networks currently and the two main network operators, Digital One (Commercial) and the BBC claim to have coverage of better than 85% of UK population (Emery, 2009) at the time of writing, with the BBC committing its coverage to increase to 90% (BBC, 2009).

Country	Status	Coverage (% Population)
Australia	DAB/DAB+ Trials	15
Belgium	DAB Launched	100
China	DAB Launched; DAB$^+$ Trials	8
Denmark	DAB Launched	90
France	DMB Launched*	20
Germany	DAB Launched; DAB$^+$ Trials	82
Ireland	DAB Trial	44
Italy	DAB/DAB+ Trials	75
Netherlands	DAB Launched	70
Norway	DAB Launched	80
Singapore	DAB Launched	99
South Korea	DAB Launched	75
Spain	DAB Launched	52
Switzerland	DAB Launched	90
United Kingdom	DAB Launched	85

**** DMB = Digital Multimedia Broadcasting***

Table 2: Worldwide DAB/DAB+/DMB Coverage (January 2009)

Further afield, the countries listed in Table 2 have adopted the DAB standard as of January 2009 and begun deployment (Pedersen, 2009) (a number of other countries have adopted the standard but have either not begun building the infrastructure or have minimal coverage at present).

4.3 DAB SYSTEM

4.3.1 System Clock

All units in the DAB system are derivations of the system clock frequency. DAB runs on a fundamental frequency of 2.048 MHz, from which the fundamental unit ***T*** can be defined as in ***4.1***:

$$T = {}^{1}/_{2.048 \times 10^{6}} \qquad 4.1$$

The unit ***T*** represents a measurement of time of around 0.48828μs. For the remainder of this document, this unit will be principally used when referring to periods of time.

4.3.2 DAB Transmission Modes

The DAB signal may be transmitted in any one of four transmission modes (I – IV). These modes and their primary characteristics are listed in Table 3 recreated from (European Broadcasting Union, 1997).

Mode	Carriers *(K)*	Maximum Transmission Freq
I	*1536*	*375 MHz*
II	*384*	*1.5 GHz*
III	*192*	*3 GHz*
IV	*768*	*750 MHz*

Table 3: DAB Transmission Modes

In the UK, Mode I is the terrestrial transmission mode used and will be the only mode referred to throughout the remainder of this document. The mode was designed for large-area coverage as it has a long guard interval allowing the effects of long-delayed

secondary or multipath signals to be removed. Mode II is mostly used in L-band transmissions, whilst Mode III is primarily used for satellite transmissions.

4.3.3 Broadcast Frequencies

In the UK, the VHF Band III portion of the spectrum is subdivided into a number of channels or blocks which are used by DAB in the UK and Europe. The UK currently uses seven active blocks, detailed in Figure 4-2, giving a total frequency range of just over 10MHz. Further blocks are used to test additional services and these may be used for full-time transmissions in the future.

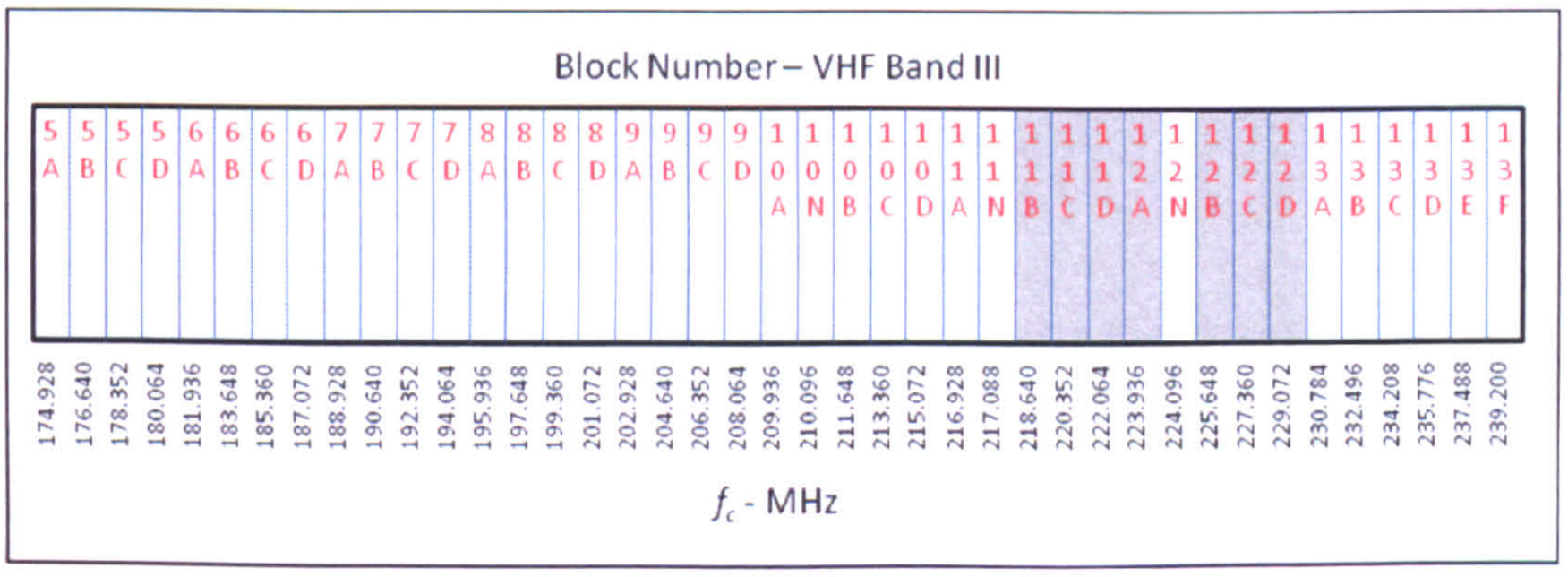

Figure 4-2: DAB Block/Channel Locations in VHF Band III

4.4 DAB Signal Structure (Frequency Domain)

The DAB signal in the frequency domain uses a Coded Orthogonal Frequency Division Multiplexing (COFDM) technique as the primary means of signal modulation (European Broadcasting Union, 1997). This technique was chosen as it was a rugged means of transmission for mobile receivers, such as vehicle entertainment systems (Shelswell, 1996).

COFDM modulation uses a large number of closely spaced frequency divided sub-carriers (or sinusoids) to create a wideband signal. In the case of the DAB standard, there are 1536 sub-carriers spaced at 1 kHz intervals plus one suppressed central

carrier, see Figure 4-3. Each of these 1536 individual sub-carriers is then additionally modulated by Differential Quadrature Phase Shift Keying (DQPSK). As the information transmitted is spread over the width of the wideband signal, each individual carrier modulates slowly relative to narrowband signal modulation. The width of the signal also helps to mitigate any fading that might be present. Although fading may occur and obscure a portion of the signal, information may still be relayed through the remainder of the spectral width.

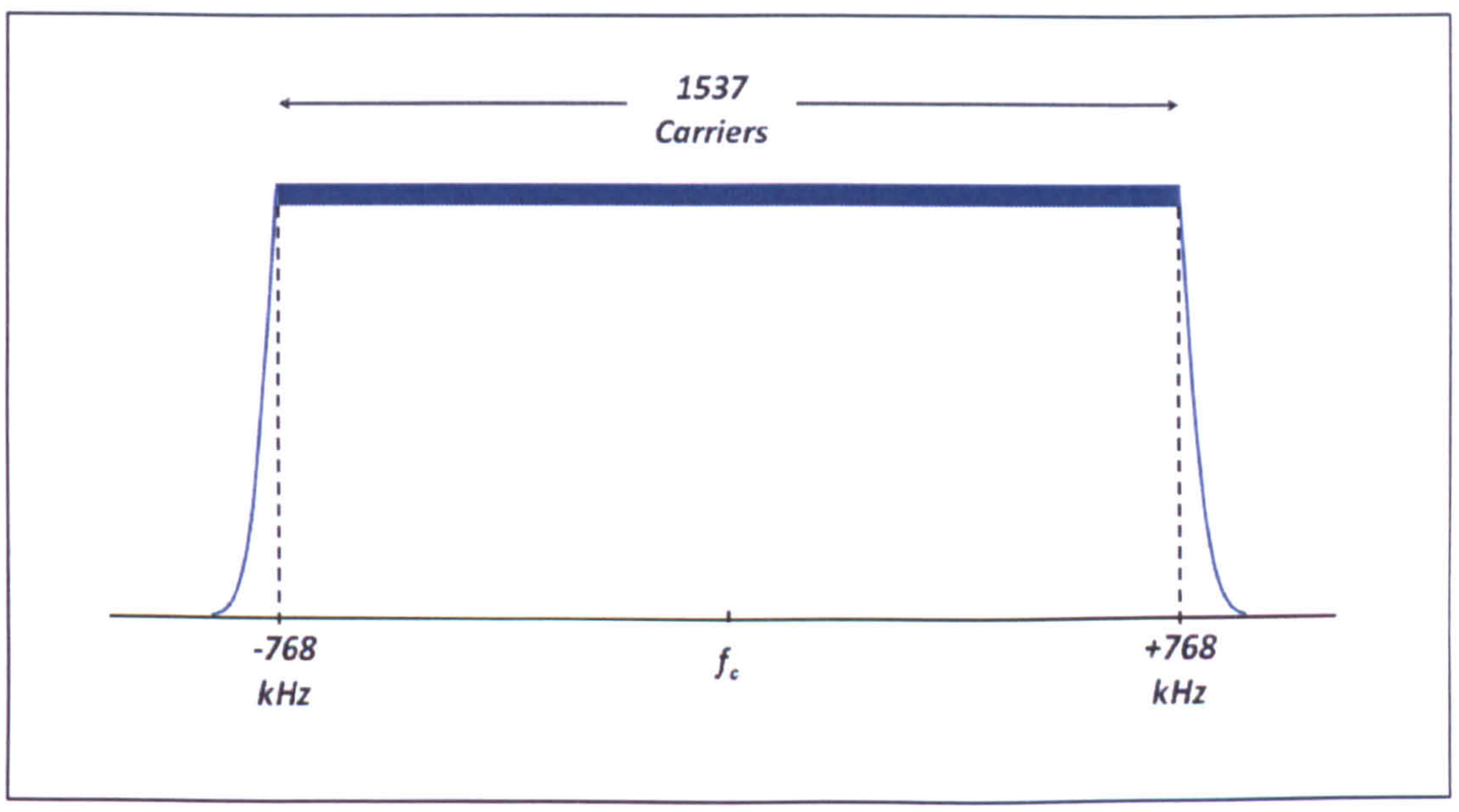

Figure 4-3: DAB signal structure in the frequency domain highlighting the signal width and central frequency f_c

As was mentioned previously, each of the subcarriers is sub-modulated by the DQPSK technique. This digital encoding technique will now be described as it will become important later in the document.

Digital information is broadcast by the modulation of a basic sine wave signal, which can be defined as follows with the amplitude A_c, the frequency f_c, the time t and the phase φ in equation 4.2:

$$A_c \cos(2\pi f_c t + \varphi) \qquad \textbf{4.2}$$

This can be expressed graphically in Figure 4-4, which shows the state of a sine wave at a point in time *t* using a Polar coordinate system.

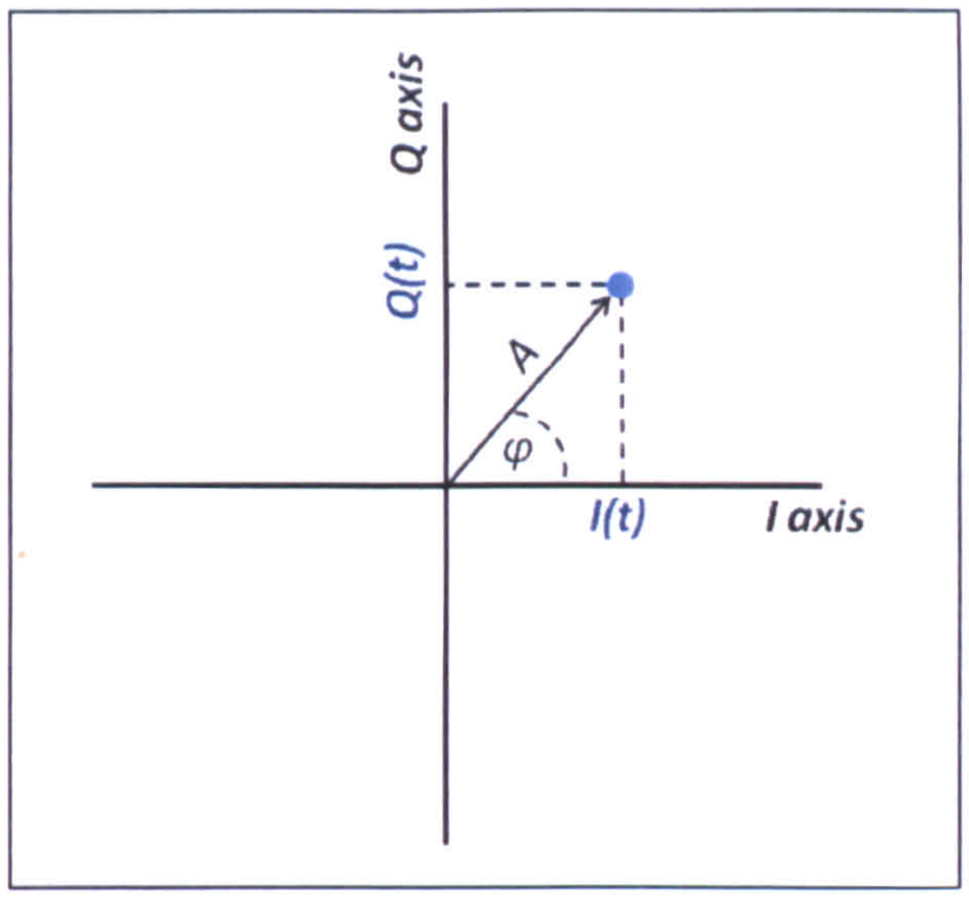

Figure 4-4: Description of the I and Q planes

The length of the arrow represents the amplitude of the wave, and the angle of the arrow is the relative phase φ at time *t*. The I and Q planes can be thought of as a conversion of the Polar coordinate system (amplitude and phase) into a Cartesian coordinate system, with the I value the intercept on the horizontal axis and the Q (complex) value the intercept on the vertical axis. The example in Figure 4-4 would have an I value of $I(t) = A(t)\cos(\varphi(t))$ and a Q value of $Q(t) = A(t)\sin(\varphi(t))$.

By breaking down DQPSK into two areas, the Quadrature Phase Shift Keying aspect is examined first. The binary data is modulated by changing (shifting) the phase of the subcarrier by either 0°, 90°, 180° or -90° (as opposed to just 180° as used in Binary PSK) giving any one of four states for the phase to be in. To show this comparison in diagrammatic form, Figure 4-5 shows the I and Q maps of both BPSK and QPSK signals respectively.

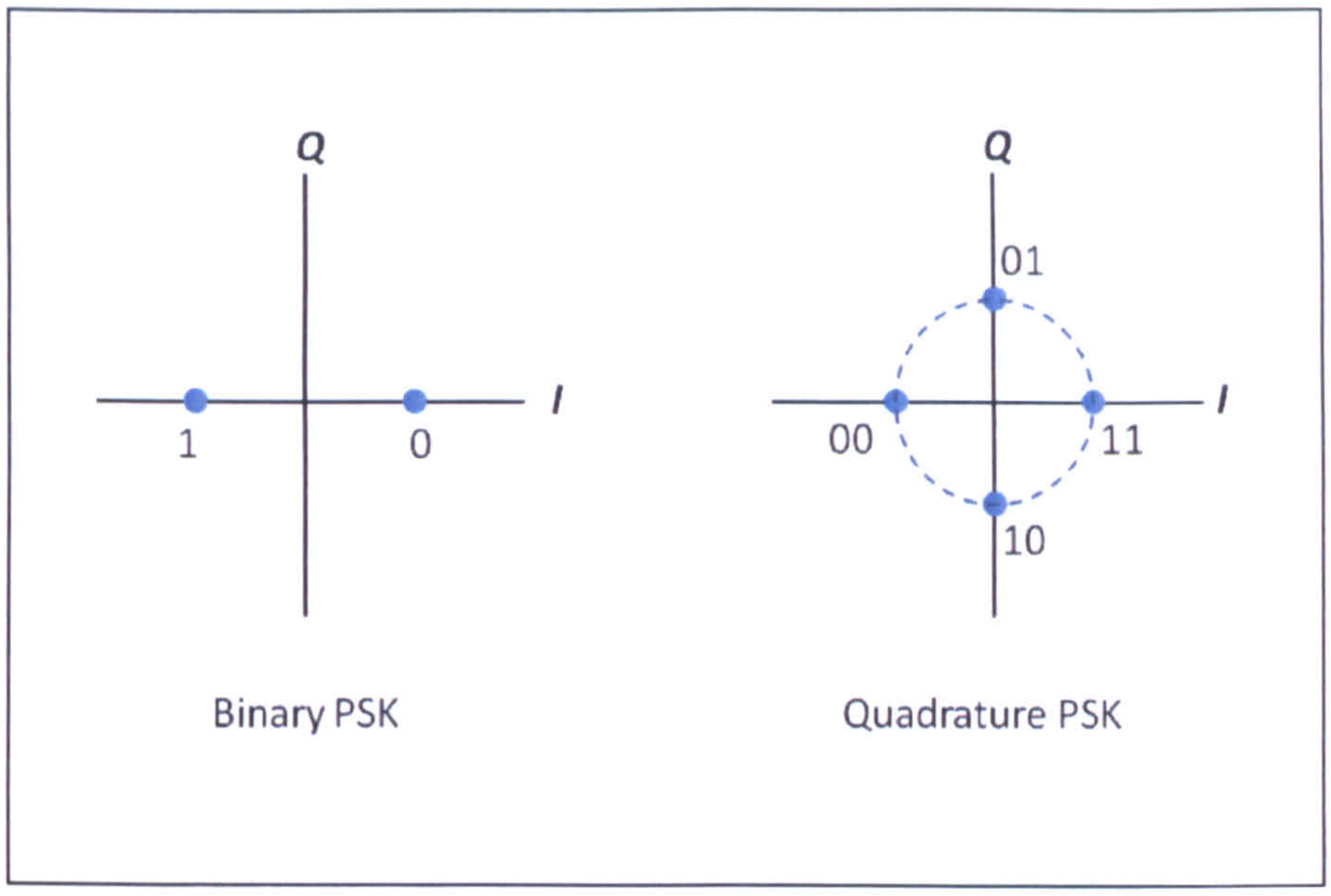

Figure 4-5: Comparison of BPSK and QPSK in the IQ planes

Where BPSK delivers only 1 bit per symbol, QPSK delivers 2 bits. The Differential aspect of the modulation means that rather than each of the four states having a set value of 00, 01, 10 and 11, the shift is relative to the current state with the sequence starting at 0° phase shift. For example, in Figure 4-6 the three modulation schemes are examined modulating the same baseband message on a simple sine wave (as QPSK and DQPSK schemes have 2 bits/symbol, the message is delivered in half the time). The DQPSK scheme, although beginning the sequence identically to QPSK at +90° position (01), shifts its second symbol through +90° again (to +180° position - 11), whilst the QPSK signal remains at the +90° (01) position. Although requiring slightly more computation due to the decoder having to constantly compare the current and previous symbols, this creates a more robust signal structure when transmitted through a physical communications channel.

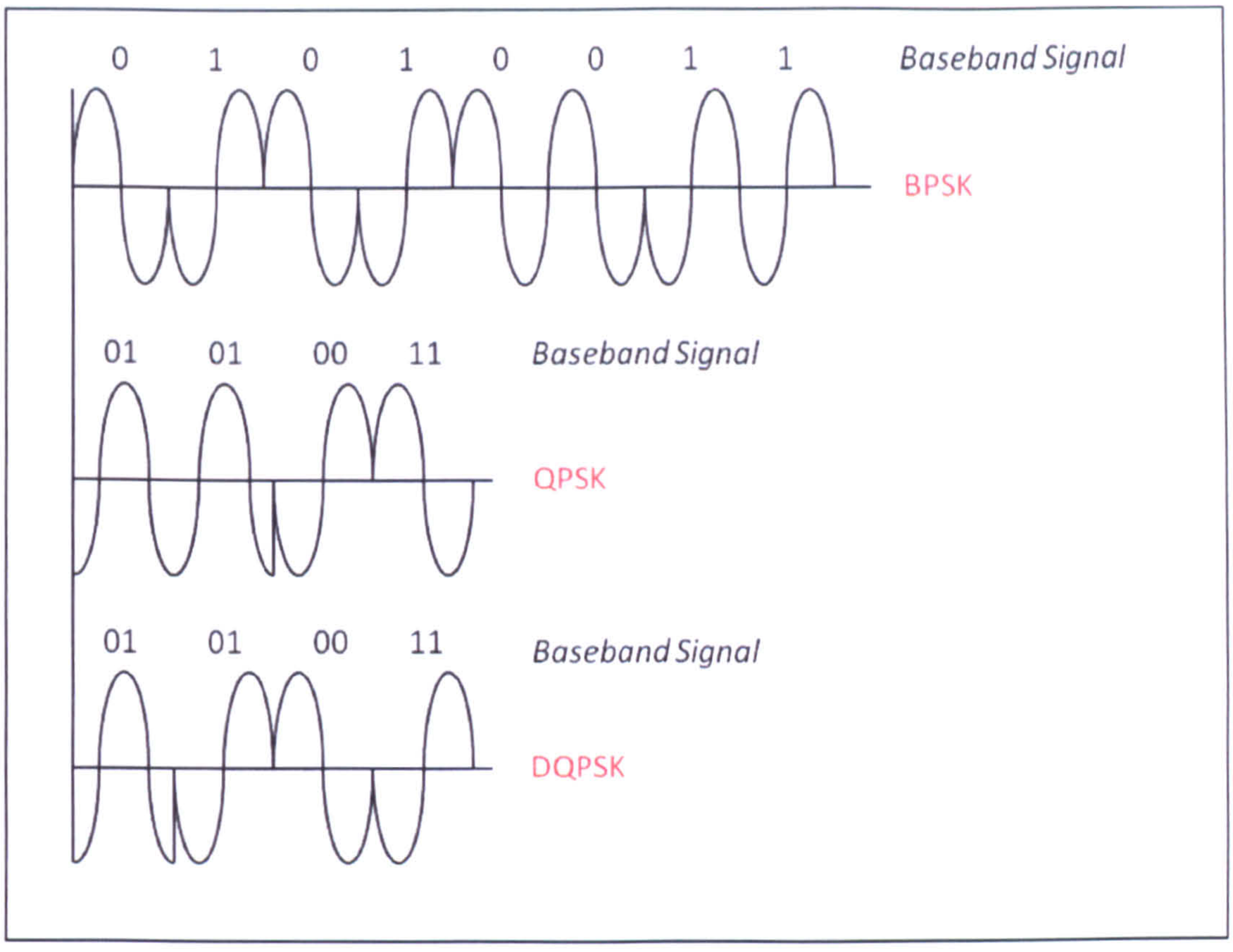

Figure 4-6: Comparison of BPSK, QPSK and DQPSK

Broadcasting the same baseband signal, note that QPSK and DQPSK messages broadcast in half the time of the BPSK signal

4.5 DAB SIGNAL STRUCTURE (TEMPORAL DOMAIN)

The DAB signal in the time or temporal domain is segmented into frames, each of which is subdivided into three main channels which are broadcast in sequence. Each DAB frame is broadcast over approximately 96ms, giving a frame-rate of roughly 10 frames/second. The individual channels are all, with the partial exception of the Synchronisation Channel, subdivided into groupings of OFDM symbols. An OFDM symbol is composed of two parts, a useful symbol portion and a Guard Interval or Cyclic Prefix, (see Figure 4-7). The useful symbol contains all of the information the receiver requires, whilst the Guard Interval is composed of a duplicate of the final section of the useful symbol of length (504T) which is then appended to the front, creating a total symbol length of 2552T (Hoeg and Lauterbach, 2003).

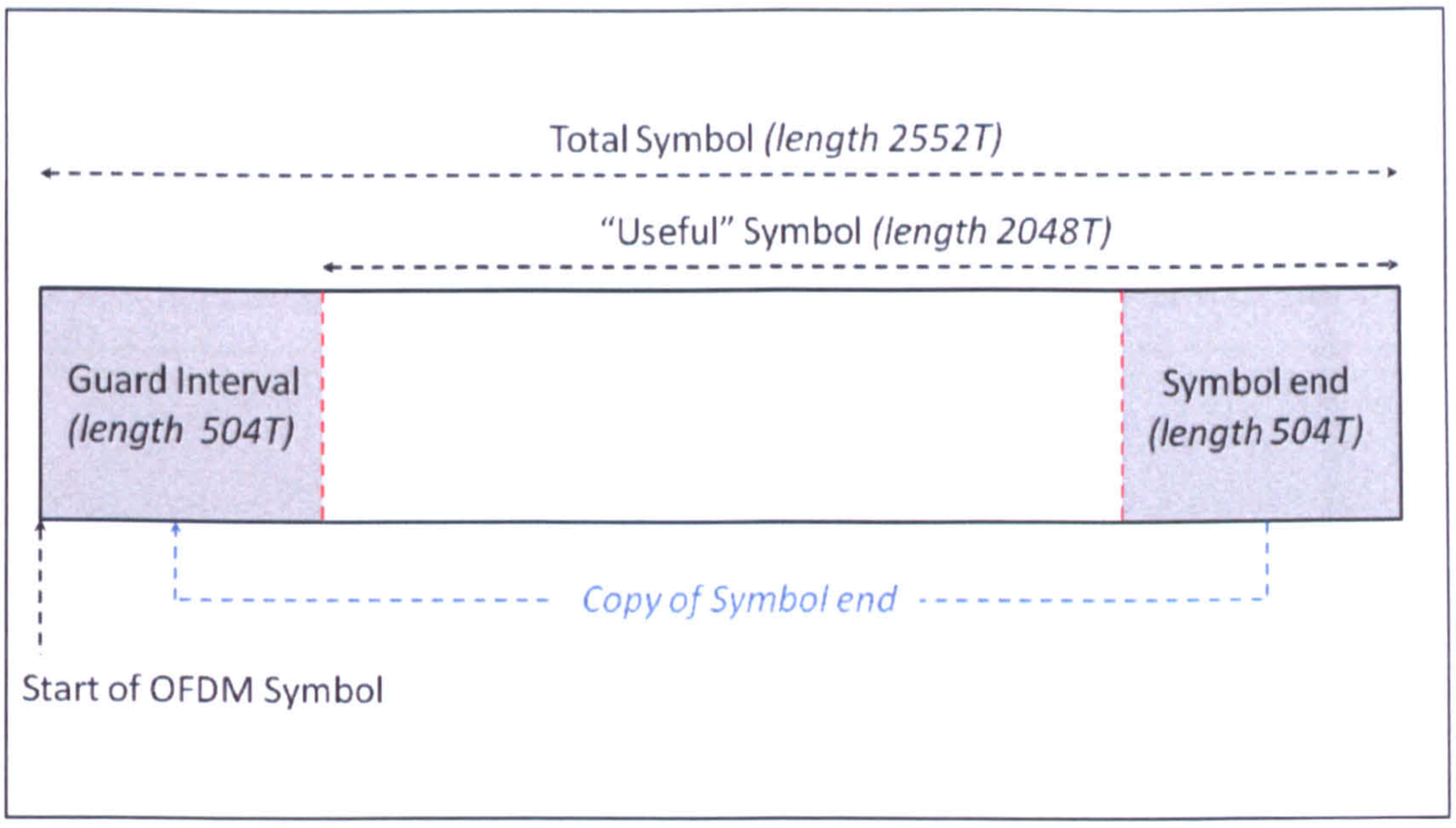

Figure 4-7: Composition of an OFDM Symbol in the temporal domain

Each of the three channels which compose a DAB frame will now be briefly examined in turn. Although only one channel is used for the remainder of this thesis, a high-level breakdown of each is presented for completeness.

4.5.1 The Synchronisation Channel (SC)

The first of these channels is the Synchronisation Channel. This is the shortest channel in the frame and is composed of two parts (Figure 4-8). The frame begins with a null or zero period, when all of the subcarriers are switched off - with the exception of every second frame - in order to provide an easily locatable (providing the signal is strong enough) yet approximate start of the frame. In every other frame, the null symbol is populated with very simple codes known as Transmitter Identification Information (TII) codes. These codes allow a receiver to unambiguously identify the region it is currently in and the transmitters it is receiving. This information becomes vital later on when discussing the positioning characteristics of the signal as a whole. The second part of the channel is the first OFDM symbol in the frame and is known as the Time Frequency Phase Reference (TFPR) Symbol. This symbol allows the receiver to precisely find the position of the

beginning of the second channel and align the decoder to find the first and subsequent DQPSK symbols.

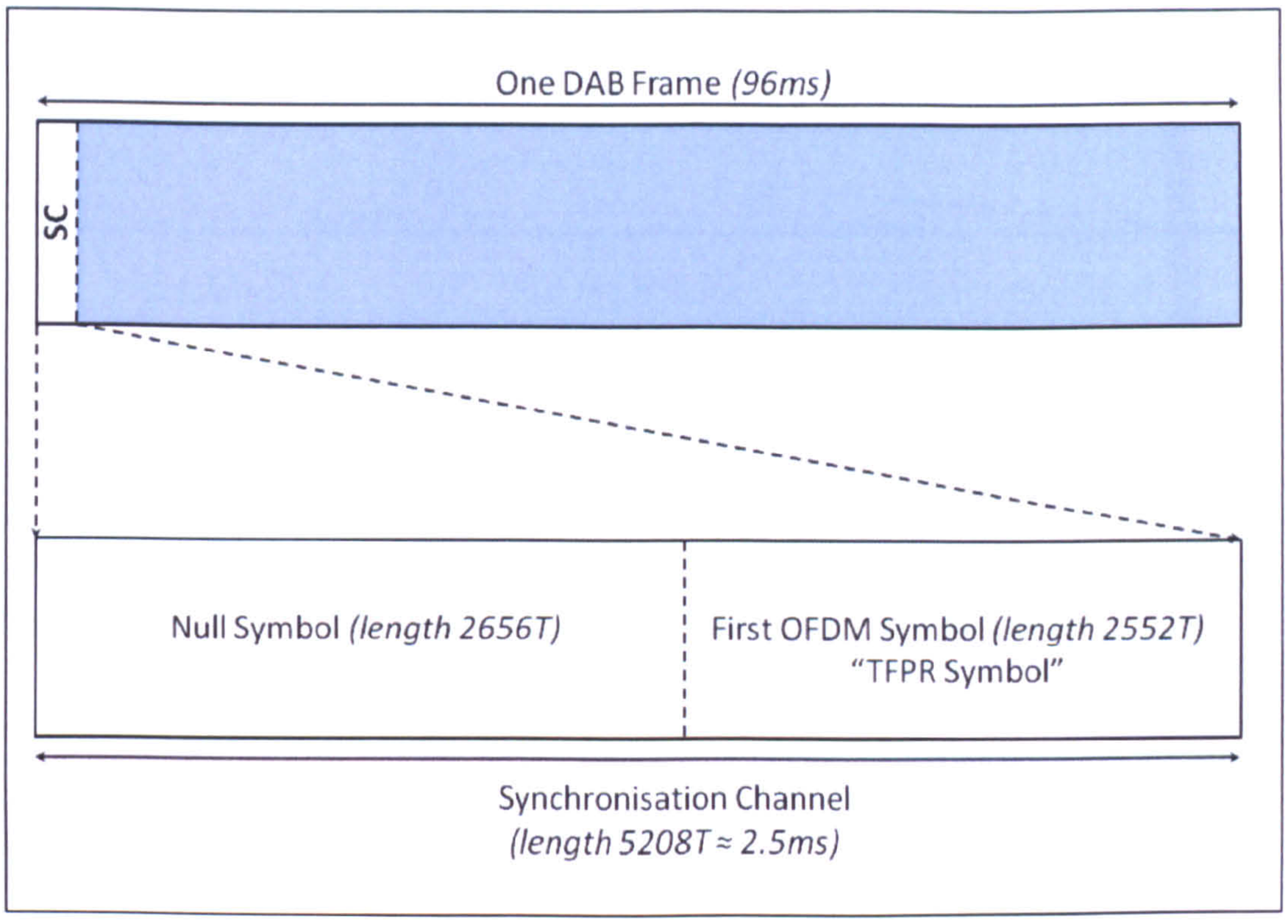

Figure 4-8: Composition of the Synchronisation Channel

4.5.2 The Fast Information Channel (FIC)

The Fast Information Channel is the second channel. This is composed of three OFDM symbols which are in turn broken down into Fast Information Blocks (FIBs). As the receiver requires this information instantly in order to understand the multiplex configuration of the Main Service Channel, this part of the signal is not time interleaved. The Fast Information Blocks are further broken down into groups (Fast Information Groups) which can be distinguished by field codes in order to decode a variety of different pieces of information about the current multiplex.

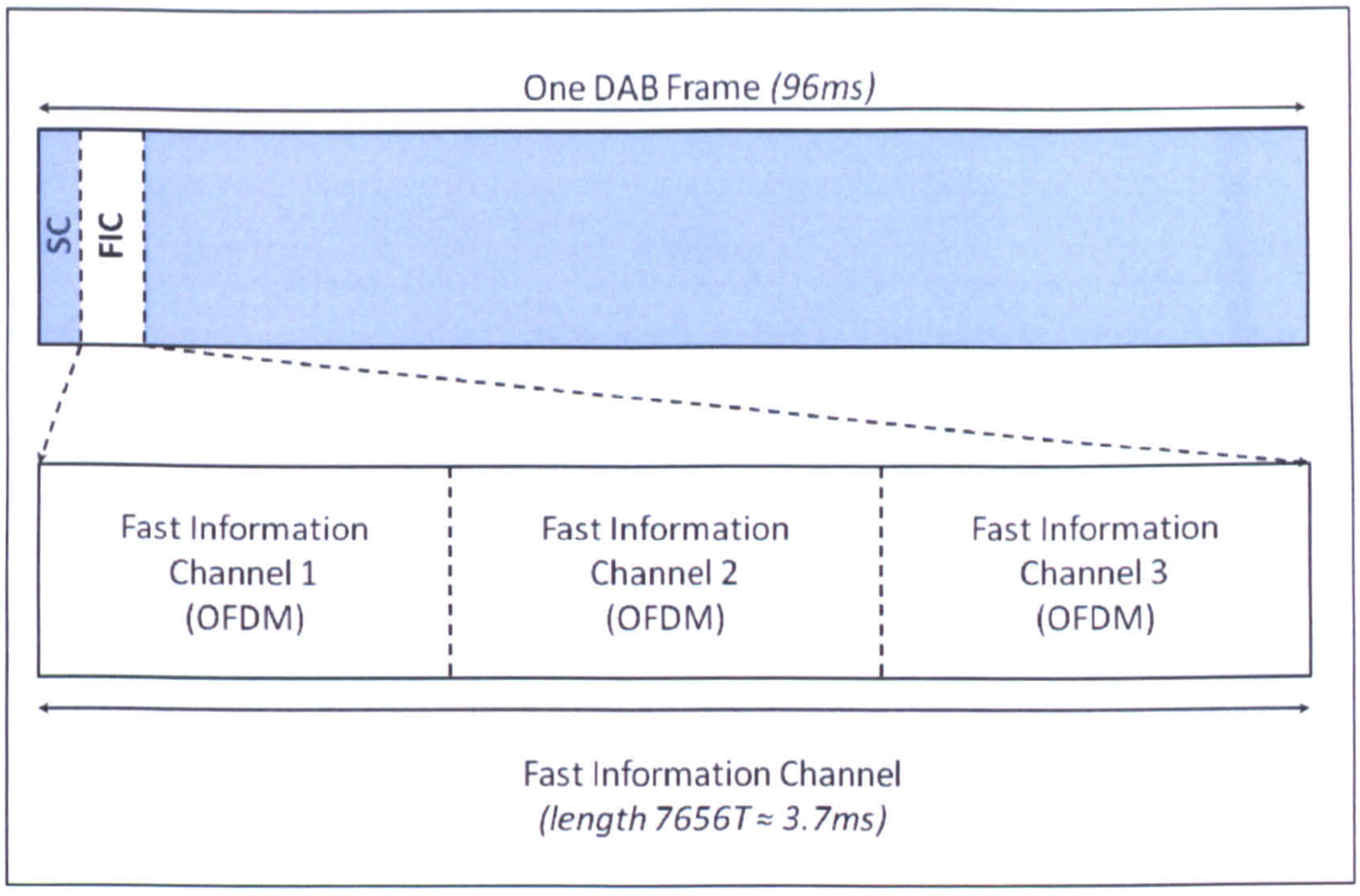

Figure 4-9: Composition of the Fast Information Channel

4.5.3 The Main Service Channel (MSC)

The Main Service Channel is the third and final channel and is composed of the programming data. It is made up of 72 OFDM symbols, each of which is broken down into Common Interleaved Frames (CIFs). The CIFs are closely linked by the FIBs in the Fast Information Channel (see 4.5.2). The capacity of the channel can vary considerably depending on the number of stations being broadcast in the multiplex, the quality of the audio and the quality of the error correction coding. The MSC is the only channel to have time and frequency interleaving.

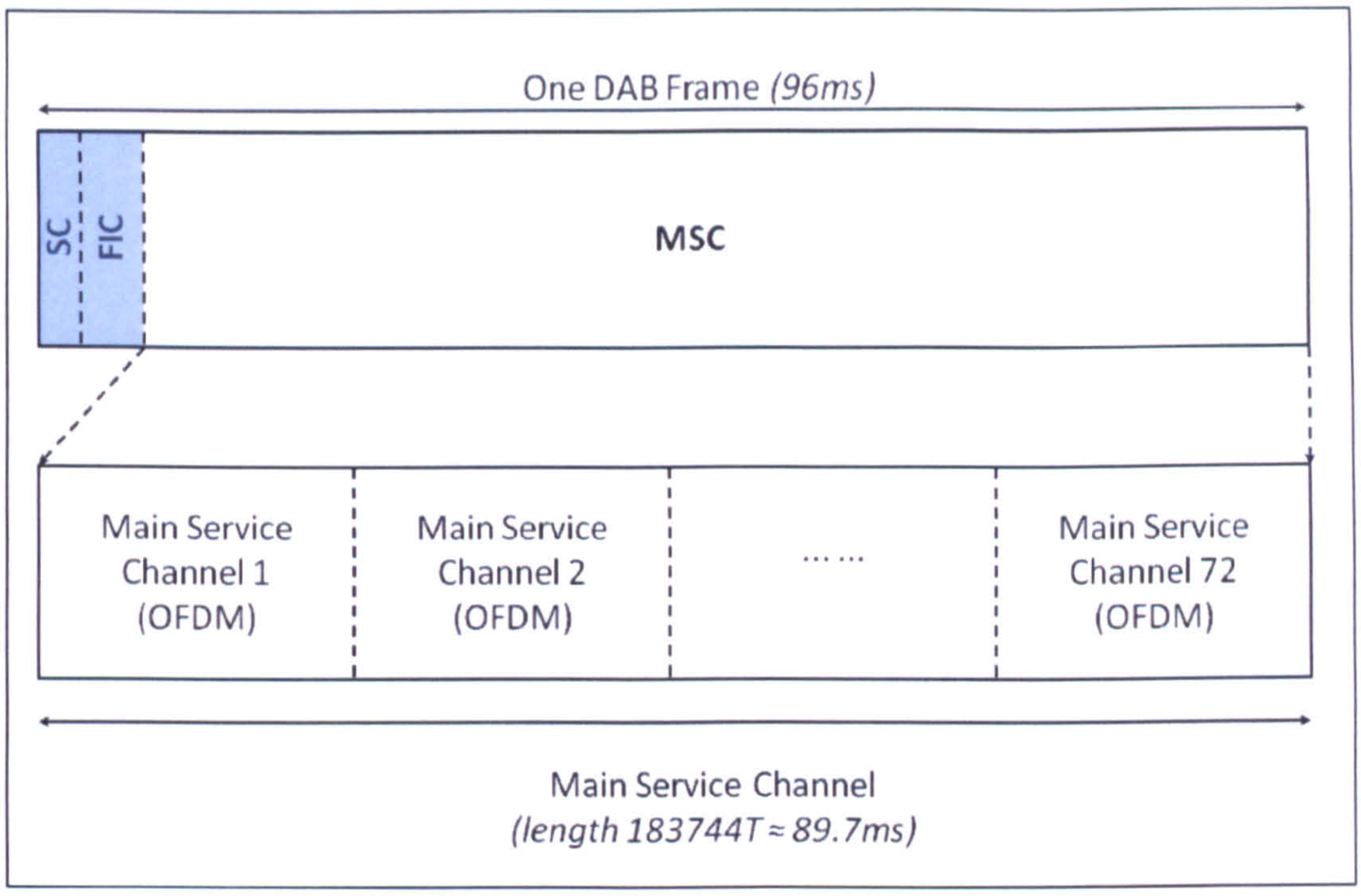

Figure 4-10: Composition of the Main Service Channel

4.6 SINGLE FREQUENCY NETWORKS

The DAB signal is delivered over what are known as Single Frequency Networks (SFNs) (Liebenow and Zimmermann, 1998). These networks consist of a number of transmitters, all of which are synchronised by GPS time giving an accuracy of 300ns or better for the majority of the time (Evans and Baily, 1997). During periods of prolonged GPS outage, the synchronisation of the transmitter clocks falls to approximately 1μs (M. Ellis, pers. comm.). This allows a DAB channel to be broadcast on the same frequency or block using very precise timing measurements. The diagram in Figure 4-11 shows a network of three transmitters (Tx_1 – Tx_3) and their associated footprints. The DAB receiver (R) lies in an area where the three transmitter footprints overlap, this means that the network must be very precisely synchronised so that the multiple transmissions do not interfere with each other. The Guard Interval inserted before each OFDM symbol in the temporal domain (see 4.5), acts as a buffer for the arrival of these subsequent transmissions.

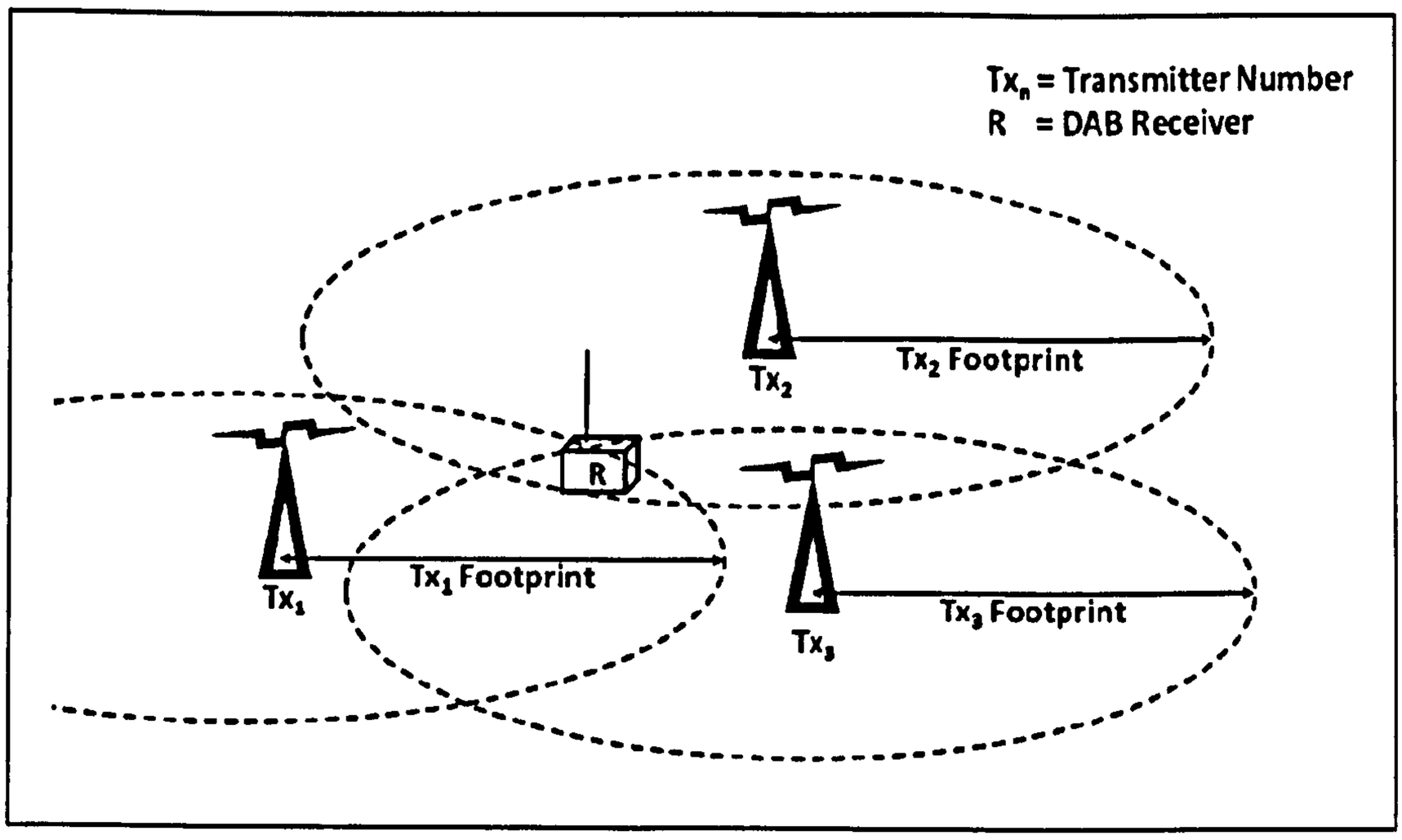

Figure 4-11: Single Frequency Network Example

When a network transmits the data, all transmitters broadcast their signals at precisely the same time or Inter-Symbol Interference (ISI) can be caused at the receiver. On occasion however, the best (highest) site for a transmitter may lie in an area which means it would interfere with another transmitter's footprint. If a secondary signal arrived at the receiver outside of the guard interval then this would cause inter-symbol interference to the primary transmission source. Therefore, certain transmitters may use a constant offset bias from one transmitter in order to mitigate this effect.

The use of this process means that to a DAB receiver, the signals *are not* broadcast simultaneously, meaning that this bias must be known and accounted for before any positioning algorithms are used.

5 POSITIONING TECHNIQUES

There are a number of different methods to estimate the position of a receiver when using terrestrial signals. In this chapter, five of the better known techniques will be examined with the purpose of finding a suitable method.

5.1 TIME OF ARRIVAL (TOA)

Time of arrival position estimation simply involves the precise measurement of a wireless signal's arrival time at a receiver. In order to calculate the three-dimensional position of the receiver, a minimum of four transmissions from four different transmitters must be received (three transmitters for a two-dimensional position) with the position of the transmitters known.

Figure 5-1 shows a basic TOA system with four transmitters. Initially, the three transmitters Tx_1 to Tx_3 are considered. It is assumed that the receiver and transmitter clocks are synchronised and the transmitters broadcast the transmission time of each signal in addition to their precise location.

As the precise transition time of each signal is known, the range can be calculated (ρ_1 to ρ_3) between each transmitter and the receiver by multiplying by the speed of light **c**. This is enough information to find a position in a perfect system, however, in reality

the receiver clock will not be synchronised to the transmitter clocks. Therefore, the fourth ranging measurement is required to correct this error.

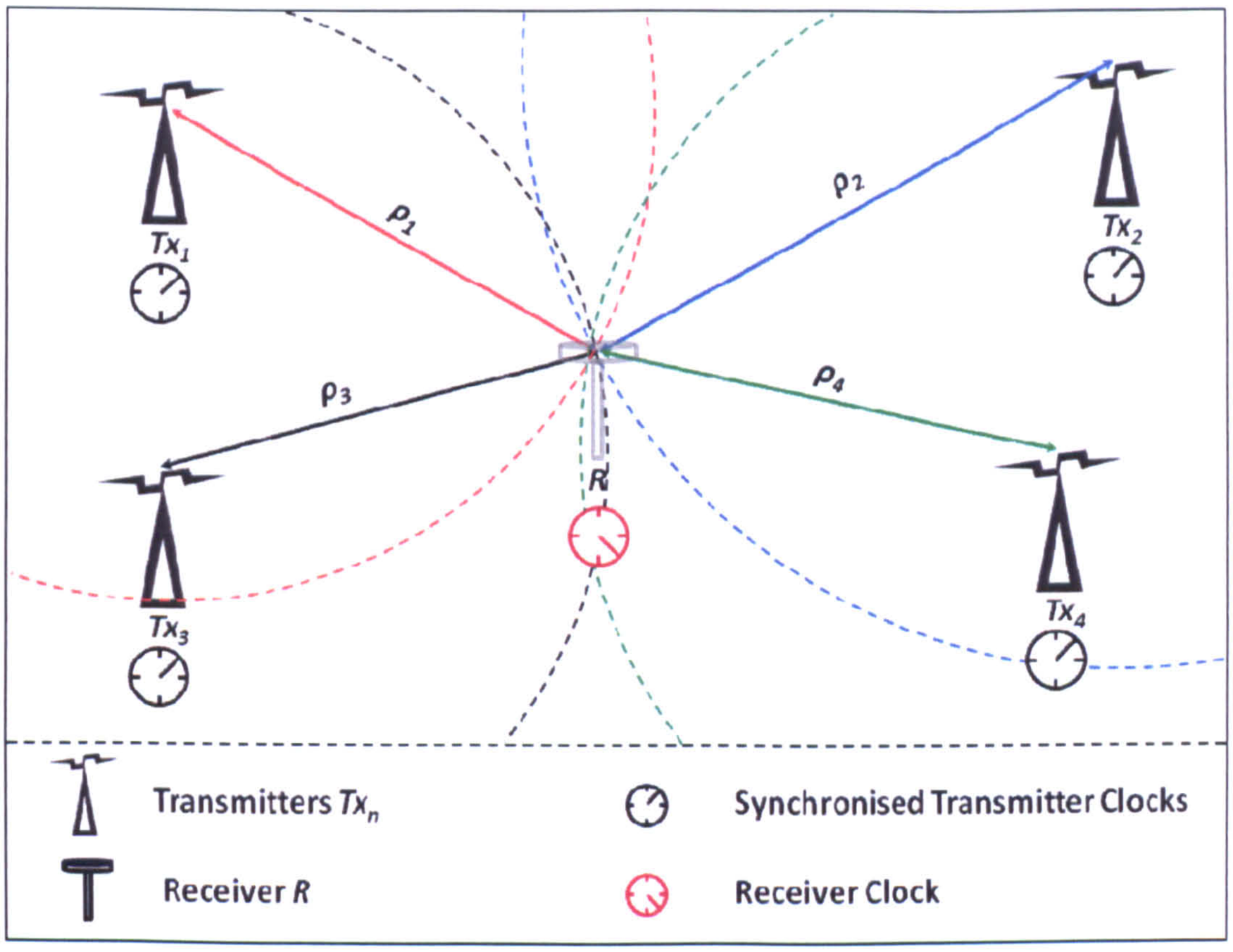

Figure 5-1: Basic TOA Position Estimation

Each range measurement creates a hypothetical sphere with the transmitter at its centre and the receiver lying somewhere on the surface of each sphere. The point where the minimum of three spheres intersect gives the 3D position. In a perfect world, each of the spheres will intersect at an infinitesimally small point giving the location, however, the number of error sources involved means that each locus of ranges has an area of ambiguity around the "true" range. This area of ambiguity is highlighted in Figure 5-2. Both diagrams *(a)* and *(b)* show a network of three transmitters on a flat earth viewed from above. This provides sufficient information to find a 2D position, however the position of transmitter Tx_3 is different in the two diagrams. Diagram *(a)* shows the transmitter geometry is fairly evenly spaced, giving a relatively small area

of ambiguity (the area bounded by the three pairs of solid lines) when compared to diagram *(b)* which has a much wider area of ambiguity.

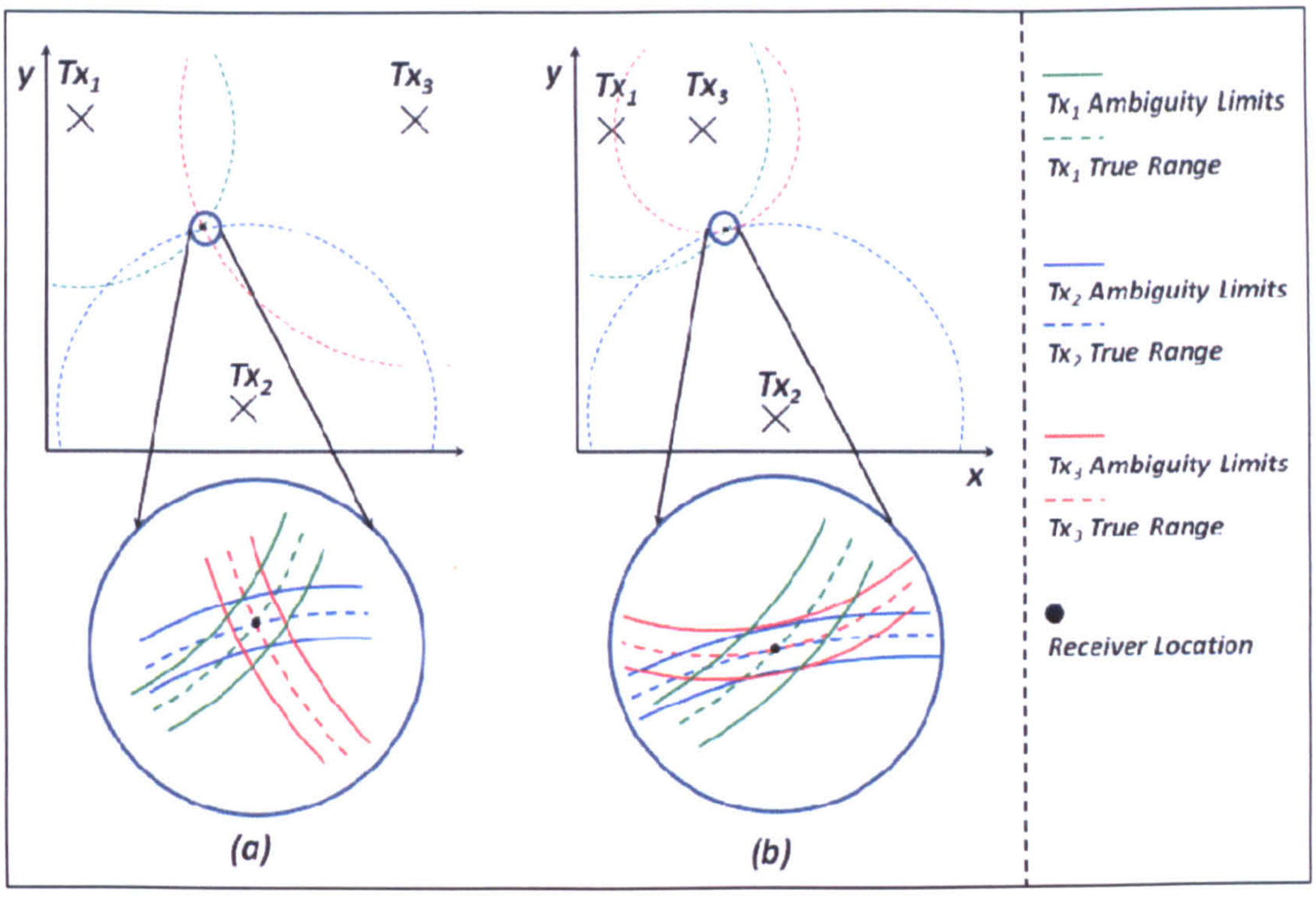

Figure 5-2: TOA Areas of Ambiguity

5.2 TIME DIFFERENCE OF ARRIVAL (TDOA)

Time difference of arrival works in a similar way to TOA and also requires a synchronised network of transmitters (if using one receiver) at known locations. Unlike the TOA technique, TDOA does not need to know the transmission time of a reference symbol. Instead, a receiver observes the signal transmitted from pairs of transmitters as follows (see Figure 5-3).

A receiver between two synchronised transmitters, Tx_1 and Tx_2, receives the reference information at slightly different times due to the receiver being closer to one transmitter (Tx_1 in this case). The time difference of arrival of this information places the receiver somewhere on a hyperbola *a* between Tx_1 and Tx_2. To find the location of the receiver in two dimensions, a third transmitter Tx_3 is required to create a second

hyperbola. This produces a series of hyperbolae between Tx_1 and Tx_3, placing the receiver on hyperbola *b*. Hyperbolae *a* & *b* intersect at the receivers location allowing the 2D position of the receiver to be found.

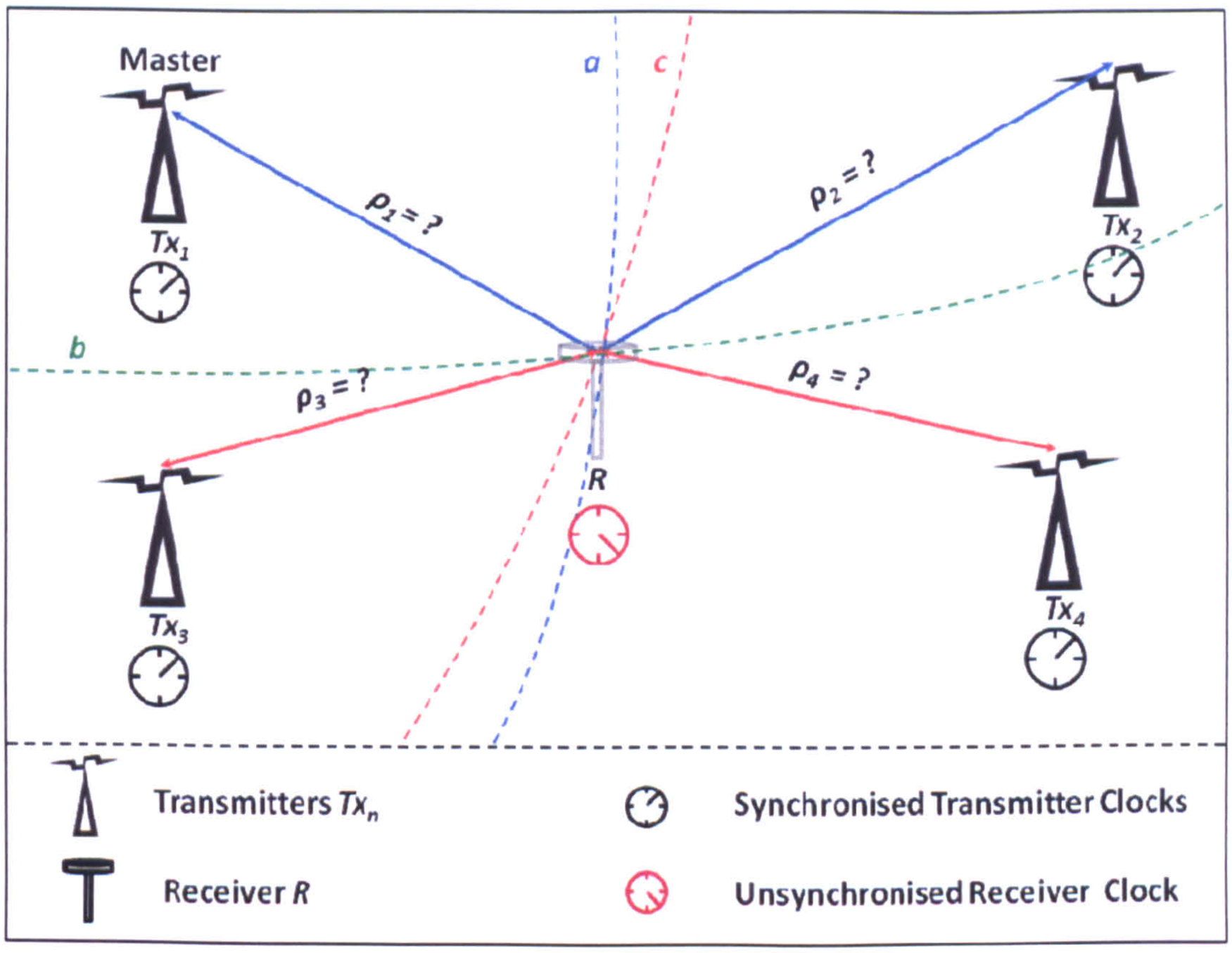

Figure 5-3: Basic TDOA Position Estimation

In order to expand this to find the 3D position, then a fourth transmitter is required (Tx_4) giving a third pairing and therefore a third intersecting hyperbola *c* at the receiver's location.

This technique may use non-synchronised transmitters by deploying a second receiver at a known location to act as a reference. Both receivers monitor the same radio frequency/frequencies and share a data link in order to apply corrections to the roving receiver. However, this technique is limited to the data link range between the two receivers in order for them to remain synchronised.

Although the transmitter to receiver ranges (ρ_1 to ρ_4) and therefore the signal propagation times are not known initially, the difference in arrival times of each signal are known. Therefore these range difference measurements can be used in place of the range measurements in order to calculate the receiver location.

5.3 ANGLE OF ARRIVAL (AOA)

The Angle of Arrival technique works by determining the direction of arrival of two or more signals to obtain a position estimate, rather than the signal timing techniques discussed previously. The network transmitters must be stationary and at known locations, although not necessarily synchronised (Küpper, 2005).

This requires either a directional antenna or preferably an antenna array to determine the Time difference of arrival or the phase difference at each array element. This technique in theory could use one receiver but due to the complexity involved, it is preferable to use one base station and one rover connected by a data link. One of the benefits of this technique is that the system can use as few as two transmitters to obtain a rough fix (although this is highly dependent on the quality of the array resolution and the distance from each transmitter – the closer the better).

The example described in Figure 5-4 shows a network of three transmitters (Tx_1 to Tx_3). By measuring the TDOA or phase difference at each array element, the incoming angles (pseudo-angles) from each transmitter may be found assuming this is in an open environment initially as this technique is also extremely vulnerable to multipath. Each angle is measured in this case with respect to a predetermined reference plane, R.

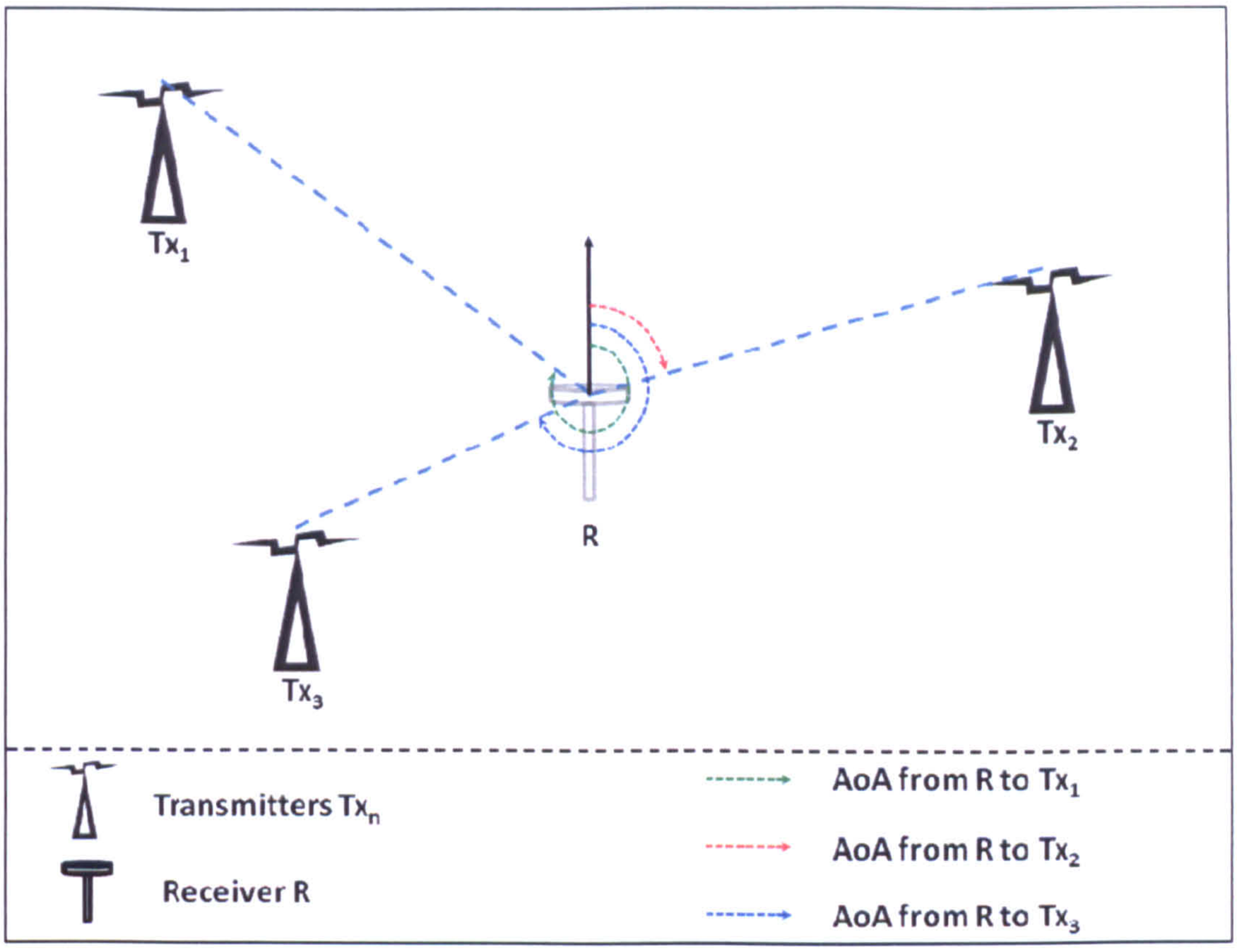

Figure 5-4: Basic AOA Position Estimation

The array resolution is a major problem as it determines the accuracy of the perceived arrival angle of each signal. The more diffuse this angle, the larger the error surrounding the position estimate. This can be mitigated to an extent using multiple base stations, but naturally this requires pre-planning.

5.4 Signal Strength Comparison

Signal strength measurement positioning is probably the most simple to realise multi-lateration system. It involves the monitoring of the change in strength of three or more omni-directional transmission sources, and then by using a mathematical model, the path loss attenuation of each signal can be found (Küpper, 2005) and a position estimation calculated.

The attenuation is a function of the range between transmitter/receiver, the wavelength of the signal of interest and the path loss gradient. Due to the different propagation

properties of radio-waves at different frequencies, these models will vary depending on the signal. This technique works well if there is no infrastructure between each transmitter and receiver. However, this is unfeasible and therefore this positioning technique is prone to significant errors due to multipath and fading in built up areas.

This technique was not investigated further due to the greatly varying quantity and density of obstructions between terrestrial based transmitters.

5.5 Carrier Phase Measurement

Ranging using a signal's carrier phase involves monitoring the phase shift of a signal/s carrier phase at each epoch.

The diagram in Figure 5-5 shows a simple two-dimensional example using this technique. At the first epoch (top diagram), the receiver is monitoring two signals from transmitters Tx_1 & Tx_2. If the receiver location at position R at this epoch is unknown, then the number of complete wavelengths between each transmitter and the receiver are unknown. These complete wavelengths are known as the *Integer Ambiguities* (distance A to Tx_1 and distance B to Tx_2).

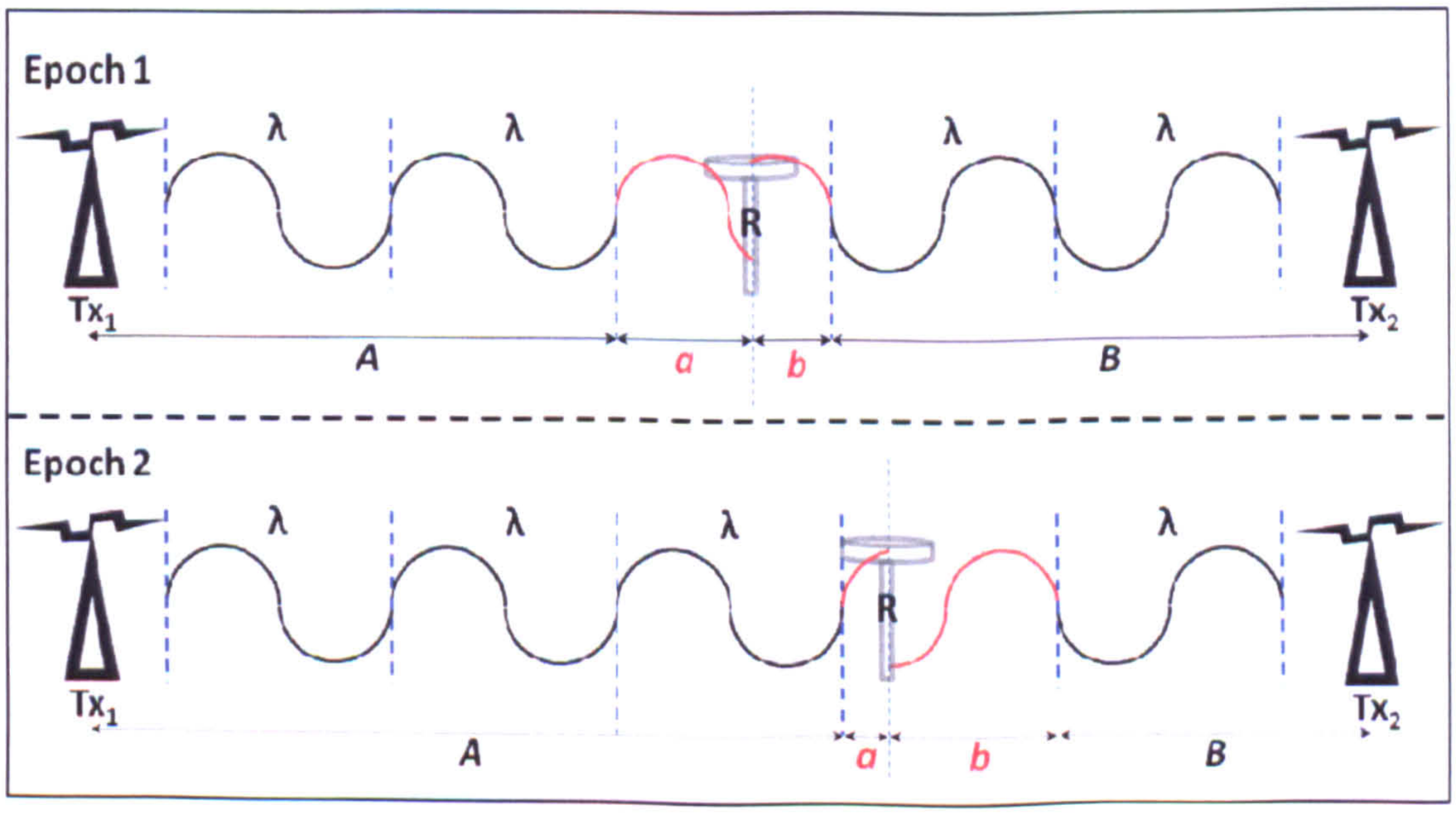

Figure 5-5: Carrier Phase Positioning Example

However, if the receiver initial position is known along with the position of each transmitter, then each integer ambiguity may be resolved instantly. As the receiver moves from this point, the phase change in each signal indicates the amount the receiver has moved in a certain direction.

If a signal source is masked for any reason for a period of time, the integer ambiguity must be recalculated. Again, as with all previous techniques, multipath and shadowing (complete loss of signal lock) will cause problems.

5.6 SUMMARY

Of the positioning techniques examined in this chapter, one technique stands out as the most likely contender for use within this investigation. The Time Difference of Arrival (TDOA) technique has been chosen due to the DAB signal not broadcasting a precise transmission time (thus eliminating Time of Arrival as a possibility). It is known that DAB networks are synchronised, therefore only requiring the need for a single receiver. Angle of Arrival requires the use of a complex antenna array which contradicts the simple off-the-shelf objective of this project and is also severely affected by multipath, as is the carrier phase measurement solution. The signal strength measurement technique is not realistic in such an environment due to the vastly changing surroundings of a receiver when in transit. Such surroundings would change the received signal strength at a nonlinear rate making measurements very unreliable.

Therefore the remainder of this project will use the Time Difference of Arrival method as the chosen positioning technique.

6 DAB SIGNAL PROCESSING

6.1 INTRODUCTION

This chapter concentrates on, and describes in detail, the methodology behind the capture of the DAB signal and its subsequent processing. The aim of the processing is to extract information for two or more Time Difference of Arrival measurements in order for a positional fix to be generated. As this project was examining the DAB signal from a positioning perspective, the raw spectrum was initially captured so that suitable software could be built to decode the signal in post-processing. The chapter continues describing this capture process and the hardware and software involved.

6.2 SIGNAL CAPTURE

6.2.1 Software Defined Radio (SDR)

This section describes the hardware and software used to capture and store the raw DAB spectrum. From early on in the project, a Software Defined Radio (SDR) approach was adopted to in order to capture the signal. A SDR essentially replaces most of the hardware required to decode a particular signal and replaces it with user-defined software with the tasks being operated by the host computers CPU. This

allows a host computer to have the potential to decode any radio signal (provided the hardware includes a sufficiently fast Analogue-Digital converter which is connected to an antenna capable of capturing the band of interest), and creates a single platform system where the reconfiguration is done in software alone.

As a Software Defined Radio system requires both particular hardware and software, the combinations used in this project were as follows.

6.2.2 Hardware – The Universal Software Radio Peripheral

One of the aims of this project was to investigate the DAB signal using relatively simple, cost-effective off-the-shelf equipment. This was successfully achieved with the use of the Universal Software Radio Peripheral (USRP).

The USRP is a piece of hardware that sits between the antenna and a computer. The device was developed and built by Ettus Research LLC (Ettus, 2008) and designed specifically to be used with the GNU Radio software described in 6.2.3. The device acts as a radio front-end and consists of two pairs of Analogue-Digital Converters (ADCs) and two pairs of Digital-Analogue Converters (DACs), allowing it to accept up to two receiver inputs and two transmitter outputs at any one time. The 12-bit ADCs are capable of capturing up to 64 Mega-samples/second, whilst the 14-bits DACs are capable of producing up to 128 Mega-samples/second. The system is controlled by a Field Programmable Gate Array (FPGA) which sits in the centre of the motherboard (*Altera Cyclone FPGA*). This chip runs the software defined radio from information received from the host computer.

The USRP connects to a computer via a USB2.0 interface, allowing a maximum transfer rate of 32MB/s. This transfer rate acts as the major limitation of the device as it limits the width of spectrum the radio front-ends can capture. Each receiver and transmitter bay inside the casing can house one of many daughter-boards, each of which are designed to operate over a particular frequency range. Figure 6-1 shows an

annotated picture of the USRP motherboard (original photograph from http://www.ettus.com/products) and highlights the positions of the major components.

As mentioned previously, the daughter-boards come in several different types. As this project was examining the DAB signal, a board was needed which would be able to sufficiently capture one or more DAB blocks in VHF Band III (170 – 240 MHz). To achieve this, the TVRX daughter-board was used as it could capture any 8MHz window between 50 and 870 MHz, giving it the ability to capture up to four signals simultaneously. Figure 6-2 shows a photograph of the USRP in its enclosure and also shows four of the available daughter-boards, the TVRX being top left, with the pen in the foreground present to give an idea of scale.

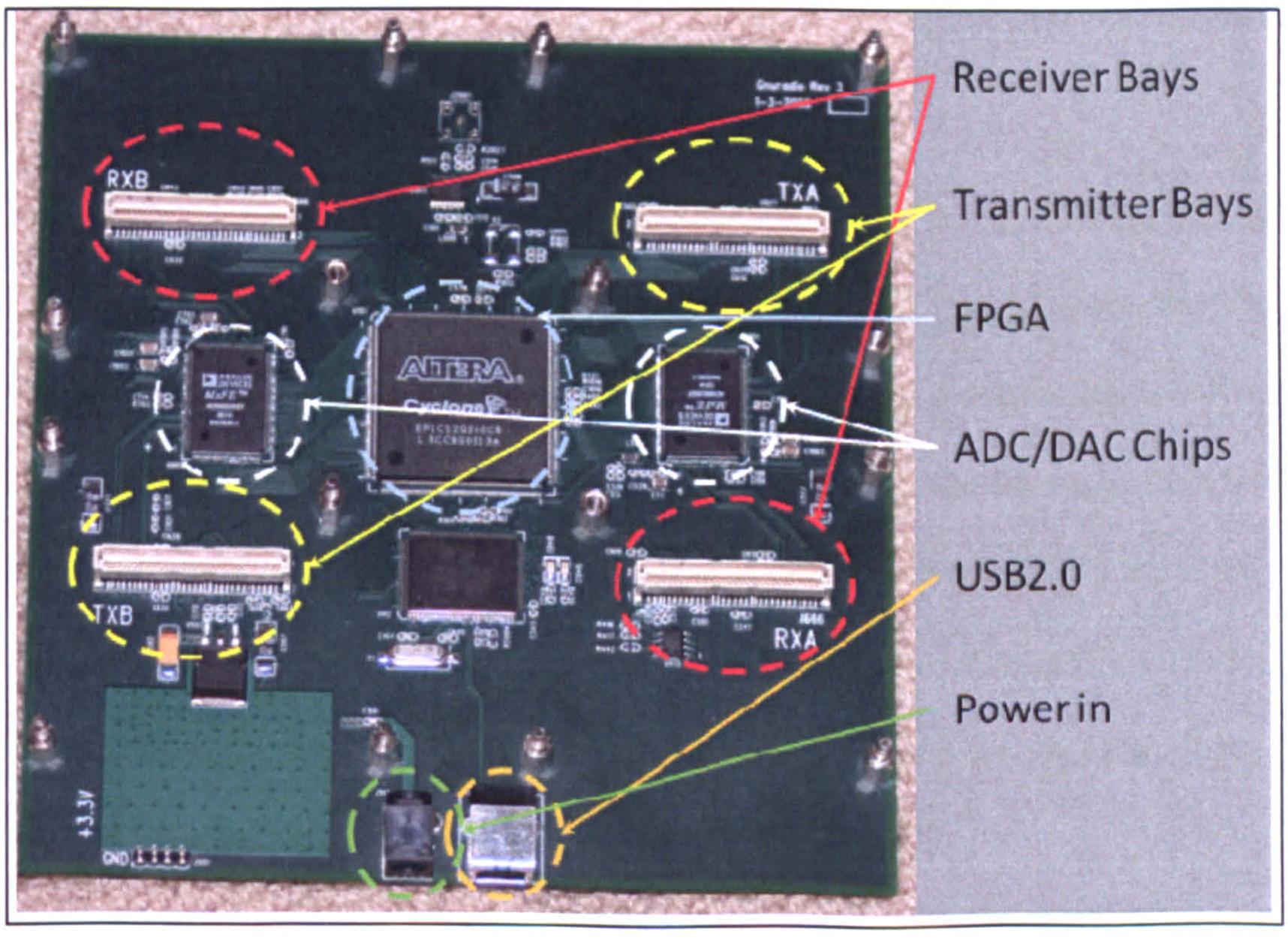

Figure 6-1: USRP Motherboard (http://www.ettus.com/products)

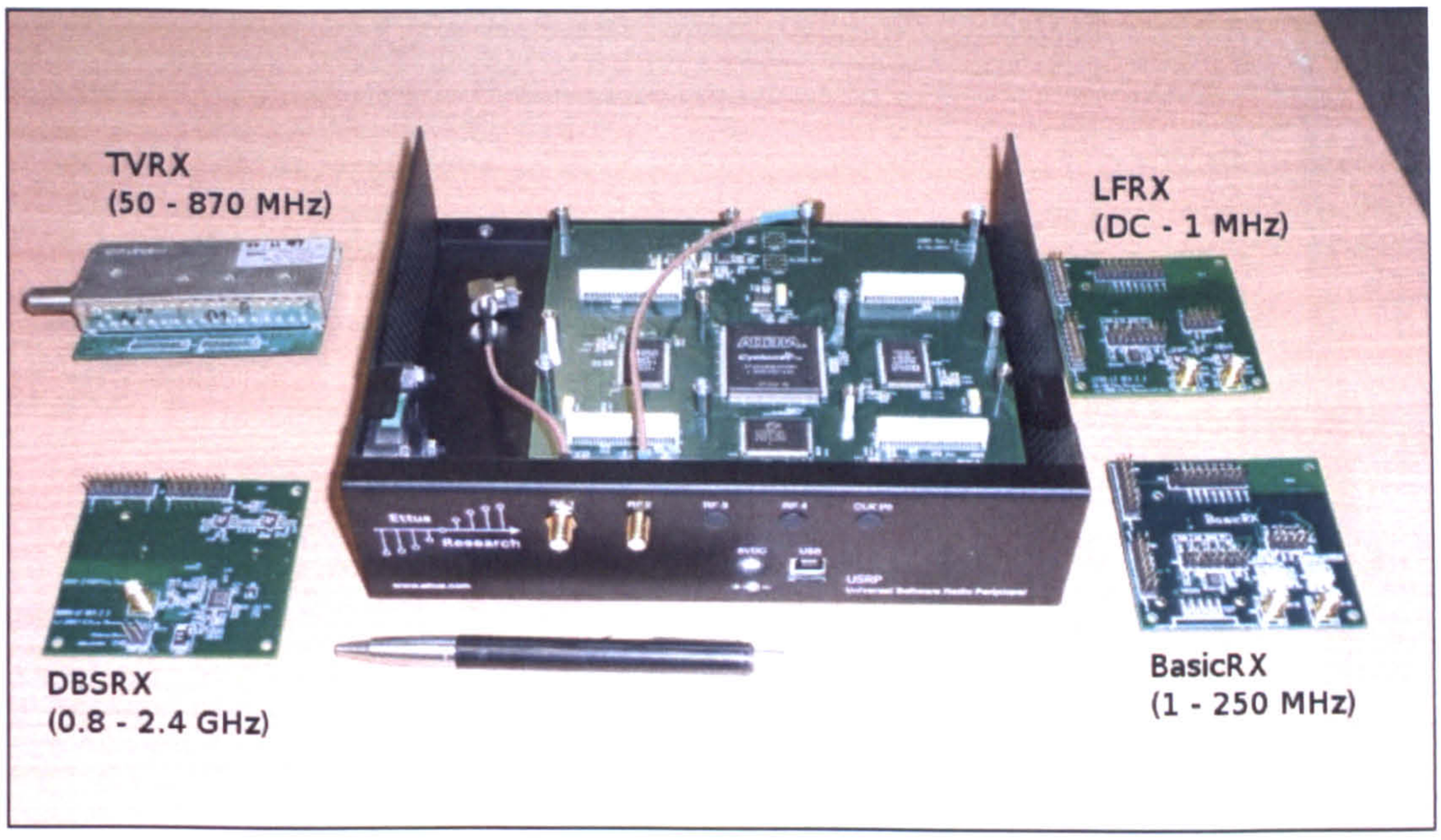

Figure 6-2: USRP in enclosure including a selection of daughter-boards

6.2.3 Software – GNU Radio

The software used to control the USRP is called GNU Radio (Lang, 2010) and is open source software and freely available. It consists of a library of signal processing block sets built using C++ and Python and is used as the building blocks to run a Software Defined Radio. Whilst a substantial amount of processing can be done using GNU Radio, this project uses a relatively small amount of it due to the experimental nature of the work. In this instance, the software is used only to convert a signal of interest to baseband and then capture and store the raw I and Q values for post-processing in Matlab™ or equivalent software.

The software script has a variety of basic input parameters, including the ability to alter the gain of the software receiver, the frequency and width of the capture, length of capture etc. Figure 6-3 shows a screen capture of GNU Radio running a Fast Fourier Transform (FFT) over an 8MHz window. In this instance, three DAB signals can be seen in the frequency domain.

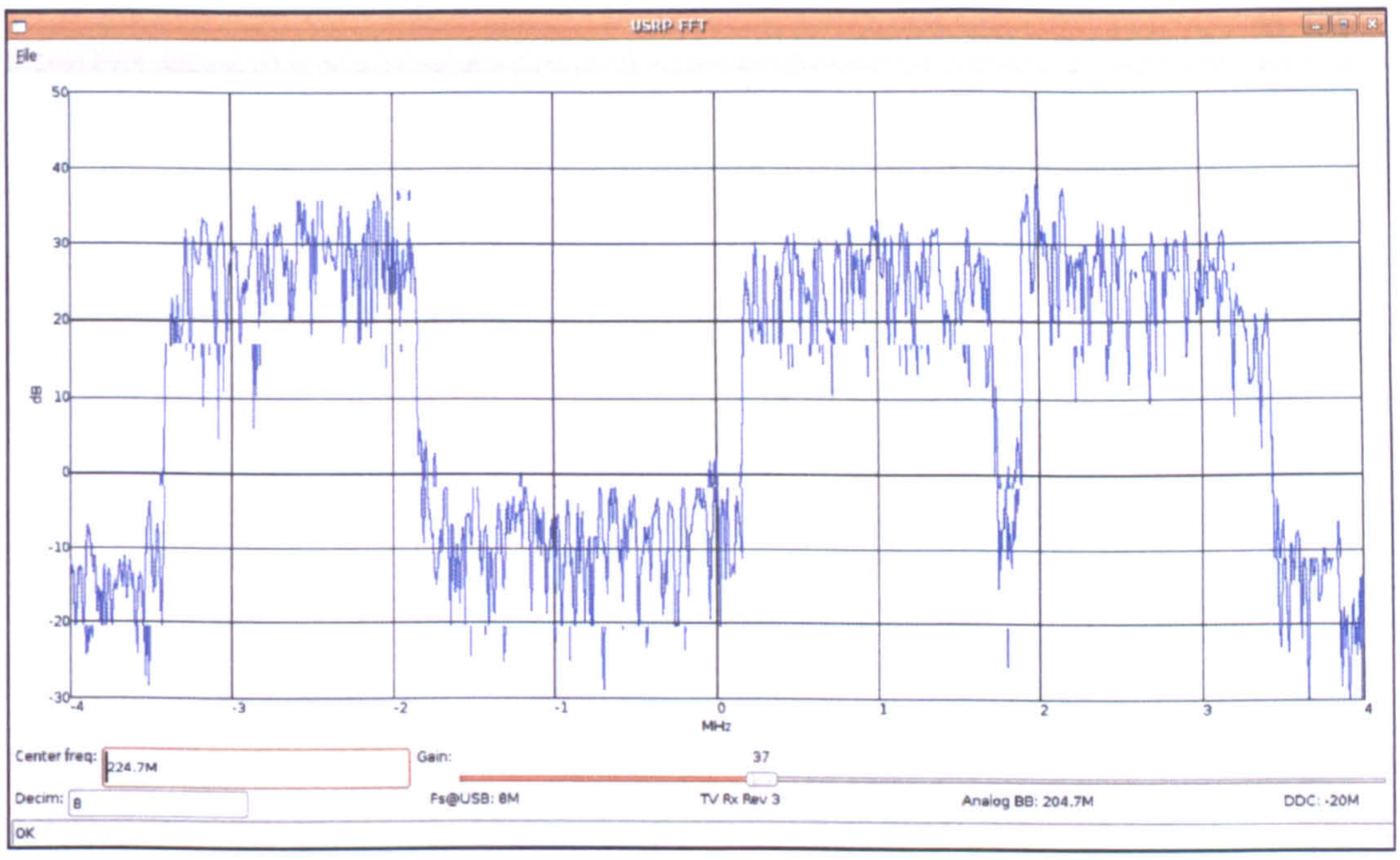

Figure 6-3: Screen capture of GNU Radio running an FFT over an 8MHz spectral bandwidth

6.2.4 Antennas

Two antennas were used in the data capture trials for this project for one of the experiments. The main antenna was a passive omni-directional dipole antenna with a 360° beam-width and 2.2dBd (dipole) gain (Figure 6-4, right image). This antenna is designed for use as a permanent static vertical mounting on a building in areas where a basic telescopic antenna does not produce sufficient reception quality.

The second was a significantly smaller active in-car glass-mounted antenna (Figure 6-4, left image). This required a +12v input giving a gain of 9dBi (isotropic, where 0 dBd = 2.15dBi), but only in the direction of the glass, essentially forming a beam of 180° away from the vehicle.

Figure 6-4: The two antennas used in this project

(i) internal side-window mounted antenna left

(ii) external roof mounted dipole right

6.2.5 Data & Pre-processing

Data captured by the USRP is stored on the computer hard drive as a complex binary number which initially must be converted to a 32-bit complex number in order for any processing to take place.

The resulting converted data file is now a string of samples in the temporal domain, the parameters of which are determined by those used in the initial capture. At this point the first 100,000 samples are ignored to avoid any interference from the TVRX/USRP front end tuning to the desired frequency when the capture was made.

One limitation of the USRP is the sampling rates of the hardware. As the main clock on the motherboard runs at 64MHz, any capture must be a decimation of this frequency. For example, while the DAB clock frequency (section 4.3.1) runs at

2.048MHz, the closest window available to the USRP is 2MHz, a decimation rate of 32. This gives a capture window of 2MHz, whereas a DAB receiver would use a window of 2.048MHz. This does not cause a problem as the bulk of the information captured does not require decoding as will become clear later, but in order for the Fast Fourier Transform to work most efficiently and to avoid confusion when determining symbol length etc, the received signal is up-sampled marginally to 2.048MHz. This makes computations simpler and allows all computations to work with integer values of T (section 4.3.1).

If capturing multiple signals then the same process is applied, a 4MHz window (two DAB signals) is up-sampled to 4.096MHz and an 8MHz window (four signals) to 8.192MHz.

The received dataset is now in a useable state to begin processing the OFDM symbols.

6.3 FINDING THE NULL SYMBOL

For the purposes of the following worked example, the basic assumption is that the dataset has been captured using the parameter values listed in Table 4 below and pre-processed as detailed in 6.2.5:

Capture Parameter	Value
DAB Broadcast Frequency (f_c)	225.648 MHz
USRP Capture Window width	2 MHz (re-sampled to 2.048 MHz)
Decimation Rate (of receiver clock)	32
Number of DAB signals	1
Total Capture Length	2.1×10^6 samples
Useable Capture Length	2.0×10^6 samples
Useable Capture Length post re-sampling	2.048×10^6 samples

Table 4: Example Data Capture Parameters

The first and most important stage of the post-processing is to detect the presence of the Null symbol in the temporal domain, and hence the start of the transmission frame. The length of a single frame is known to be 196,608T and it is known that at some point this will contain the Null symbol to signal the start of the next frame, so this number of samples is extracted and the absolute values of the signal in its current state are plotted (see Figure 6-5).

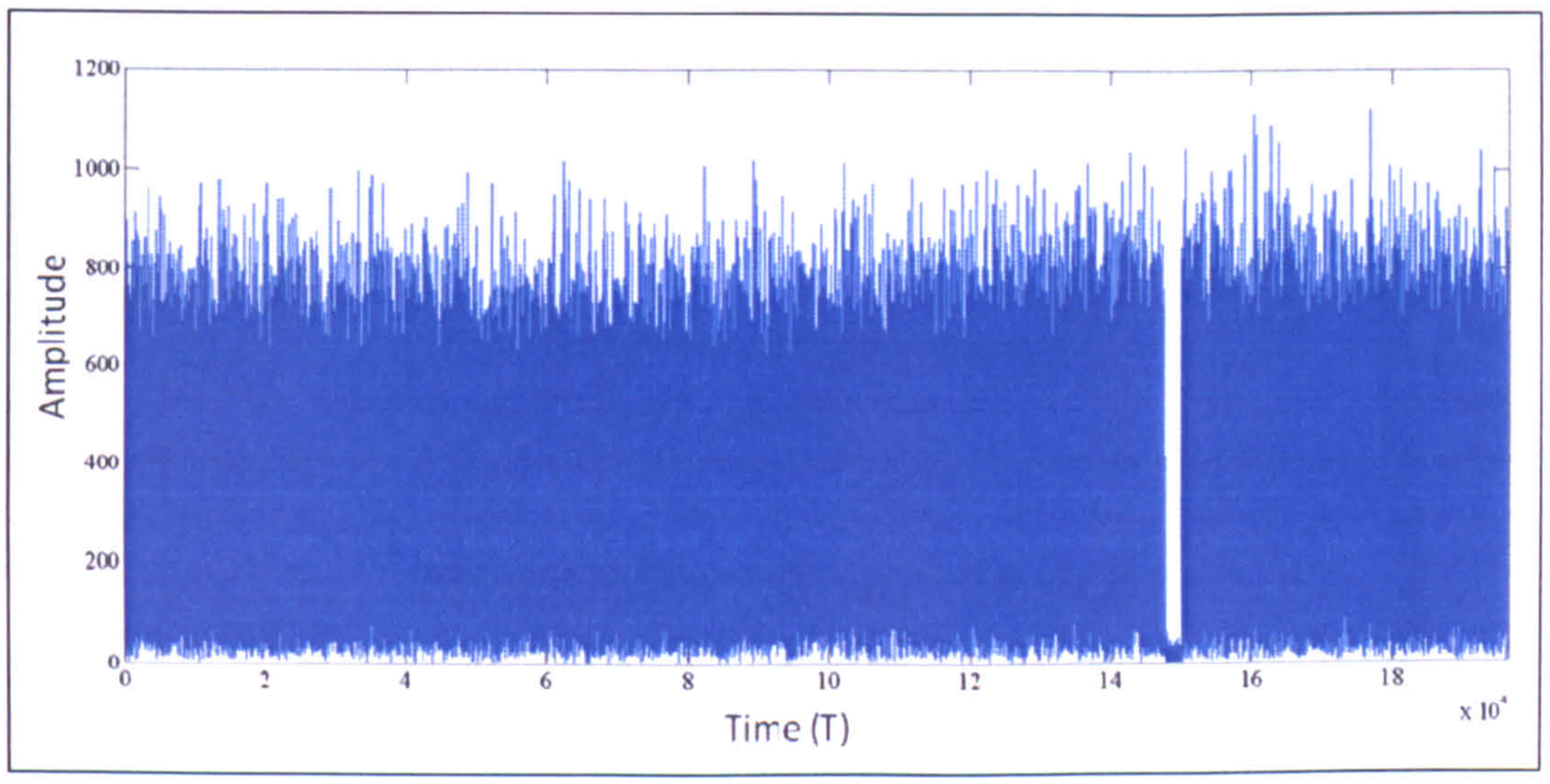

Figure 6-5: Plot of a DAB frame in the temporal domain

By eye, it is immediately obvious where the null symbol is located. It is known that the Null length is exactly 2656T; however, this is not the length seen when the null region in Figure 6-6 is examined closely. As this signal contains transmissions from multiple transmitters, a slight overlap is present and the end of the secondary signal's final OFDM symbol overlaps that of the primary signal as may be seen highlighted in the figure.

At this point in the processing, it is not important that an overlap is present as it is the end of the Null Symbol that is needed in order to align for the next processing stage. Therefore, the search for the first null symbol is an iterative process which runs from left to right in the plot, testing the absolute amplitude of the current position in the

frame with those around it. Whilst the Null Symbol length may not be detectable as 2656T due to secondary transmissions, it is known that the period will be no less than 2152T due to the DAB signal design.

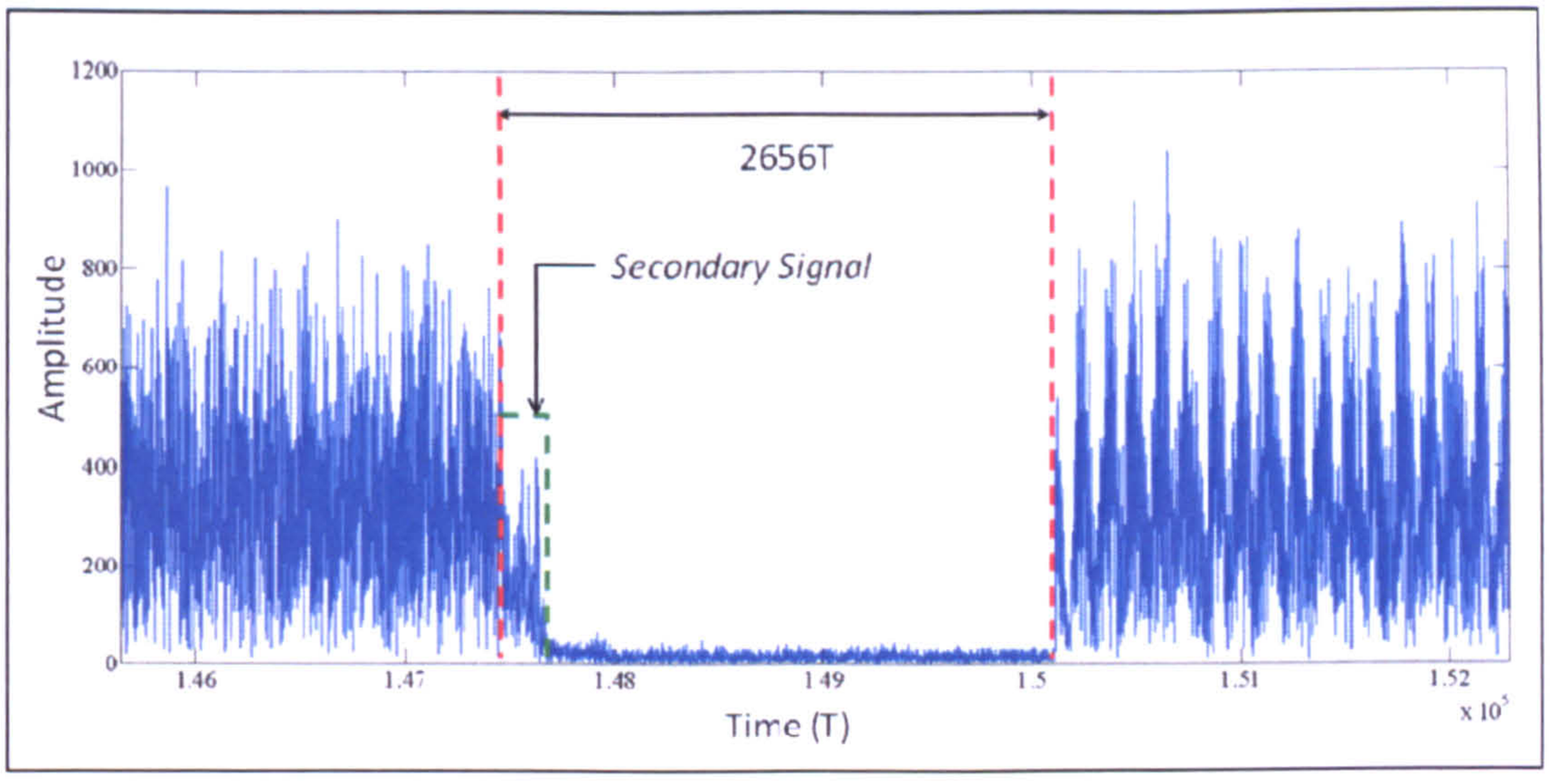

Figure 6-6: Closer view of Null Symbol

The search window T_{WIN} can be defined as:

$$T_{WIN} = T_{NULL} - T_{GI} \tag{6.1}$$

Where T_{NULL} is the length of the Null Symbol and T_{GI} is the length of the OFDM Guard Interval. This gives a minimum window length to search for and after a number of iterations, identifies the Null Symbol. Having found this region, the end of it must be found precisely in order to correctly identify the second part of the Synchronisation Channel, the TFPR symbol. This is relatively simple to find by testing each null point against the next in the sequence until a rise in the value is encountered. At this point it is assumed that the rough start of the OFDM symbols has been found and processing can continue.

6.4 DEFINING THE FIRST OFDM SYMBOL

The first OFDM Symbol in the DAB frame is the Time-Frequency-Phase Reference Symbol, the sole purpose of which is to align the remainder of the frame and to allow for decoding of the Fast Information Channel. The rough start of this symbol has been identified, or at least the Guard Interval associated with it, therefore the length of an OFDM Symbol (T_{OFDM}) is defined as below, where T_{USE} is the length of the useful symbol portion, and T_{GI} the length of the Guard Interval:

$$T_{OFDM} = T_{USE} + T_{GI} \qquad 6.2$$

With this in mind, the symbol itself can be extracted and the Guard Interval defined (Figure 6-7).

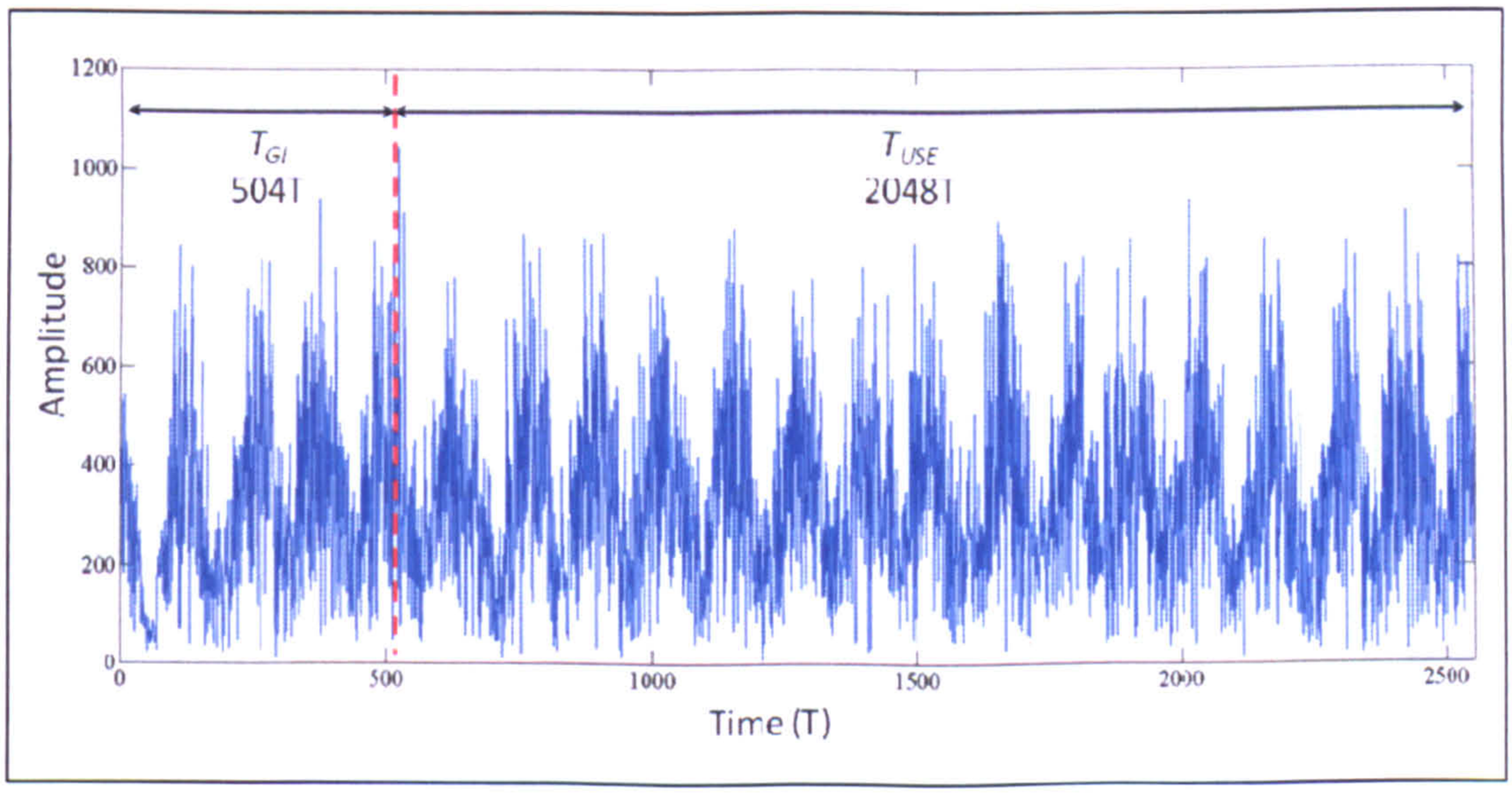

Figure 6-7: Defining the first OFDM Symbol (TFPR Symbol)

The useful symbol portion (T_{USE}) can now be extracted and run through a Fast Fourier Transform algorithm (Cochran et al., 1967) to display the OFDM symbol in the frequency domain. This is performed so that the frequency errors can be removed.

6.5 CORRECTING THE FREQUENCY OFFSET

In its current state, the symbol being processed contains errors in the frequency domain. This is discussed in detail in (Rugini and Banelli, 2005) and is due to errors in the receiver oscillator (the USRP front-end in this case) and the channel the signal travels through from transmitter to receiver. This is a two-stage process involving the correction of the coarse frequency (integer number of kHz) offset and the fine frequency (fraction of kHz) offset.

6.5.1 Fine Frequency Offset

The fine frequency offset correction involves the comparison of the symbols Guard Interval (GI) with its duplicate section (refer to Figure 4-7). Although these regions are identical when transmitted, because of secondary signals and other error sources through the channel, they do not arrive at the receiver as such. It is the comparison of these regions which allows the receiver to calculate the fine frequency offset, by plotting these symbol portions side-by-side (Figure 6-8), it can clearly be seen that although the two vectors largely map to each other, the left side of the plot shows some interference.

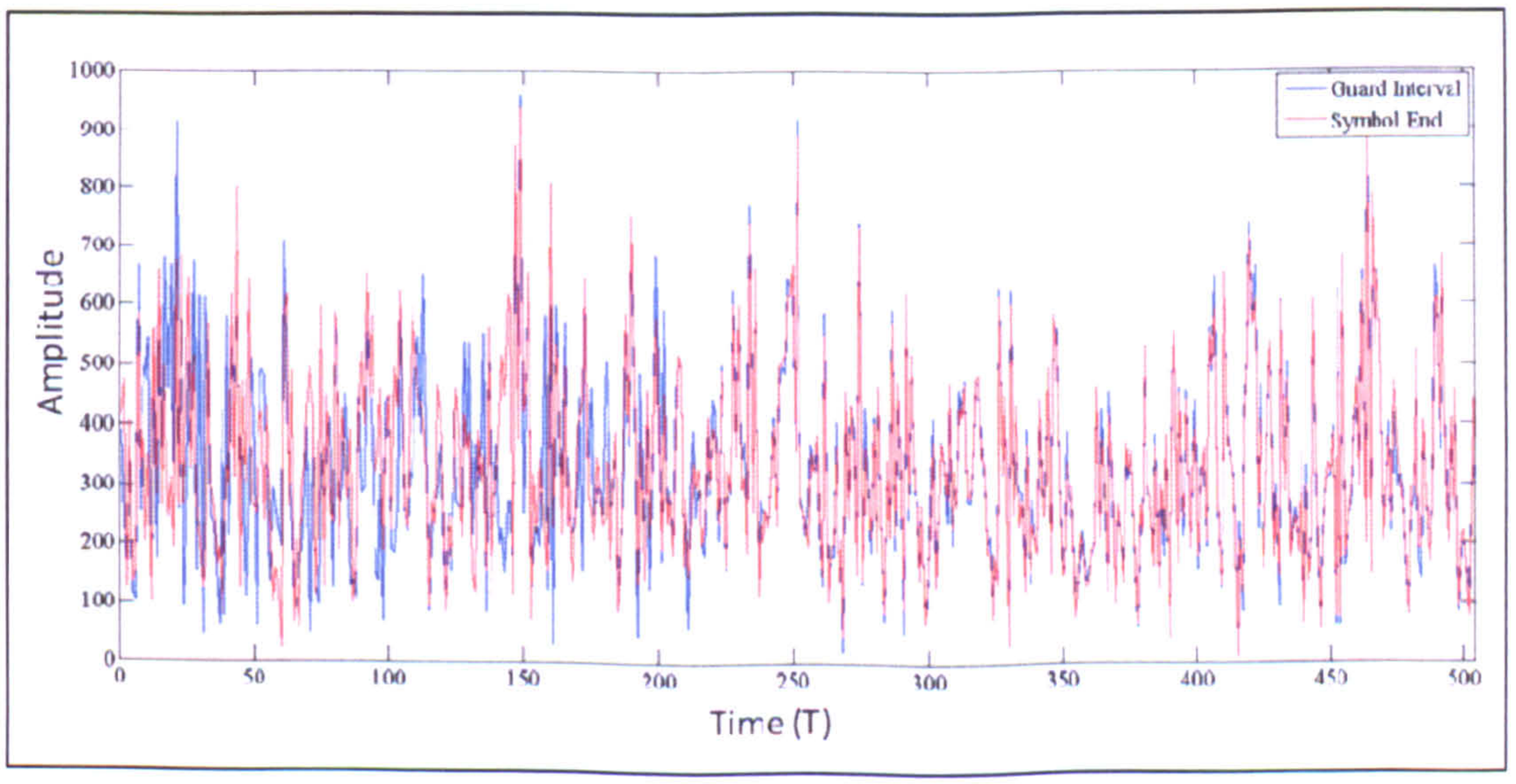

Figure 6-8: Comparison of Guard Interval with OFDM Symbol end

This difference can then be calculated by taking the dot product of the two complex vectors (van de Beek, 1998) - Figure 6-8 only shows the absolute values for ease of viewing - as shown below where **a** is the complex vector of the Symbol End (504T), **b** is the complex vector of the Guard Interval and E_{FINE} is the resulting correction value in Hz:

$$\mathrm{E_{FINE}} = \left(\frac{\mathbf{atan2}\left(\Im(\mathbf{corr}), \Re(\mathbf{corr})\right)}{2\pi}\right) \tag{6.3}$$

Where: $$\mathbf{corr} = \mathbf{a} \times \mathbf{b}^{T} \tag{6.4}$$

The current symbol can then be corrected for the fine frequency offset by the calculation as follows:

$$\mathbf{d} = \mathbf{c} \cdot e^{j2\pi \cdot E_{FINE} \cdot \mathbf{f}} \tag{6.5}$$

Where **d** is the symbol corrected for fine frequency offset, **c** is the same symbol before correction and **f** is the vector of values defined as:

$$\mathrm{f} = \sum_{i=0}^{2047} \frac{i}{2.048 \times 10^{6}} \tag{6.6}$$

6.5.2 Coarse Frequency Offset

Having corrected the fine frequency offset, the coarse frequency offset must now be calculated and applied. For this purpose, the symbol of interest is represented in the frequency domain by applying a FFT algorithm (Figure 6-9). This technique requires the comparison of the empty carriers lying to the sides of the signal with the carriers switched on. The purpose of this is to move the symbol an integer number of carriers

(integer number of kHz) so that it 'fits' precisely in the processing window to continue decoding.

This is done by moving a comparison window over the signal fringes denoted by A and B in Figure 6-9. It is known that when the signal is centred correctly, it will lie in the region ±768 kHz of 0, with the central suppressed carrier f_c at 0 kHz. This gives a total width of 1537 carriers including f_c.

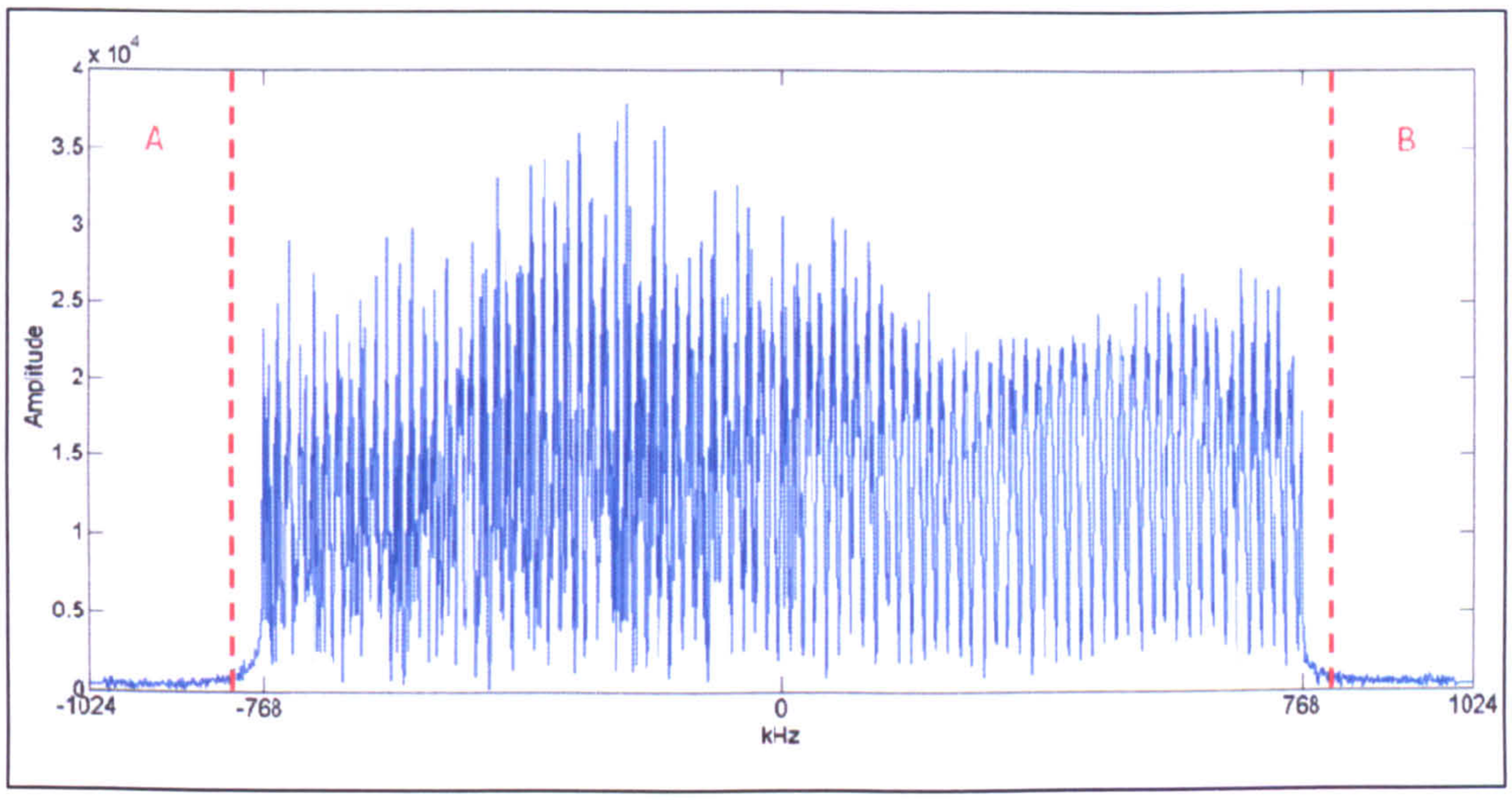

Figure 6-9: OFDM Symbol represented in the frequency domain following fine error correction

As the partial (fine) frequency offset has been calculated previously, this is simply a testing algorithm by shifting the window until the local maximum sum of 1537 carriers is found. This completes the frequency offset correction.

6.6 GENERATING THE TFPR SYMBOL

The Time Frequency Phase Reference Symbol was briefly introduced in 4.5.1 as the first OFDM symbol in the DAB frame. As this frame is always identical in all DAB transmissions, as part of the ETSI 300 401 standard (European Broadcasting Union, 1997), it can be re-created locally in the receiver.

6.6.1 CAZAC Sequence

The symbol is composed of a complex sequence known as a Constant Amplitude Zero Auto-Correlation (CAZAC) code. As the name suggests, CAZAC codes have the following properties (Heimiller, 1961):

- Constant amplitude in the frequency domain
- Zero out-of-phase auto-correlation in the frequency domain
- In-phase correlation of modulus one in the temporal domain

6.6.2 Symbol Generation

One of the most critical stages of the processing involves the generation of the correct CAZAC sequence within the receiver so that cross-correlation may be performed with the received symbol later in the process. The symbol is defined in (European Broadcasting Union, 1997) by equation 6.7 where $l = 1$.

$$z_{l,k} = \begin{cases} e^{j\varphi_k} & for -K/2 \le k < 0 \; and \; 0 < k \le K/2 \\ 0 & for \; k = 0 \end{cases} \qquad 6.7$$

Where:

$$\varphi_k = \frac{\pi}{2}(h_{i,k-k'} + n) \qquad 6.8$$

The values of k, k', n and i can be found in Table 12 on page 216 and the values of j and h can be found in Table 13 on page 217. This gives sufficient information to create the TFPR code for transmission mode I. The phases are calculated from equation 6.8 and plotted against $\boldsymbol{T}$ as shown in Figure 6-10.

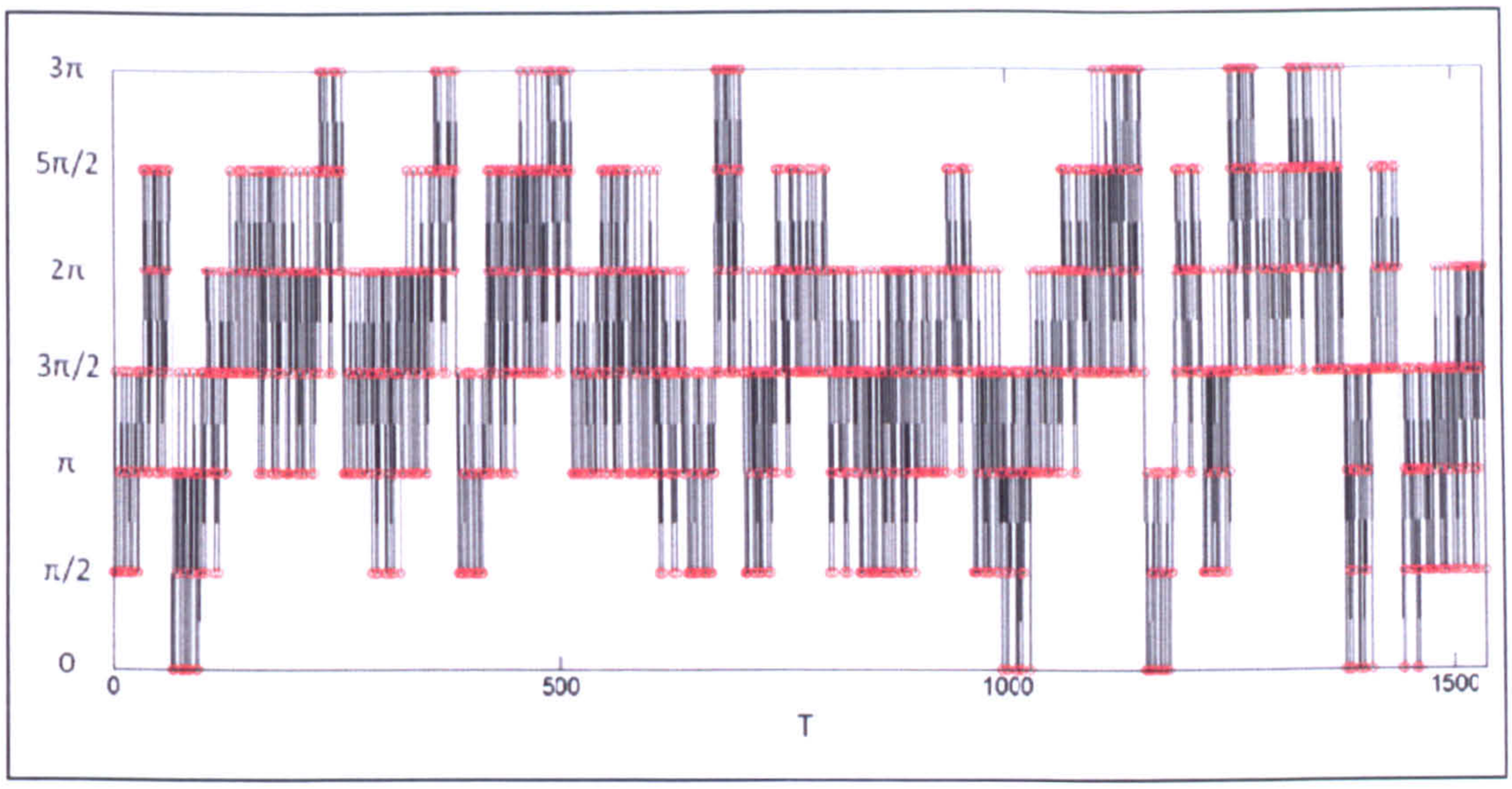

Figure 6-10: TFPR Sequence Phases

At this stage the central suppressed carrier has not been taken into account, therefore this is inserted into the central position of the phase sequence to increase the length from 1536T to 1537T (central carrier at 769T). The in-phase (I) and quadrature (Q) components of the symbol are then calculated from equation 6.7, and can be seen plotted in the 2D I-Q planes and 3D I-Q against time ***T*** in Figure 6-11.

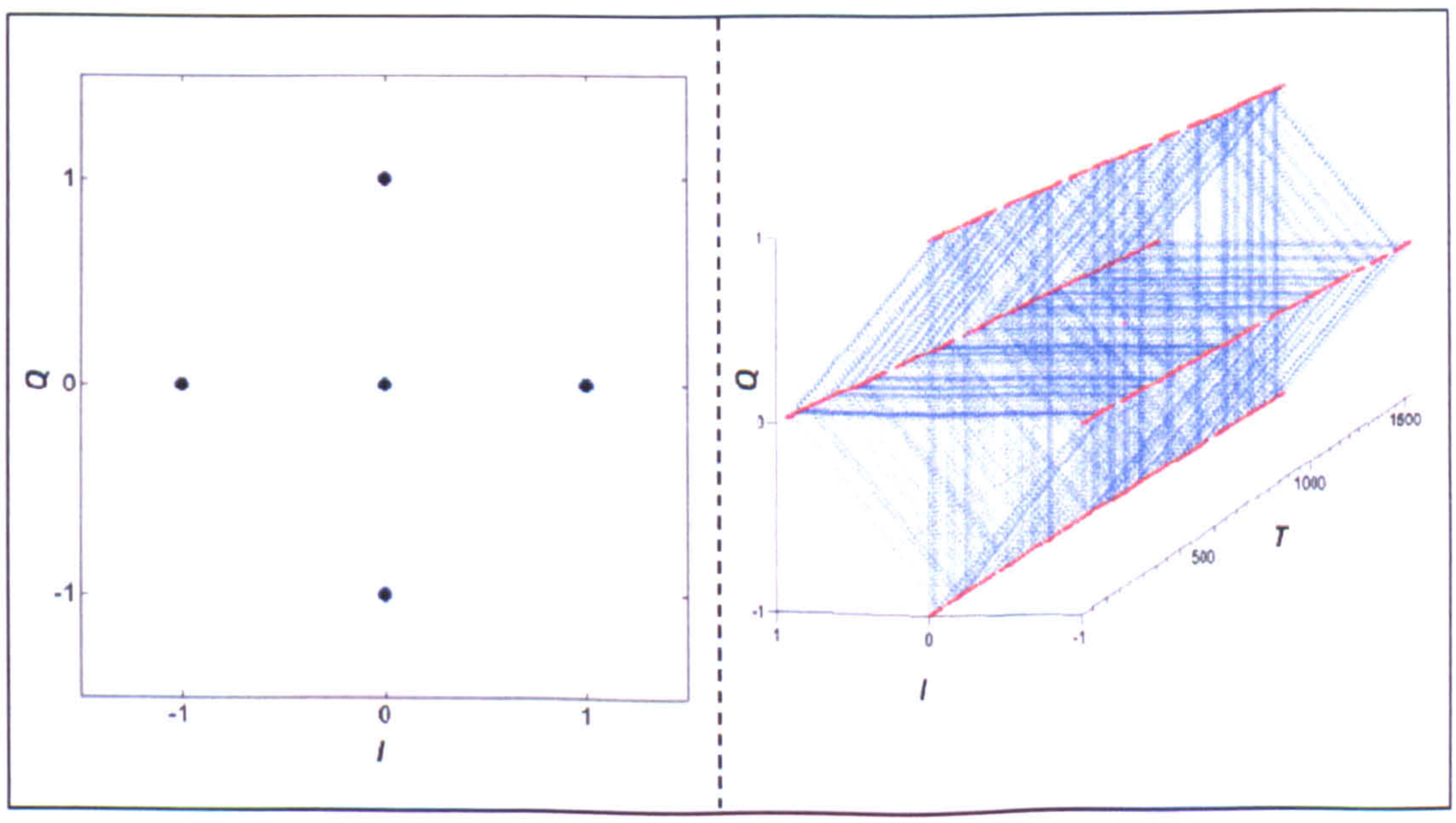

Figure 6-11: TFPR Symbol plotted as I-Q (left) and I-Q against time T (right)

This gives the basic TFPR symbol represented in the frequency domain. This symbol can now be passed through an inverse FFT to show the constant amplitude nature of the sequence in the frequency domain when compared to that of the temporal domain.

Figure 6-12 shows the modulus of the sequence in both the frequency (blue) and temporal (red) domains, plotted on the same axis. The central suppressed "tuning" carrier can be seen clearly at position 769T on the frequency plot.

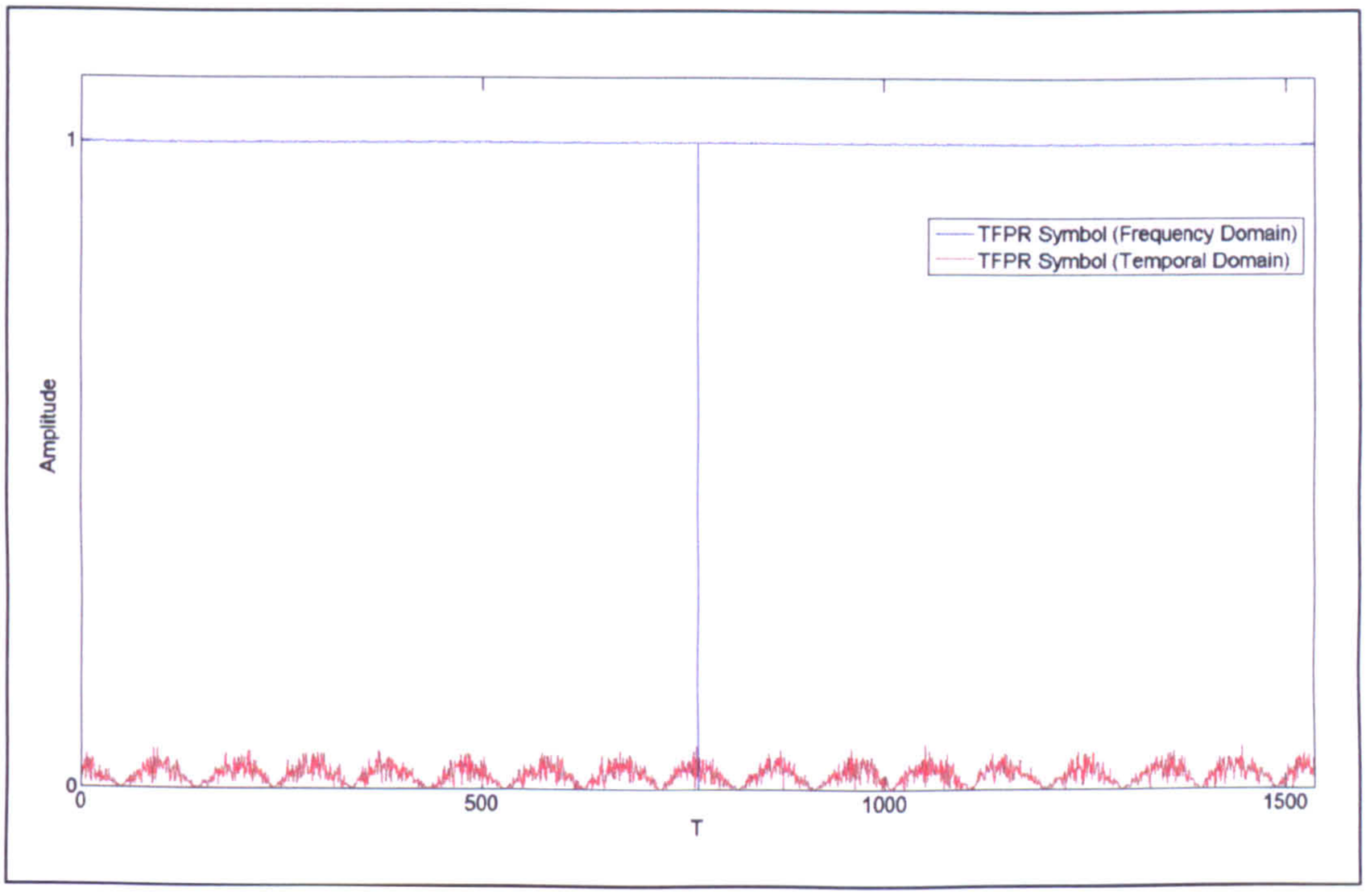

Figure 6-12: Comparing the TFPR Symbol in Frequency/Temporal Domains

By performing an auto-correlation of this 1536T sequence and plotting the modulus of the result, the following can be seen in Figure 6-13.

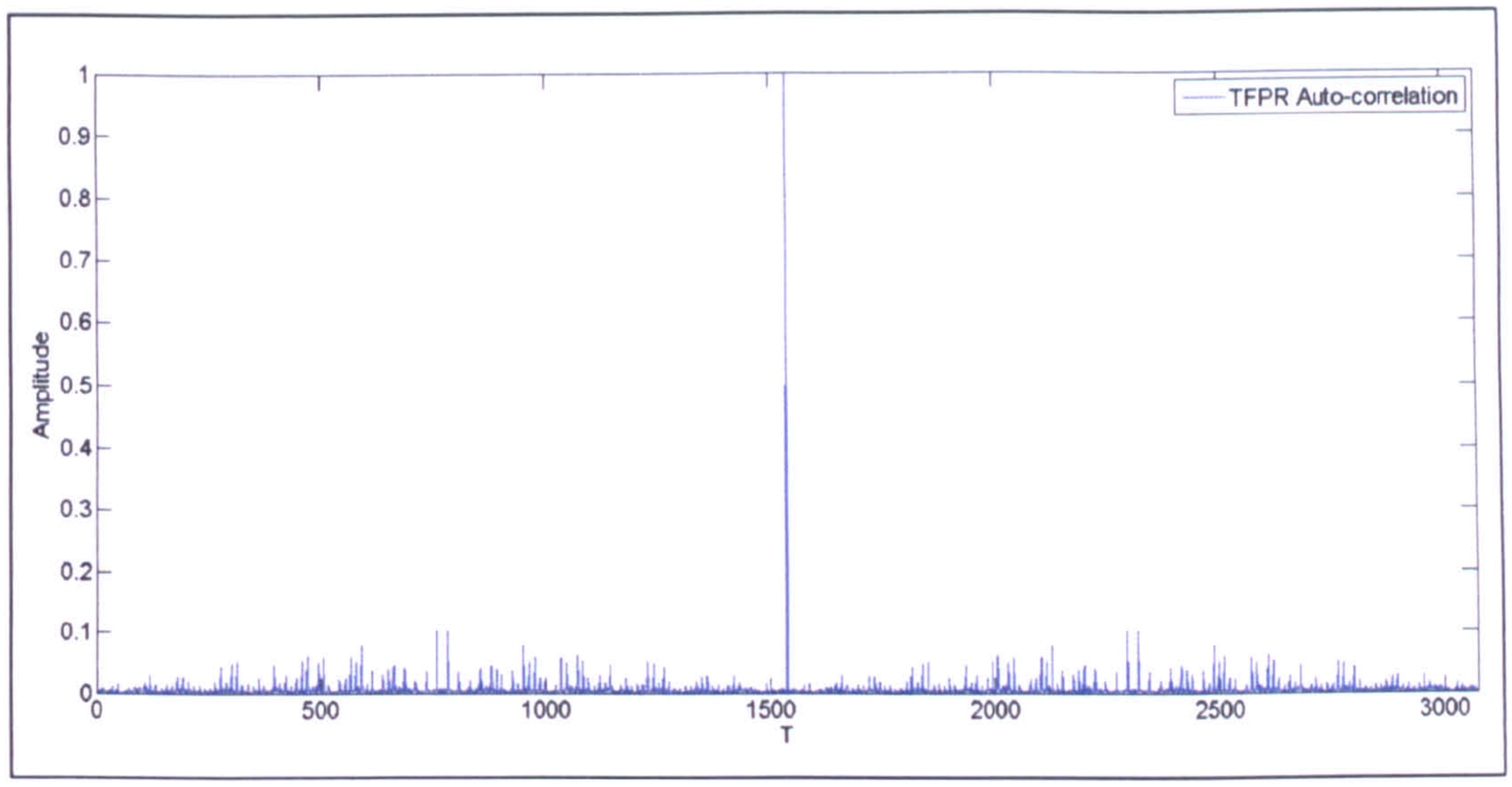

Figure 6-13: Auto-correlation of generated TFPR symbol

In this plot it can clearly be seen that the auto-correlation maximum at position 1536T has amplitude of |1|.

6.6.3 Zero-padding

Now the symbol has been successfully created using the parameters described in (European Broadcasting Union, 1997), zero-padding must be applied in the frequency domain in order to match the size of the capture window.

The re-sampled capture window has a length of 2048T, which is composed of 1536 useful OFDM carriers, 1 suppressed central carrier and a fringe either side of the signal of length 256T (from -769 to -1024 kHz and +768 to +1024 kHz). The TFPR symbol as it stands currently has a window width of 1537T. Therefore, in order to match the received symbol, the fringes of the generated symbol must be zero-padded so that they match.

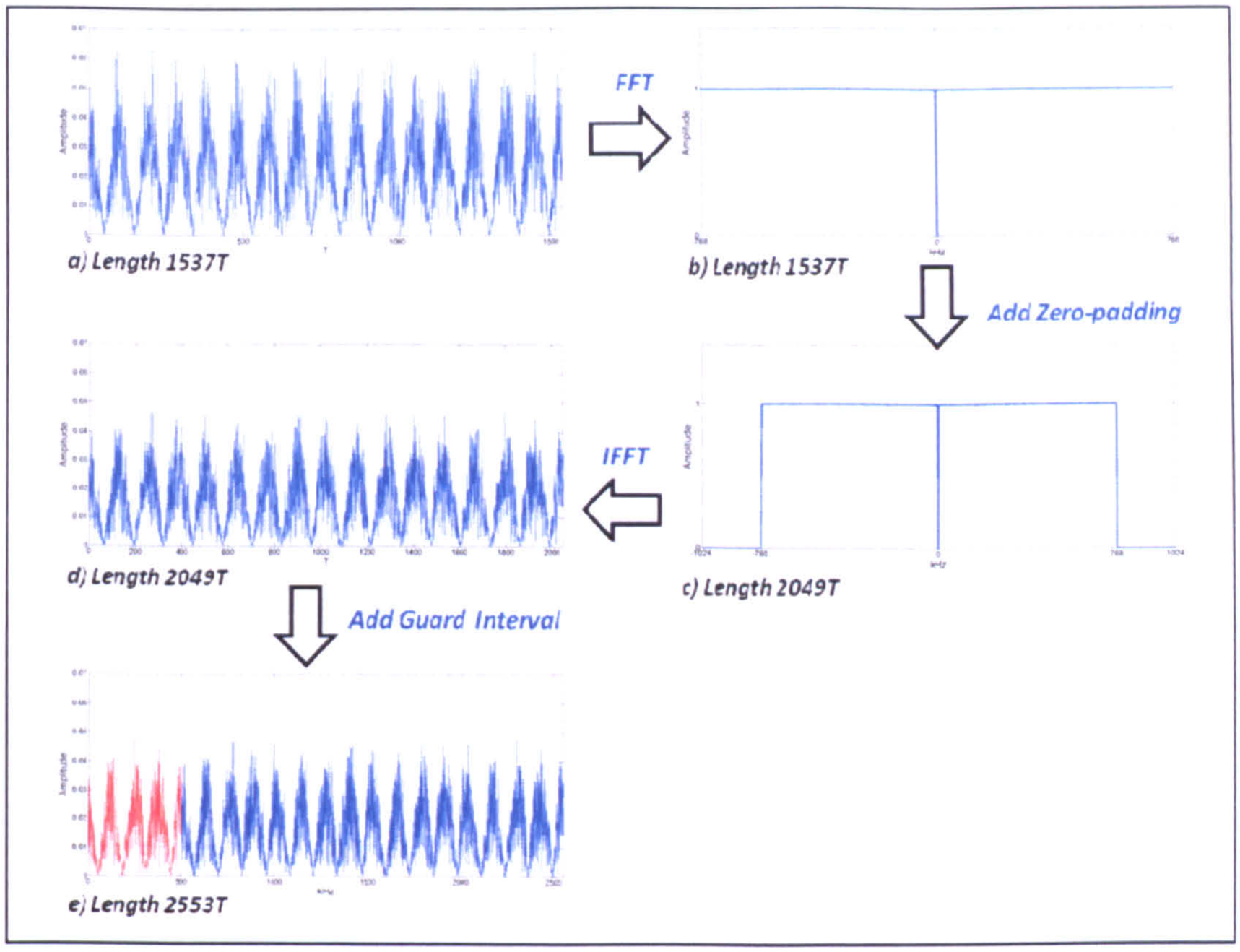

Figure 6-14: Modification of the basic TFPR symbol within receiver

The charts (***a*** – ***e***) in Figure 6-14 show the five step process the receiver generated TFPR symbol must undergo in order to match the received signal. This process is undertaken as opposed to further processing of the received signal in order to provide the longest possible code length which becomes important in the following section.

Chart ***a*** shows the modulus of the TFPR symbol as defined by the ETSI specification (European Broadcasting Union, 1997) and represented in the temporal domain. This symbol is processed using an FFT in order to present the symbol in the frequency domain. Chart ***b*** in Figure 6-14 shows the result of this process and highlights the constant amplitude nature of the symbol in the frequency domain. Chart ***c*** shows the position of the zero-padding placed either side of the OFDM symbol in order to expand and match the capture window (2049T). This is passed back through an inverse FFT to represent the signal in the temporal domain. The symbol is now in a

position to perform cross-correlation with the received symbol established in section 6.5.

6.7 TFPR Cross-Correlation

The cross-correlation process involves the comparison of the IQ values in the received and generated symbols in order to establish the correlation coefficients of each. It has already been shown that the auto-correlation function (the correlation of the generated function with itself) has excellent and easily distinguishable code correlation properties.

There are a number of additional factors to examine at this point. Firstly it is known that each signal will travel through a unique channel containing background additive white Gaussian noise (AWGN) and or channel fading dependant on the surrounding structures. Secondly, there will likely be more than one signal arriving at the receiver on the same frequency, and this could arrive before, at the same time or after the arrival of the primary (strongest) signal. The signal that the software receiver initially locks on to is defined by the null symbol search and subsequent definition of the first OFDM symbol as detailed in 6.3 and 6.4.

In order to establish the strongest possible cross-correlation, simulations can be performed involving changing some of the key characteristics of the incoming signals. The following sections (6.7.1 to 6.7.5) show the simulation processes and the conclusions that can be drawn from them.

6.7.1 Comparing the TFPR sequence length (auto-correlation)

This simulation compares the varying lengths of the TFPR symbol which were shown in 6.6.2, using the symbol in the following states:

1. The sequence as defined in the ETSI specification - length 1536T.

2. As 1 with the addition of the central carrier – length 1537T.
3. As 2 with the addition of the zero-padding in the frequency – length 2049T.
4. As 3 with the addition of the guard interval – length 2553T.

The correlation is performed using the complex signal in the temporal domain and is displayed in Figure 6-15, with the results of the maximum peak correlation coefficients in the table below. The side lobes represent the amplitude of the correlation coefficients at ± 1 lag from the maximum peak. The importance of this will become relevant later when multiple signals and multipath are examined.

TFPR Symbol Length	*Max Peak Amplitude*	*Side "Lobes" Amplitude*
1536T	1.0000	0.0004
1537T	0.9993	0.0007
2049T	0.7496	0.2245
2553T	0.9326	0.2761

Table 5: Results when comparing TFPR sequence length for cross-correlation

Clearly the shortest length of symbol yields the highest maximum peak amplitude possible in this test.

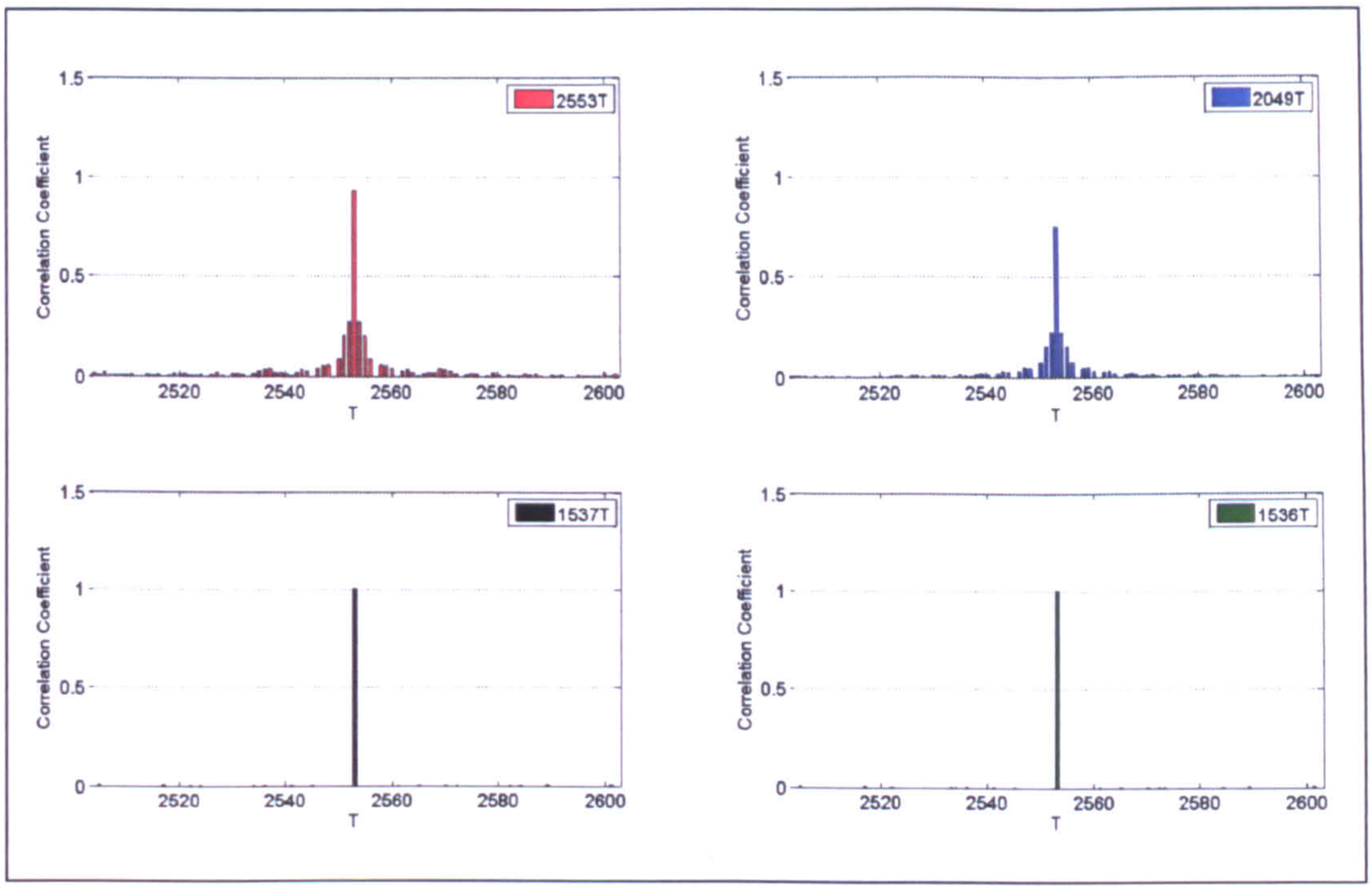

Figure 6-15: Comparison of TFPR length auto-correlation

6.7.2 Comparing TFPR sequence length with additional delayed signals

The process now moves on to look at adding an additional two signals to this channel and performing the test again. The two weaker signals will be simulated so one arrives slightly before the primary (strongest) signal and the second slightly after. The values for this simulation are shown below:

Signal	*Lag (T)*	*Relative Power*
Signal 1 (Primary)	0	100%
Signal 2	-25T	60%
Signal 3	+35T	30%

Table 6: Simulation parameters

Each TFPR signal is produced from the basic generated sequence, with the channels zero-padded in the temporal domain to create the correct length (for example, zero-pad of 25T, the 2553T of the TFPR symbol and zero-pad of 35T). Signals 2 and 3 are

also given a reduced power as a percentage of the primary signal, which is the signal the earlier processing will align with.

For example, Figure 6-16 shows this process in diagrammatic form. Three signals are shown with different lags. Diagram a) shows the null end position of the strongest signal being found and the total symbol length and hence guard interval and useful symbol defined. Diagram b) shows the removal of the remainder of the two secondary signals while diagram c) shows the final portion of the incoming signal about to be passed through a FFT.

This means that power is being lost from the secondary signals, which are thus receiving less-obvious correlation peaks.

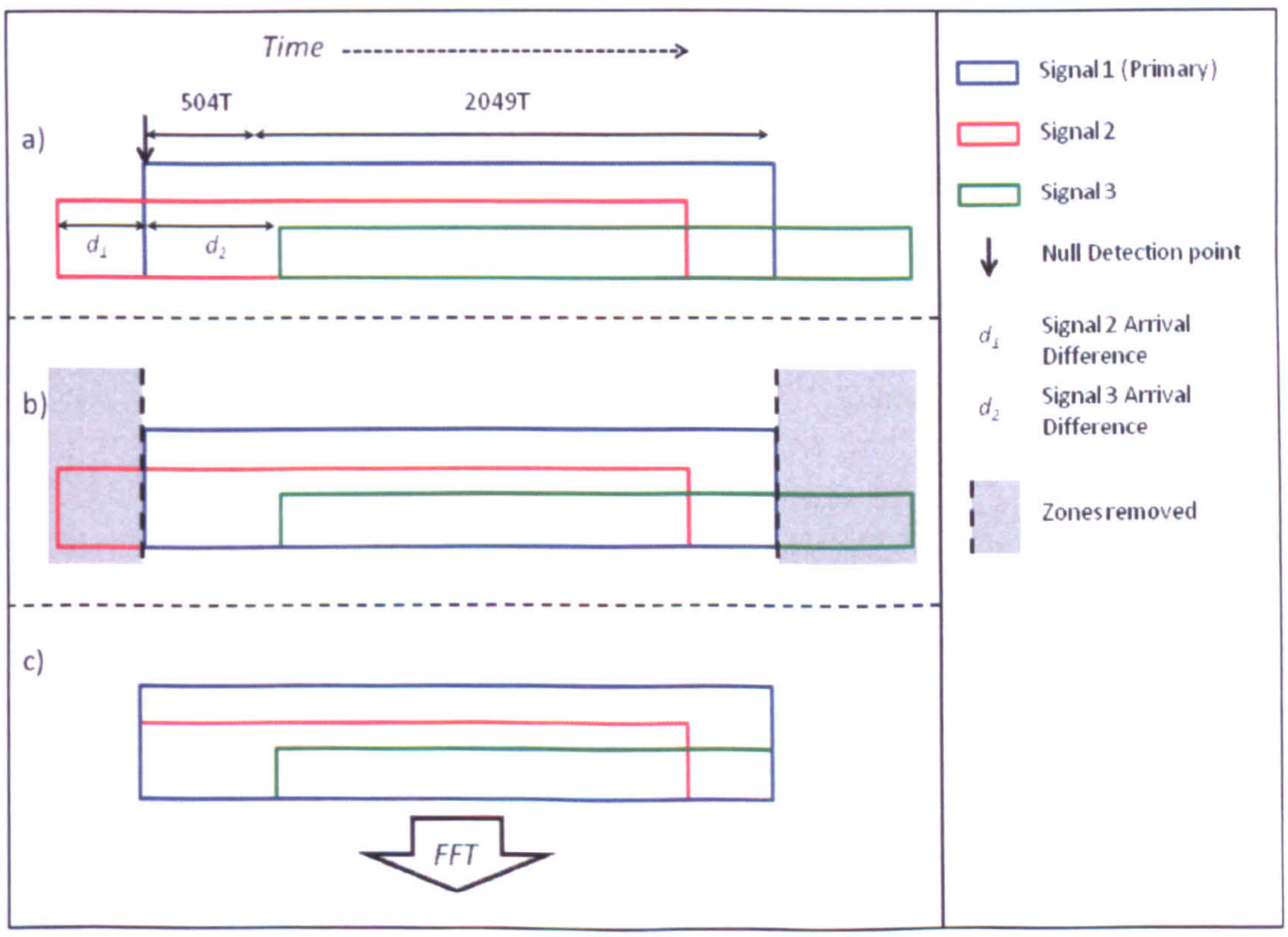

Figure 6-16: Processing window problem

The outcome of this simulation can be seen in Figure 6-17.

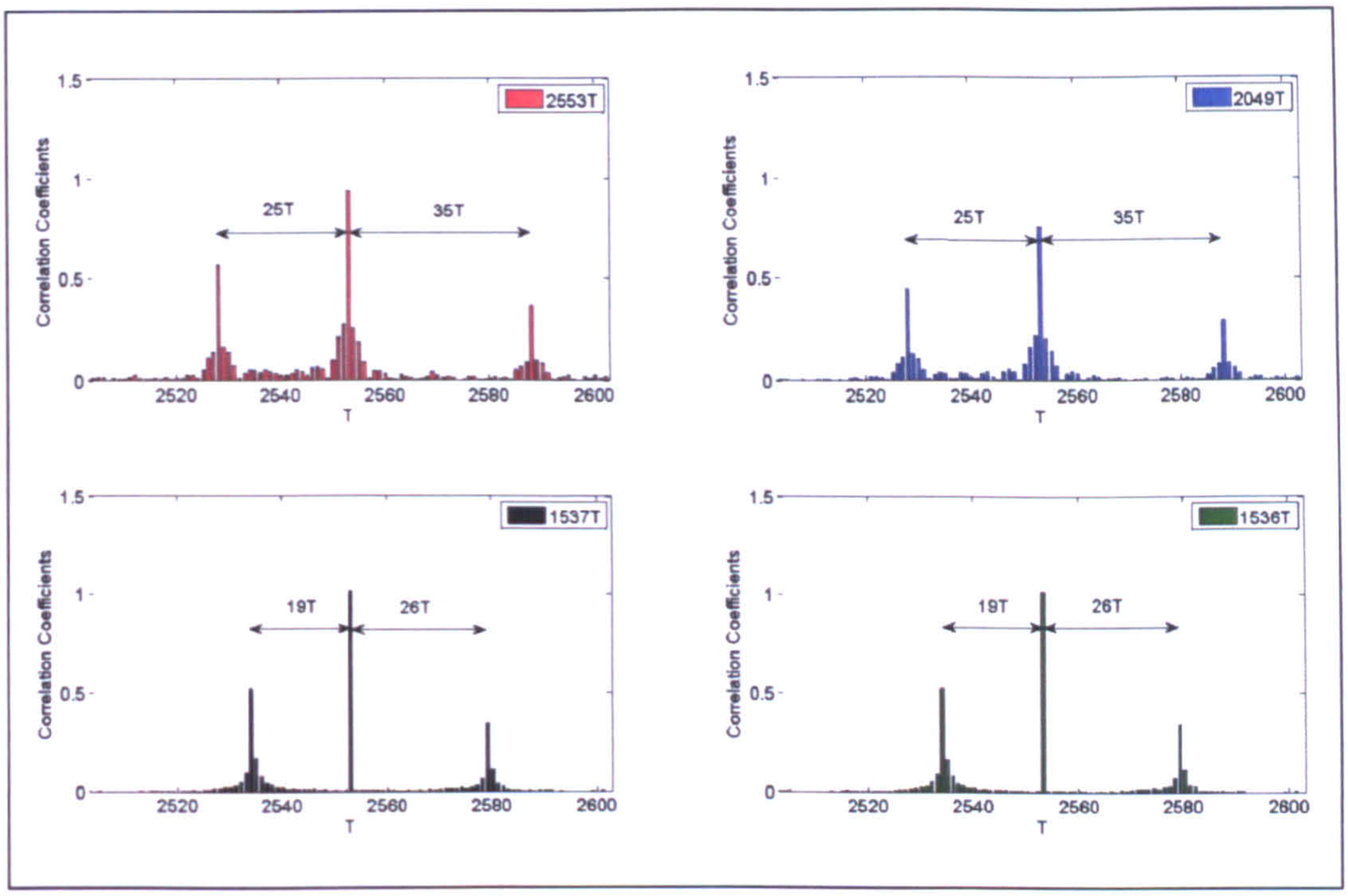

Figure 6-17: Comparison of TFPR symbol length cross-correlation

All four of the cross-correlation functions clearly show the three signals, with the results shown below in Table 7.

Sequence	*Measurement*	*Signal 1*	*Signal 2*	*Signal 3*
1536T	*Correl. Coeff.*	1.008	0.5272	0.3464
	Measured Lag (T)	0	-19	+26
1537T	*Correl. Coeff.*	1.007	0.5234	0.3483
	Measured Lag (T)	0	-19	+26
2049T	*Correl. Coeff.*	0.7556	0.4472	0.2936
	Measured Lag (T)	0	-25	+35
2553T	*Correl. Coeff.*	0.9405	0.5634	0.3691
	Measured Lag (T)	0	-25	+35

Table 7: Results from simulation of multiple delayed signals

This immediately shows that the two secondary signals lag measurements for the sequence lengths 1536T and 1537T are incorrect (highlighted in grey), although their cross-correlation properties appear to be better defined.

The error in these sequences is directly related to the ratio of the difference in sequence length:

$$T_t = \left(\frac{2048}{1536}\right) \cdot T_c \qquad 6.9$$

Where T_c is the measured signal delay and T_t the true signal delay. This difference provides the Time Difference of Arrival measurement required to calculate the position of a receiver.

6.7.3 Comparing TFPR sequence length through noisy channels

The same simulation in 6.7.2 is now performed but in this instance varying amounts of AWGN are added to each channel. It is assumed that the weaker the incoming secondary signal is relative to the primary signal, then the lower the Signal-to-Noise ratio (SNR) will be. The values applied are shown below in Table 8:

Signal	*Lag (T)*	*Relative Power*	*SNR (dBW)*
Signal 1 (Primary)	0	100%	50
Signal 2	-25T	60%	30
Signal 3	+35T	30%	15

Table 8: Simulation parameters for 6.7.3

As it is known where the cross-correlation peaks are going to be already, it is still easy to spot them (Figure 6-18), however, using a searching algorithm for this process may prove more difficult due to the amplitude and proximity of peaks which are not secondary transmissions. In particular, signal 3 (the smallest of the three peaks, marked with an arrow on each chart) has a number of correlation peaks in the vicinity of the true signal which could cause an incorrect match in the receiver. As would be expected, the ambiguous correlation peaks are most apparent in the two smaller code

sequences of 1536T and 1537T, with the maximum code length of 2553T yielding the clearest correlation spikes.

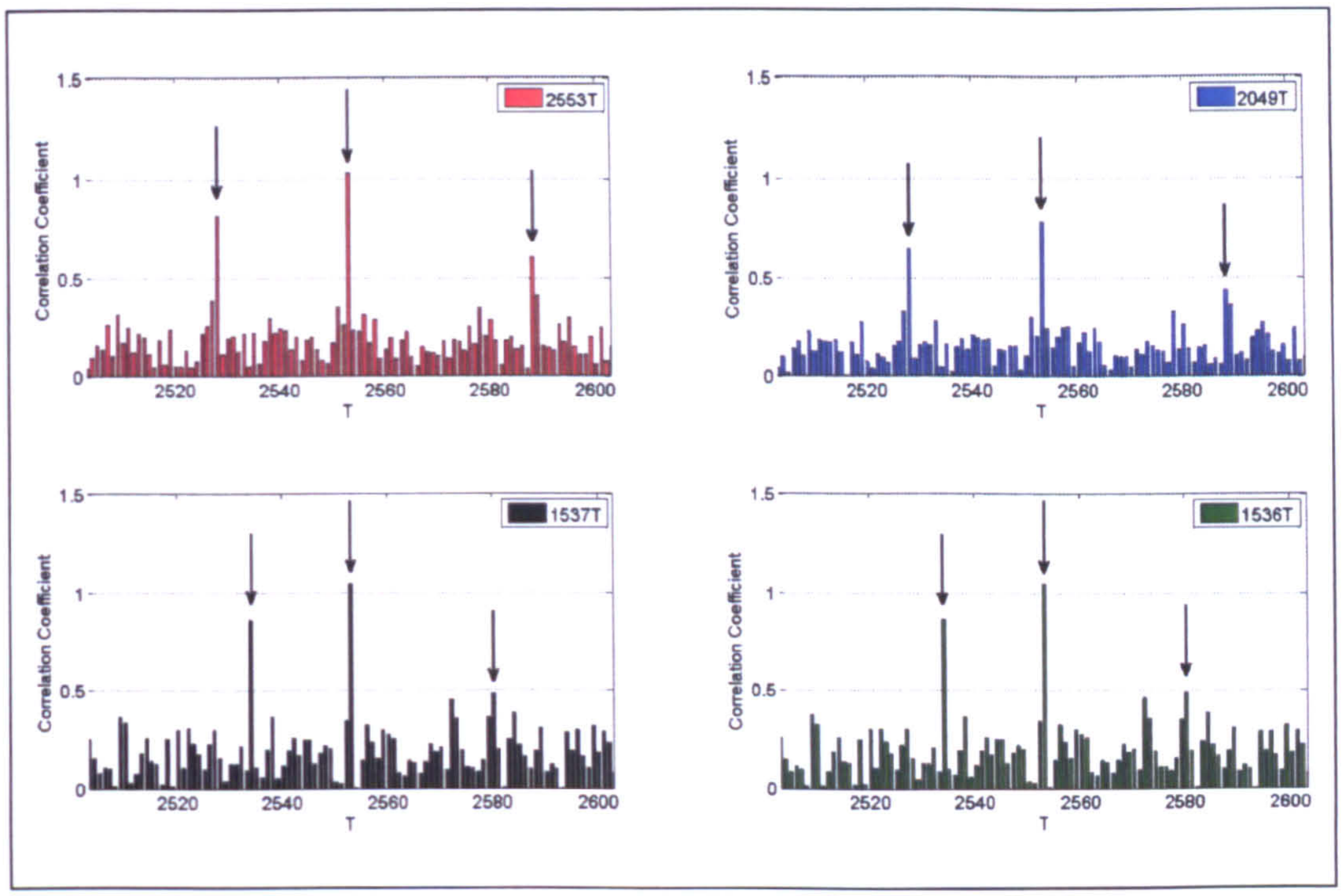

Figure 6-18: Comparing TFPR symbol length cross-correlation with varying SNR

The scenarios in 6.7.2 and 6.7.3 have both used the same secondary signal delays; however, as the null detection algorithm "locks" onto the strongest signal which then defines the symbols (+2553T from the null detection position), the full power of these additional signals is not being used (as shown earlier in Figure 6-16).

6.7.4 Cross-correlation over a wider input window

The problem highlighted in section 6.7.3 can be recovered by running the cross-correlation over a longer symbol length. This means that the two shorter TFPR sequences (1536T and 1537T) can no longer be used, as in order to do this the incoming symbol must be passed in the temporal domain through a FFT, remove the

"empty" carriers and then back through an IFFT to perform the cross-correlation in the temporal domain.

Therefore, both the 1536T and 1537T sequence lengths can now be ignored. The remainder of this section will concern only the 2553T sequence as the tests undertaken so far have shown that it has outperformed the 2049T sequence, giving results with higher correlation-peak to noise ratios and correct lag times.

This simulation, as with previous ones, assumes that the null detection algorithm has run meaning that the process is in a position to define symbols. Rather than extract the 2553T length of the incoming signal, this is extracted in addition to ±504T (guard interval length) giving a total incoming symbol length of 3561T.

This can be done as it is known that any overlapping transmitter footprints are designed to arrive in the guard interval of each, due to the precise synchronisation of the networks (European Broadcasting Union, 1997, Hoeg and Lauterbach, 2003).

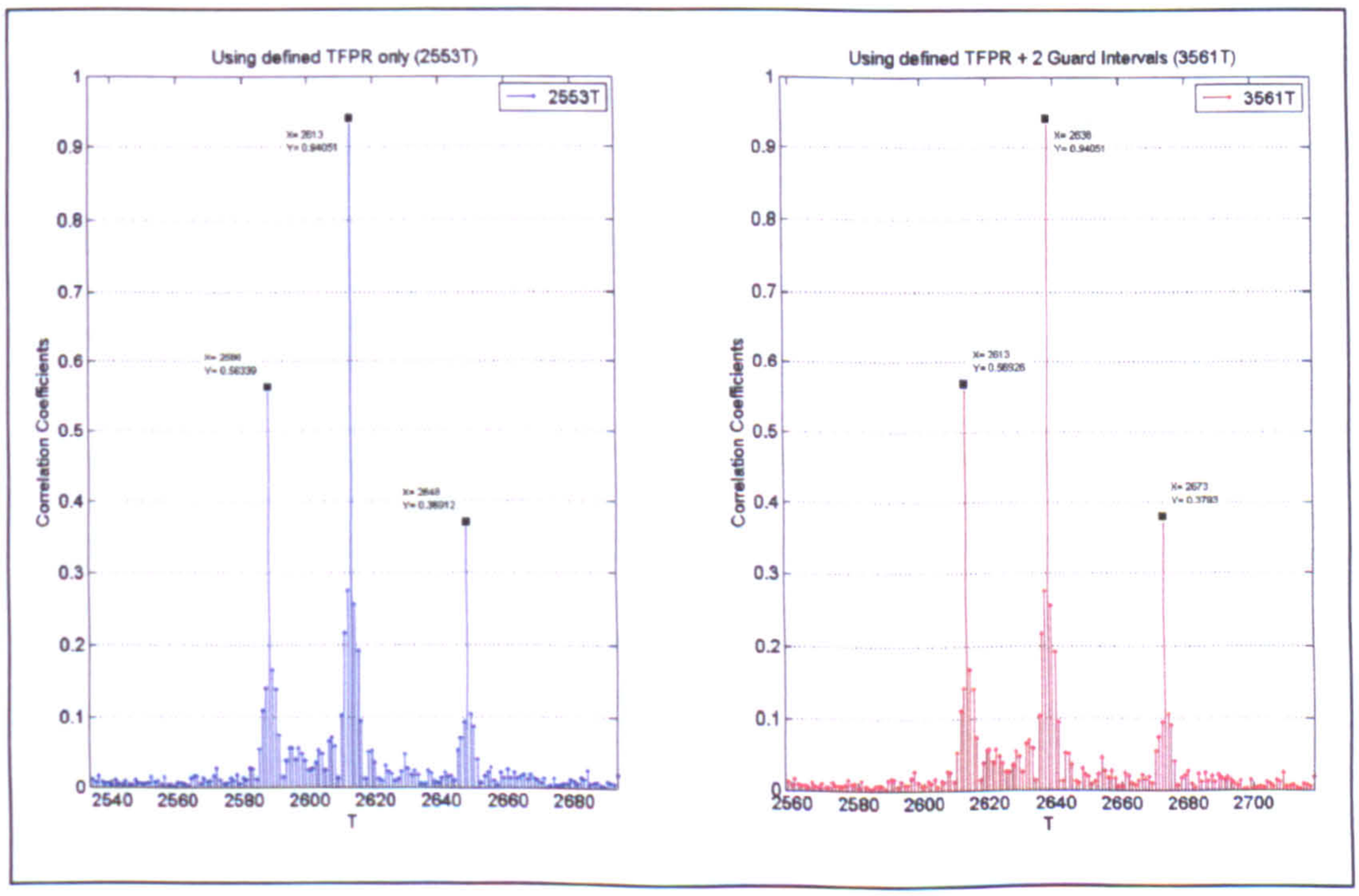

Figure 6-19: Comparing TFPR Symbols

Using the defined TFPR symbol only (2553T) (left) and the defined TFPR plus two Guard Intervals (504T + 2553T + 504T) (right)

The charts in Figure 6-19 show the process used previously on the left (comparing the incoming 2553T and the generated 2553T), and the process proposed above using an additional 504T at either end of the defined symbol (right plot). As would be expected, the correlation coefficient value of the primary signal remains the same as the complete symbols energy are used in both cases; however, the two secondary signals show a marginal increase in amplitude on the right plot. Although the increases shown here are small, if the secondary signal lag was measured in the hundreds of T, then a substantial amount of signal power would be lost using the earlier method. Reclaiming this power helps to define the correlation peaks at their maximum amplitude and allow the receiver to identify them as easily as possible.

6.7.5 Conclusions

This section has examined the variety of ways lags might be measured between multiple arriving signals. Simulations have been used to investigate the addition of noise, the separation of multiple signals arriving at different lags and at different SNR. The use of different sequence lengths has also been examined in addition to their auto and cross-correlation properties, and deciding upon a particular approach to use in the processing of real signals.

The distance between lags (in T) will be used as the TDOA measurements to calculate the position of a receiver using the Least Squares process (described in 6.10). However, before this can be performed, the locations of the transmitters themselves must be determined. The subsequent chapter will examine this process.

6.8 TRANSMITTER IDENTIFICATION INFORMATION (TII)

The Transmitter Identification Information (TII) codes embedded in the DAB signal are broadcast every second frame and contain unique codes allowing a receiver to theoretically identify the region it is located in and the transmitters that information is currently being received from.

The code is defined by a basic Frequency Division Multiplexing (FDM) approach with each transmitter switching on pairs of carriers during the TII null period which are subsequently decoded in the frequency domain. The code is divided into two parts; firstly the region code or pattern number p is defined by the pattern of the switched-on neighbouring carrier pairs in the frequency domain and secondly, the transmitter code or comb number c is represented by the position of these carrier pairs on the frequency axis.

In transmission mode I, this code is spread over a bandwidth of 384 kHz and then repeated three times to cover a total bandwidth of 1537 kHz (1536 with the removal of the suppressed central carrier). The purpose of this is to allow a receiver to decode the TII even when there is heavy fading present on the broadcast channel.

The TII signal $S_{TII}(t)$ broadcast from a particular transmitter is defined by equations 6.10 to 6.14, found in (European Broadcasting Union, 1997):

$$S_{TII}(t) = Re\left\{e^{2j\pi f_c t}\sum_{m=-\infty}^{+\infty}\sum_{k=-K/2}^{K/2} z_{m,0,k} \times g_{TII,k}(t - mT_F)\right\} \qquad 6.10$$

Where: $$g_{TII,k}(t) = e^{2\pi jk(t-T_{NULL}+T_U)/T_U} \times Rect(t/T_{NULL}) \qquad 6.11$$

T_{NULL} is the length of the null symbol (2656T); T_U is the length of the useful OFDM symbol (2048T) and f_c is the centrally tuned frequency of the DAB signal.

The function Rect(t) is defined as:

$$\text{Rect}(t) = \begin{cases} 1 & if\ 0 \leq t < 1 \\ 0 & if\ t < 0\ or\ t \geq 1 \end{cases} \qquad 6.12$$

$$z_{m,0,k} = A_{c,p}(k) \times e^{j\varphi_k} + A_{c,p}(k-1) \times e^{j\varphi_{k-1}} \qquad 6.13$$

The sequences are encoded within the null symbol of the relevant frame and, as with the processing of the OFDM symbols, are decoded in the frequency domain. During the null period, a number of sub-carrier pairs are switched on and each of these sub-carriers broadcasts a complex number ($z_{m,0,k}$) which is defined by equation ***6.13***, where the individual carrier positions (k) are defined by the region and transmitter codes.

$$A_{c,p}(k) = \begin{cases} \sum_{b=0}^{7} \delta(k, -768 + 2c + 48b) \times a_b(p), & -768 \leq k < -384 \\ \sum_{b=0}^{7} \delta(k, -384 + 2c + 48b) \times a_b(p), & -384 \leq k < 0 \\ \sum_{b=0}^{7} \delta(k, 1 + 2c + 48b) \times a_b(p), & 0 < k \leq 384 \\ \sum_{b=0}^{7} \delta(k, 385 + 2c + 48b) \times a_b(p), & 384 < k \leq 768 \end{cases} \qquad 6.14$$

The values for $a_b(p)$ can be found in Table 14 on page 217, where δ is known as the *Kronecker* symbol. This is defined as:

$$\delta(i,j) = \begin{cases} 1 & if\ \ i = j \\ 0 & if\ \ i \neq j \end{cases} \qquad 6.15$$

6.8.1 TII Example

Once broadcast and defined at the receiver, the TII signal is presented in the frequency domain. Figure 6-20 shows how a perfect TII signal would appear. In this instance

the region code 69 is being broadcast (binary value 1 1 1 1 0 0 0 0). Each black line represents a pair of carriers spaced by 1kHz, with each bit in the 8-bit sequence separated by 48kHz. As the code is repeated three times across the bandwidth of the signal, the code is represented twice either side of the central frequency f_c.

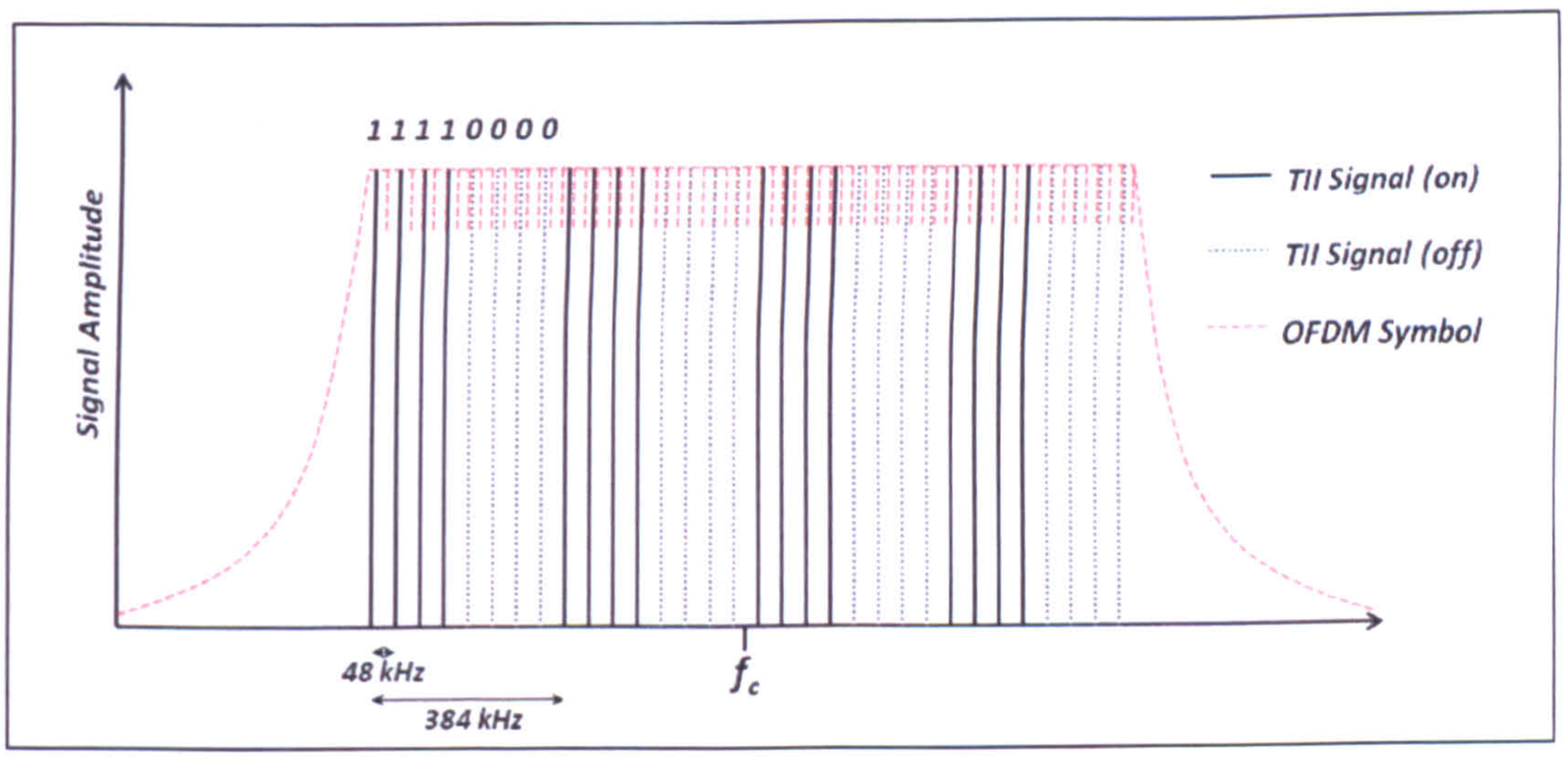

Figure 6-20: Example of TII signal represented in the frequency domain

This process makes the TII symbol easy to identify if there is only one transmitter present, but to be able to position the receiver then a minimum of three (or later, two) transmitters on one transmission block is required in addition to the need to distinguish between them.

6.8.2 Code Separation

The following section will examine the use of real data captured and processed at a known location, and attempt to separate and identify multiple transmitter TII signals within a capture. In this process, the primary null has already been identified and therefore the symbol lengths defined. The length of the null symbol is known so this portion can be extracted, however at this point the reader should refer again to Figure 6-6 on page 76. This plot shows where the null symbol is, providing there is only one

signal present. It also shows the region (green box) where the overlap from subsequent signals is present.

As has been stated previously, it is known that signals can only arrive in the guard interval of the closest/strongest signal; therefore it is subsequently known that the minimum portion of the null symbol where the TII symbol is not swamped by the final OFDM of the secondary transmission (the useful portion of the null symbol) will be:

$$T_{WIN} = T_{NULL} - T_{GI} \qquad \textbf{6.16}$$

Where T_{NULL} is the length of the null symbol and T_{GI} the length of the guard interval. In the case of transmission mode I, the value for T_{WIN} used here is 2152T. Therefore a window of length 2049T can be defined back from the null symbol detection position in the temporal domain and the result run through an FFT, giving the correct carrier 1 kHz separation allowing the receiver to decode the TII.

If trying to detect the presence of multiple weak signals, this process can be performed iteratively (see Figure 6-21), shifting the 2049T window by 1T (Δ) until the start of the TFPR symbol is reached.

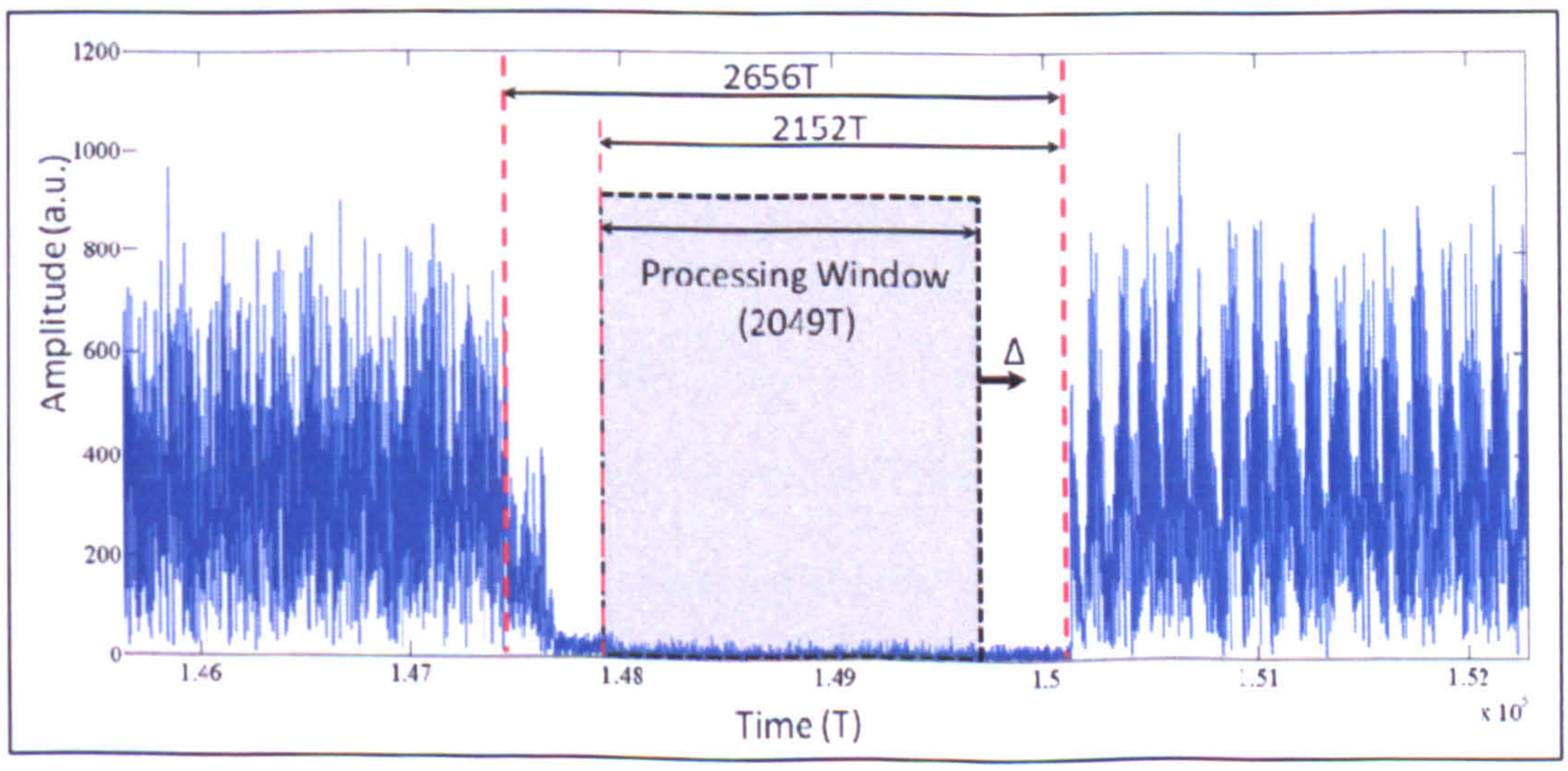

Figure 6-21: Processing the TII using an iterative processing window

The results may then be averaged in order to extract as much power from each signal as possible. The result is then displayed in the frequency domain (Figure 6-22).

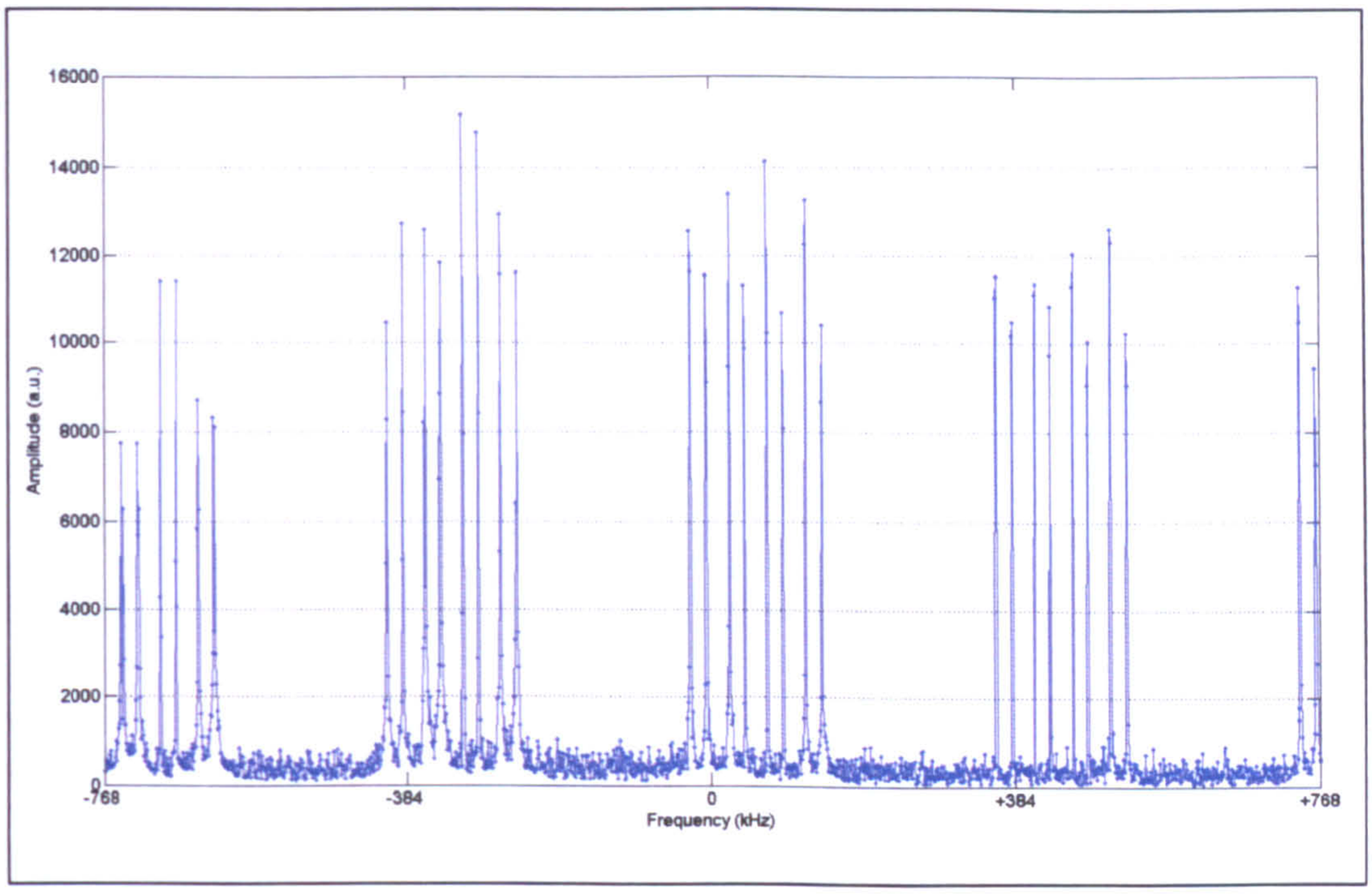

Figure 6-22: TII Signal in the frequency domain

It is known that the TII code is broadcast four times over the bandwidth of the signal, therefore, the resulting frequency plot can be divided into four with the result being averaged in order to search for the region codes used in the broadcast. The result of this is shown plotted in Figure 6-23. This is the maximum TII power that can be received in a single frame.

6.8.2.1 Finding the Region Codes

In order to identify the transmitters received and hence the transmitter positions, the region (or regions) currently being received must be correctly identified. As has been shown previously, there are a maximum of 70 region codes (0 - 69) used on band III transmissions in the UK, so in order to identify the correct regions, each code in the frequency domain must be constructed with the purpose of testing these against the received code.

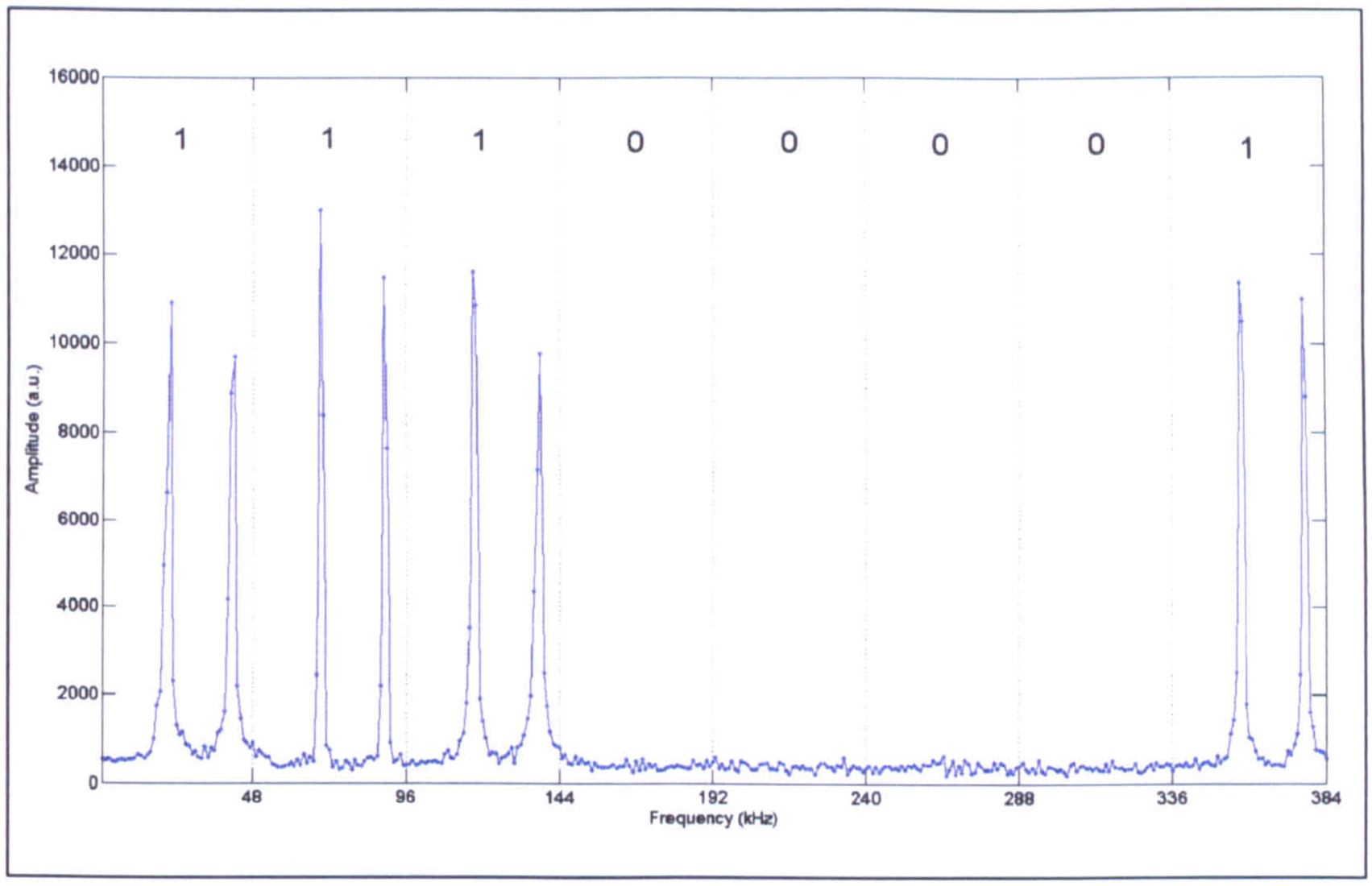

Figure 6-23: Averaging the four TII quadrants

Referring again to Figure 6-23, it can be seen that the frequency axis has been subdivided into the eight 48kHz TII code bits, and in this scenario it is clear that the region code has a binary value of "**1 1 1 0 0 0 0 1**". This code can be cross-referenced with Table 14 on page 217 in order to determine the final region (65 in this case).

In order to perform this in the receiver with optimum efficiency, the region codes used in the UK at the current time are generated. At the time of writing there were 18 different regions in the UK, therefore the binary values of each are used to switch bits on and off accordingly. The mean value of the amplitudes of each carrier pair are taken for each code. This can be visualised by plotting, as seen in Figure 6-24 and then by "flattening" the 3D plot along the Region Codes axis, giving the maximum amplitude of all codes at each 1kHz spacing and identifying the code associated with each maximum. In Figure 6-24, the right hand plot shows this flattening, allowing identification of the maxima in each code.

A similar example is shown in Figure 6-25; however in this example the receiver is using the national commercial network and receiving transmissions from seven transmitters across three regions.

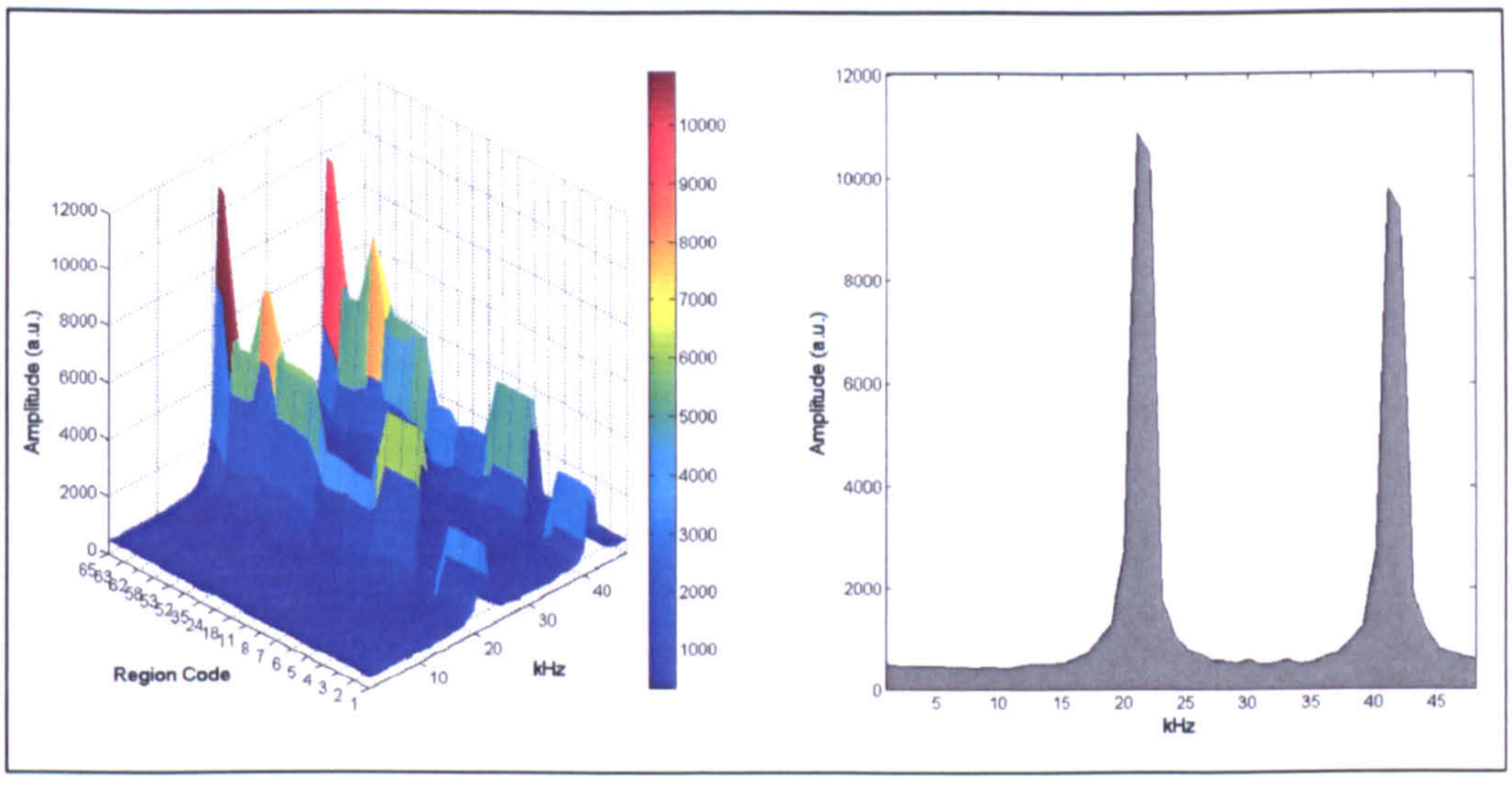

Figure 6-24: Testing UK region codes against received TII – Simple example

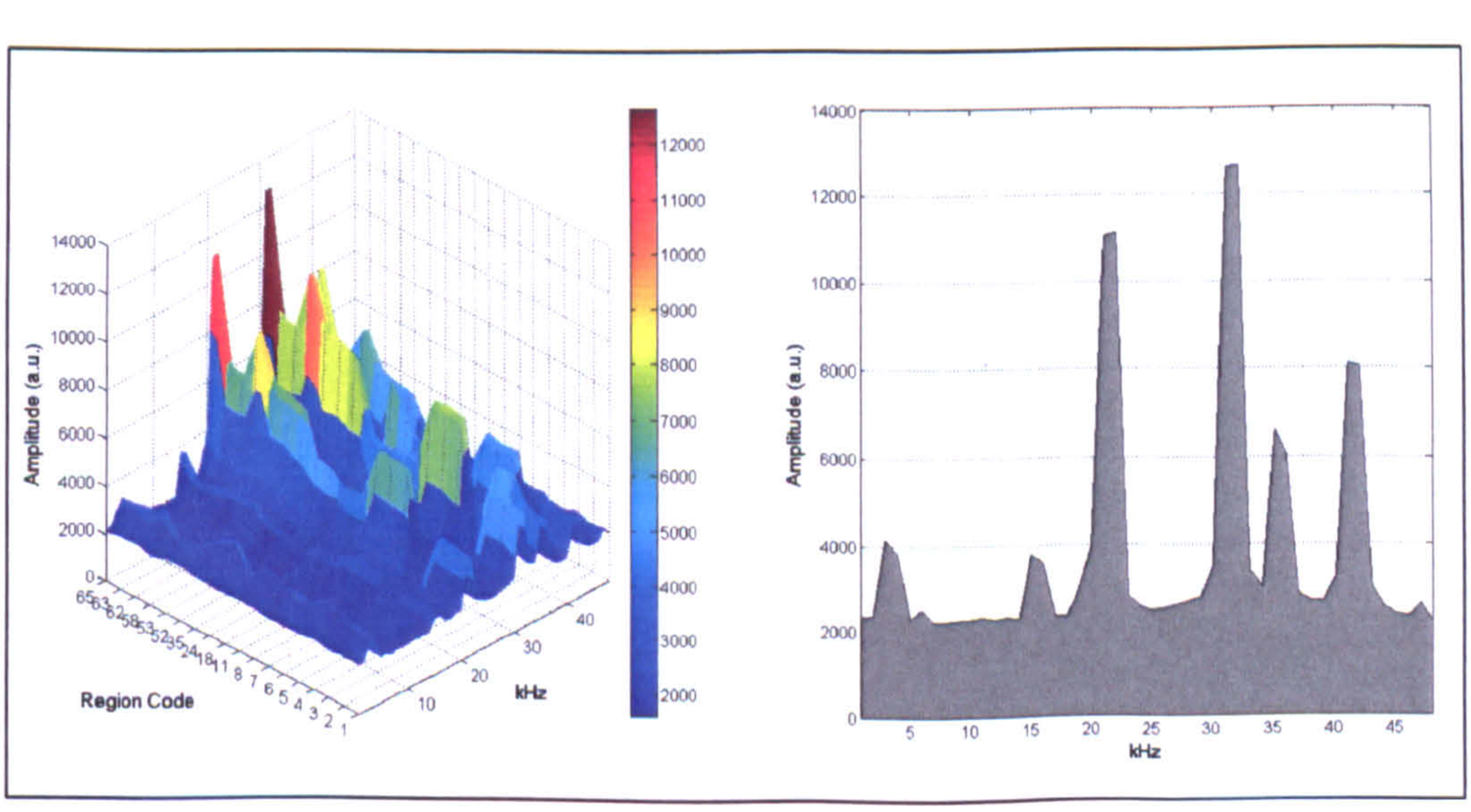

Figure 6-25: Testing UK region codes against received TII – Complex example

At this stage a position has been reached to identify the individual transmitter codes.

6.8.2.2 Finding the Transmitter Codes

As has been mentioned previously, each transmitter broadcasts its signal as a pair of carriers when viewed in the plots in Figure 6-24 and Figure 6-25. The region codes for each of the identifiable carrier pair peaks are now known and the transmitter itself may be identified by identifying the x-axis intercept of these peaks and using equation 6.14. Once identified, this code can be cross-referenced with a database of individual transmitter codes available from (Moldon, 2010). This gives the location of each transmitter using the standard UK reference frame, OSGB36.

6.8.2.3 Transmitter Position Database Accuracy

The accuracy of the DAB transmitter database as found in (Moldon, 2010) is limited to an OS grid reference of $100m^2$, with each location listed as an OS grid reference. The grid reference details the lower left corner of the grid square the transmitter is located in, thus giving a position ambiguity of up to 141m (Figure 6-26).

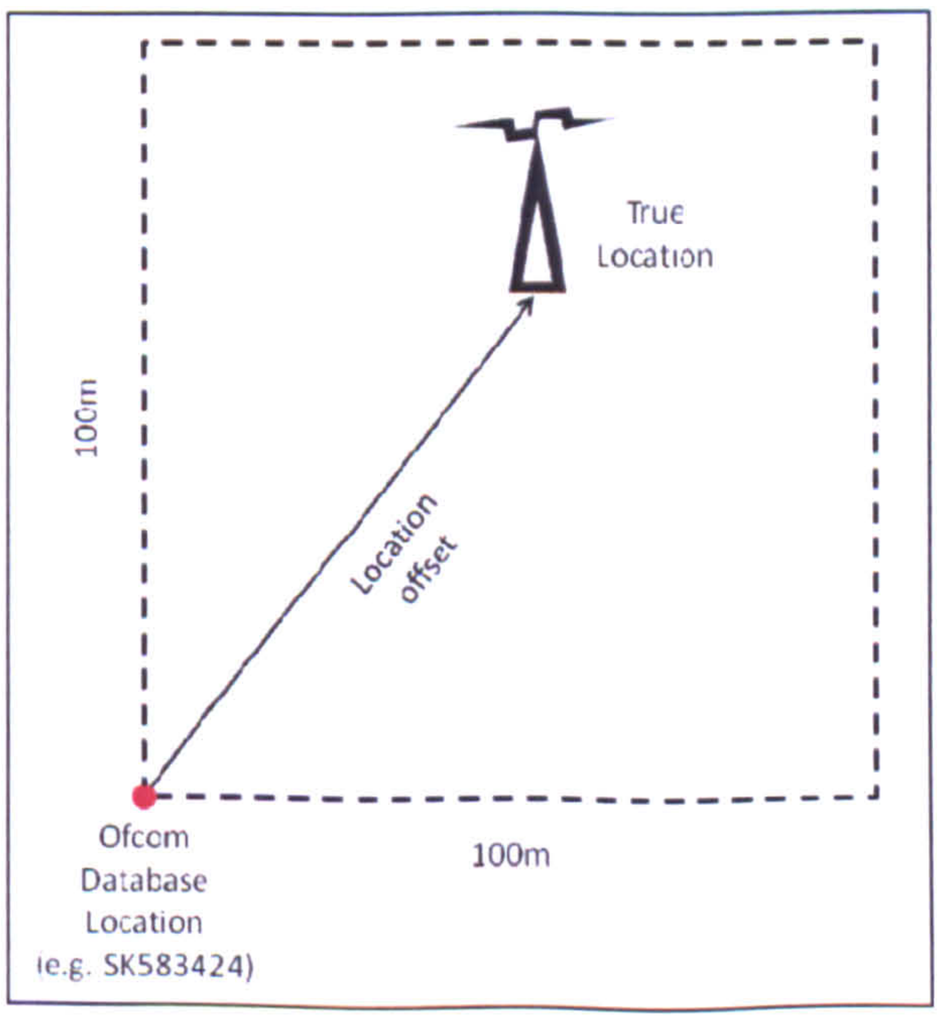

Figure 6-26: Transmitter location database accuracy

The effect of this potential offset will be examined later during the system testing phase of this project.

6.9 MATCHING CORRELATION COEFFICIENTS TO TII

At the current stage in the process, information from the raw signals has been successfully extracted; the timing information from the cross-correlation of the TFPR symbol and the transmitter identification from decoding the TII codes.

This now means that the two must be matched in order to be able to use the least squares positioning process. It can be seen in the following two charts (Figure 6-27 and Figure 6-28) that at least six transmitters are being received at the receiver's location. The transmitter TII codes as presented in Figure 6-27 show the varying amplitudes of each signal represented in the frequency domain, whilst the associated correlation coefficients in Figure 6-28 are represented in the temporal domain.

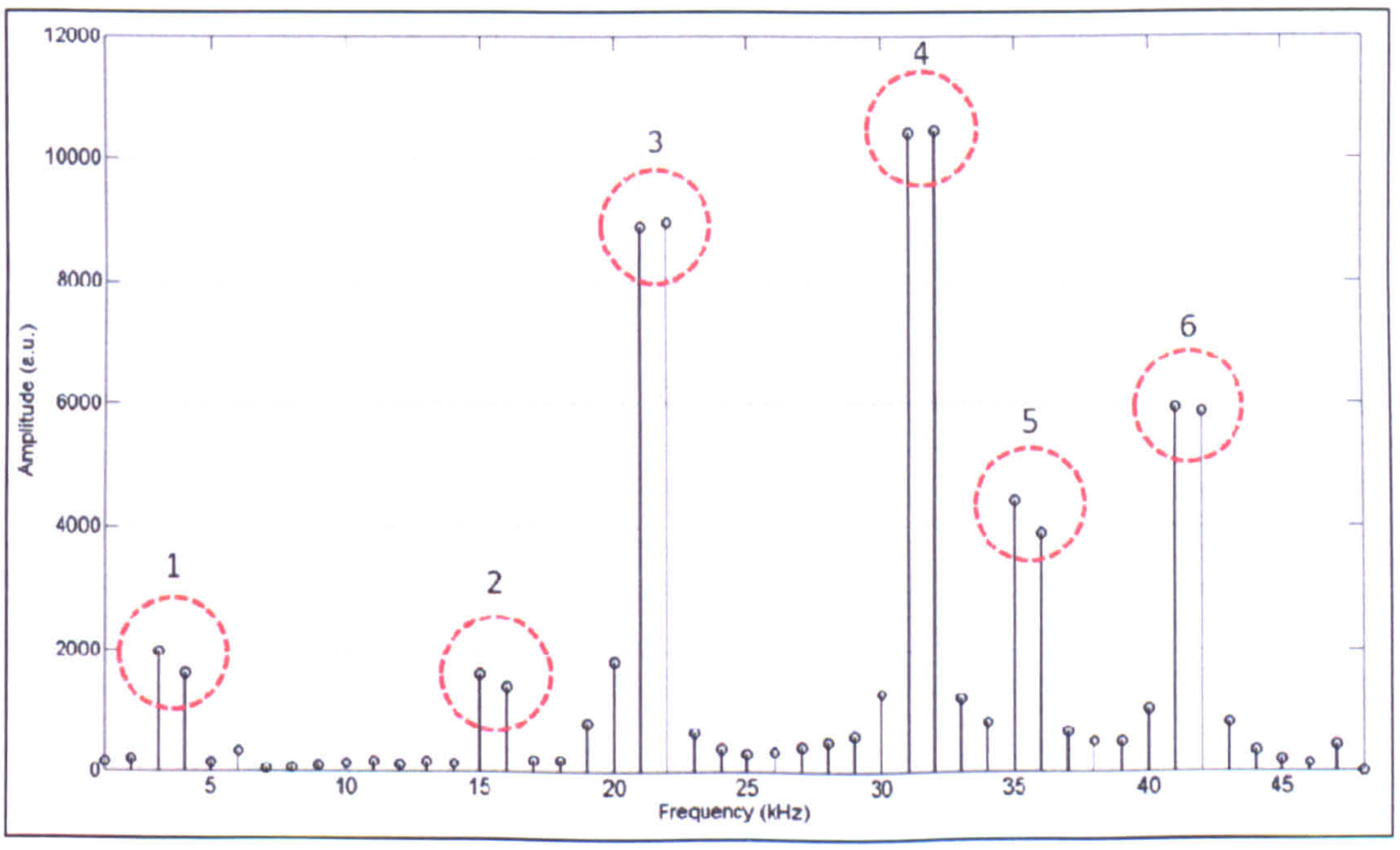

Figure 6-27: Example incoming TII Code

For each TII pair present, the average value of both carriers is taken and compared to the detected correlation peak values. When comparing Figure 6-27 and Figure 6-28, it can be seen that peaks occur at approximately the same amplitudes. For ease of viewing, these have been highlighted and numbered in both charts.

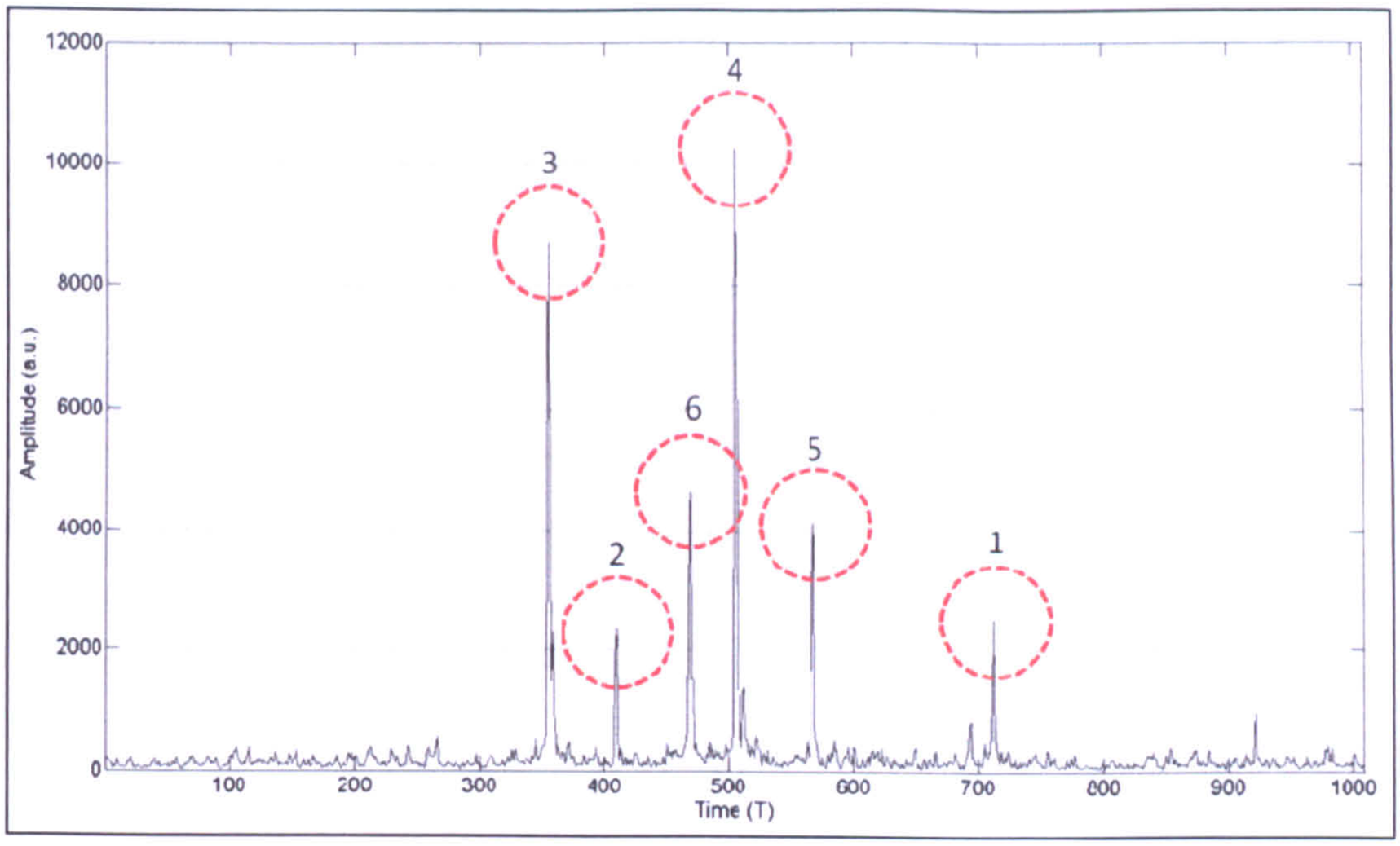

Figure 6-28: Example cross-correlation plot for Figure 6-27

Due to all transmissions emitting the same TFPR symbol, there is no way to separate them based on transmitted code. This also means that errors can be introduced into the system when two or more transmitter's timing information are incorrectly matched. Therefore, a threshold was built in to this part of the signal processing where coefficients of similar amplitudes are compared to all TII values extracted. This is an iterative process with each tested pair being passed to the following Least Squares process where most incorrectly matched pairs will not converge on a result. If more than one converged result occurs, then that with the lowest HDOP value is taken as the correctly matched pair.

6.10 POSITION ESTIMATION USING LEAST SQUARES

As the two key factors have now been established allowing the system to position a receiver, these values must be fed into a least squares process. This process is defined as follows. Firstly, as the position of the transmitters is known by decoding the TII signals, these positions can be plotted and the relative positions of the receiver as seen in Figure 6-29. In this case, the minimum of three transmitters have been identified, sufficient for a 2D position.

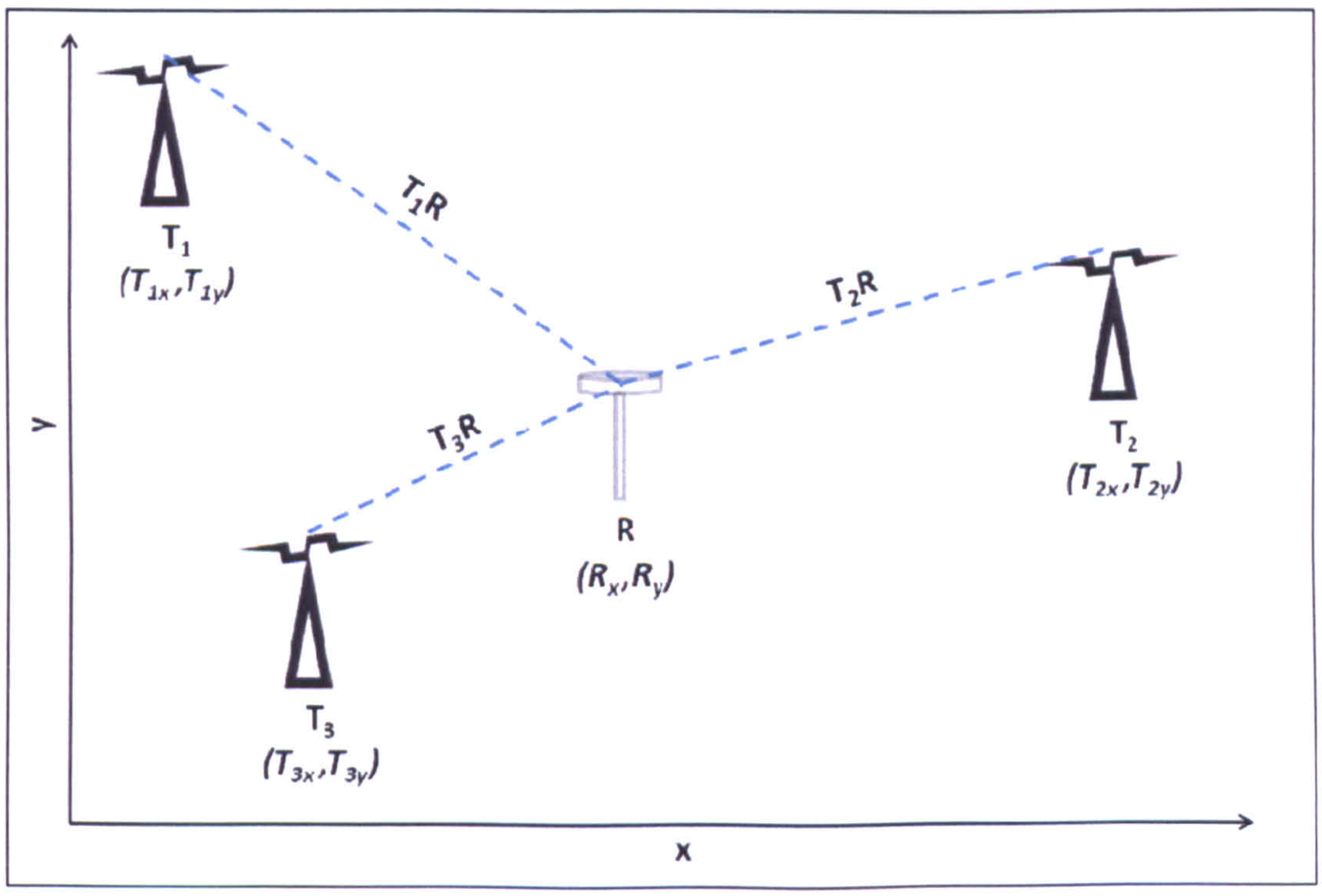

Figure 6-29: Test Layout of Transmitters & Receiver

The unknown ranges between each transmitter and the receiver R can be defined by equations 6.17 to 6.19:

$$T_1R = \sqrt{(R_x - T_{1x})^2 + (R_y - T_{1y})^2} \qquad 6.17$$

$$T_2R = \sqrt{(R_x - T_{2x})^2 + (R_y - T_{2y})^2} \qquad 6.18$$

$$T_3R = \sqrt{(R_x - T_{3x})^2 + (R_y - T_{3y})^2} \quad 6.19$$

Each range (T_1R to T_3R) can be expressed in terms of signal transition time (t_n) by dividing by the speed of light in a vacuum, c:

$$t_n = \frac{T_nR}{c} \quad 6.20$$

As the precise transmission time of each signal is not known, the TDOA values are used rather than TOA (both discussed in chapter 5); therefore two independent TDOA measurements at the receiver are defined relative to the ranges as:

$$TDOA_1 = |t_2 - t_1| \quad 6.21$$

$$TDOA_2 = |t_3 - t_1| \quad 6.22$$

Therefore the difference in ranges (z_{21} & z_{31}) can be defined as:

$$z_{21} = \sqrt{(R_x - T_{2x})^2 + (R_y - T_{2y})^2} - \sqrt{(R_x - T_{1x})^2 + (R_y - T_{1y})^2} \quad 6.23$$

$$z_{31} = \sqrt{(R_x - T_{3x})^2 + (R_y - T_{3y})^2} - \sqrt{(R_x - T_{1x})^2 + (R_y - T_{1y})^2} \quad 6.24$$

The terms in brackets can be defined and then expanded:

$$z_{nm} = \sqrt{a_n} - \sqrt{a_m} \quad 6.25$$

Where:
$$a_n = (R_x - T_{nx})^2 + (R_y - T_{ny})^2 \quad 6.26$$

And:
$$a_m = (R_x - T_{mx})^2 + (R_y - T_{my})^2 \quad 6.27$$

Expanding:
$$a_n = [R_x{}^2 - 2R_xT_{nx} + T_{nx}{}^2] + [R_y{}^2 - 2R_yT_{ny} + T_{ny}{}^2] \quad 6.28$$

$$a_m = [R_x{}^2 - 2R_xT_{mx} + T_{mx}{}^2] + [R_y{}^2 - 2R_yT_{my} + T_{my}{}^2] \quad 6.29$$

This equation is then differentiated wrt a:

$$\frac{\delta z}{\delta a} = \frac{1}{2}a^{-\frac{1}{2}} \quad 6.30$$

$$\frac{\delta a}{\delta xR} = 2R_x - 2T_{nx} \quad 6.31$$

$$\therefore \qquad \frac{\delta z}{\delta xR} = \frac{1}{2\sqrt{a}}(2R_x - 2T_{nx}) = \frac{R_x - T_{nx}}{\sqrt{(R_x - T_{nx})^2 + (R_y - T_{ny})^2}} \qquad 6.32$$

$$\frac{\delta z}{\delta xR} = \frac{R_x - T_{nx}}{T_1 R} \qquad 6.33$$

Therefore the final partial differentials are as follows to solve for the first transmitter pair:

$$\frac{\delta z_1}{\delta xR} = \frac{R_x - T_{1x}}{T_1 R} - \frac{R_x - T_{2x}}{T_2 R} \qquad 6.34$$

$$\frac{\delta z_1}{\delta yR} = \frac{R_y - T_{1y}}{T_1 R} - \frac{R_y - T_{2y}}{T_2 R} \qquad 6.35$$

And therefore the second transmitter pair:

$$\frac{\delta z_2}{\delta xR} = \frac{R_x - T_{1x}}{T_1 R} - \frac{R_x - T_{3x}}{T_3 R} \qquad 6.36$$

$$\frac{\delta z_2}{\delta yR} = \frac{R_y - T_{1y}}{T_1 R} - \frac{R_y - T_{3y}}{T_3 R} \qquad 6.37$$

The position of the receiver can then be solved for by least squares using the following matrix operations. $TDOA_1$ and $TDOA_2$ represent the observation measurements taken by the receiver which can be expressed as ranges (from equation 6.20).

TDOA measurements: $$\bar{z} = \begin{bmatrix} TDOA_1 \\ TDOA_2 \end{bmatrix} = \begin{bmatrix} ct_1 - ct_2 \\ ct_1 - ct_3 \end{bmatrix} \qquad 6.38$$

$$H = \begin{bmatrix} \frac{\delta z_1}{\delta xR} & \frac{\delta z_1}{\delta yR} \\ \frac{\delta z_2}{\delta xR} & \frac{\delta z_2}{\delta yR} \end{bmatrix} \qquad 6.39$$

Where:

$$\bar{x} = (H^T H)^{-1} H^T \bar{z} \qquad 6.40$$

$$\delta\bar{x} = (H^T H)^{-1} H^T \delta\bar{z} \qquad 6.41$$

$$\delta\bar{z} = z - \hat{z} \qquad 6.42$$

Where $\hat{z}$ is the initial guess of the receiver's position and z is the value from the receiver. After the first iteration, $\hat{z}$ is updated with z and the process then continues. The accuracy of the initial guess defines the number of iterations required before a usable solution is found. This can take a number of iterations, depending on the quality of the initial guess input to the system.

Solutions which do not converge on a result are rejected, with the system then continuing with the following DAB frame. The raw measurements are extracted from this frame and the process continues.

6.11 SUMMARY

This chapter has presented the complete signal processing flow, from the capture of the raw DAB data, to establishing the Time Difference of Arrival measurements based on the signal lags and finally the positioning process solved using Least Squares. It has also been shown how to find the position of any transmitter by decoding every second null symbol and to match these results to the correlation coefficients. The system at this stage has been constructed for the purpose of static positioning only. A number of key differences are shown in chapter 8.11 for the dynamic positioning experiments.

7 UK DAB COVERAGE

7.1 INTRODUCTION

This chapter will examine the current potential positioning performance of the DAB networks in the UK by modelling the true locations of transmitter antennas heights and the varying height of a receiver. An analysis has been performed by placing a hypothetical grid over the UK, based on OSGB36 coordinates (Easting/Northing) and calculating the Horizontal Dilution of Precision (HDOP) at each grid intersection. Figure 7-1 shows how the simulation has been constructed.

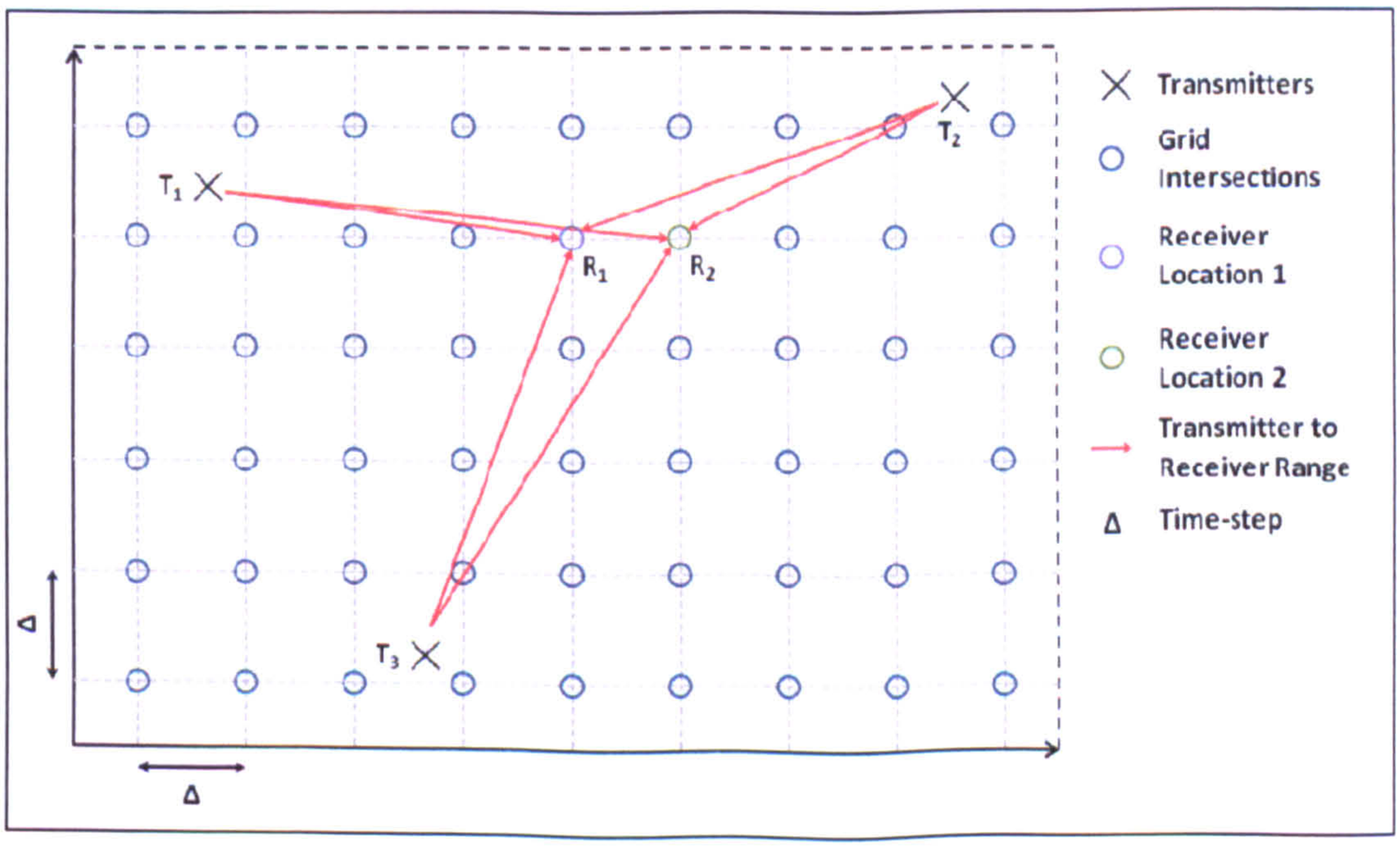

Figure 7-1: HDOP Simulation Setup

At each grid intersection (circled in the figure), the linear distance is calculated to the three transmitters (T_1 to T_3). As the position of both receiver (grid intersection) and transmitters is known during this simulation, the HDOP value of the transmitter layout can be calculated based on the TDOA timing expected from these positions. The resolution of the grid acts as the time-step (Δ) of the calculation, which can be as detailed as required. The transmitters are located at their true locations (details taken from the *Ofcom* website (Moldon, 2010)) which may lie between intersection points.

The HDOP measurements at each grid intersection were calculated based on TDOA measurements from the transmitters within a range defined by the heights of the transmitting and receiving antennas. The transmitter's receivable range at each receiver position was calculated using the Hata model (discussed earlier in section 3.6.5) and the subset of available transmitters in the area created based upon this analysis.

7.2 Simulation 1: National Coverage

The first simulation examines the UK as a whole on a grid of 700km × 1000km. The spatial resolution (Δ) used was 1km. The results from this are shown in Figure 7-2 through to Figure 7-7. Each figure shows both the individual transmitter coverage footprint (left chart) and the HDOP values based on a minimum of three transmitters to find a 2D position.

Block 11D is the only national network presented here due to the lack of transmitter height information available for the BBC national network (12B). The remaining blocks represent either local or regional networks. For this simulation, the receiving antenna is fixed at an altitude of 3 metres (value chosen as this was the approximate height of the dipole antenna when fitted to the test vehicle).

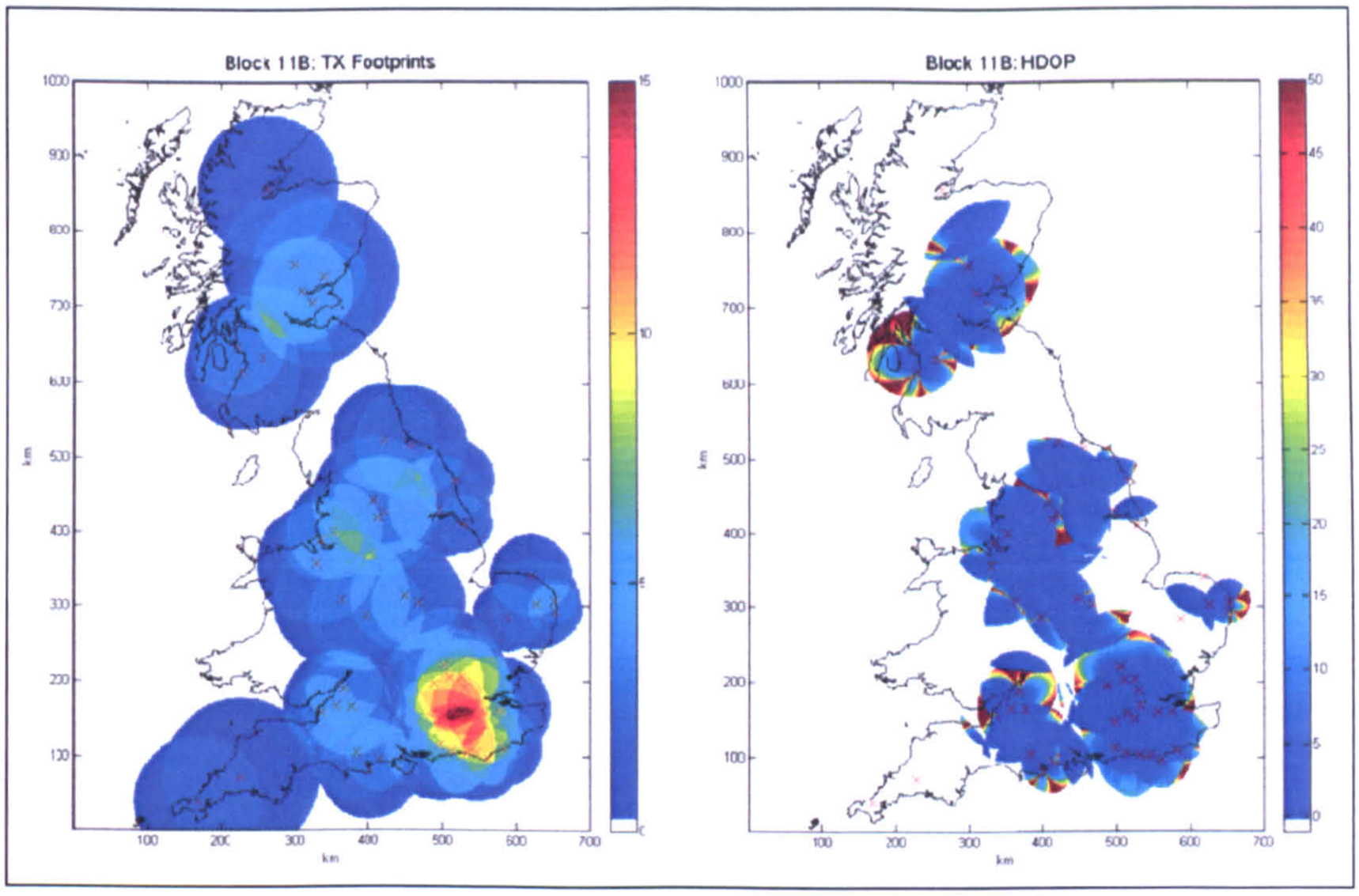

Figure 7-2: Simulation using DAB transmitters on block 11B

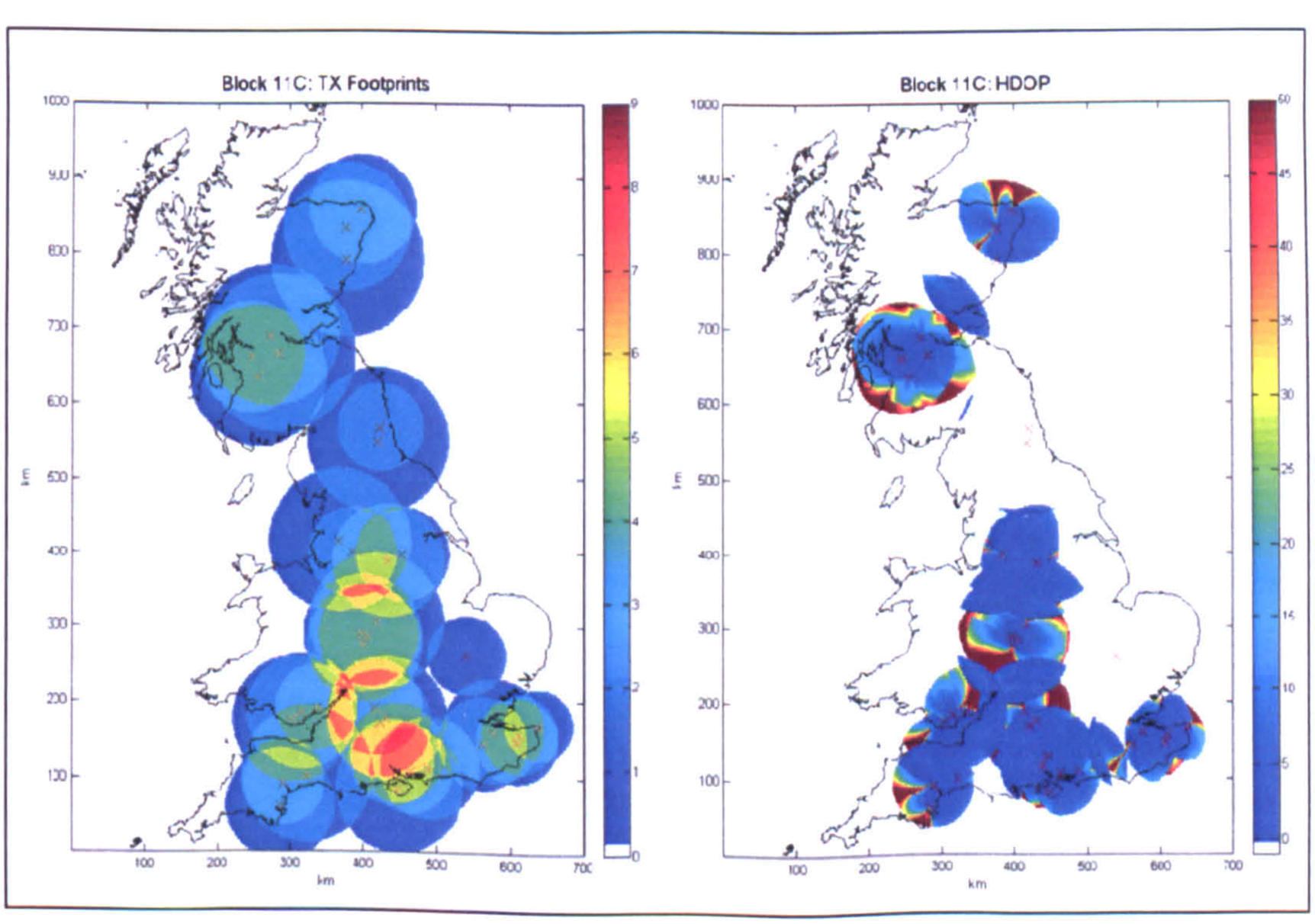

Figure 7-3: Simulation using DAB transmitters on block 11C

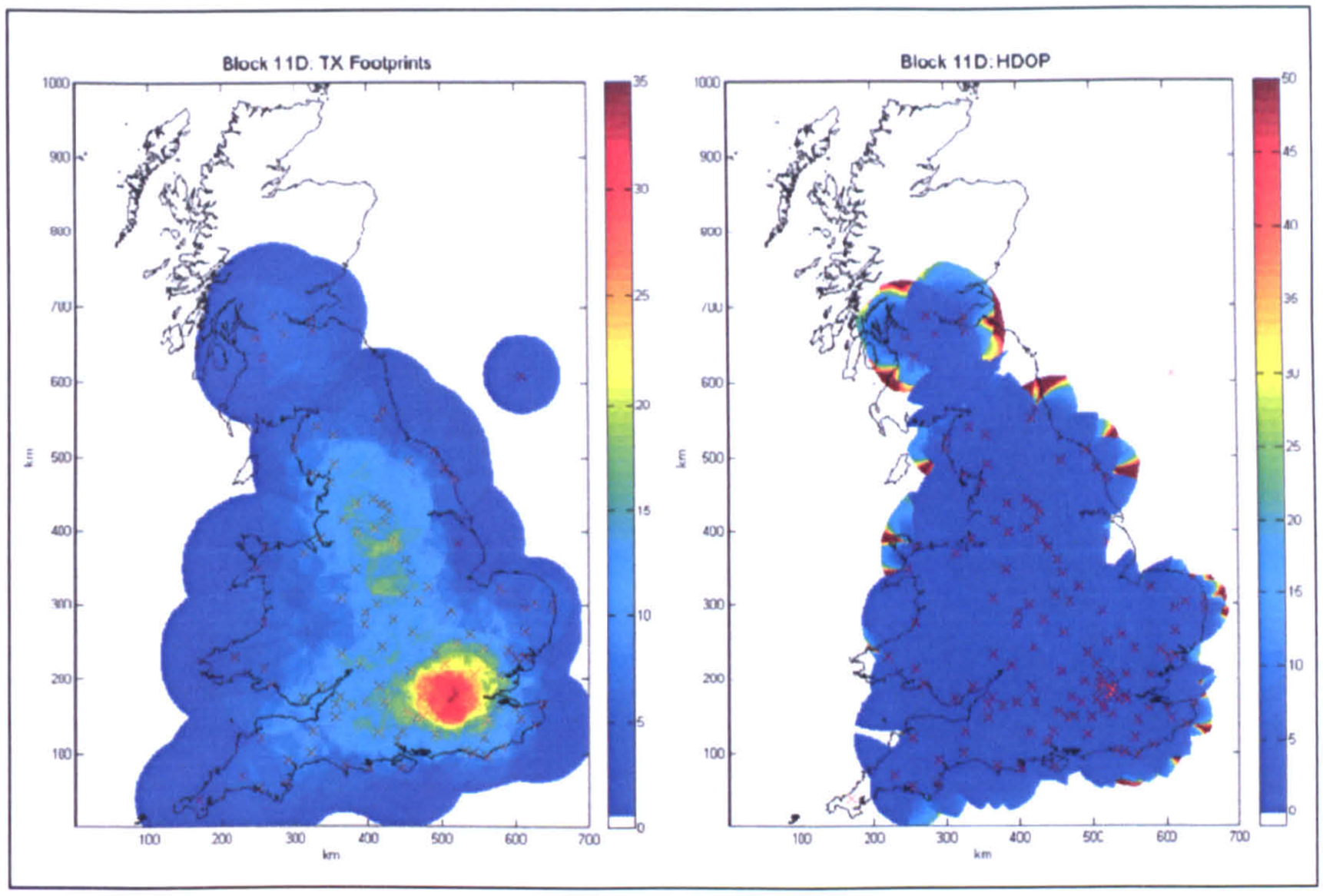

Figure 7-4: Simulation using DAB transmitters on block 11D

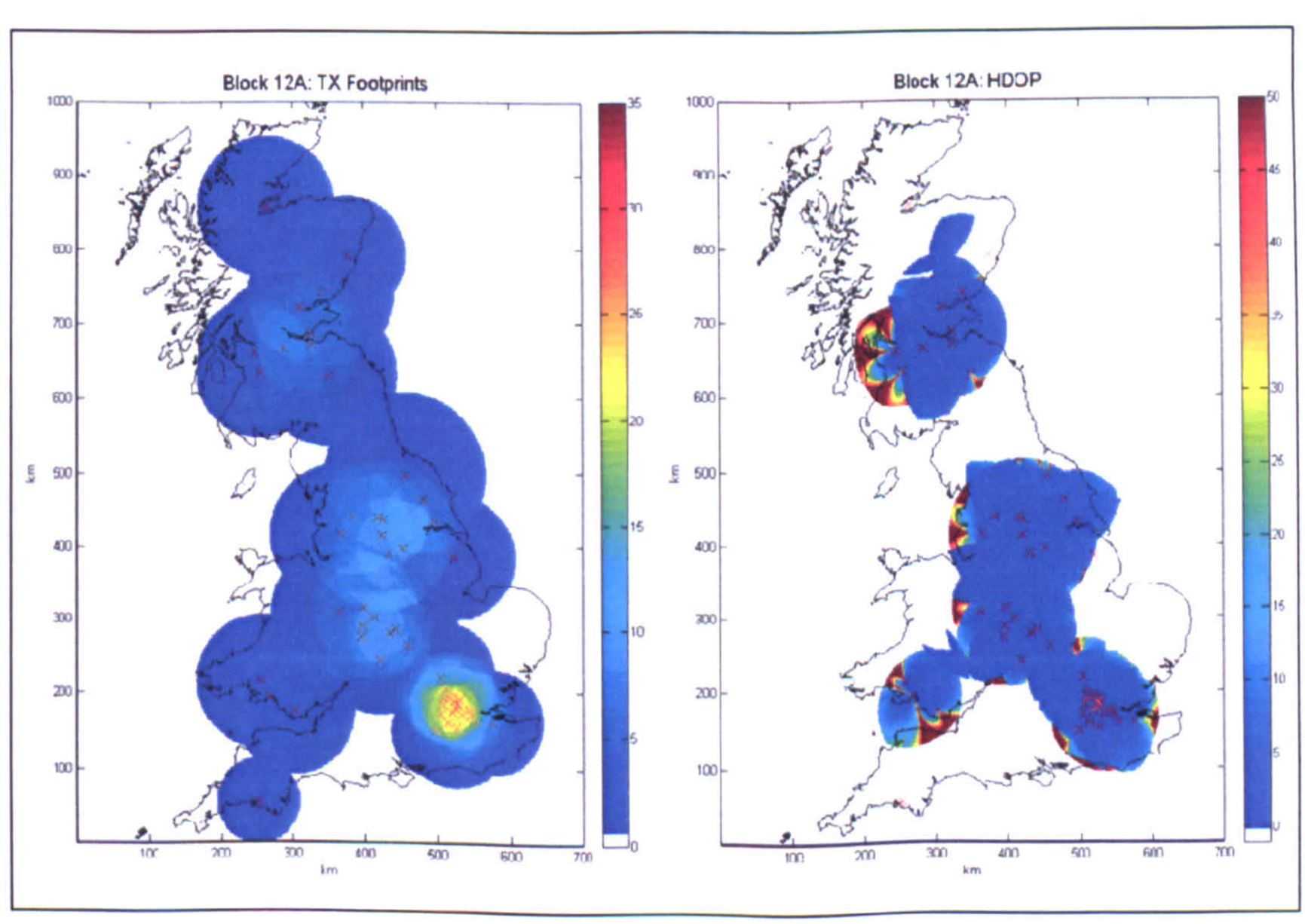

Figure 7-5: Simulation using DAB transmitters on block 12A

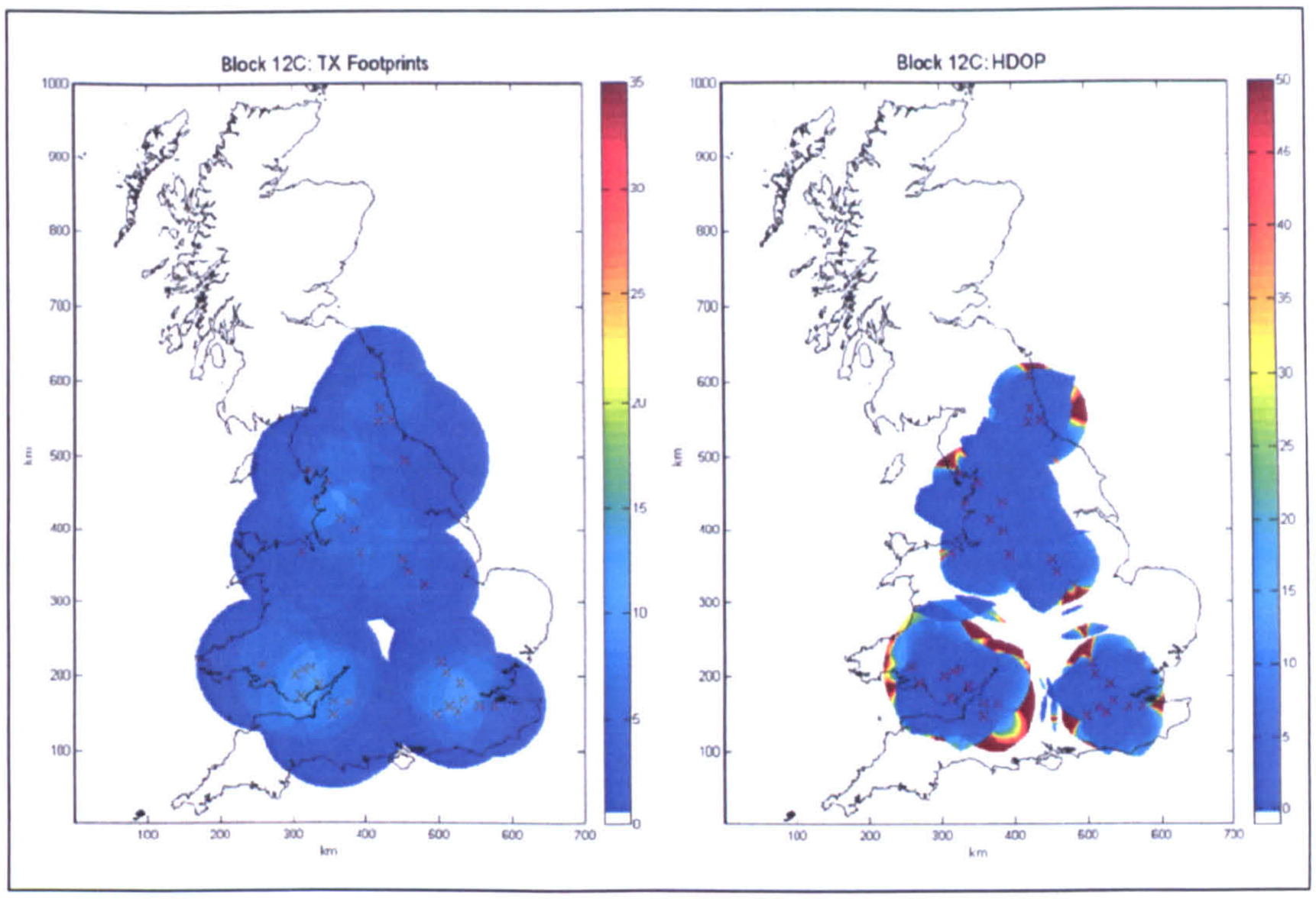

Figure 7-6: Simulation using DAB transmitters on block 12C

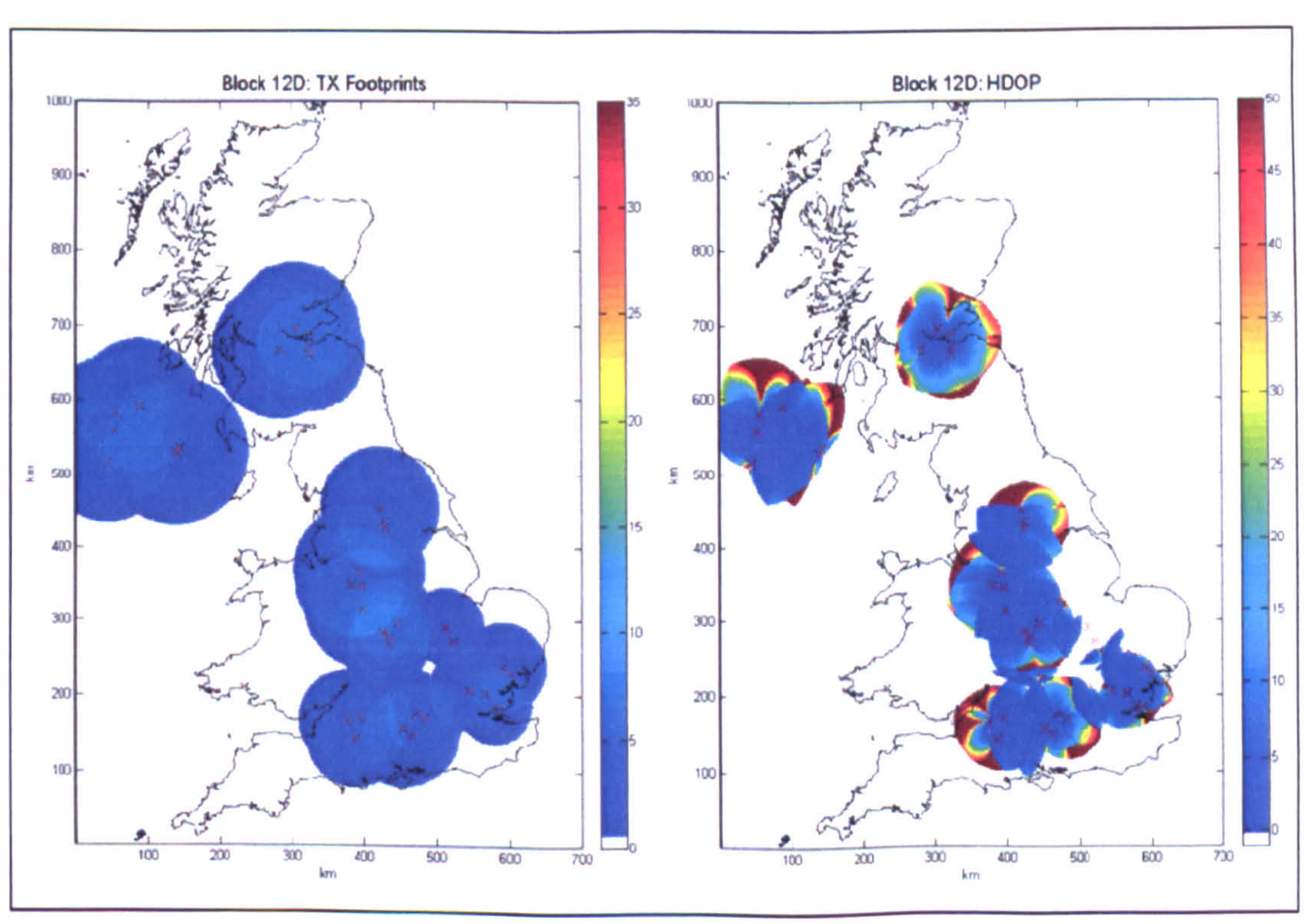

Figure 7-7: Simulation using DAB transmitters on block 12D

As can be seen from these results, the coverage of transmitters around the UK varies depending upon the DAB block from which they are broadcast from. HDOP values on block 11D shows that the majority of the country lies in a region where two or more transmitters are viewable at any one time, from a national network alone. Areas not covered by this approach tend to lie in regions where GPS would not suffer poor coverage (urban environments). This also provides the motivation of a terrestrial based alternative to GNSS.

7.3 SIMULATION 2: LOCAL COVERAGE

This simulation examines the testing region used in DAB positioning tests which follow this chapter. In this scenario, the focus of the simulation is shown on the UK map below in Figure 7-8 within the black rectangle. This area is grid of 100km × 105km with a spatial resolution of 100 metres. This region was chosen as it contains many areas which will later be used for system testing. Results follow in Figure 7-9 through to Figure 7-14.

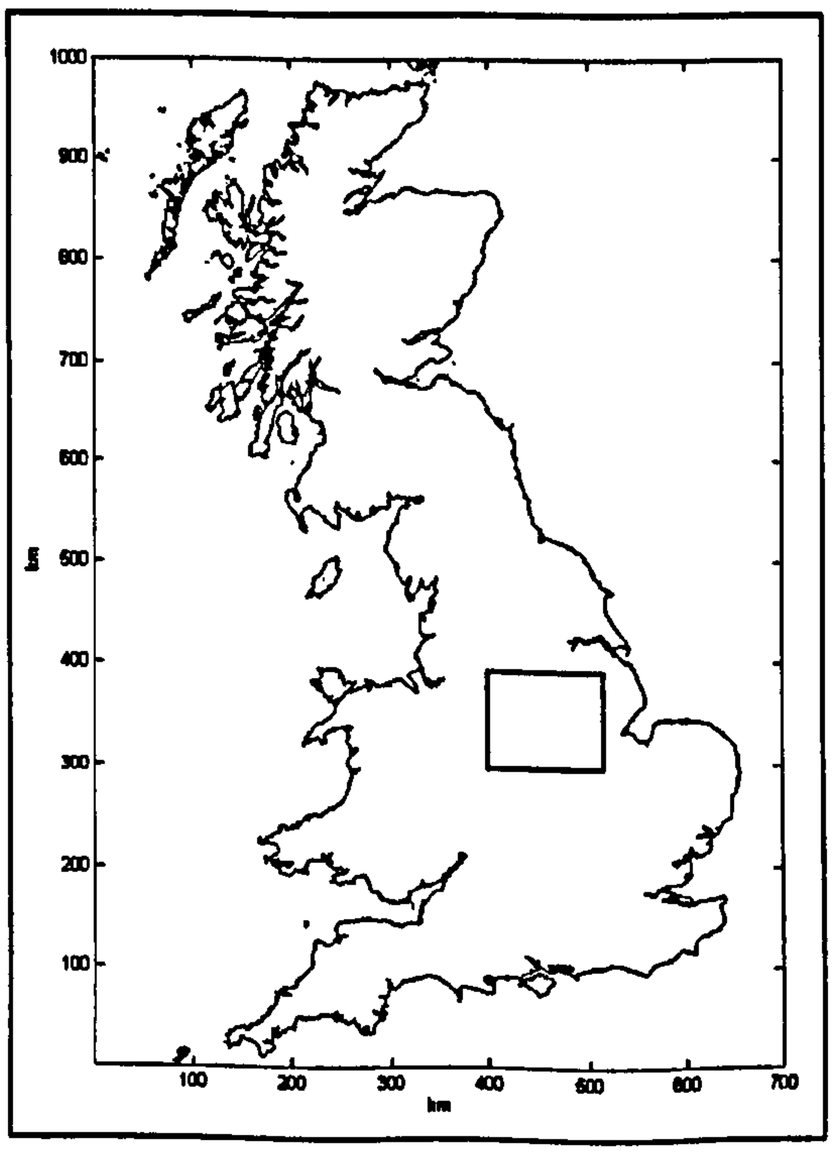

Figure 7-8: Region used for local region simulation

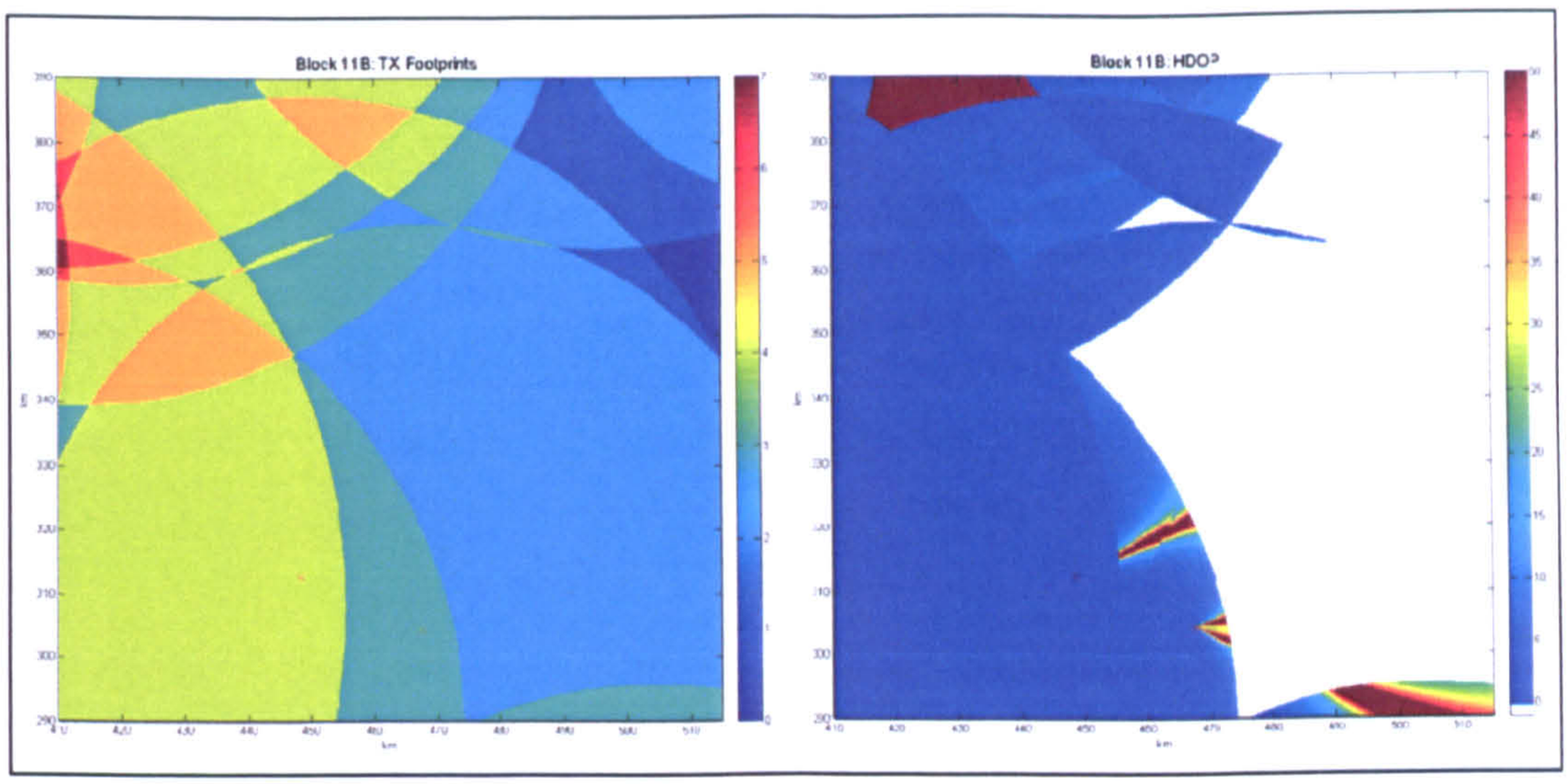

Figure 7-9: Simulation using DAB transmitters on block 11B (local region)

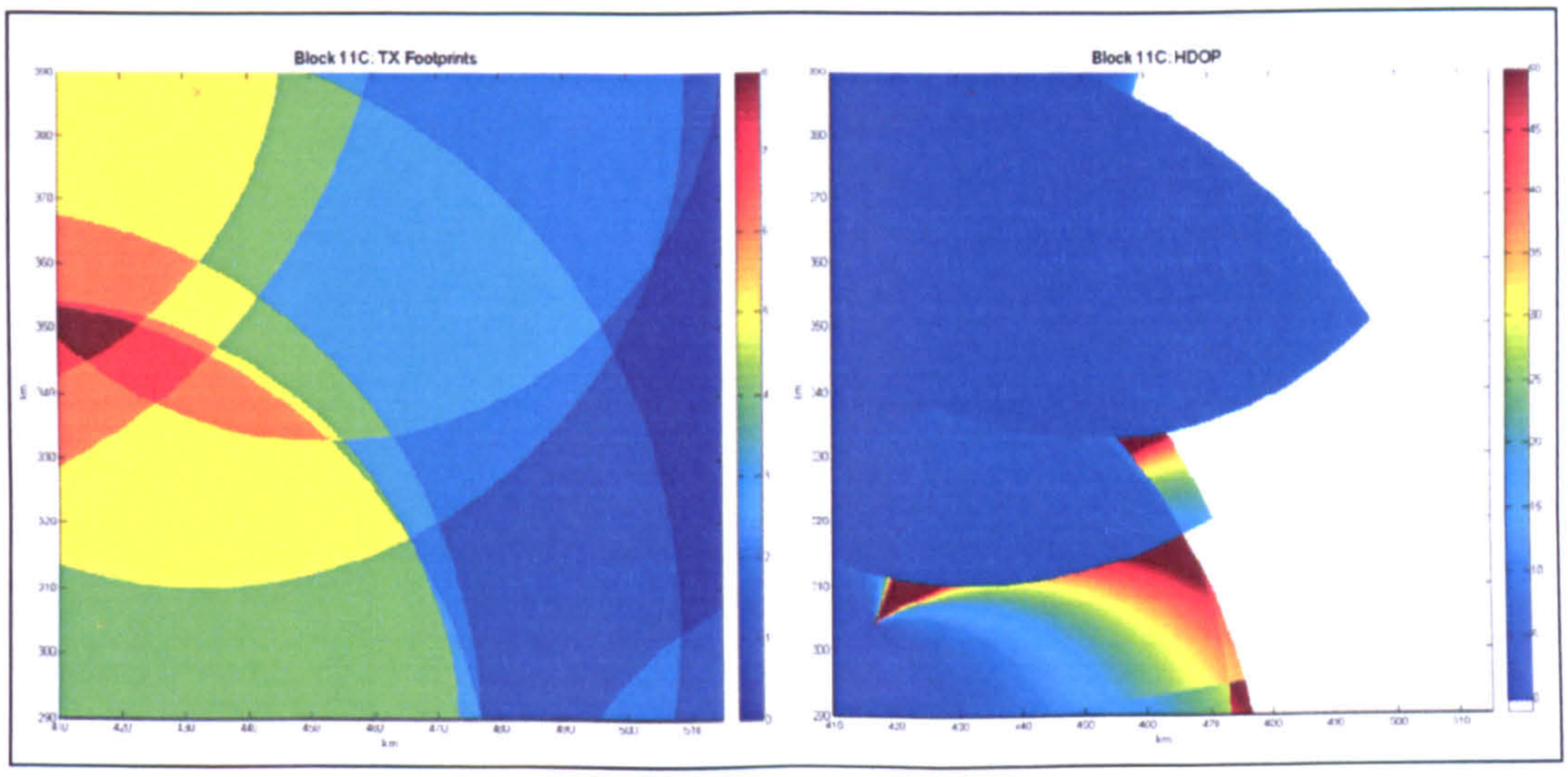

Figure 7-10: Simulation using DAB transmitters on block 11C (local region)

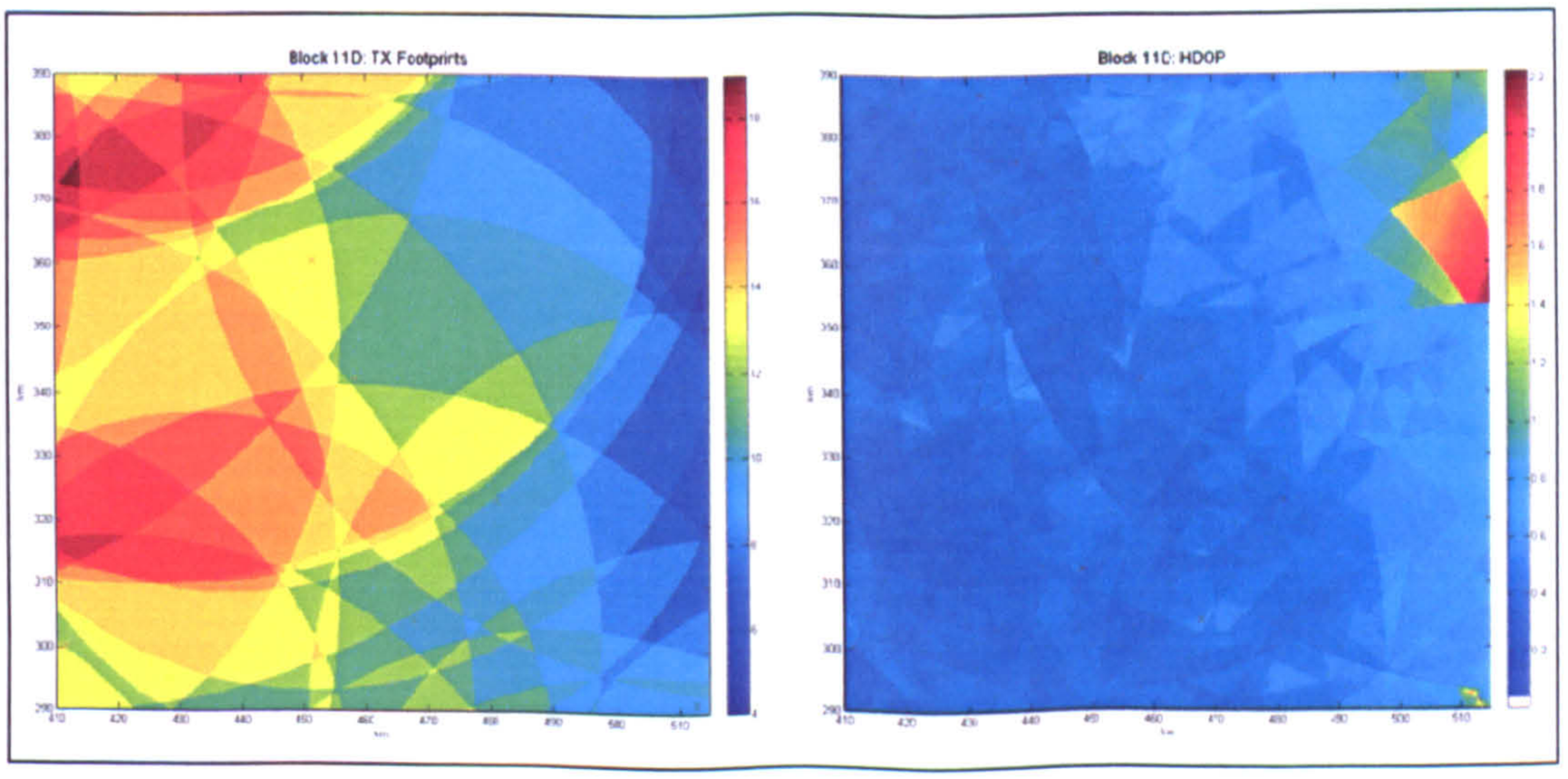

Figure 7-11: Simulation using DAB transmitters on block 11D (local region)

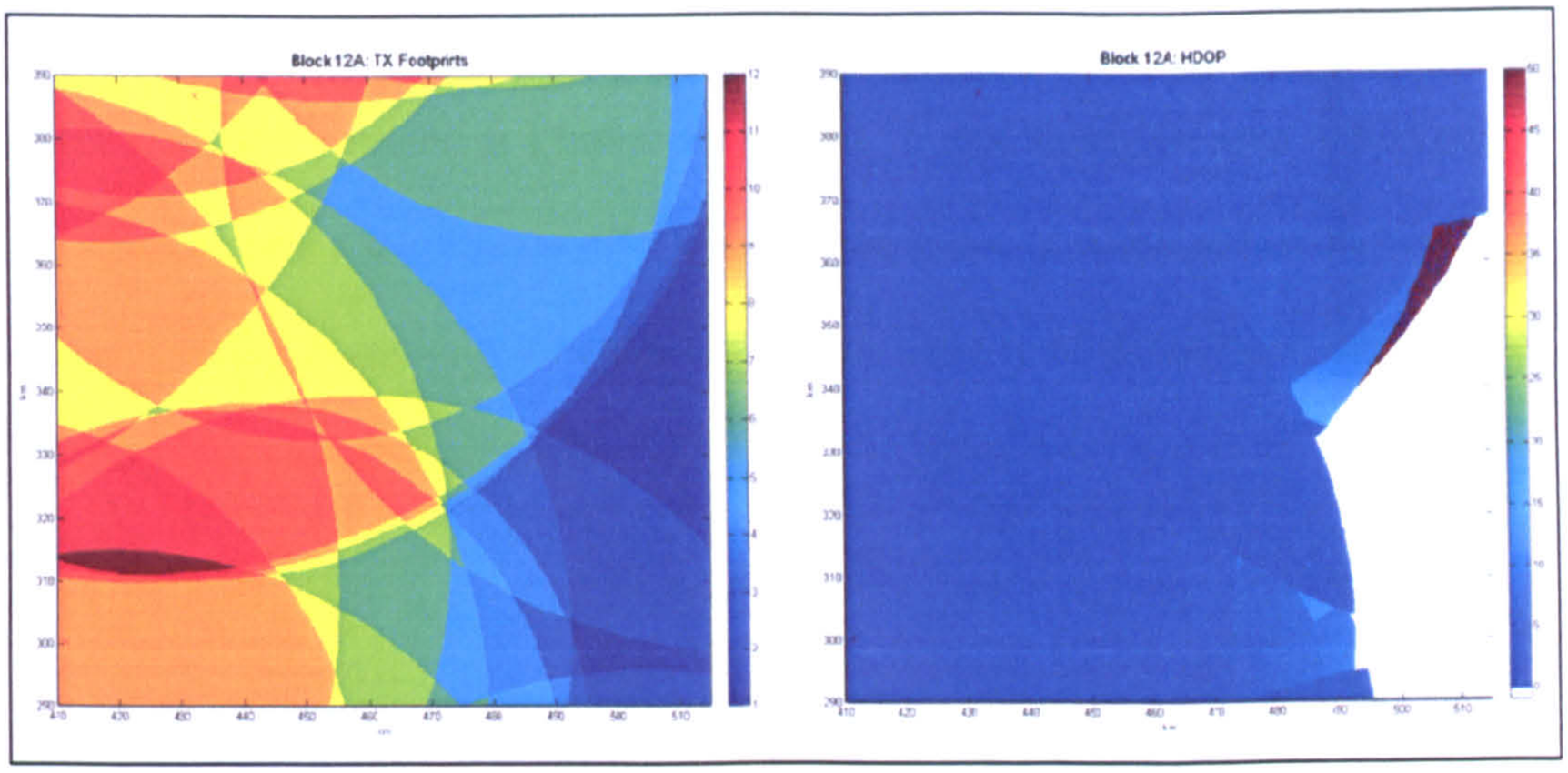

Figure 7-12: Simulation using DAB transmitters on block 12A (local region)

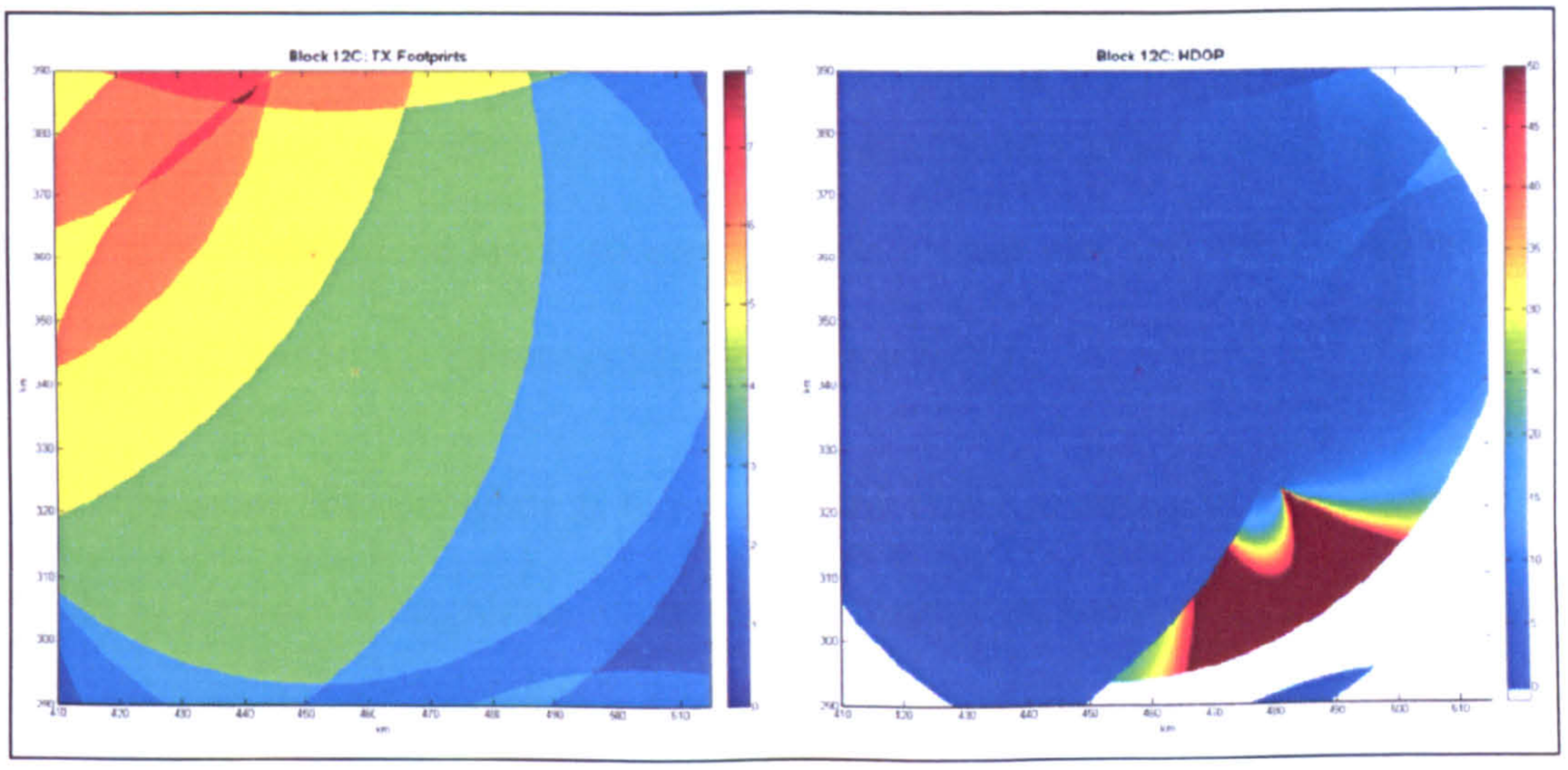

Figure 7-13: Simulation using DAB transmitters on block 12C (local region)

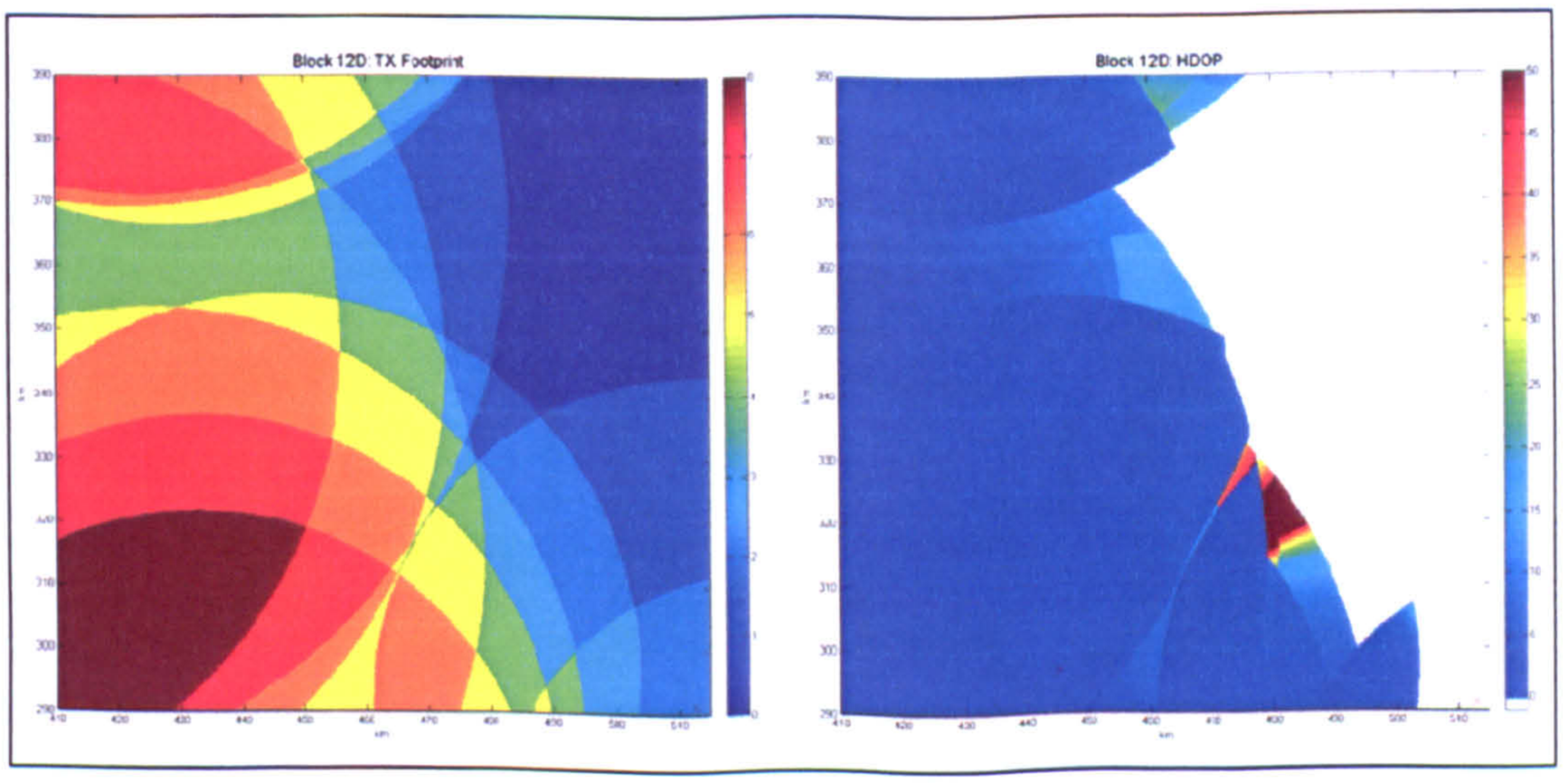

Figure 7-14: Simulation using DAB transmitters on block 12D (local region)

The simulation has shown the same results as used for the national simulation but within a smaller area and at a higher resolution. It can clearly be seen in this region which transmission frequencies offer either a standalone or combined solution. Block 11D (Figure 7-11) naturally contains the highest number of transmitters being one of the two current national networks.

7.4 SIMULATION 3: RECEIVER ANTENNA HEIGHT

This final simulation examines the same region (using the same spatial resolution) from section 7.3 but varies the receiving antenna height between 1 and 100 metres. Each figure shows three plots, the left plot indicates the HDOP available if the antenna is 1 metre above ground-level, 10 metres in the central plot and 100 metres for the right plot. The model is otherwise identical to that in 7.3.

The purpose of this simulation is to examine the effect of changing receiver antenna height by an order of magnitude has on a DAB positioning receiver, in order to be able to "see" sufficient transmitters to calculate a fix. The heights in this case were chosen as being the most likely range at which a DAB antenna would be situated above the Earth's surface. Figure 7-15 to Figure 7-20 over the following pages show the results of this simulation for the same transmission blocks as used previously.

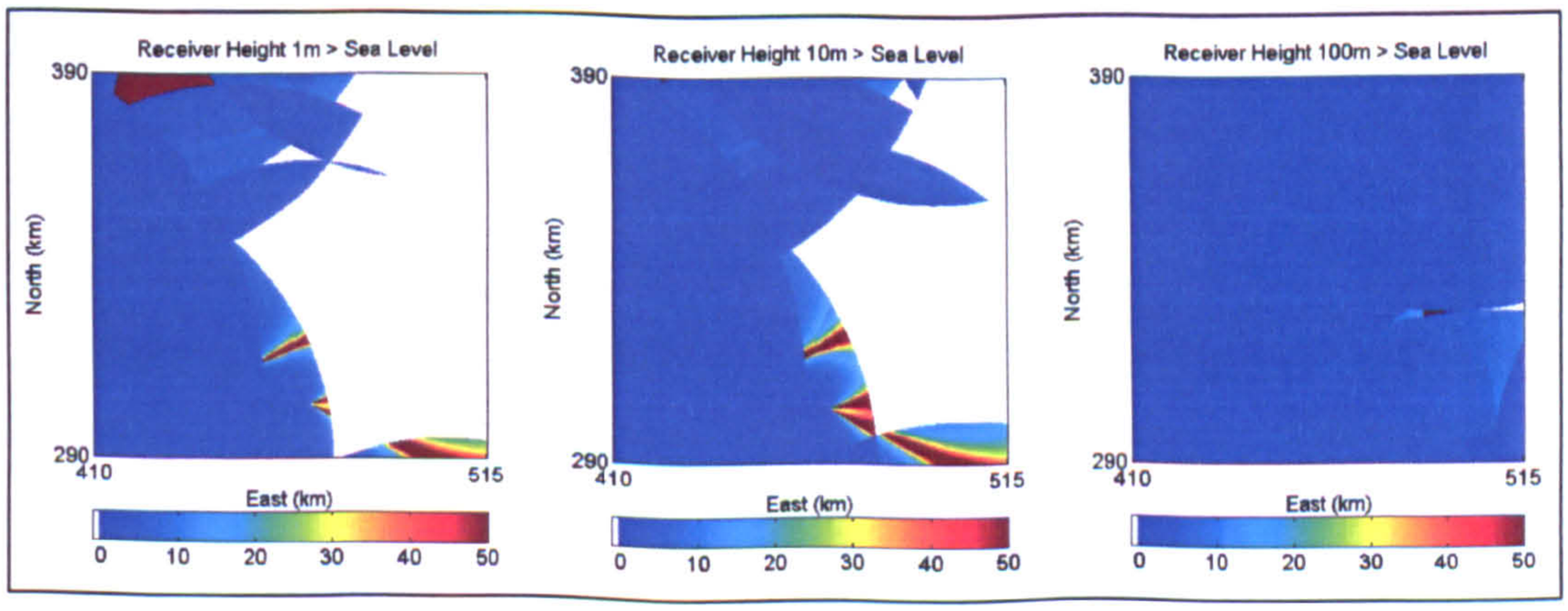

Figure 7-15: Simulation varying receiver height on block 11B (local region)

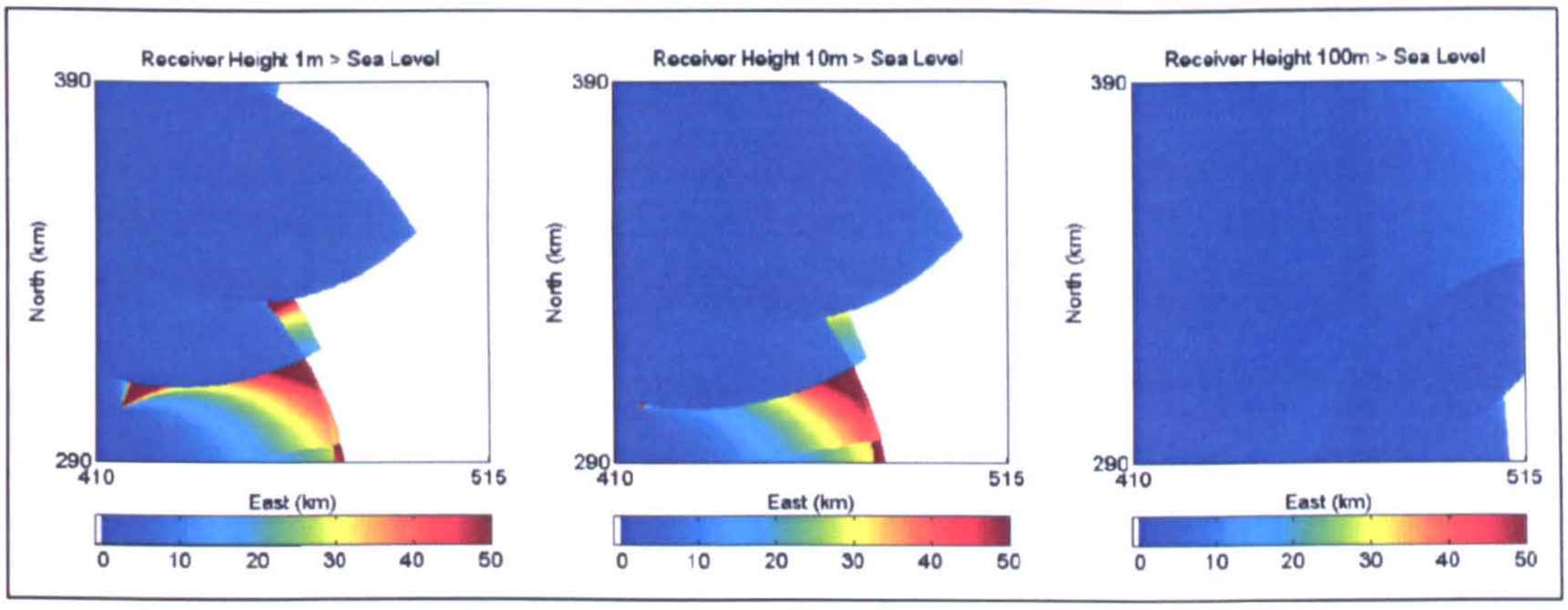

Figure 7-16: Simulation varying receiver height on block 11C (local region)

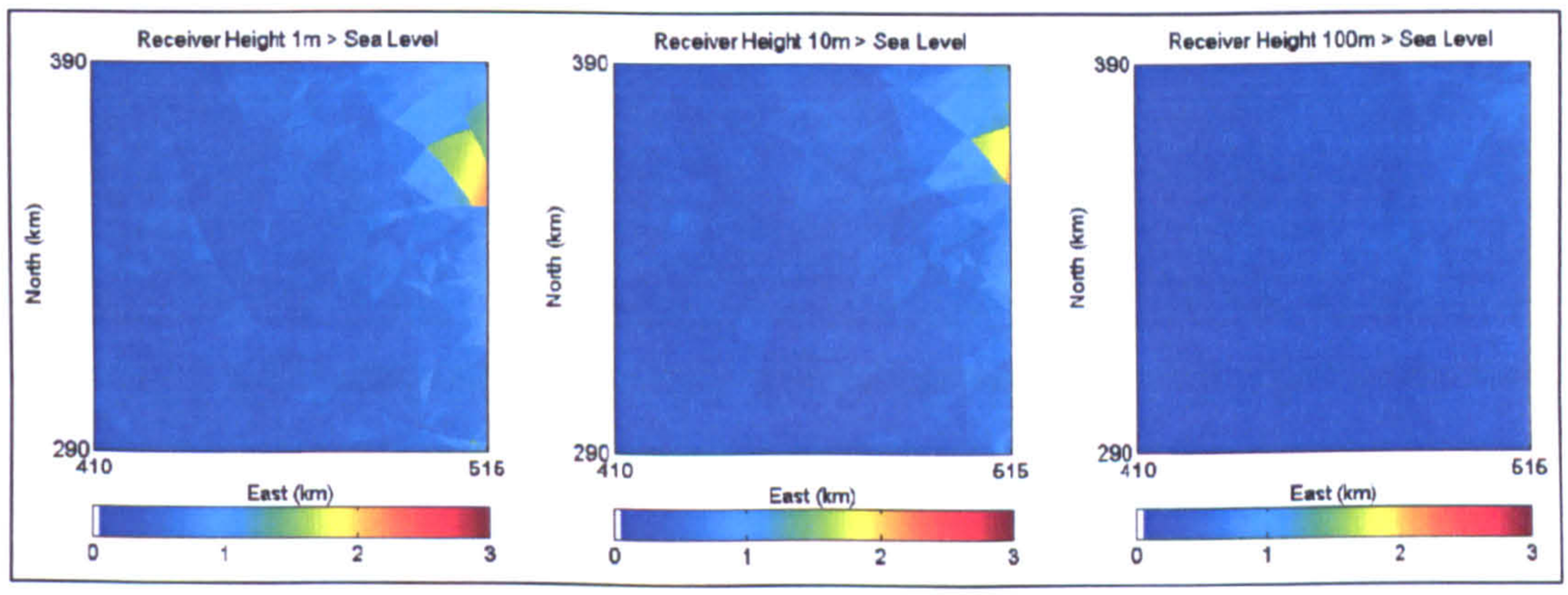

Figure 7-17: Simulation varying receiver height on block 11D (local region)

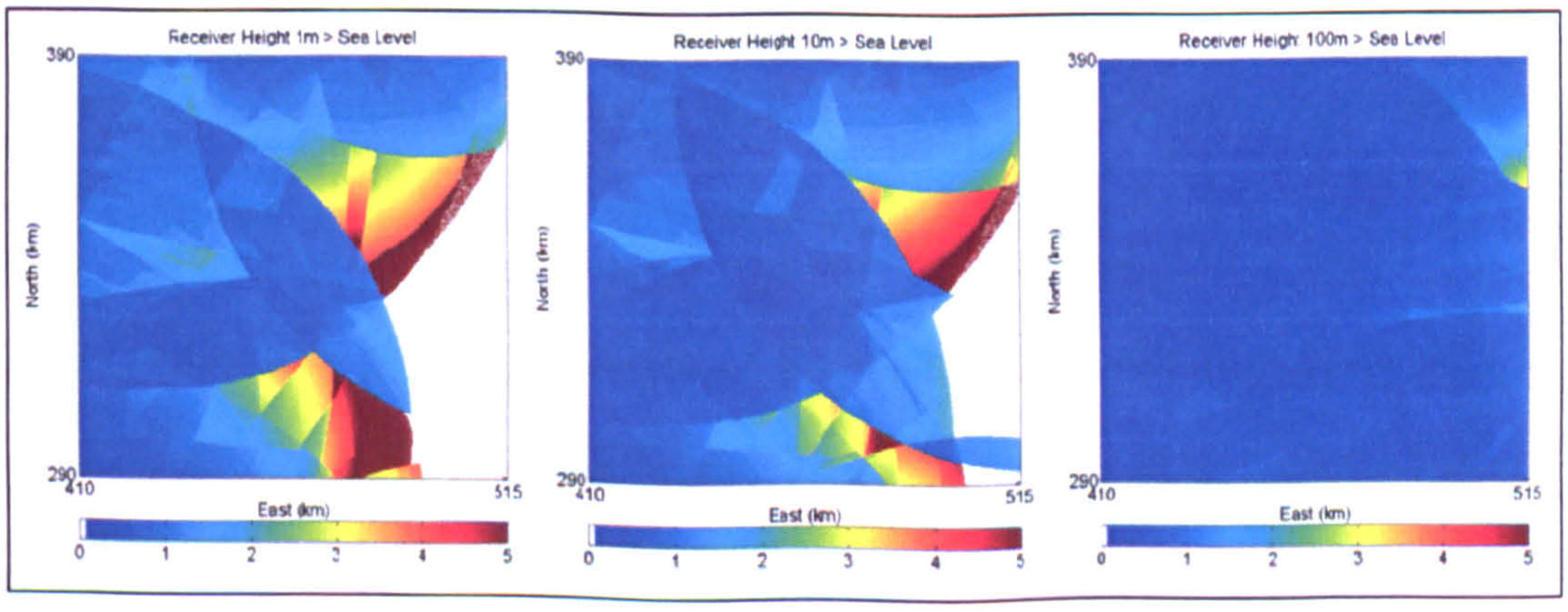

Figure 7-18: Simulation varying receiver height on block 12A (local region)

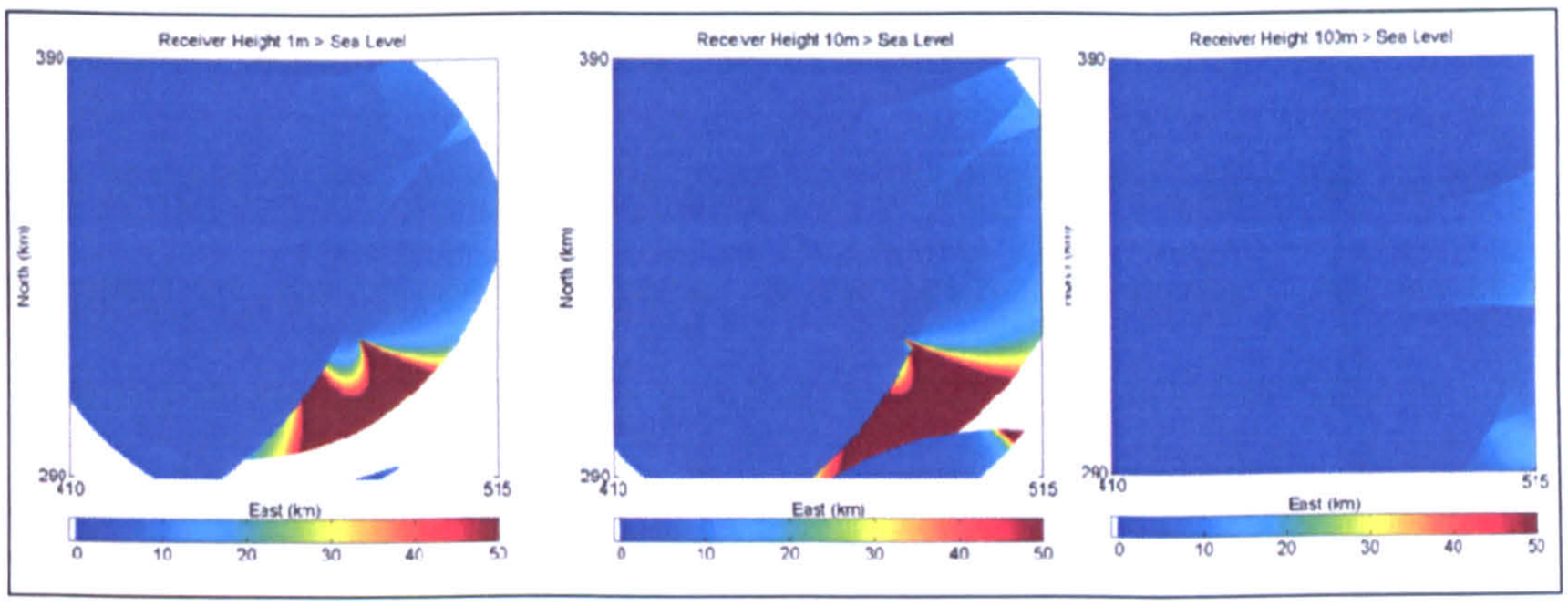

Figure 7-19: Simulation varying receiver height on block 12C (local region)

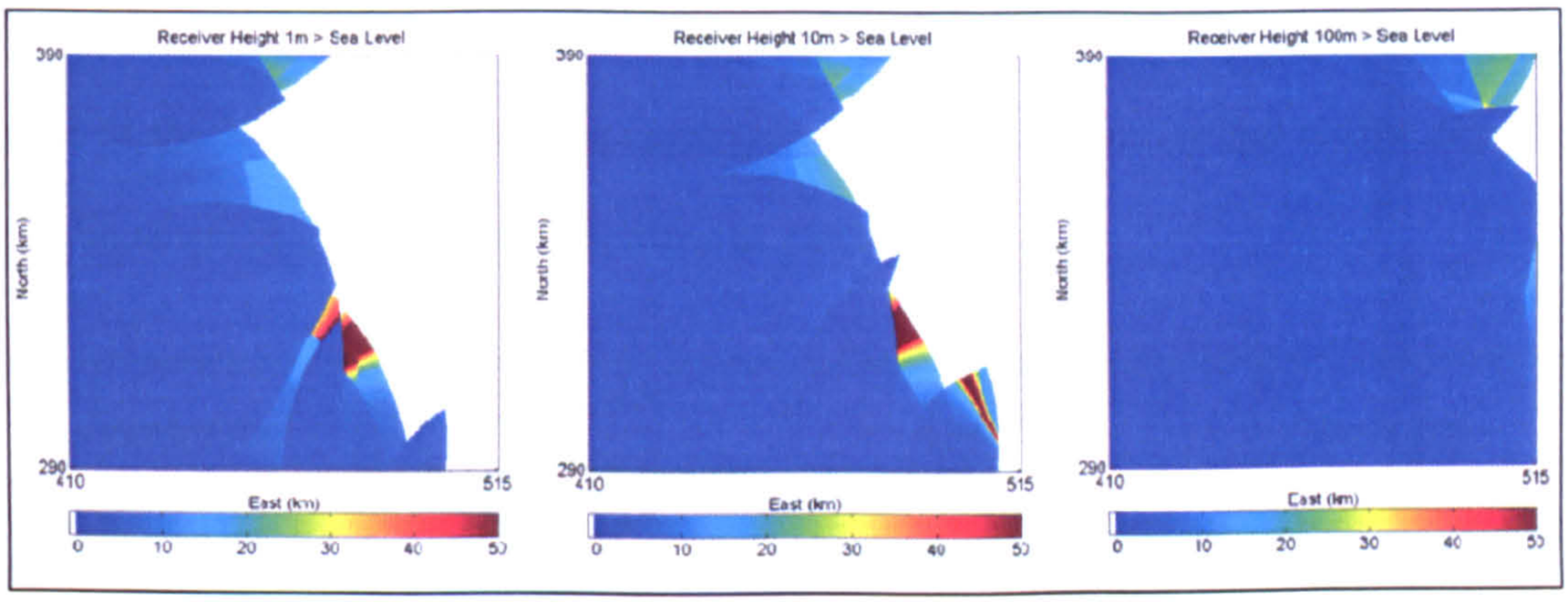

Figure 7-20: Simulation varying receiver height on block 12D (local region)

These results show the quality of TDOA positioning when the antenna is positioned above ground-level at the levels indicated on the charts. As more transmitters emerge into view to a receiver, so the HDOP value falls with block 11D once again showing the highest quality results as per the previous simulations.

These simulations give a rough idea of the number of transmitters available at a certain location and at a particular height. As these scenarios all consider the use of a spherical earth with no obstacles between transmitter and receiver, the true world results would be expected to be slightly degraded from these results. This height-testing scenario will be investigated further using real data later in the project.

7.5 SIMULATION 4: THE "*T* GRID"

This simulation was performed in order to model the effect that the receiver's sampling-rate has on the performance of the positioning system. As has been discussed previously, DAB data is broadcast at a clock rate of 2.048 MHz with the USRP front-end only having the ability to sample at 2.000 MHz. This involves the up-sampling of the signal by a small degree in order to match the broadcast clock rate and decode the information in the signal.

In section 4.3.1 the unit ***T*** was defined, giving the distance travelled by the signal in 1***T*** by roughly 146m. In this simulation, the four transmitters used are those currently used in the Nottingham/Leicester regions and the model assumes that usable signals can be received as TDOA pairs as listed in Table 9.

Transmitter	*TII Code*		*East (m)*	*North (m)*
	Region	*Transmitter*		
Mapperley	65	8	458350	342450
Waltham	65	16	480950	323350
Copt Oak	65	17	448350	312650
Houghton	65	21	467550	304450

Table 9: Transmitters used for simulation in 7.5

In this scenario, each pair creates a series of hyperbolae between the two transmitters. As the system resolution is limited to the measurement value of ***T***, this means that the hyperbolae are spaced according to this value.

The results of this can be seen in Figure 7-21 and Figure 7-22. The first of these figures shows the result of the test area on the left with a closer view of a 1km by 1km square on the right (indicated by the red square).

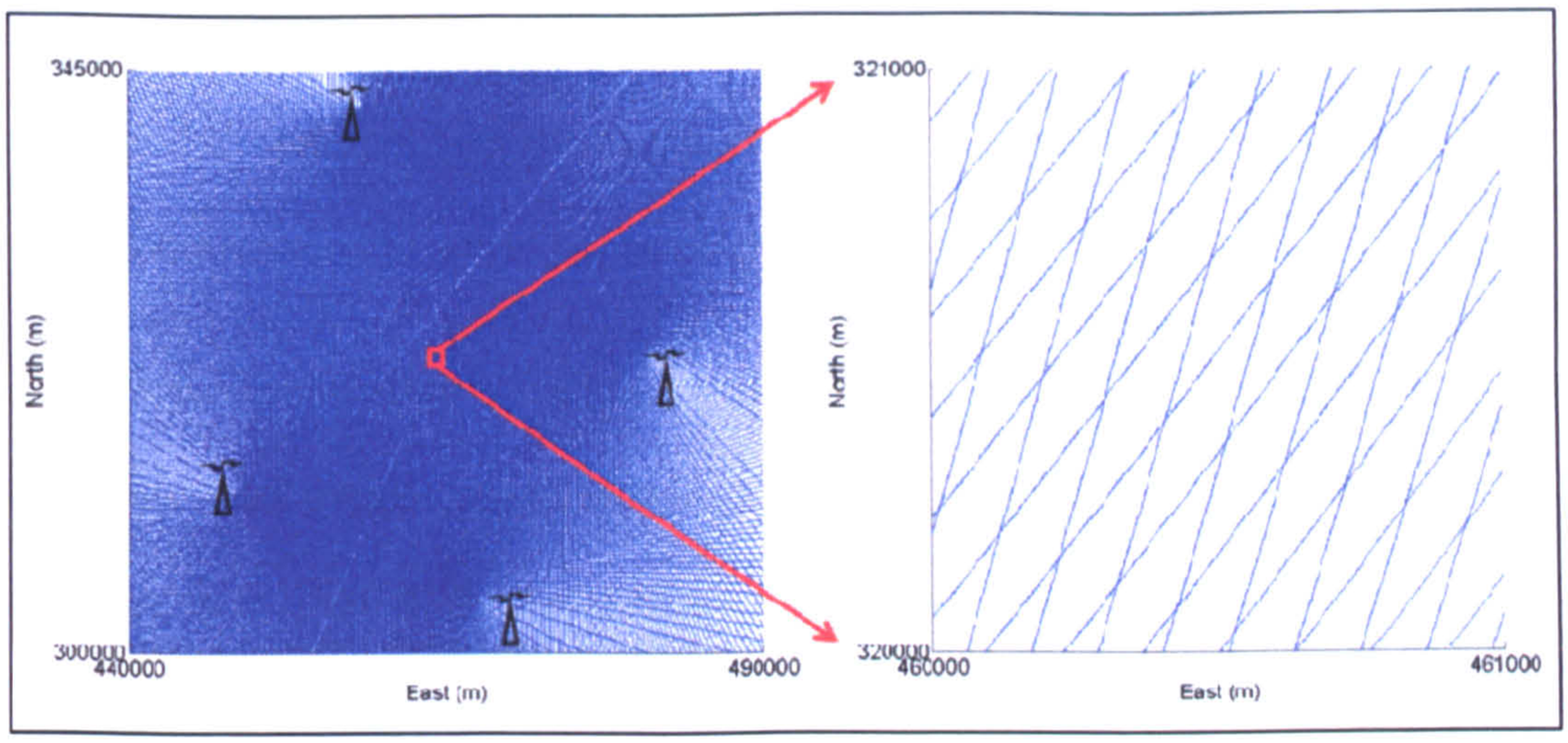

Figure 7-21: Local T Grid simulation

Two pairs of transmitters giving two TDOA measurements

It can be seen in this case that the grid structure formed by the difference in arrival times limited by integer values of ***T***, gives roughly thirty positions within a square kilometre which the TDOA measurement system will lock to. By examining a different square kilometre in Figure 7-22, it can be seen that because of the limitation due to transmitter geometry, there are only eight possible positions the system will lock to.

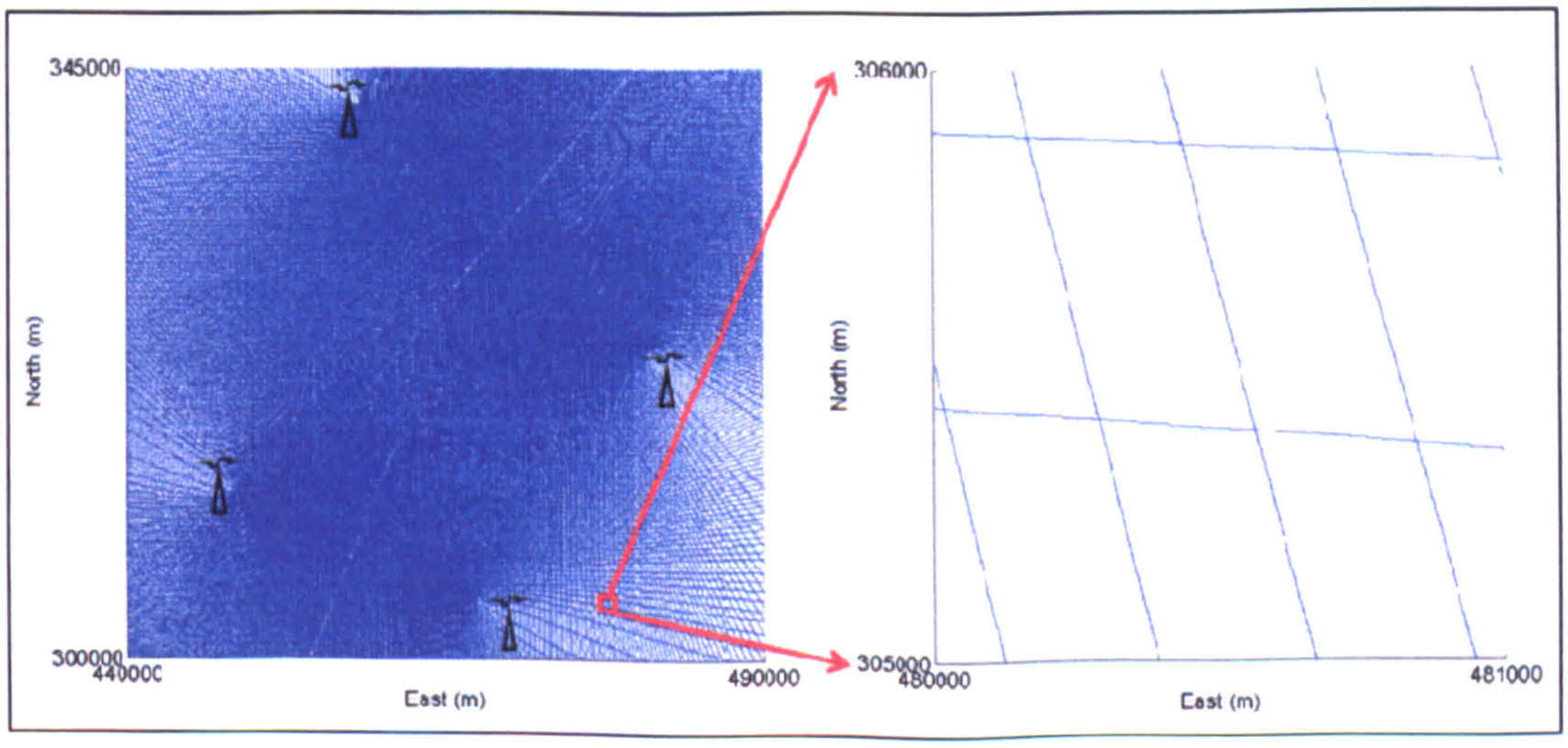

Figure 7-22: Local T Grid simulation

Two pairs of transmitters giving two TDOA measurements

Running the simulation again with the same transmitters, but this time the model is assembled so that four transmitters are received on the same frequency, such as might be received if tuning to one of the national networks.

The Waltham transmitter is assigned as the 'master' (reference transmitter), with the remaining three transmitters as secondary signals. This provides enough information to make three TDOA measurements and therefore three sets of time equidistant hyperbolae. These results can be seen in Figure 7-23 and Figure 7-24 with the left hand charts in each figure showing the simulation run over the same areas and the right hand charts highlighting the same magnified regions in Figure 7-21 and Figure 7-22.

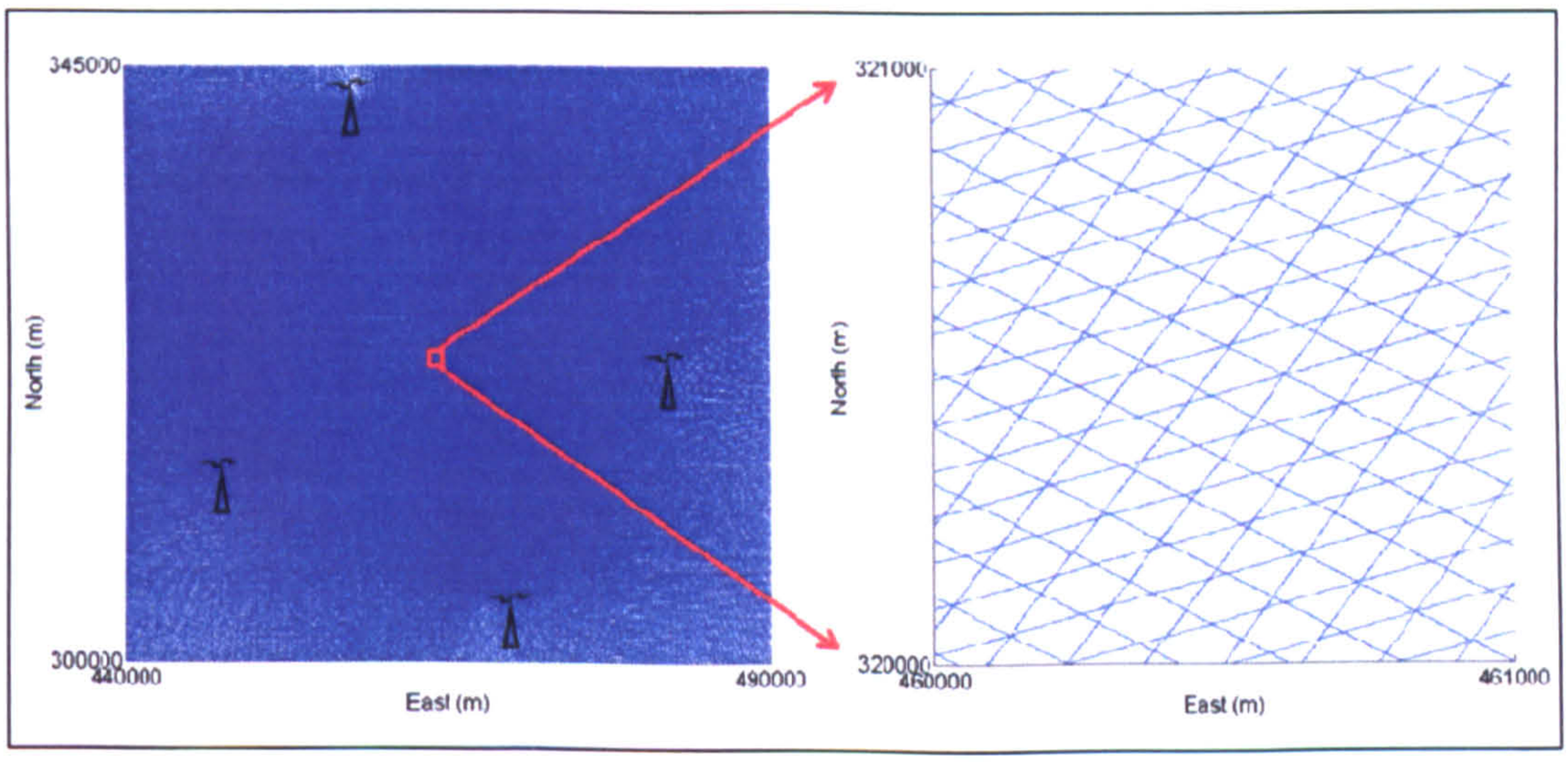

Figure 7-23: Local T Grid simulation

One master, three secondary giving three TDOA measurements

It is immediately obvious that the use of this transmitter geometry and measurement of TDOA, providing sufficient transmitters are receivable on a single frequency, gives the system a higher resolution than the previous exercise. This has limited the size of each measurement cell providing a more accurate estimation of position.

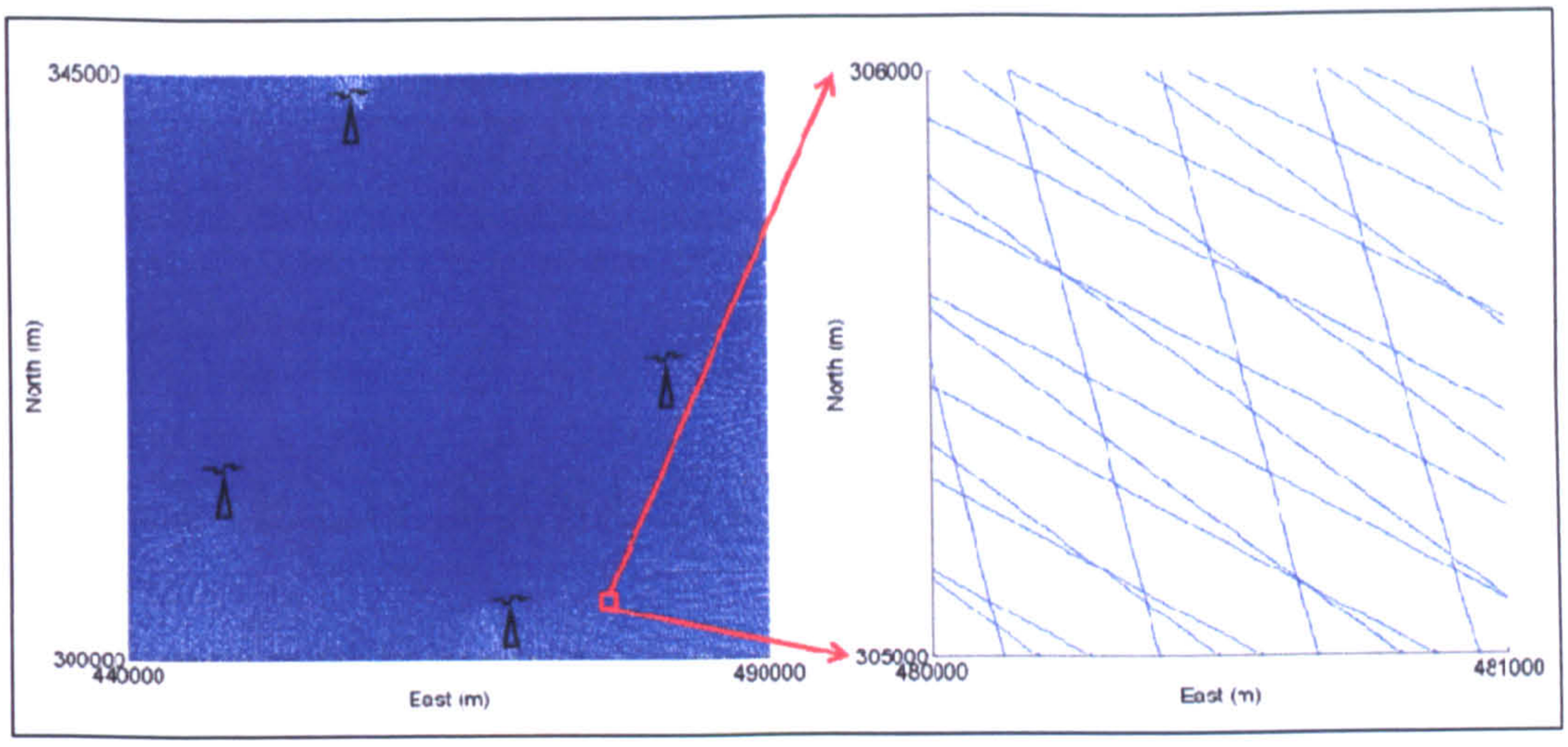

Figure 7-24: Local T Grid simulation

One master, three secondary giving three TDOA measurements

The purpose of this exercise was to highlight the difference in resolution when adding more than the fundamental two TDOA measurements, and showing that the geometry of the transmitter layout is also critical in providing the best possible resolution in this system.

8 FIELD TEST RESULTS

8.1 INTRODUCTION

This chapter will examine the results of DAB captures taken in a variety of locations, and scenarios. A number of tests were performed in order to examine the potential behind positioning using DAB alone. These tests were then expanded to explore the durability of the system in environments where the transmitter layout could vary considerably.

8.2 TRANSMITTER OSCILLATOR CONSISTENCY

8.2.1 Introduction

The purpose of this test was to monitor the stability of a transmission over a 48 hour period. If the transmitter oscillators were found to show a fluctuation of different readings over time, then this would strongly affect the positioning potential of the system. Any oscillator variations affecting the positioning system will be obvious in the cross-correlation process described previously.

In order to perform this, captures were made of the BBC national network (Block 12B – 225.648 MHz) once per hour for 48 hours. The omni-directional dipole antenna was

mounted on the roof of a building on the University Park campus; roughly fifteen metres clear of the ground. The USRP was set to run at hourly intervals and perform a one-second capture on the hour (approximately ten transmission frames). The data could then be post-processed in order to examine the stability of the transmission.

8.2.2 Results

The data was post-processed with the aim of finding the null symbol, so allowing the TII symbols (every second frame) and performing a cross-correlation of the TFPR symbol (every frame) to attain the difference in arrival times of the transmissions. The receiver oscillator error also had to be accounted for in each frame.

The results of each capture were averaged in order to create the smoothest plot. The map in Figure 8-1 shows the relative positions of both transmitters and the receiver, while the charts in Figure 8-2 and Figure 8-3 show the received TII information and TDOA measurements respectively. It can clearly be seen that at the data sampling rate used by the USRP, no fluctuations are seen in either frequency (TII) or time (TDOA), proving that the stability of transmitters in the mid-term is adequate for positioning purposes. Each figure clearly shows two peaks, with the peaks in Figure 8-2 presented as pairs of carriers which can be decoded as "Mapperley" and "Waltham" transmitters when referring to the Ofcom database. The peaks in Figure 8-3 show a constant separation of 174T, and giving a single TDOA measurement in this case.

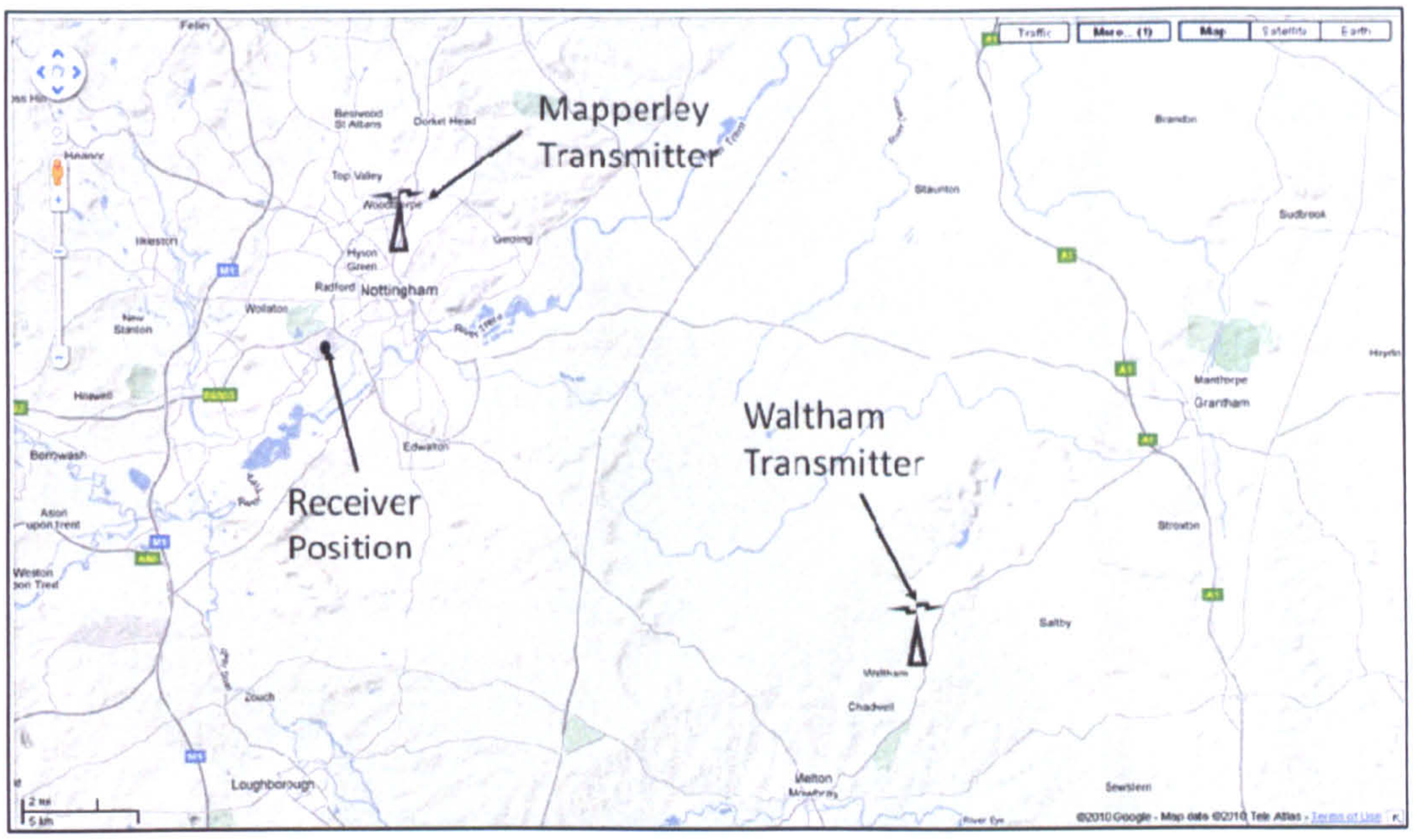

Figure 8-1: Map showing transmitter and receiver positions

(Image courtesy of Google Maps UK)

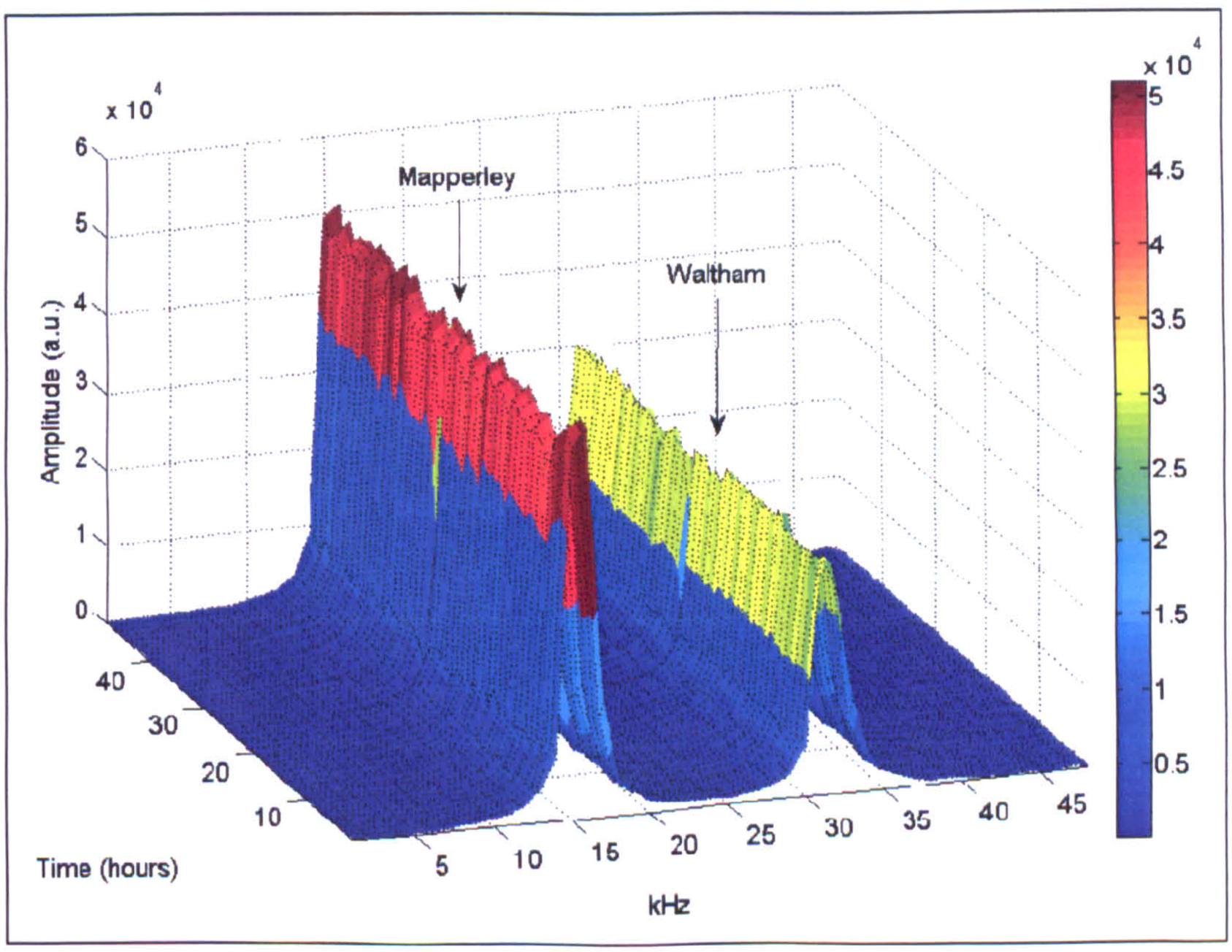

Figure 8-2: TII of block 12B captures over 48-hour period

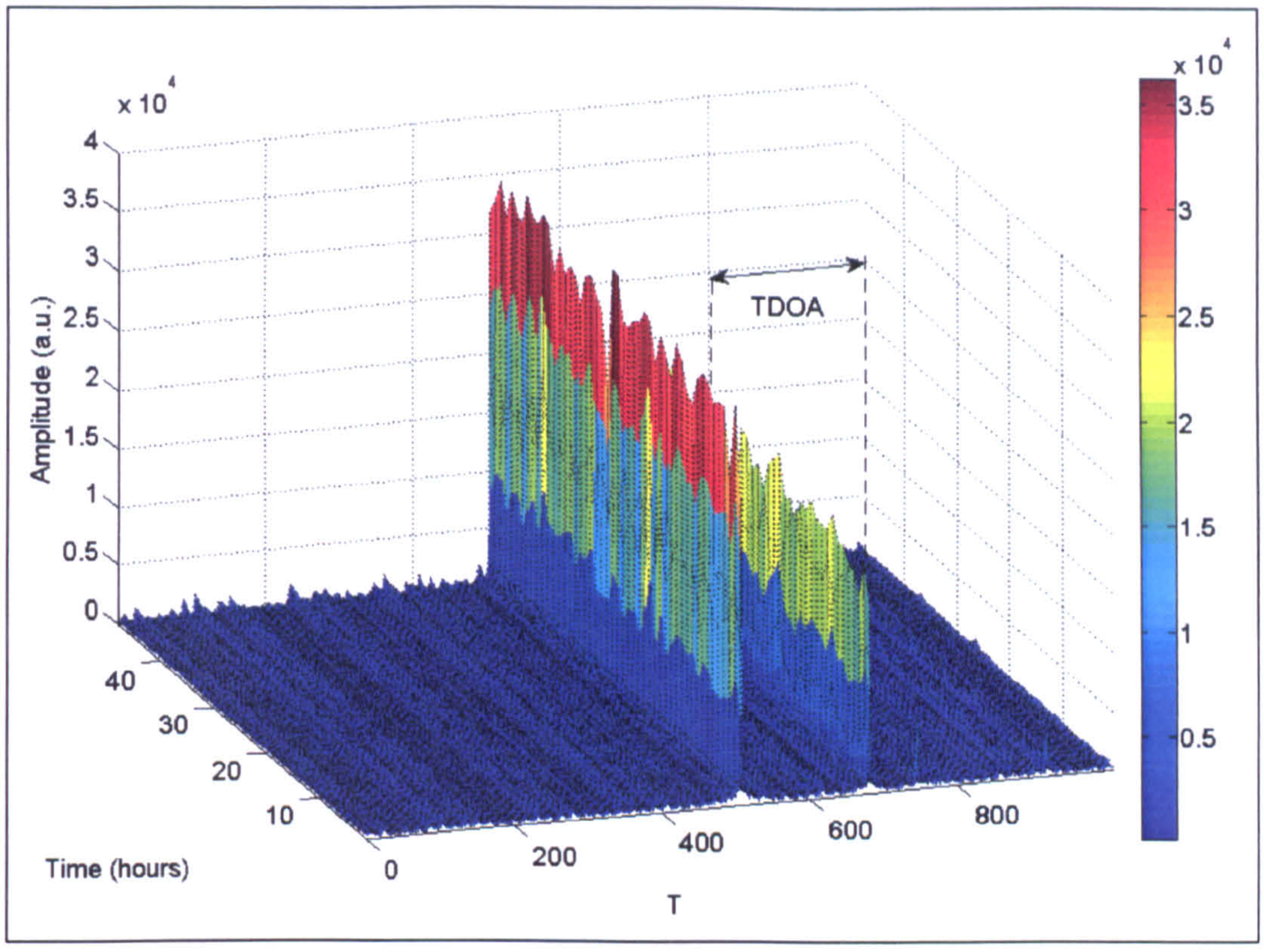

Figure 8-3: Cross-correlation of block 12B captures over 48-hour period

8.3 RECEIVER ANTENNA HEIGHT TESTING

8.3.1 Introduction

This section will examine the difference in receiver antenna height makes in real signal testing. This was performed as a simulation earlier in 7.4. In this scenario, the test equipment was initially stationed at the base of a building on the University of Nottingham campus, and then positioned on the top of a turret on the roof of the same building. The same test was then performed at the base of and the top floor of a 15-story building, based on the same campus.

The purpose of these experiments was to investigate how a large change in height affects the number of transmitters viewable from the same position. It would be expected that new transmitters would come into view if the height of the antenna is increased by a substantial degree.

8.3.2 Results

The first test examined the commercial national network on block 11D. The first capture was taken at 2 metres above ground level at the base of the building, with the second capture taken atop the turret, approximately 15 metres from ground level. It can be seen in Figure 8-4 that a significant difference in cross-correlation amplitude is present between the two DAB captures. Both captures were performed using the same gain value through the capture software, for the same period of time. The results were then averaged to show the mean value achieved over all received DAB frames.

Although the primary signal (based at 505T) shows an increase in amplitude, the secondary correlation peak (at 678T) has shown an unexpected decrease. The process is then repeated using the signal from the Nottingham local network on block 12C.

The results from this (shown in Figure 8-5) show a similar result. While the primary transmitter strength increases with height, the secondary signal decreases.

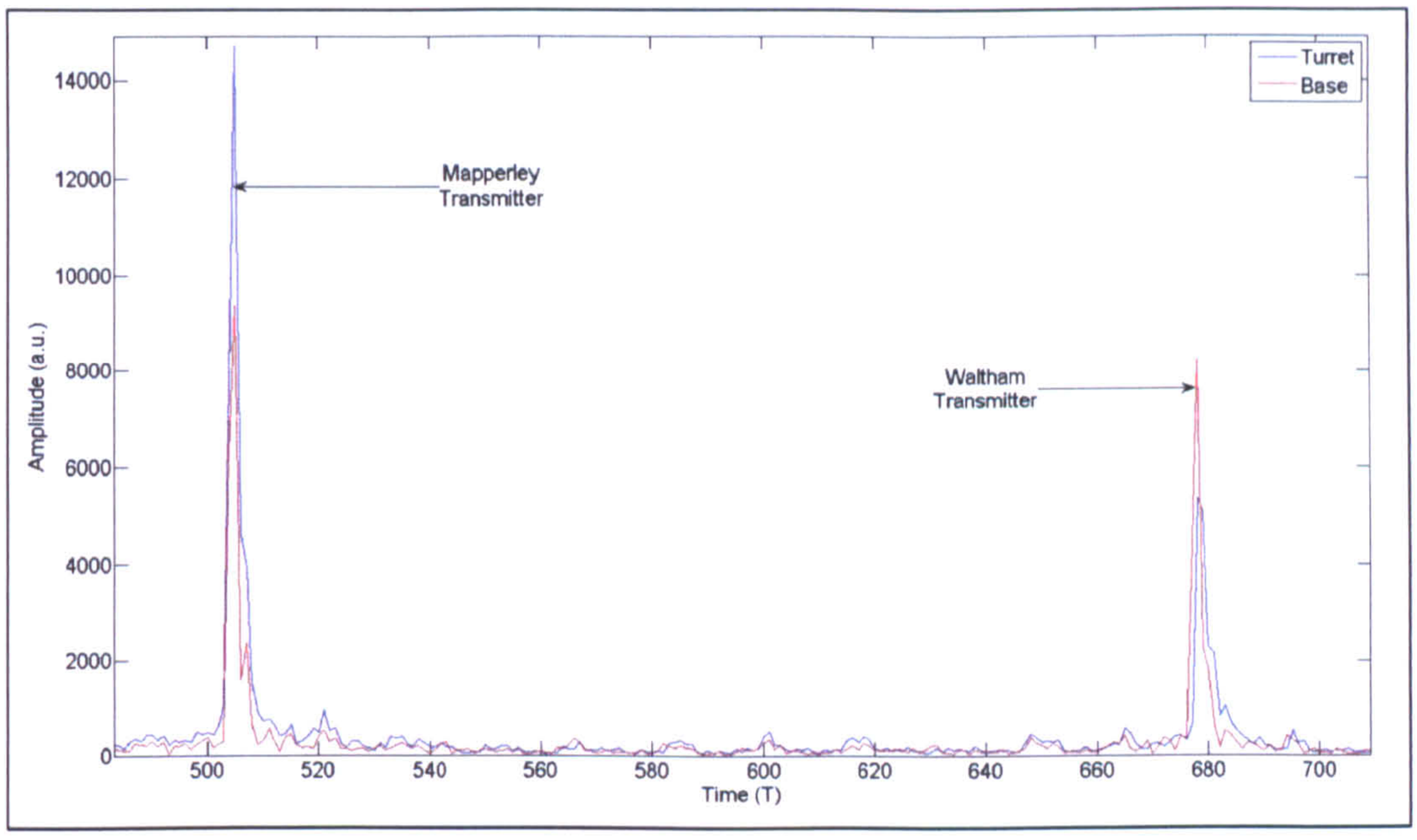

Figure 8-4: Height Testing Location 1 – Block 11D

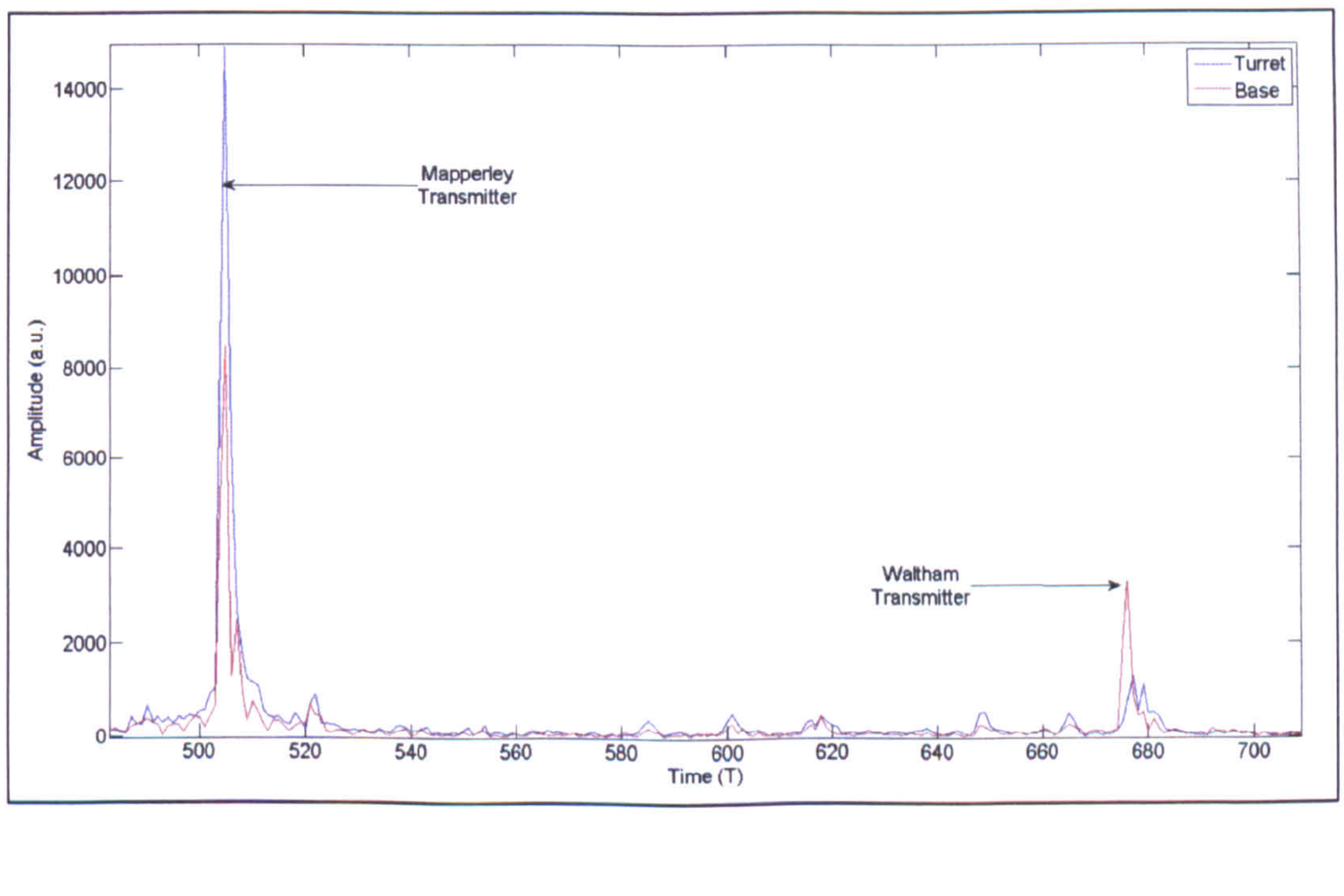

Figure 8-5: Height Testing Location 1 – Block 12C

This result is surprising, as it would be expected that the received power for both transmitters would increase. Instead, it appears that the stronger of the two transmitters 'swamps' the broadcast frequency, causing a smaller correlation peak for secondary signals.

The same experiment was then carried out at the Tower Building on campus, the tallest building in the area, with the top floor capture taken at approximately 60 metres above ground level. This time, the local network result on block 12C is examined (as it is known that a limited number of transmitters broadcast on this frequency within the region). The results of both captures can be seen in Figure 8-6, where the most noticeable change in correlation coefficients is the amount of multipath present on the capture taken from the top of the tower.

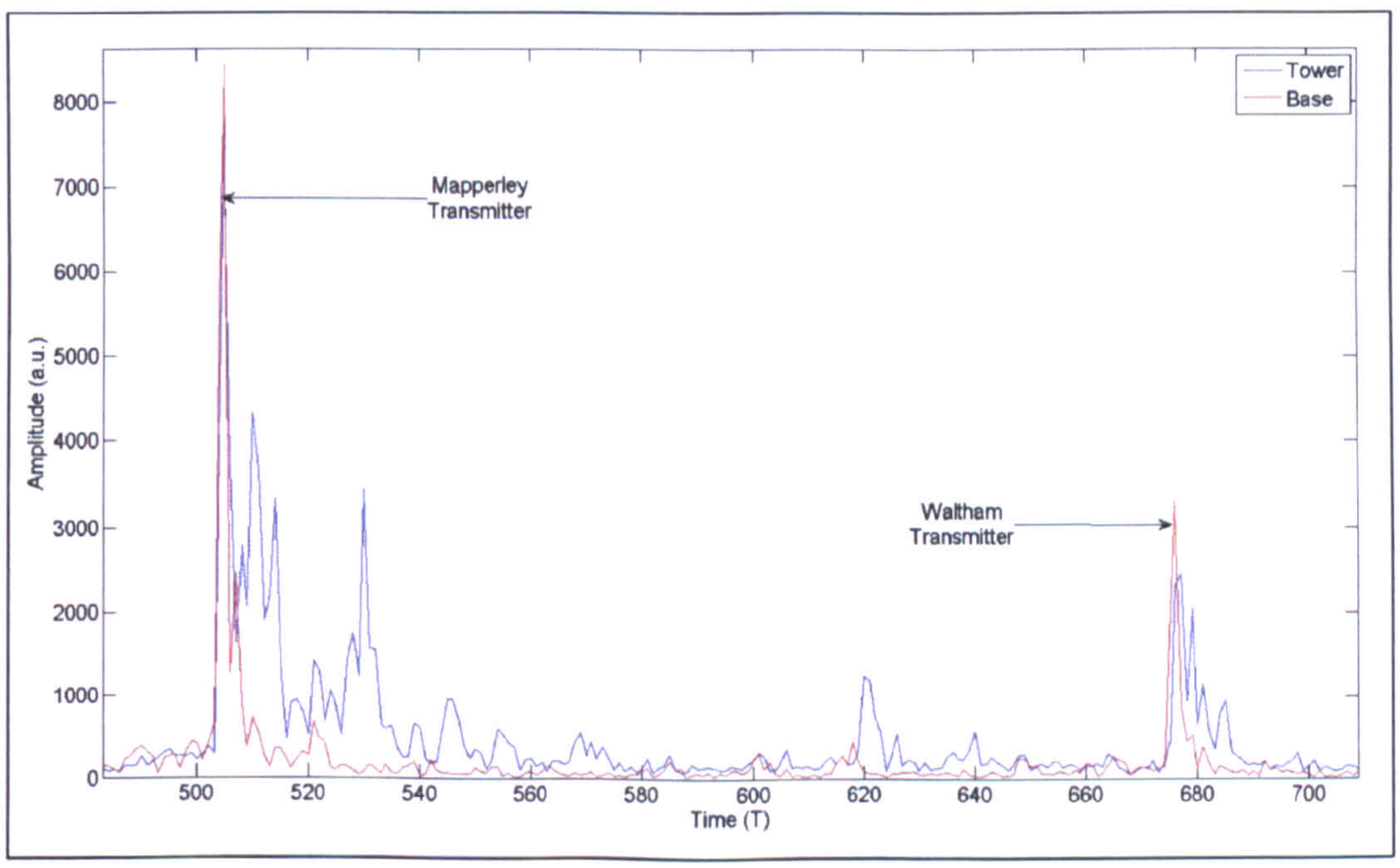

Figure 8-6: Height Testing Location 2 – Block 12C

The same test performed on the national block 11D is then shown in Figure 8-7. It is immediately obvious that a number of new transmitters may be received from the elevated position over the ground based position. In order to evaluate this capture fully, the TII information from both captures must be compared (Figure 8-8).

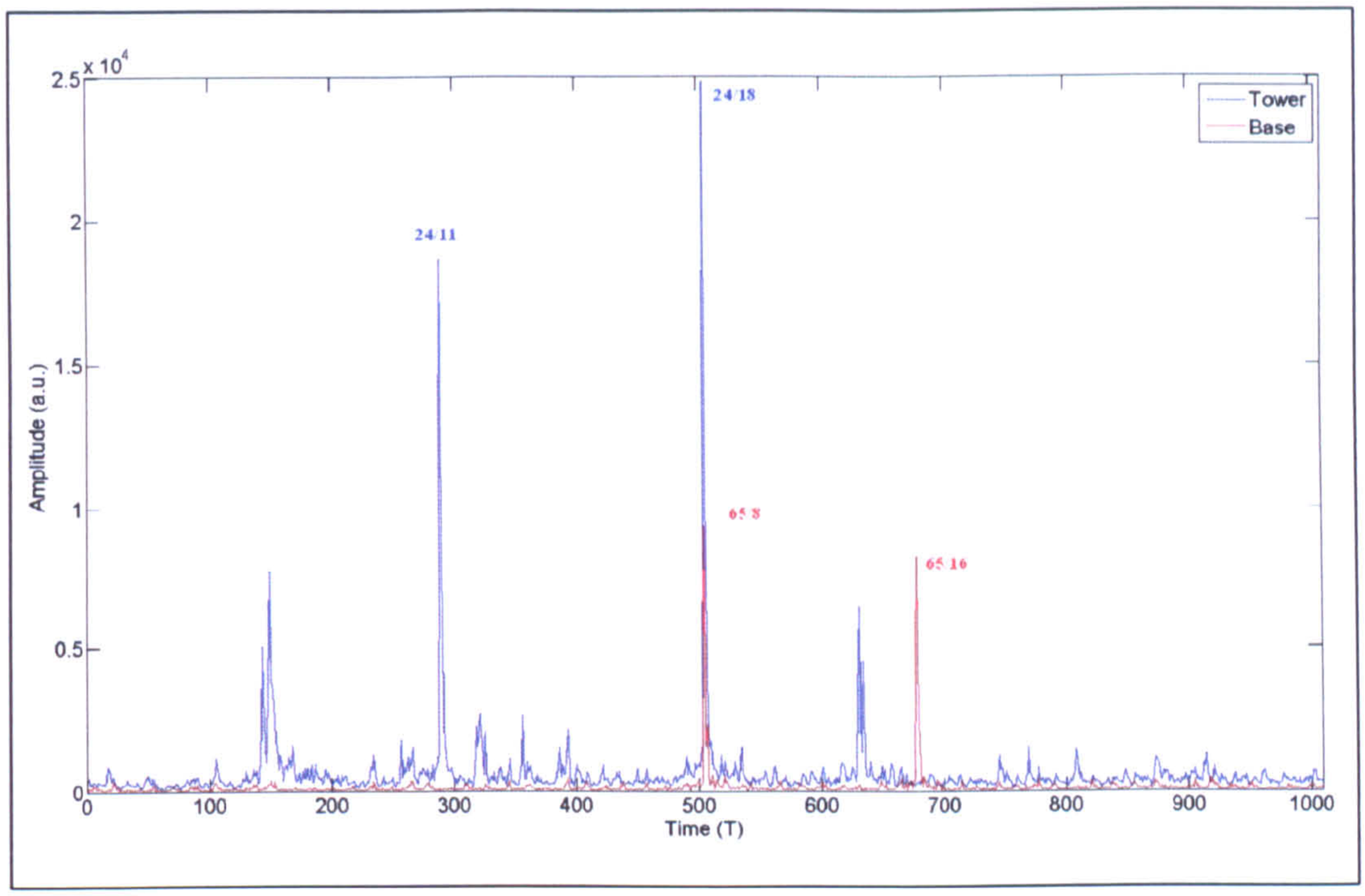

Figure 8-7: Height Testing Location 2 – Block 11D

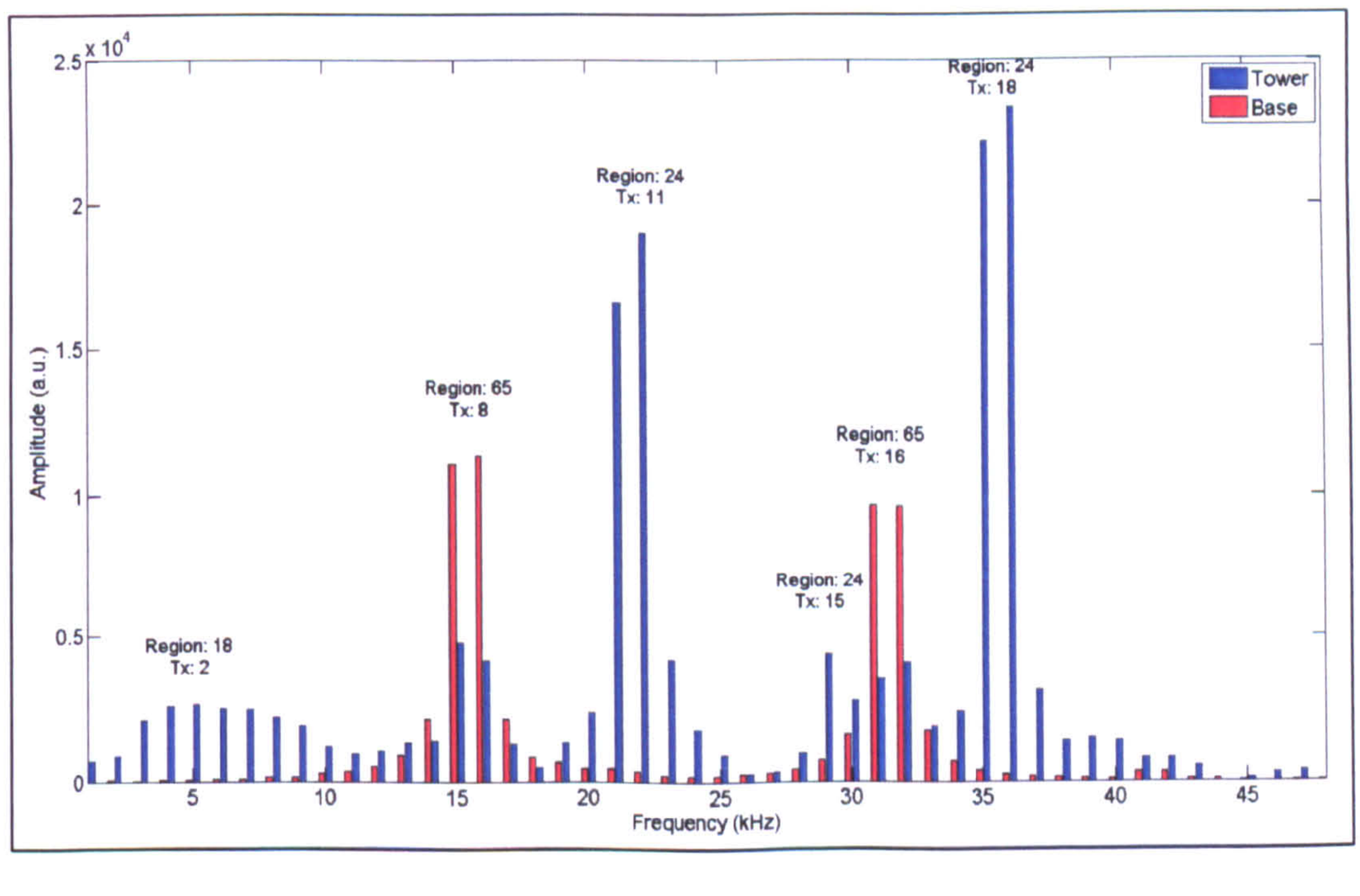

Figure 8-8: TII codes associated with Figure 8-7

While the ground based receiver automatically locks onto the correlation coefficient with greatest amplitude (referring to the TII information, this transmitter has the code

Region 65, Tx 8), the tower based receiver receives a number of more powerful transmitters that lie outside of the line-of-sight of the ground based receiver.

In this scenario, the primary transmitter locked onto by the signal processing algorithms has the TII code Region 24, Tx 18, with a number of other signals present along the frequency axis.

This shows that a difference in elevation of only 60 metres can make a significant difference in the number of transmitter's receivable. In this instance, the number of transmitters increases from 2 to 6 (N.B. further transmitters are likely to be present, however the detection algorithms detected six on this capture).

8.4 ANTENNA TESTING

8.4.1 Introduction

The purpose of this test was to establish the difference in quality of observable measurements between DAB antenna positioned at the same location. As the purpose of this project is to examine the positioning potential of DAB, the antenna that gave the better results would then be used for the main trials reported on later in this project.

For this test, the primary passive dipole omni-directional antenna was compared to the smaller active directional patch antenna (refer to Figure 6-4 on page 73 for details of both antennas). Both antennas were installed at the same height, with the same capture input parameters through the GNU Radio software.

The antennas were positioned at the following two locations for this test. Both tests capture the DAB national commercial network on block 11D. Positions were measured using Real-Time Kinematic (RTK) GPS equipment.

	Position 1	***Position 2***
East (m)	469199	482652
North (m)	380516	374236
Terrain Elevation (m)	35	8
Antennas height above terrain (m)	3	3
Total Height (m)	38	11

Table 10: DAB receiver positions

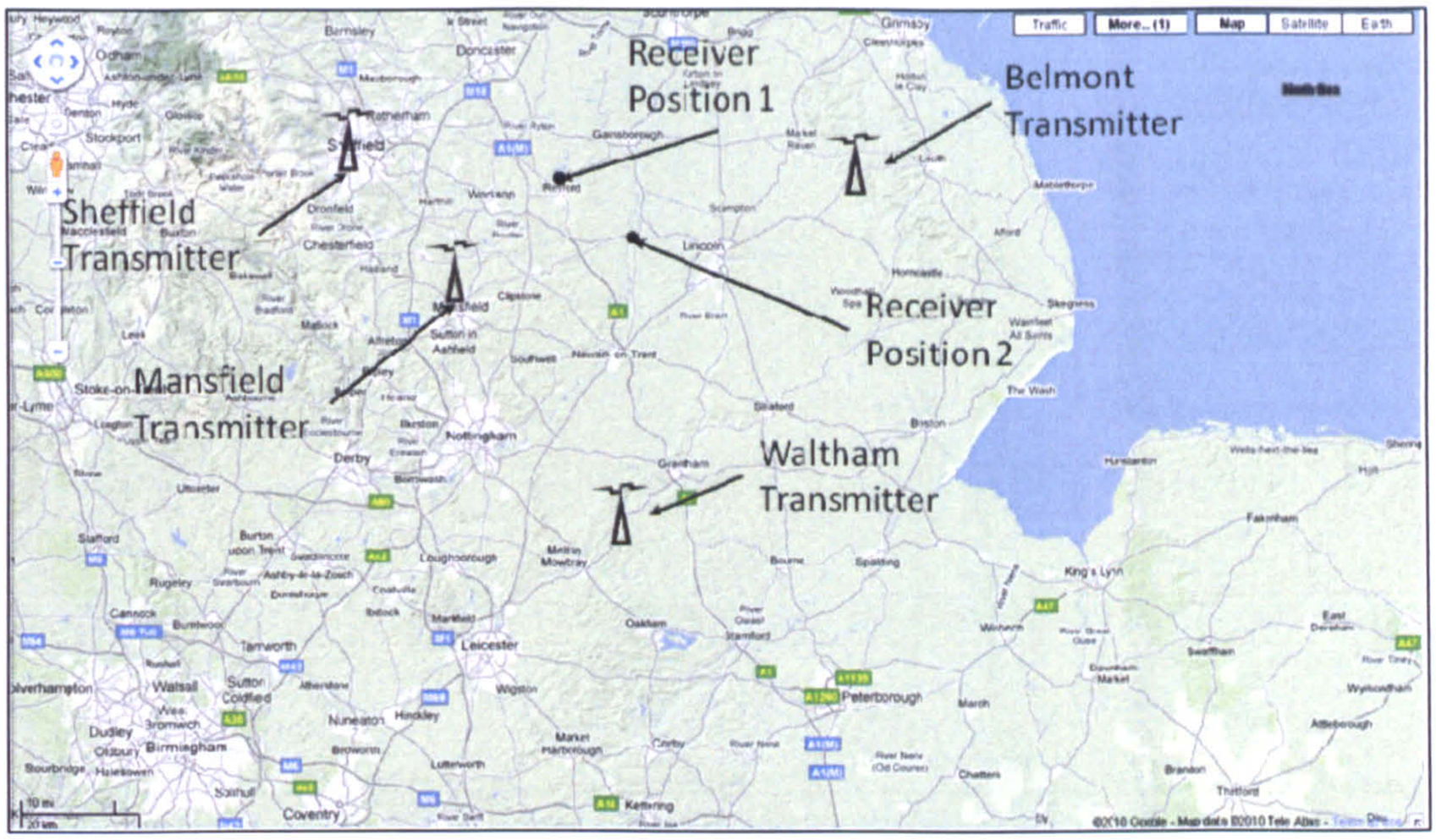

Figure 8-9: Map showing transmitter & receiver locations

(Image courtesy of Google Maps UK)

8.4.2 Results

8.4.2.1 Position 1

The received TII and TFPR cross-correlation charts for position 1 can be seen in Figure 8-10 and Figure 8-11 respectively. Three unique incoming transmissions can be identified using the dipole antenna (sufficient for a 2D fix) whilst only two transmissions can be seen from the patch antenna. The transmission from the Mansfield transmitter suffers on the patch antenna capture where the cross-correlation peak lies below the threshold associated with the primary received signal from the Waltham transmitter. The background noise level from the patch antenna result is also of greater magnitude than the dipole which can be seen in Figure 8-10.

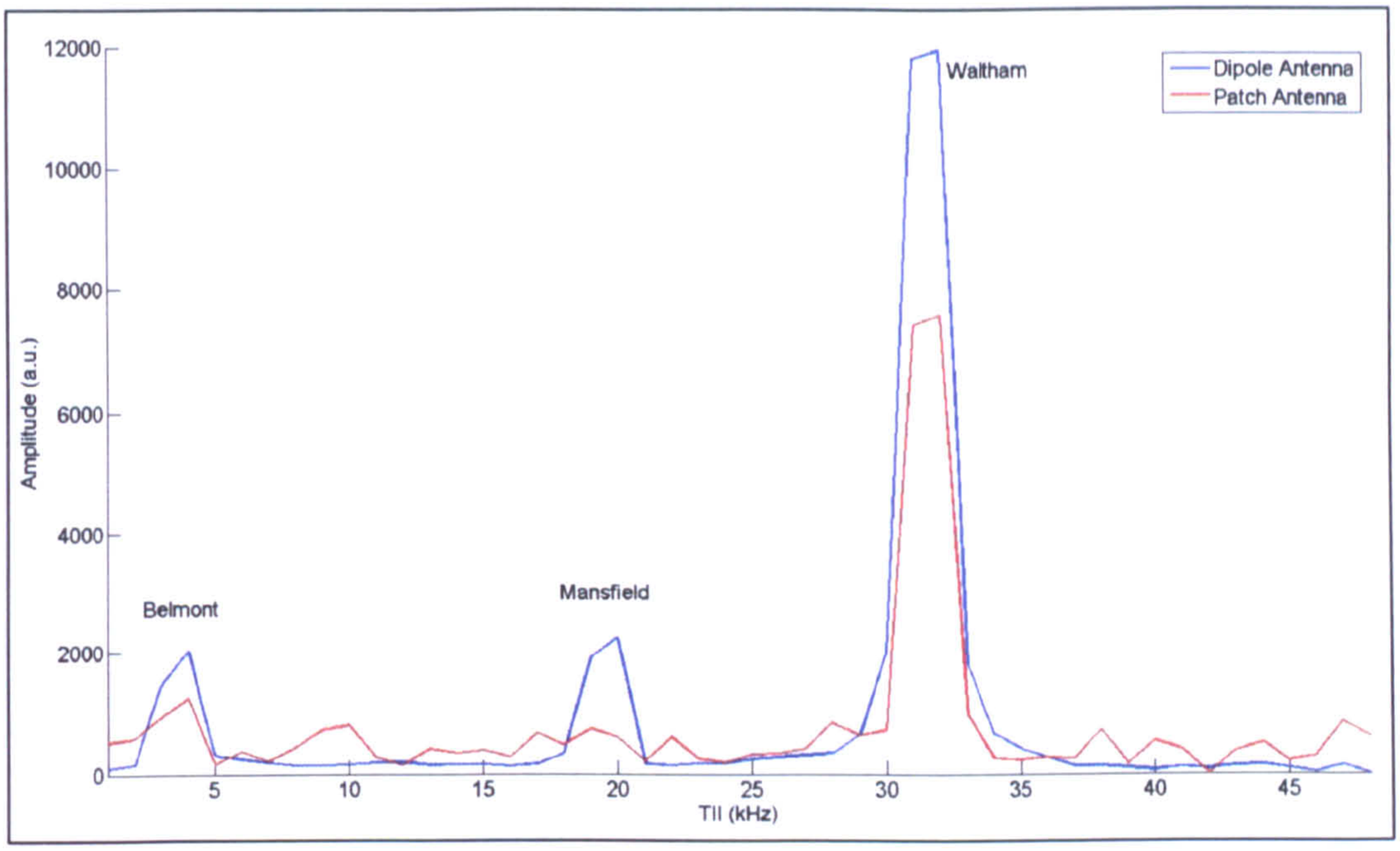

Figure 8-10: Antenna Testing Position 1 – TII

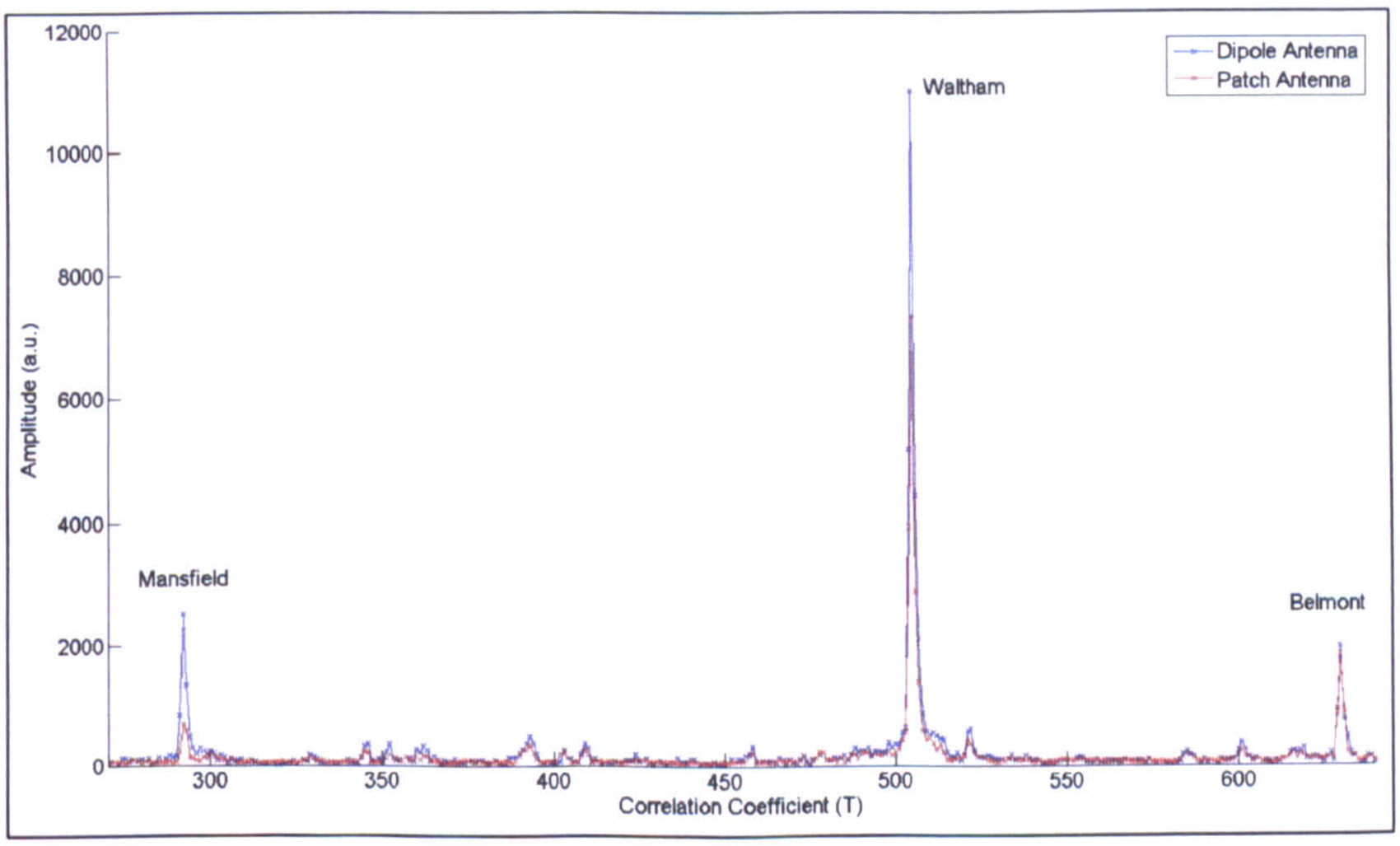

Figure 8-11: Antenna Testing Position 1 – Cross-correlation

8.4.2.2 Position 2

The results from position 2 show a higher level of noise from the patch antenna than the dipole than was seen at position 1. Four transmitters can be clearly identified from the TII information from the dipole as can be seen in Figure 8-12, whilst three can be recognised from the patch antenna.

The patch does not successfully identify the transmitter at Sheffield, whilst significantly lower signal amplitudes are detected for both the Mansfield and Belmont transmitters.

This scenario is also shown when viewing the correlation coefficients in Figure 8-13, where different primary signals are detected from the two antennas. The patch locks on to Waltham as its most powerful signal whilst the dipole locks to Mansfield.

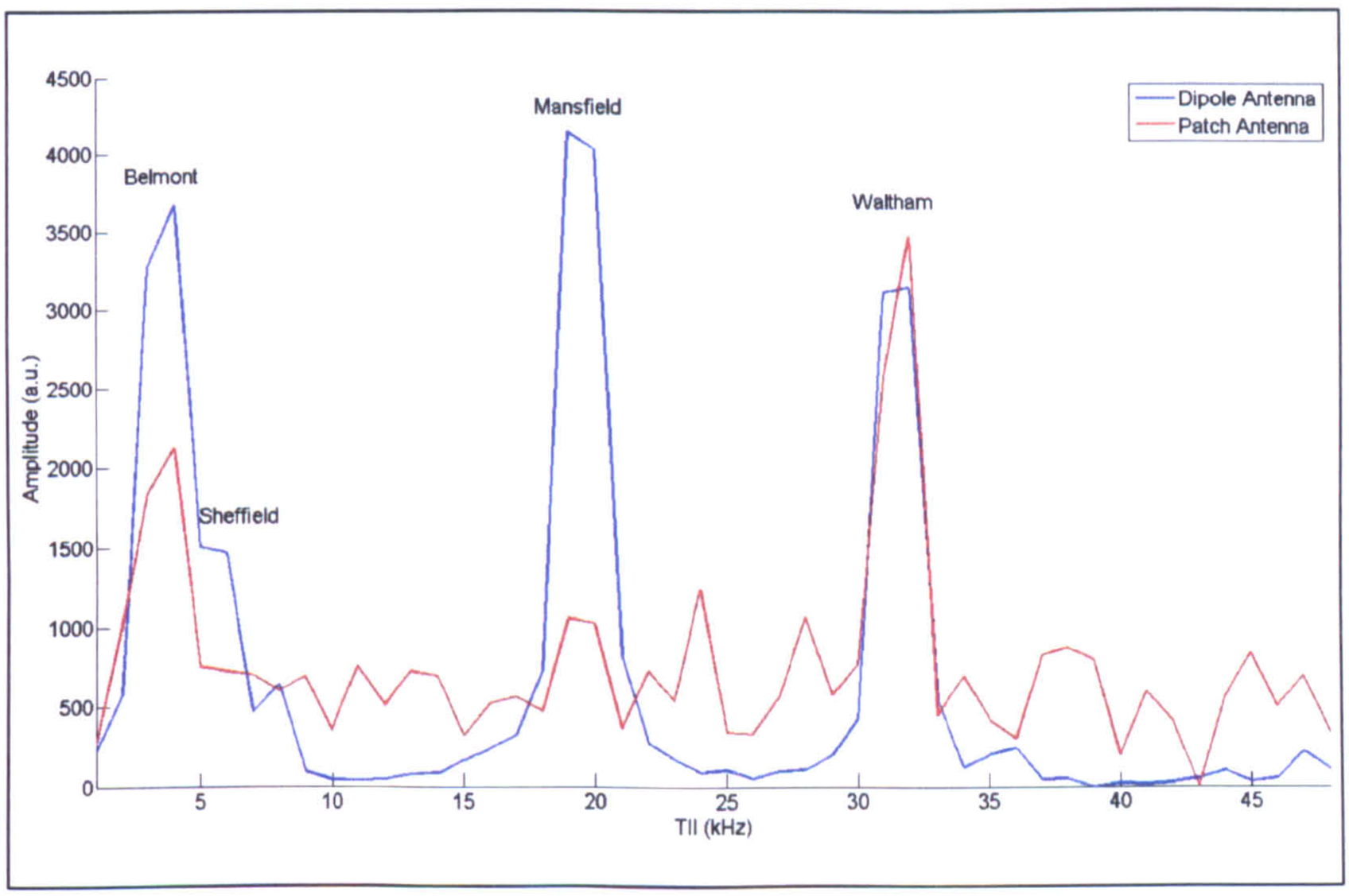

Figure 8-12: Antenna Testing Position 2 - TII

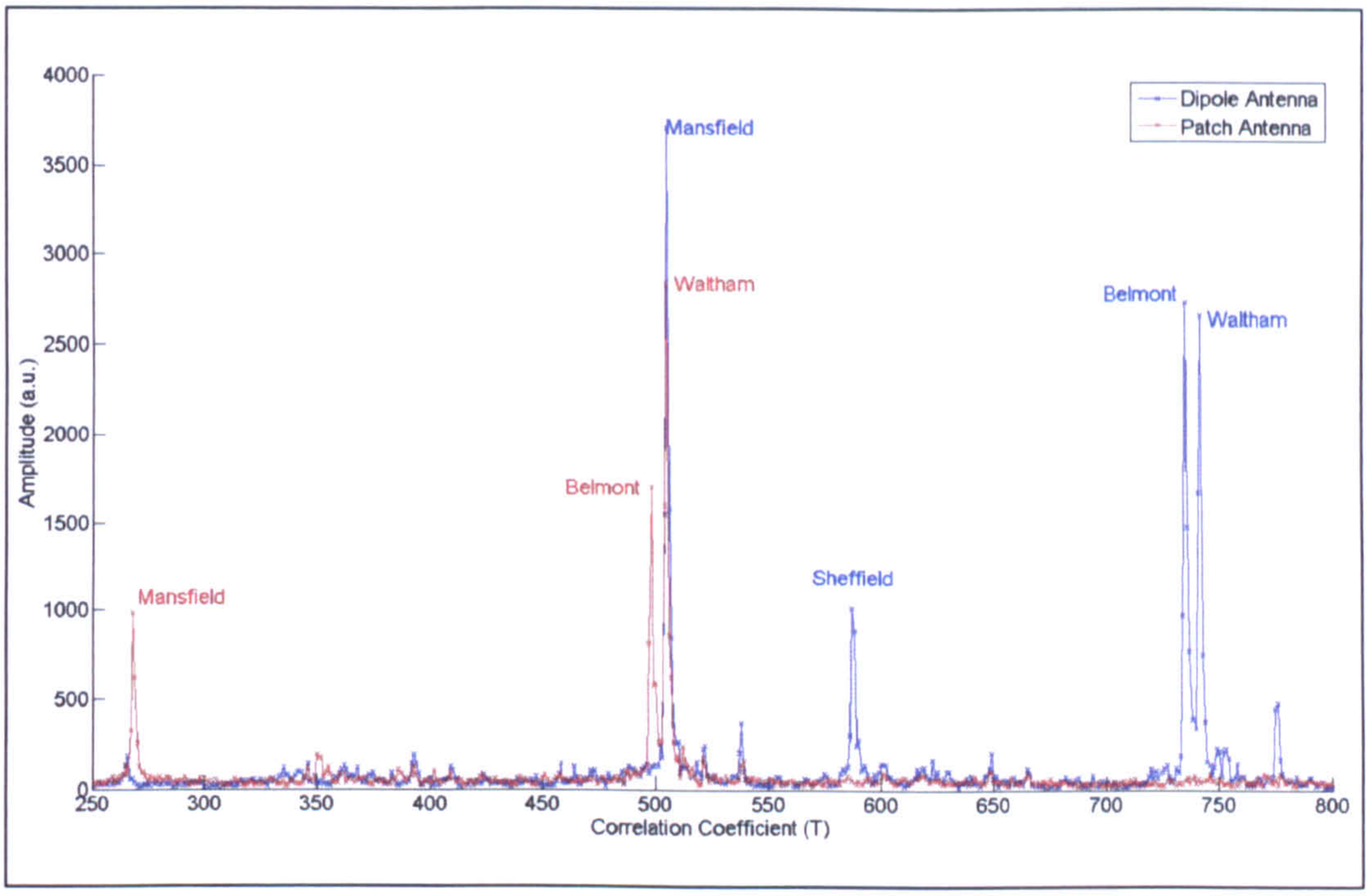

Figure 8-13: Antenna Testing Position 2 – Cross-correlation

8.4.3 Conclusions

The purpose of this exercise was to identify a receiving antenna to use for the primary static and dynamic experiments performed later in this project. It has been shown that whilst both antennas have the ability to receive and identify multiple signals on a single DAB frequency, the dipole results are shown to be far more impressive than the patch.

Naturally, the physical size of the dipole makes it less portable than the patch antenna, but as the aim of this project is to perform a feasibility study for the use of the DAB signal as a positioning source, this matter remains of relative unimportance.

Therefore, the dipole antenna was chosen for the remainder of the experiments in this project.

8.5 INDOOR TESTING

8.5.1 Introduction

The purpose of this test is to examine the system's ability to detect usable signals in an indoor location and examine the possible effect of multipath within this environment.

Three positions were chosen within an indoor environment, on different floors and at the same depth within the building. The depth of the captures lay behind one external (constructed from breeze blocks) and one internal (plasterboard) wall at a depth of approximately 5 metres from the edge of the building (see plan in Figure 8-14). Each floor had a change in height of approximately 4 metres.

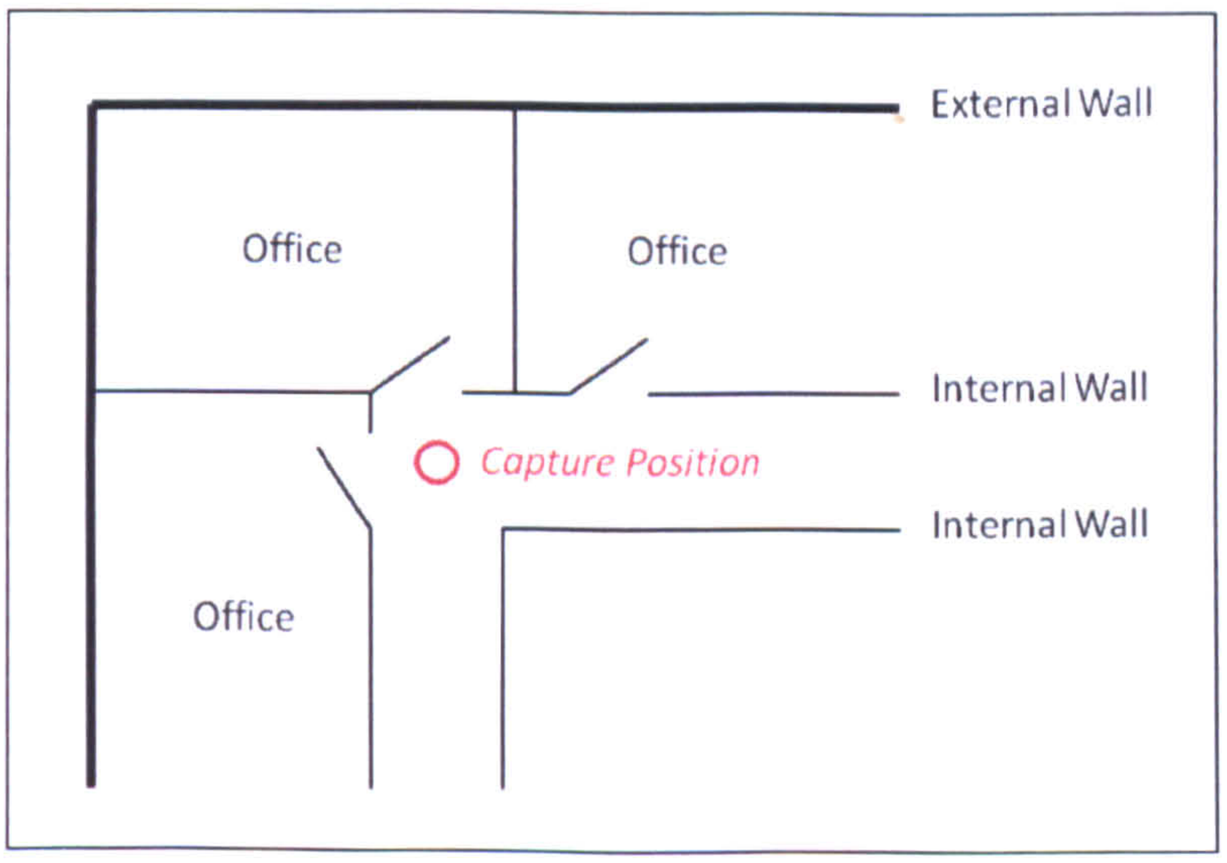

Figure 8-14: Indoor test – Floor Plan

8.5.2 Results

The results from the test were inadequate to produce a position estimate, primarily due to the transmitters in view of the receiver's antenna. The following three charts show the correlation coefficients and associated TII information measured using the commercial national network (block 11D) over three floors in the same building.

Each of the three positions had the same OS National Grid position but merely a difference in floor level (from ground to second floor).

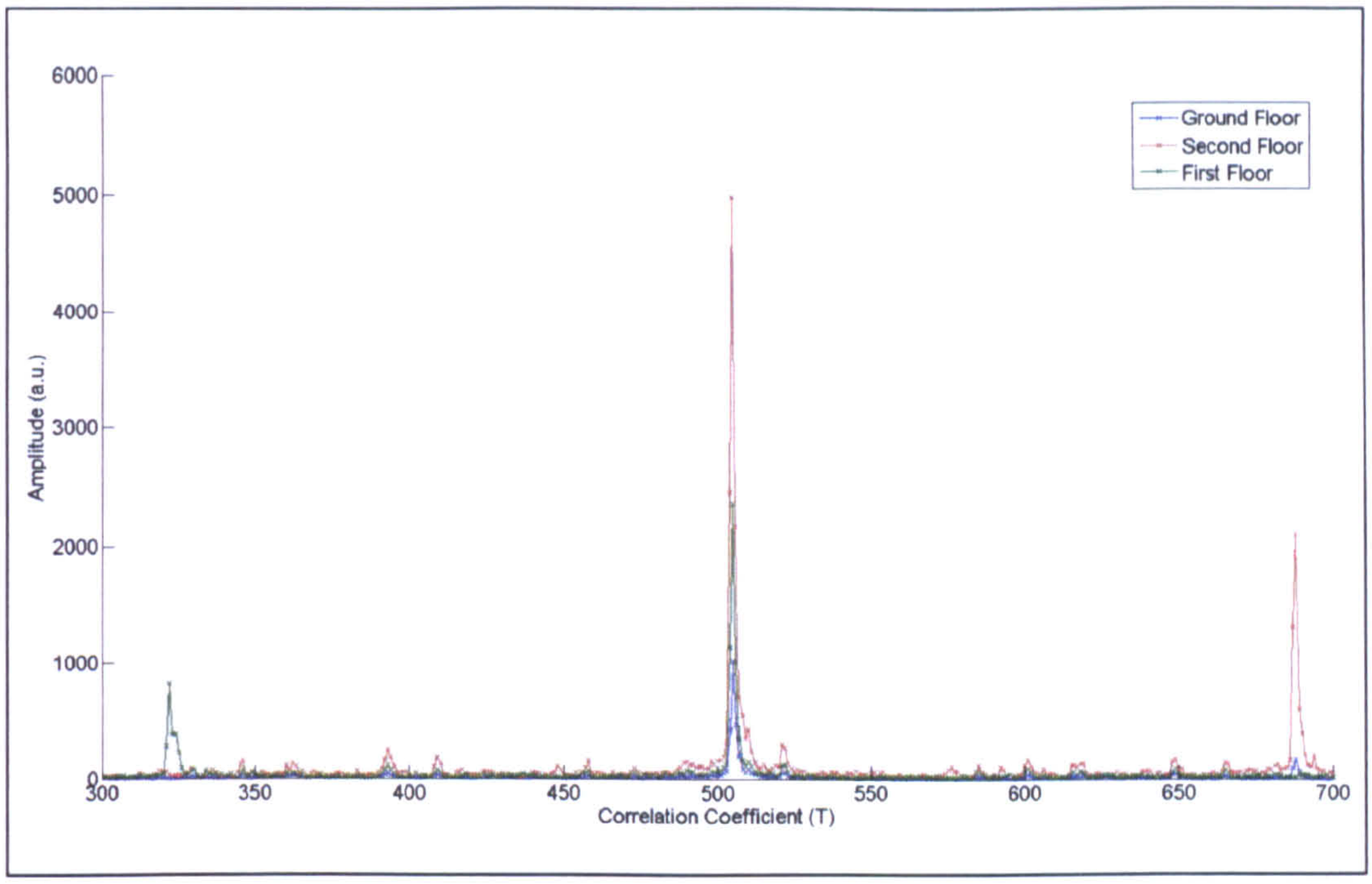

Figure 8-15: Indoor Test – Cross-correlation of TFPR symbol

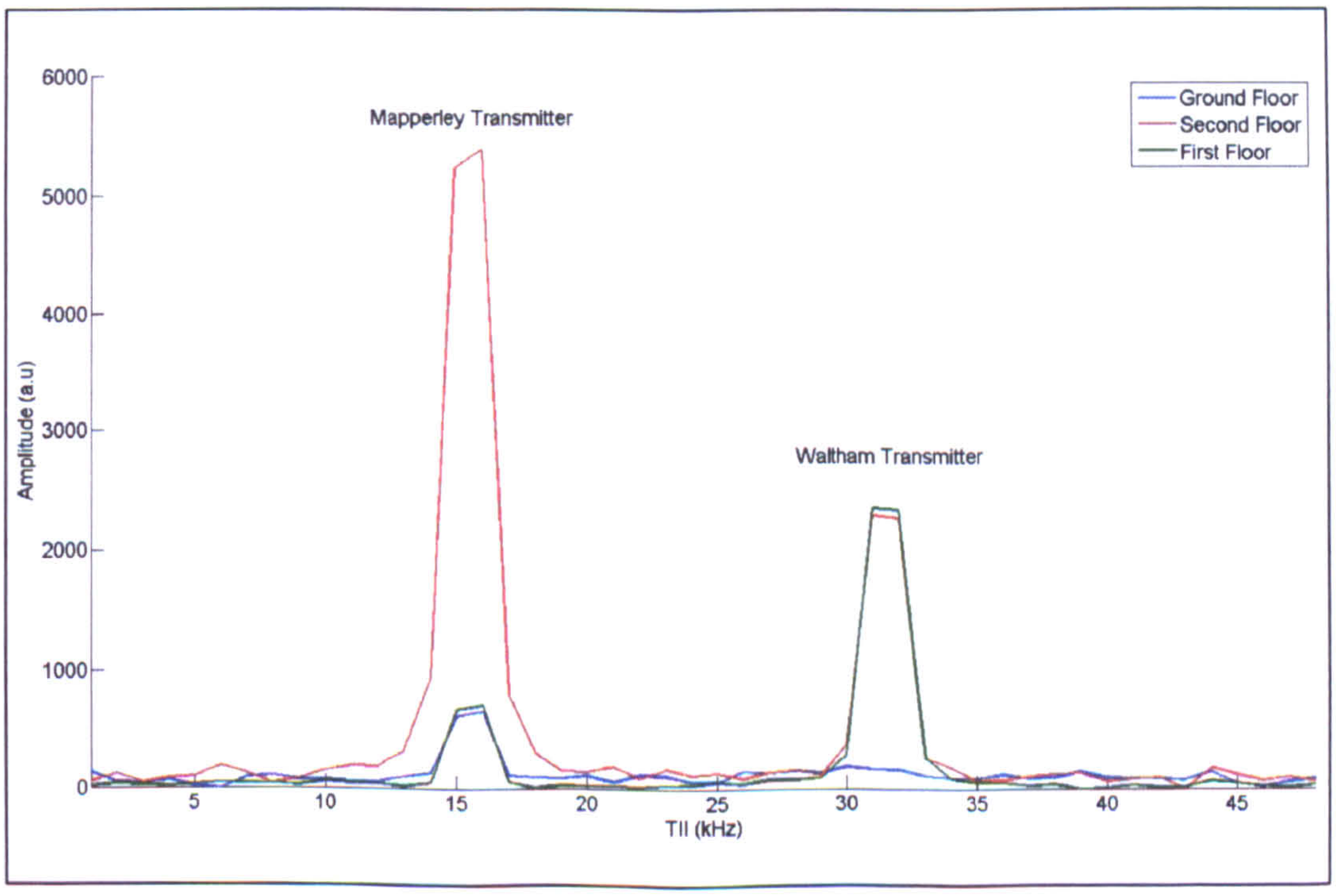

Figure 8-16: Indoor Test – TII information

The chart shown in Figure 8-15 shows the cross-correlation coefficients of each capture taken from block 11D, while Figure 8-16 shows the associated TII signal for these captures.

In this region, it would normally be possible to obtain a weak signal from transmitters based close to the city of Leicester on the local DAB block 11B when out in the open, as may be seen in subsequent experiments. However, within the indoor environment this was not possible due to the poor quality (low SNR) of the signals. It was still possible to obtain information about two transmitters on all floors, those situated at Waltham and Mapperley (highlighted in Figure 8-16), proving that multiple signals are still available to an indoor environment.

Multipath was not seen to cause a problem in this test as can be seen by the cross-correlation plots. If multipath was present here, it would be visible on a sub-T position only as the walls of the building lie within the highest possible resolution of this system (≈ 150 metres).

8.6 TRANSMITTER DATABASE ACCURACY TEST

8.6.1 Introduction

Earlier in this project (see section 6.8.2.3), the accuracy of the transmitter location database as supplied by Ofcom was investigated. It was shown that the locations provided were only as accurate as the $100m^2$ grid reference square that the transmitter was located in. The potential effect of this could be a measurement difference of more than one unit of $\boldsymbol{T}$ - therefore this issue was investigated further.

8.6.2 Transmitter Survey

Each transmitter visited had to be surveyed using a Leica *Smartstation*, due to the restricted access of the area immediately underneath and surrounding each mast. An angle of intersection was measured at two ends of a baseline, the length of which was dependant on the visibility of each mast (see Figure 8-17 for details).

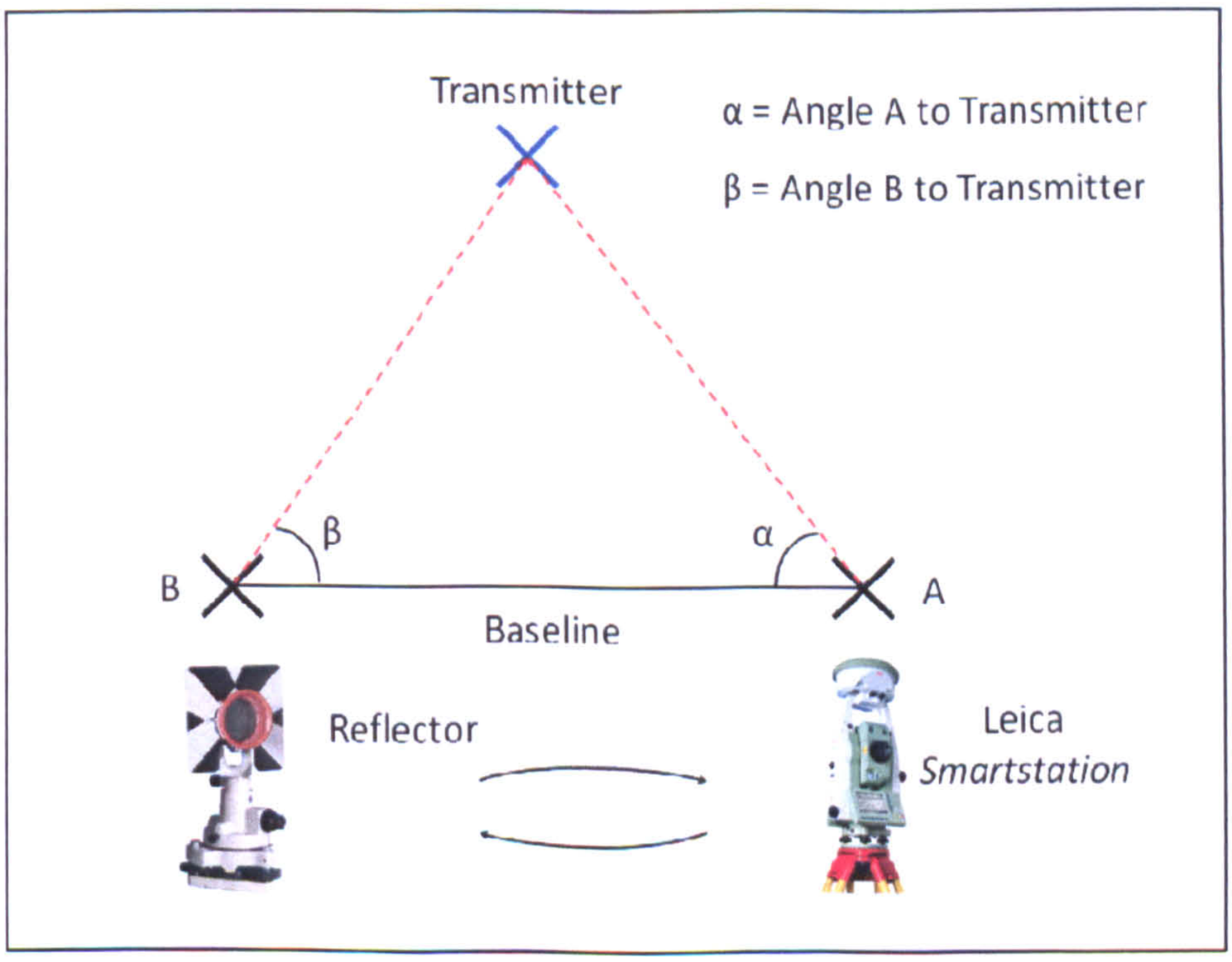

Figure 8-17: Transmitter Survey Method

A levelled tripod was positioned at each end of a baseline, with the *Smartstation* installed on one and a target reflector on the other. The *Smartstation* was then used to measure the position of the first tripod using RTK GPS and was then used to measure the angle between a point on the transmitter mast and the reflector. This process was then repeated after swapping the *Smartstation* and reflector positions, allowing for the calculation of the baseline length and angle from the second tripod to the mast. This provided sufficient information to calculate the position of each mast.

A number of locations were chosen in a region which was known to be within range of four transmitters. Data captures were taken at each position and the transmitters identified successfully. The transmitters themselves were then visited and surveyed to within an accuracy of one metre, with the results then used in place of the locations found on the database and a comparison made.

8.6.3 Results

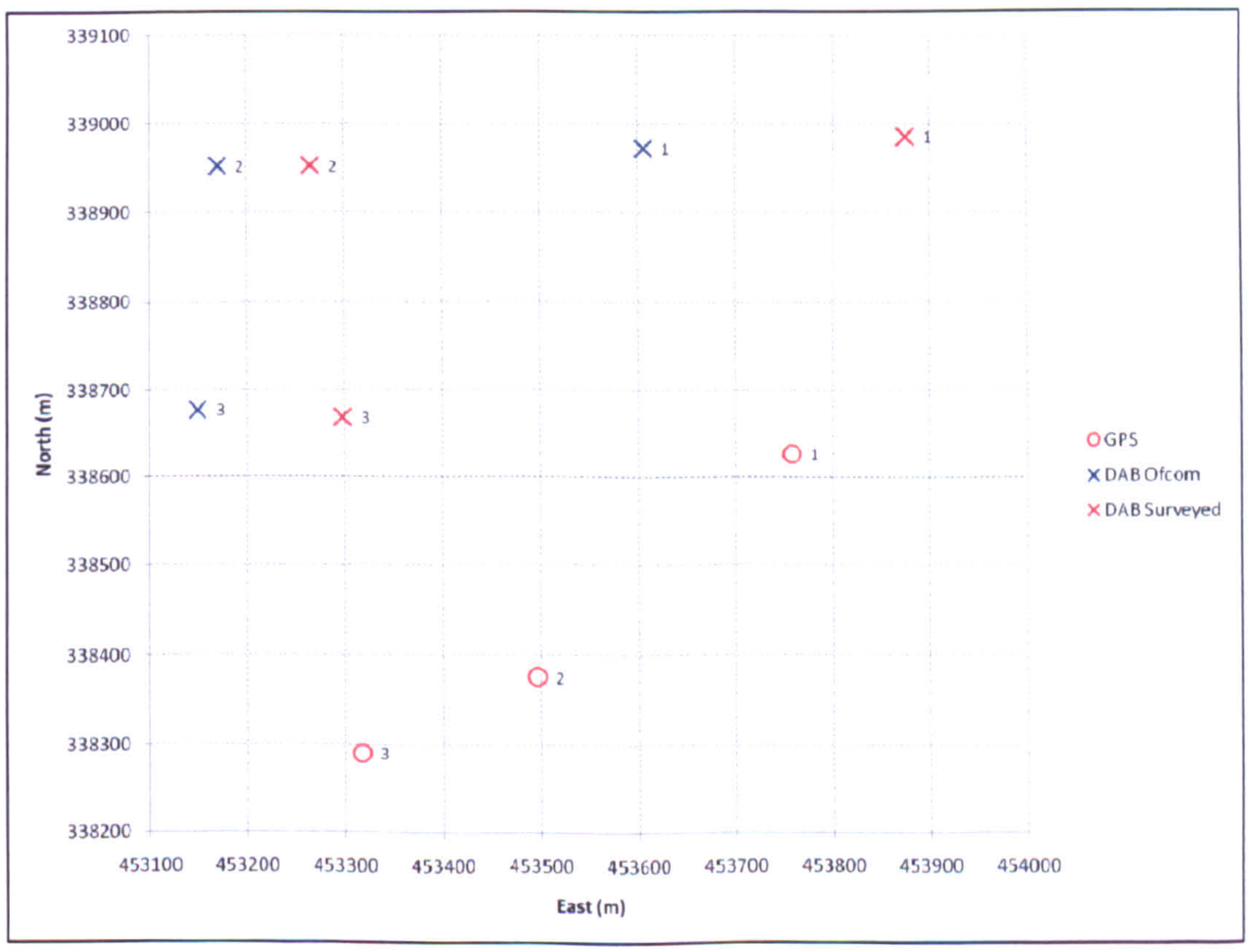

Figure 8-18: Database transmitter accuracy test

The results presented in Figure 8-18 show the difference in DAB positional estimates from both the Ofcom transmitter database and the revised transmitters found by surveying each mast. The change in position can be seen to be quite significant here, particularly in case 1, where although the offset from GPS is still at the same distance, the hyperbolic grid intersection shifts eastwards by approximately 300 metres.

The captures at locations 2 and 3 also show a smaller offset from GPS when using the surveyed transmitter masts. The Easting, Northing and total linear offsets can be seen in the charts in Figure 8-19.

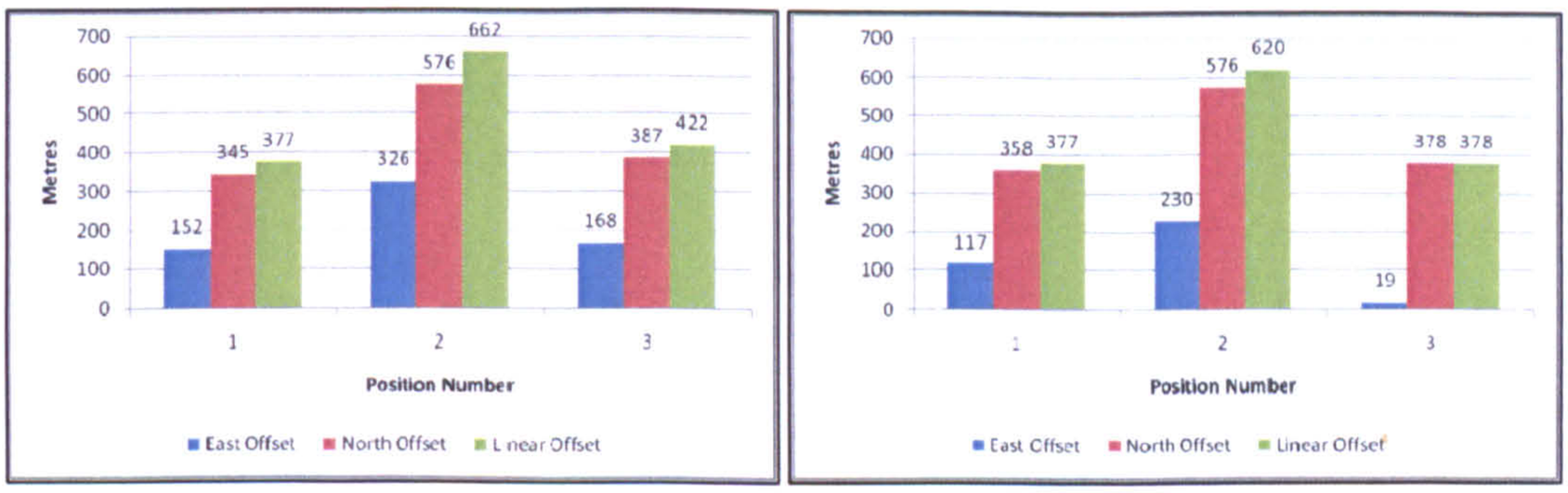

Figure 8-19: Charts showing difference in DAB/GPS offset

Left chart shows the offset from the Ofcom database; right chart shows the offset when all transmitter positions have been surveyed

Position 3 in this case makes a dramatic difference in the east offset and improves from 168 metres when using the public database to just 19 metres using the surveyed sites. In all three cases, the largest differences appear in the Easting component with only small differences in the Northings. The effect of these coordinate errors will of course depend wholly on the array of the transmitters that are visible to the receiver, but it can be seen here in this test that the difference in transmitter database positions can make a significant difference.

Due to the time taken to survey each transmitter for this test, it was decided to continue to use the Ofcom coordinates for the remainder of the experiments.

8.7 REPEATABILITY TESTING

8.7.1 Introduction

This test was performed around the interior road system on the University Park campus. The purpose of the test was to use any available DAB blocks at each static location (measured by GPS) to establish a position estimation and then repeat this process by returning to each capture point (precision within 1m) and performing the same process.

As the transmitter oscillator consistency over time was tested in experiment 8.2, the results would be expected to be identical during the repeated test.

8.7.2 Results

The plot shown in Figure 8-20 shows the positioning results as described above. Each capture location includes a precise RTK GPS solution providing sub-metre accuracy to allow the precise repeat test procedure. As this test was conducted over a relatively small region, the same transmitters were found for each capture point (detailed below).

	Mapperley 65/08	**Waltham 65/16**	**Houghton 65/21**	**Copt Oak 65/17**
Location (E/N)	*458350/342450*	*480950/323350*	*467550/304450*	*448350/312650*
Block 11B	×	×	✓	✓
Block 11D	✓	✓	✓	✓
Block 12B	✓	✓	×	×
Block 12C	✓	✓	×	×

Table 11: Transmitters & DAB Frequencies

At the majority of positions, the system could extract two TDOA measurements using the potential combinations of transmitter pairs shown in the previous table. The most common solution was to use Mapperley and Waltham as one transmitter pair (giving the first TDOA measurement) and Houghton and Copt Oak transmitters as the second. However, a number of the capture points (the locations with greater elevation) were able to extract a third TDOA measurement on Block 11D only between Houghton and either Mapperley or Waltham.

It can be seen that the DAB locations do not coincide perfectly with the GPS location which is due to the measured integer ***T*** values discussed in 7.5. The magnitude of each offset from the GPS position for Easting, Northing and the total linear offset can be seen plotted in Figure 8-21, where capture 10 shows the offset with the largest magnitude. Capture 10 also happens to have the lowest capture elevation, meaning that more distant signals may not have sufficient power to penetrate objects within the line-of-sight.

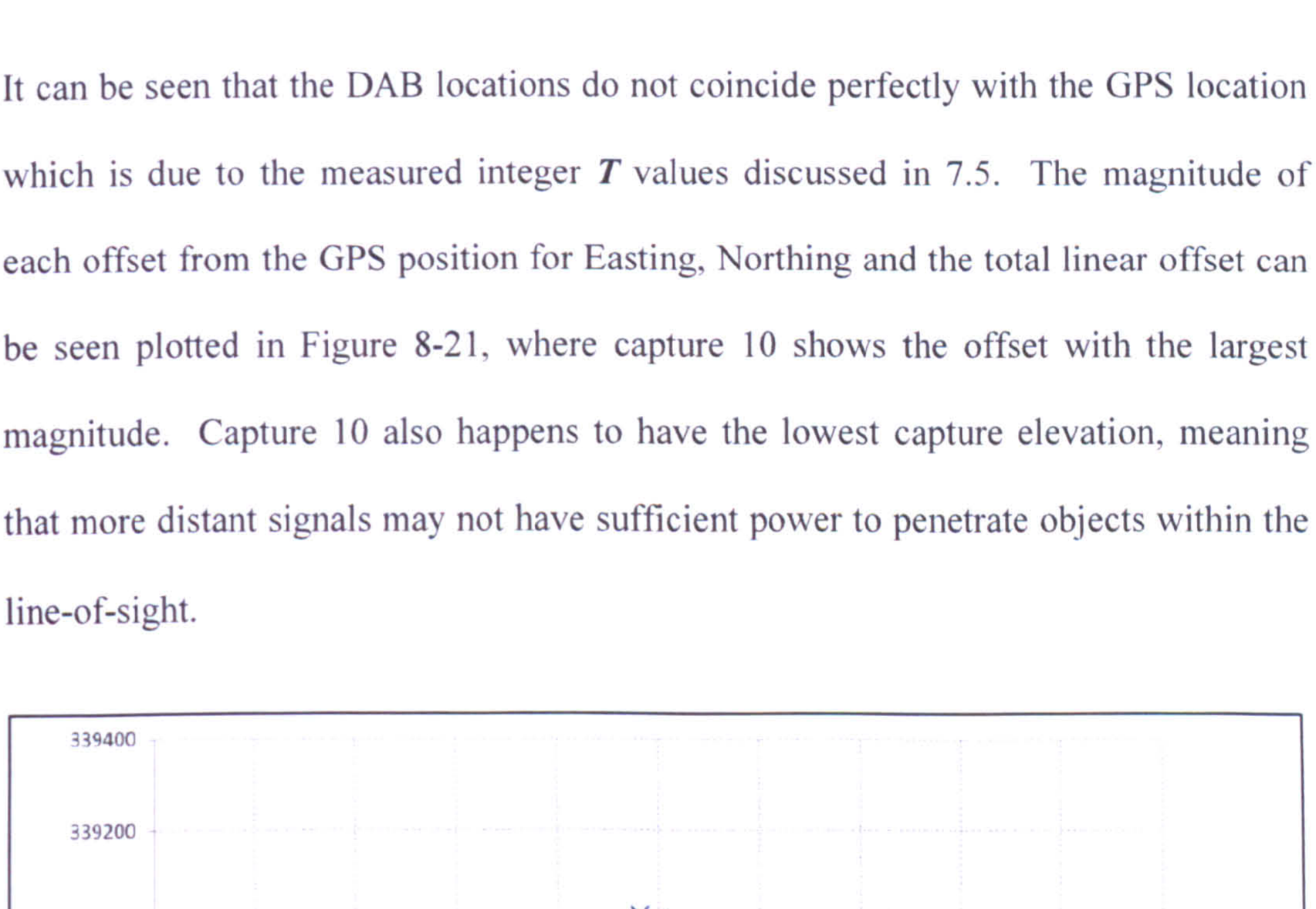

Figure 8-20: Positioning Results from test 8.6

The chart plotted in Figure 8-23 shows all captures plotted as their linear offset from GPS (y-axis) against the terrain height (x-axis). A linear trend-line drawn against this data indicates that the higher the elevation, the smaller the offset of the DAB position from the true GPS position.

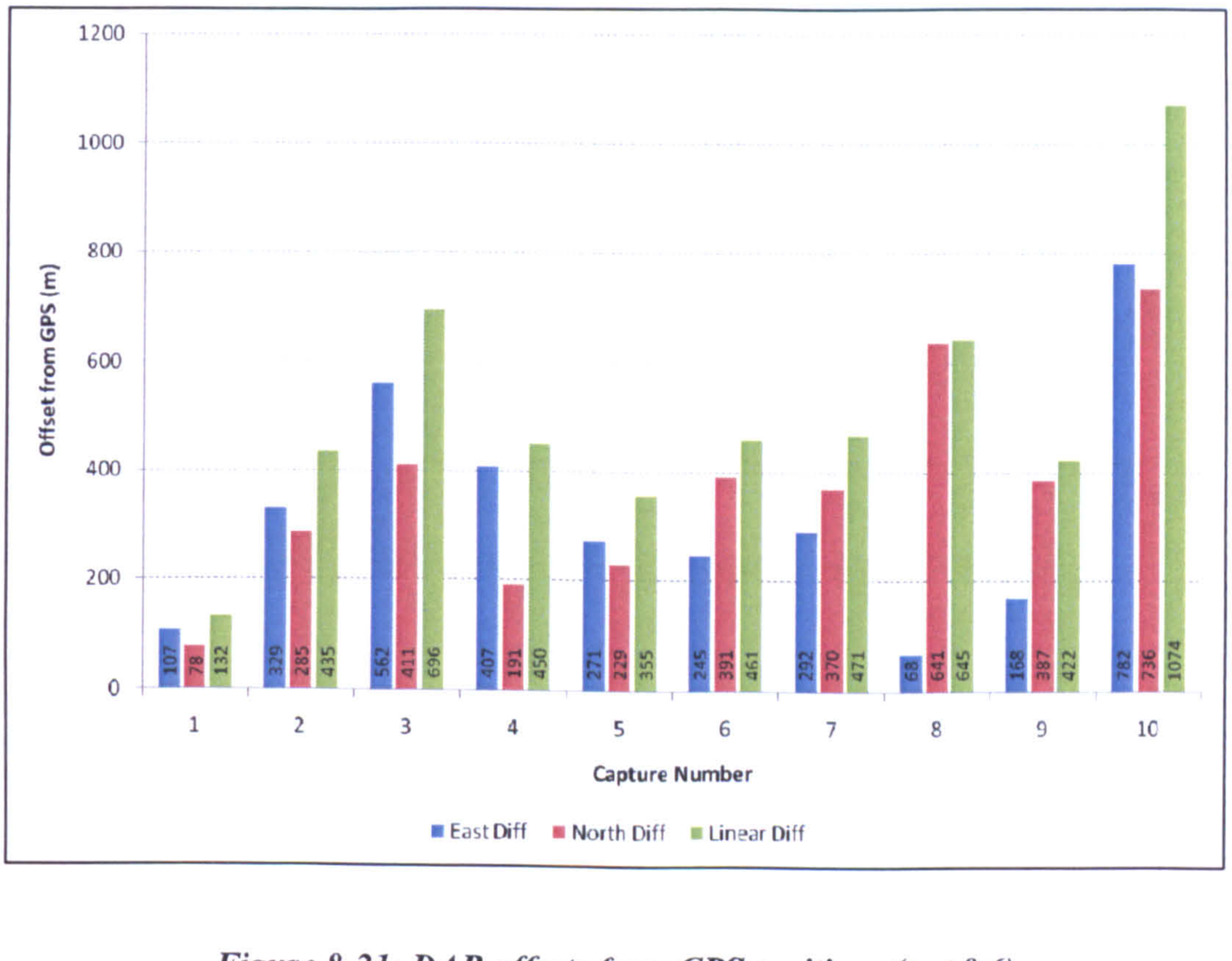

Figure 8-21: DAB offsets from GPS positions (test 8.6)

The final evaluation chart shown in Figure 8-22 shows each capture points calculated Horizontal Dilution of Precision (HDOP). Although capture point 10 has the highest HDOP value, there appears not to be any direct correlation between this value and the value of the linear offset in position.

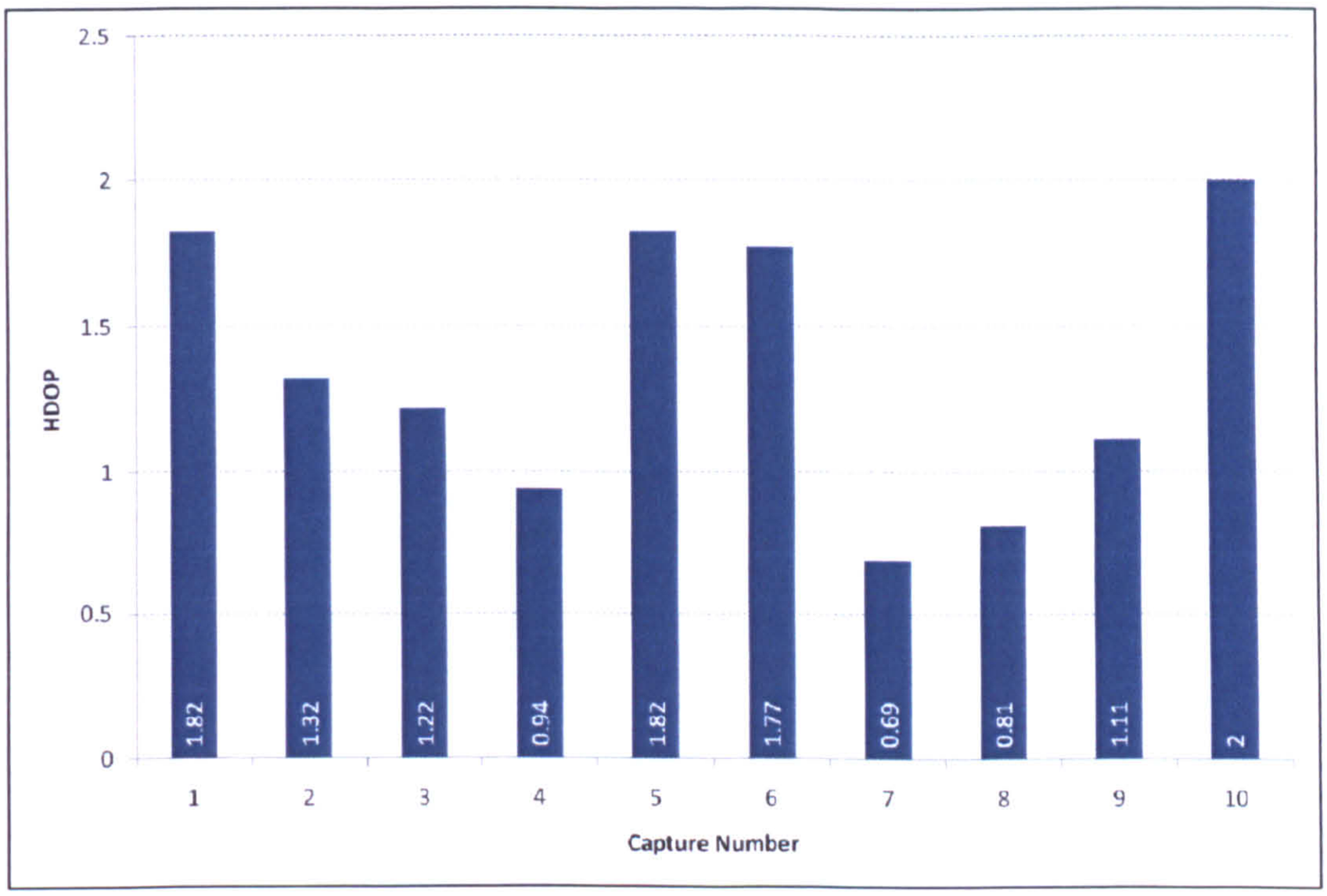

Figure 8-22: HDOP values for each capture number (test 8.6)

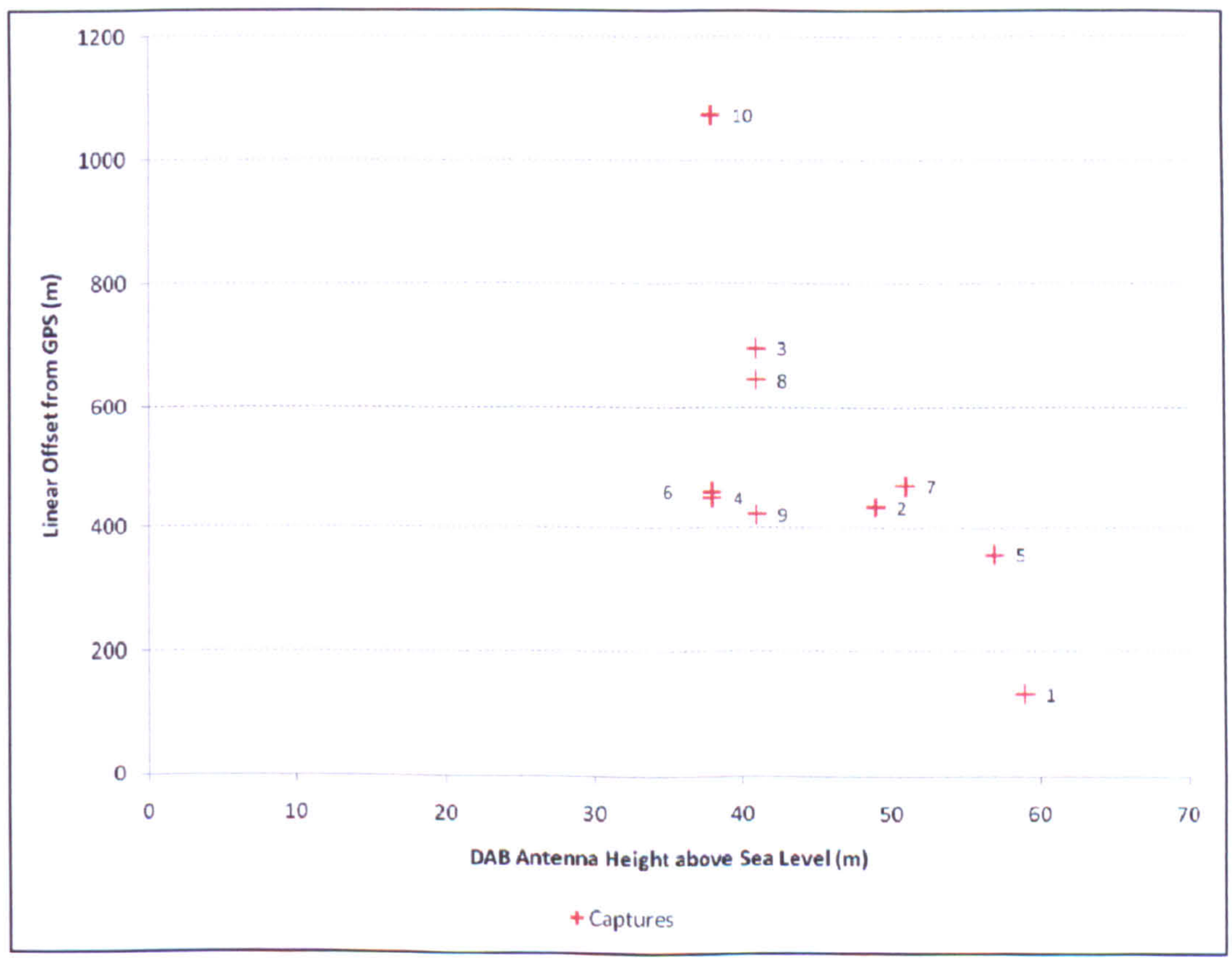

Figure 8-23: Capture height vs. linear offset from GPS (test 8.6)

The same exercise is then run again approximately an hour later by returning the antenna to precisely the same GPS coordinates as before (± 1 metre). As expected, the calculated coordinates are identical with the exception of one measurement at capture position 3 which now calculates at the same hyperbolic intersects as position 9.

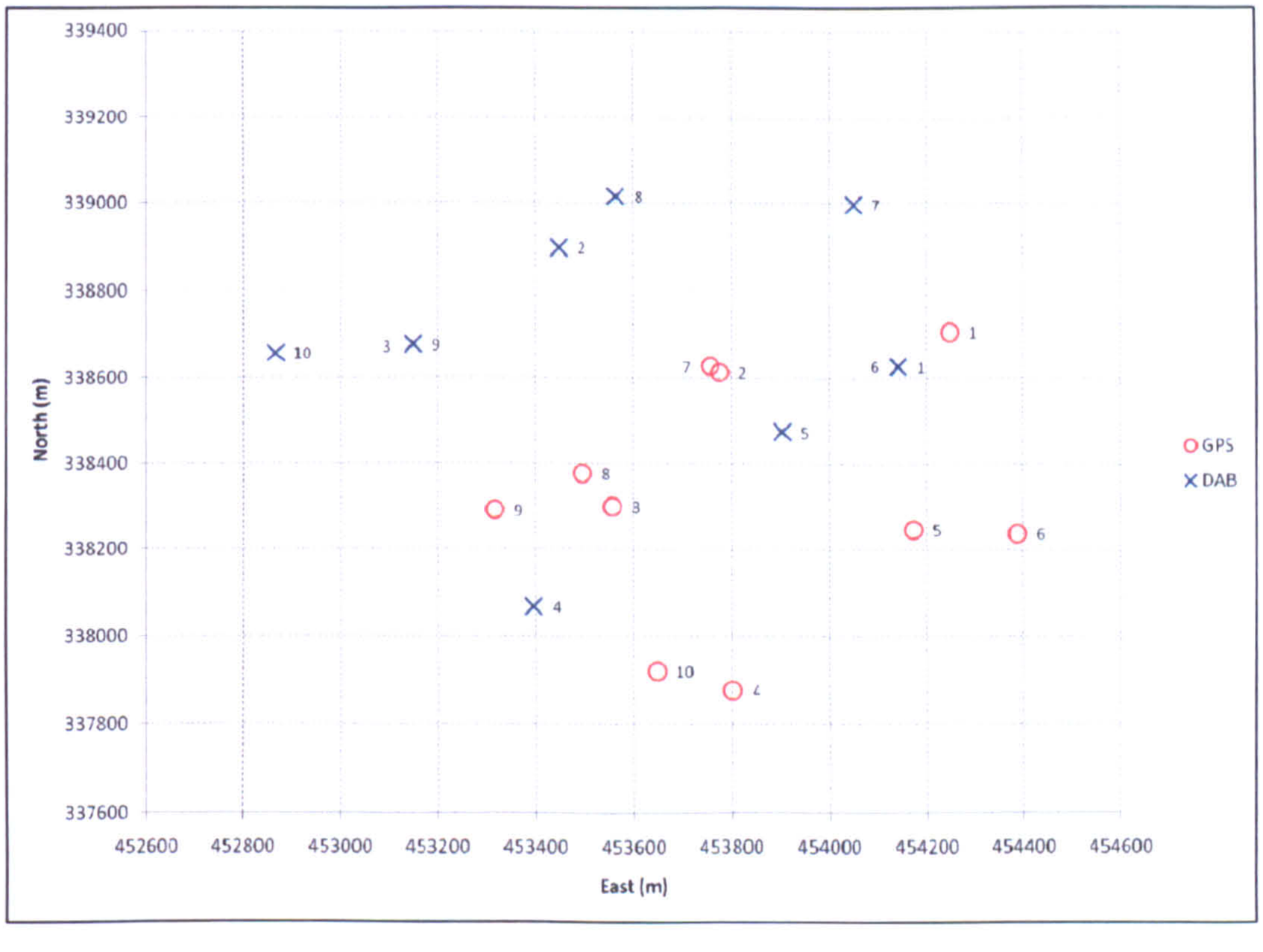

Figure 8-24: Repeated test showing GPS/DAB positions

This instance could be explained by the under-sampling of the signal by the USRP front-end. As the DAB data is sampled at a rate ×1.024 faster than the receiver sample-rate, this could give a measurement ambiguity of ±1T, enough to alter the measurement by up to 150 metres.

8.8 STATIC TEST: LEICESTER (RURAL/SUBURBAN)

8.8.1 Introduction

This test was performed using the main dipole antenna mounted to the roof of a vehicle. The aim of the test was similar to that in 8.7, but to the take the system further out in the field in order to examine measurements spaced over a wider area. This was done in order to observe the positioning capability of the system when the ranges between transmitter and receiver differ by several kilometres between captures as opposed to the hundreds of metres tested previously. At each capture position, the DAB positioning equipment has no previous knowledge of where it has been.

The region identified lay roughly between the cities of Nottingham and Leicester, composing mostly suburban and rural landscapes. Four transmitters roughly border the region used, however further transmission sources should be able to be received at certain locations, due to regional crossover.

At each capture position, the precise location was calculated using GPS, with the DAB captures performed simultaneously on all seven of the UK blocks. For each block, a capture of length $2.1e^6$ samples was taken (roughly one second) using a 2MHz bandwidth capture window, resulting in approximately ten transmission frames with the purpose of averaging the results from frames containing TII information (half of the received frames).

Each capture yields the results of both the TII and cross-correlation of the TFPR symbol, as is shown in Figure 8-25 and Figure 8-26 for four of the seven blocks receivable at this location (11D and 12B are the two national networks, 11B is the Leicester local network and 12C is the Nottingham local network).

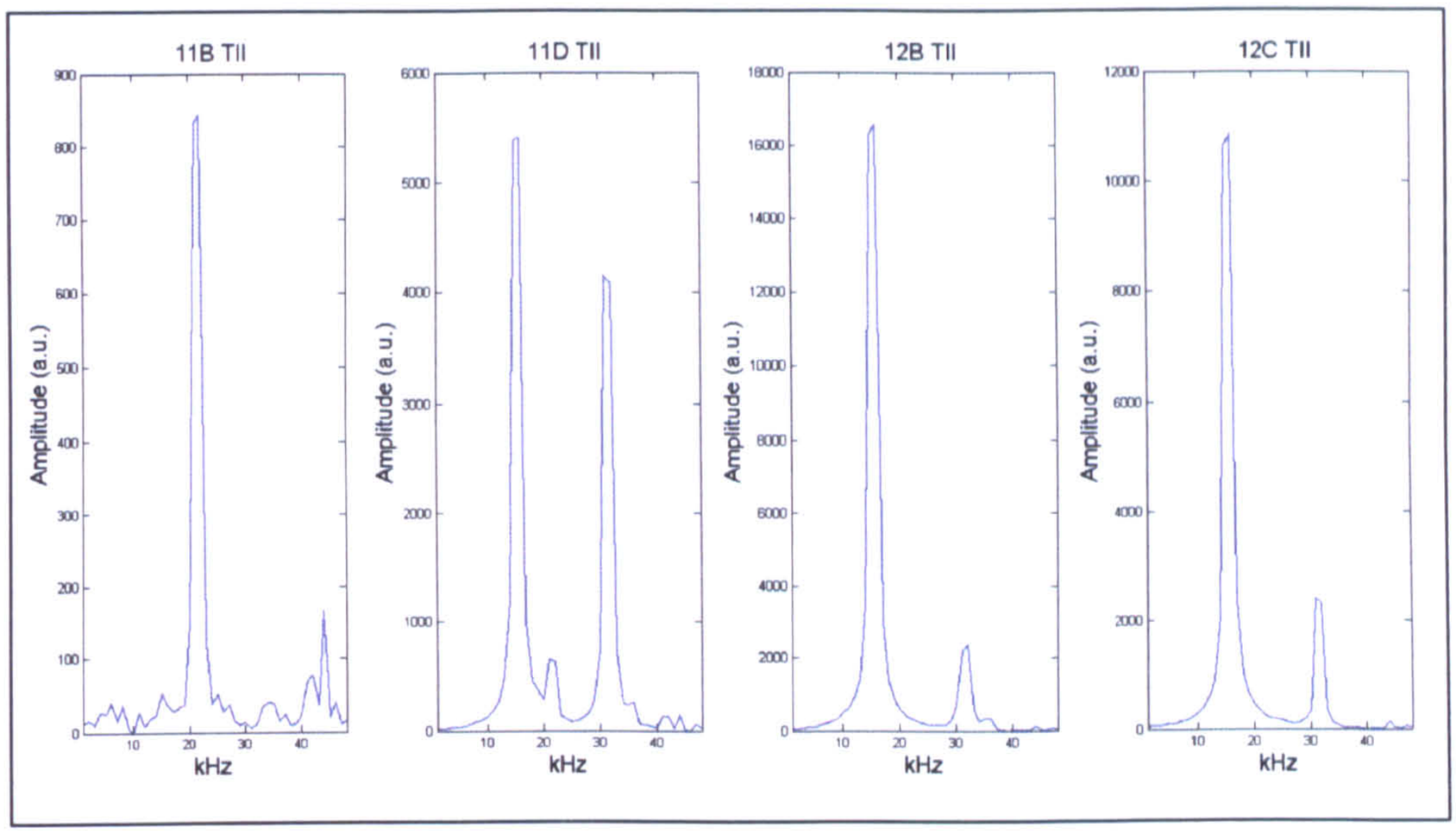

Figure 8-25: TII information Example (four DAB blocks)

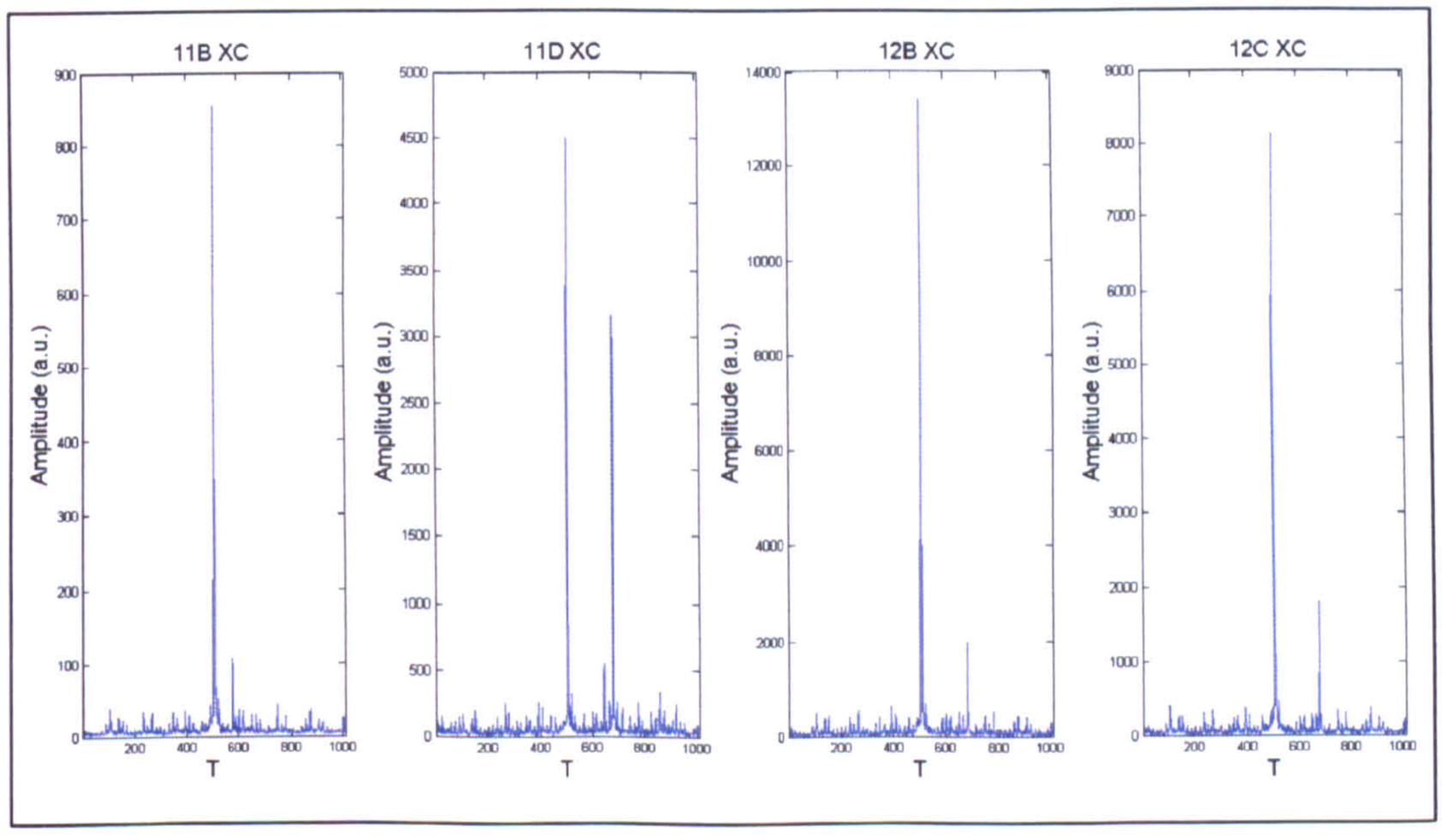

Figure 8-26: TFPR Cross-correlation Example (four DAB blocks)

8.8.2 Results

The chart shown in Figure 8-27 shows an overview of the capture positions within the region in question. Each 'true' position from the GPS receiver is indicated along with the DAB position. All discernable transmitters are shown on the plot, however, these

are not all detectable from any one location, therefore to show each positional result in further detail; these are broken down and shown over the following pages.

Figure 8-27: Test Results Overview

Figure shows the test region, transmitters used and comparison between GPS and DAB positions

Each individual result shows the transmitters used, the TDOA measurements taken, the GPS/DAB locations including the offset between the two systems, the initial 'guess' used for the least squares process along with each iteration of this process culminating in the final DAB position, and finally the HDOP of each DAB position.

1	DAB Block													
	11B		11C		11D		12A		12B		12C		12D	
TII (Region/Tx)	65 65	17 21			65 65 24	16 8 18			65 65 24	16 8 18	65 65	16 8		
TDOA (T)	52				122 224				123 225		119			

Positioning Results		
	East (m)	North (m)
GPS	458284	334549
DAB	458282	334810
Offset	2	261
HDOP	0.5889	
Height	59m	

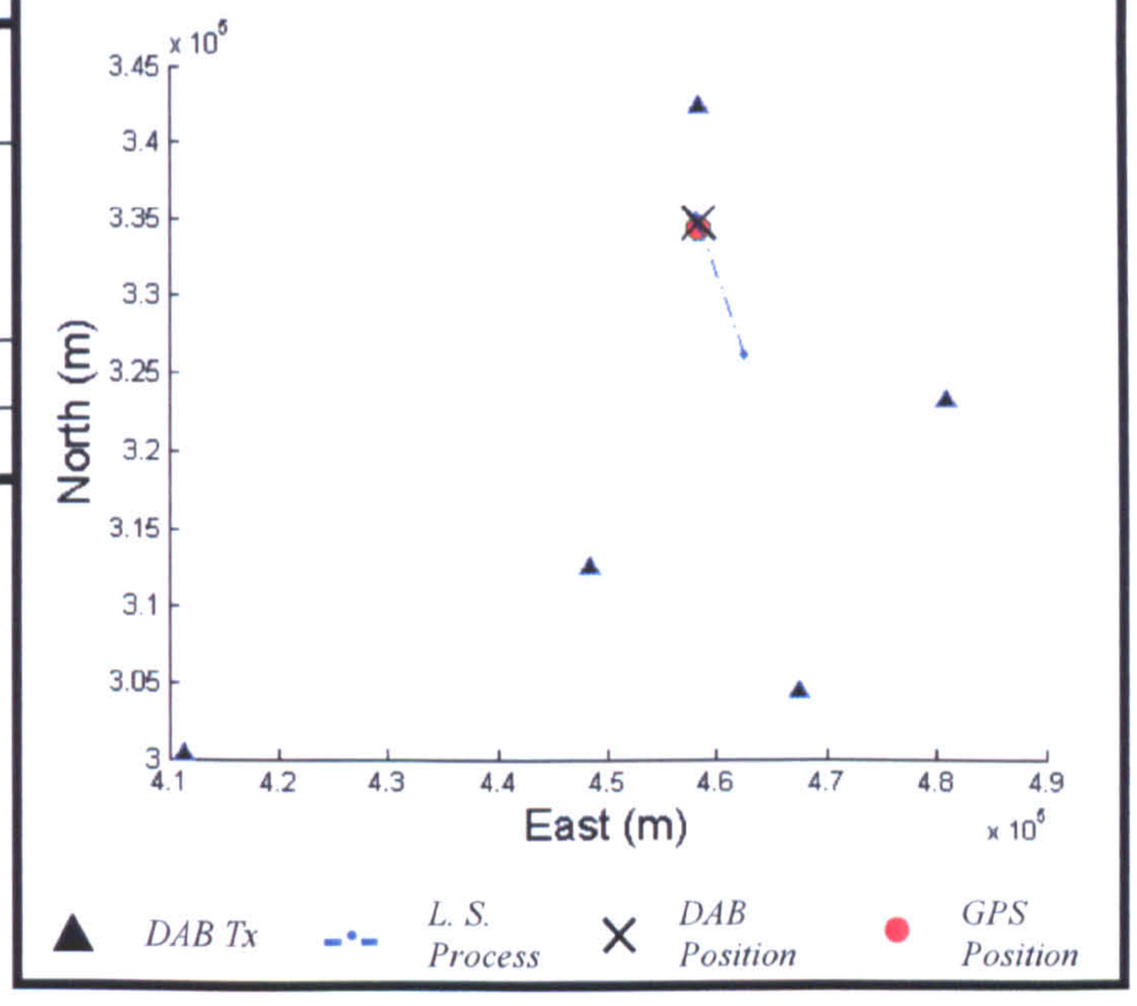

2	DAB Block													
	11B		11C		11D		12A		12B		12C		12D	
TII (Region/Tx)	65 65	17 21			65 65 58	16 8 2					65 65 65	8 16 10		
TDOA (T)	3				2 430						0 137			

Positioning Results		
	East (m)	North (m)
GPS	465867	328277
DAB	465587	328182
Offset	280	95
HDOP	1.5404	
Height	90m	

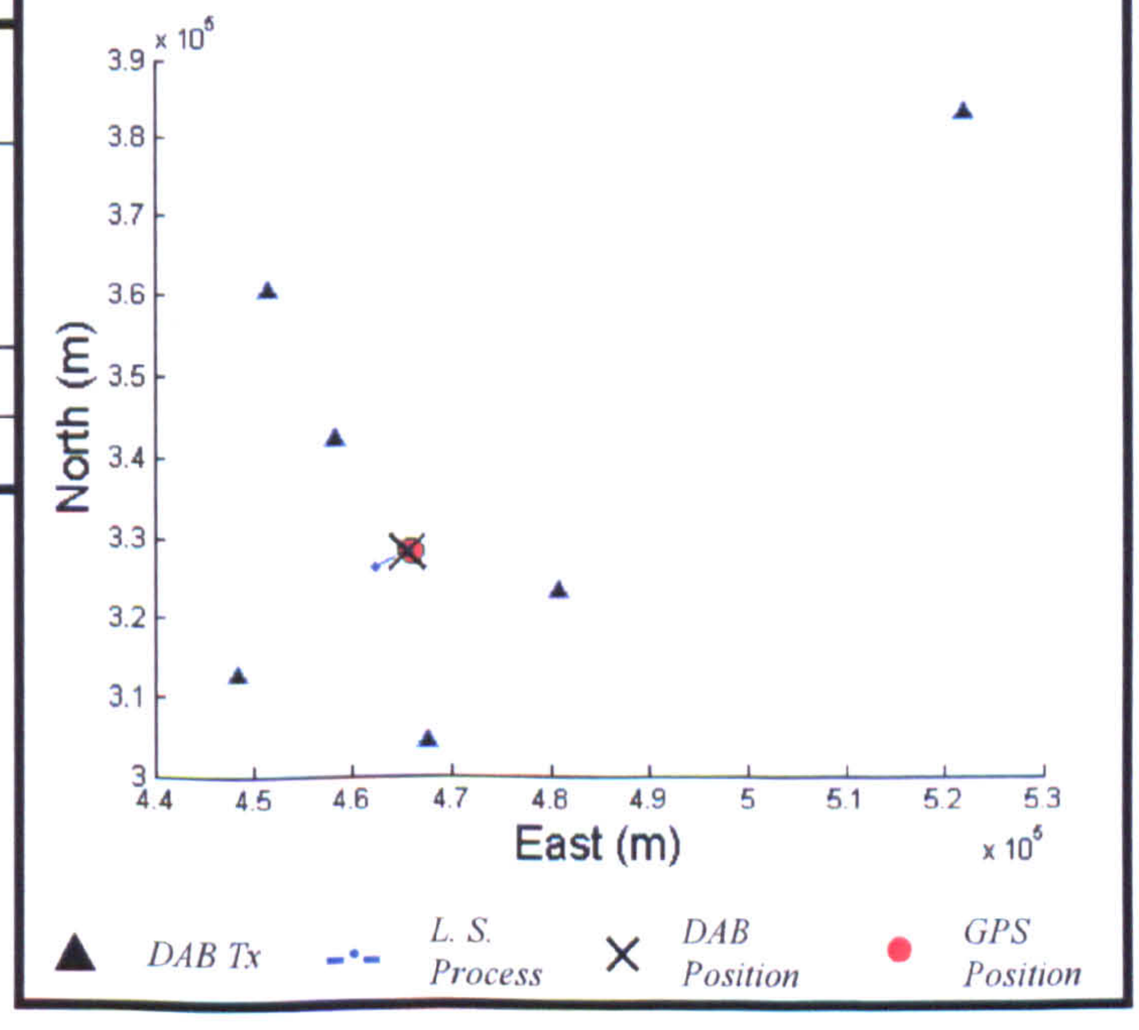

3	DAB Block													
	11B		11C		11D		12A		12B		12C		12D	
TII (Region/Tx)	65 65	17 21			65	8					65	8		
TDOA (T)	69													

Positioning Results		
	East (m)	North (m)
GPS	474742	320129
DAB		
Offset		
HDOP		
Height	86m	

Insufficient Information for standalone DAB position estimation

▲ *DAB Tx* -·- *L. S. Process* × *DAB Position* ● *GPS Position*

4	DAB Block													
	11B		11C		11D		12A		12B		12C		12D	
TII (Region/Tx)	65 65	17 21			65 65	16 11			65	16	65	16		
TDOA (T)	51				9									

Positioning Results		
	East (m)	North (m)
GPS	466495	315155
DAB	334769	-268370
Offset	131725	583525
HDOP	39.0860	
Height	69m	

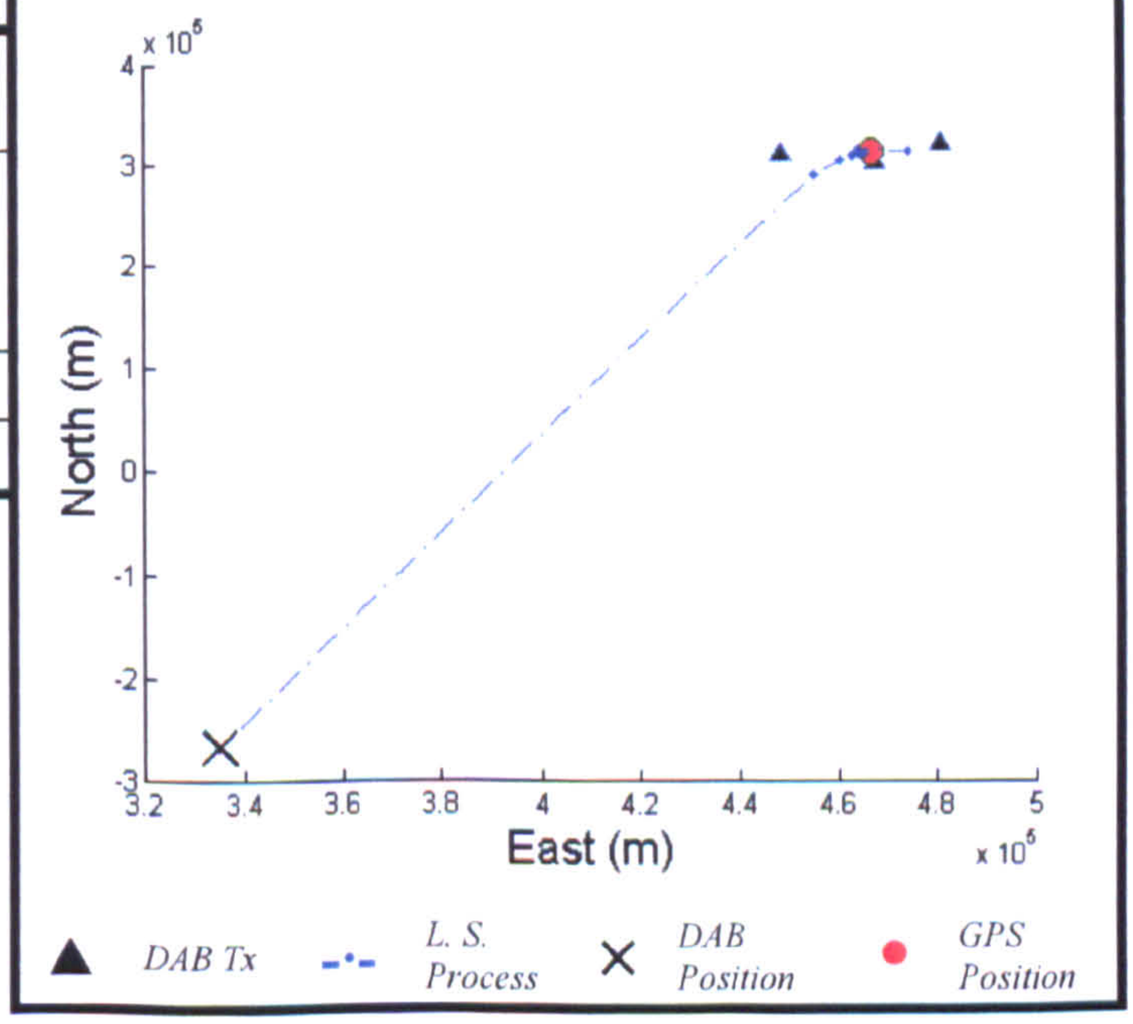

5	DAB Block													
	11B		11C		11D		12A		12B		12C		12D	
TII (Region/Tx)	65 65	21 17			65 65	21 16			65 18 65	16 2 8	65 65	16 8		
TDOA (T)	8				106				153 36		39			

Positioning Results		
	East (m)	North (m)
GPS	458149	310477
DAB	458082	310506
Offset	67	29
HDOP	0.6522	
Height	77m	

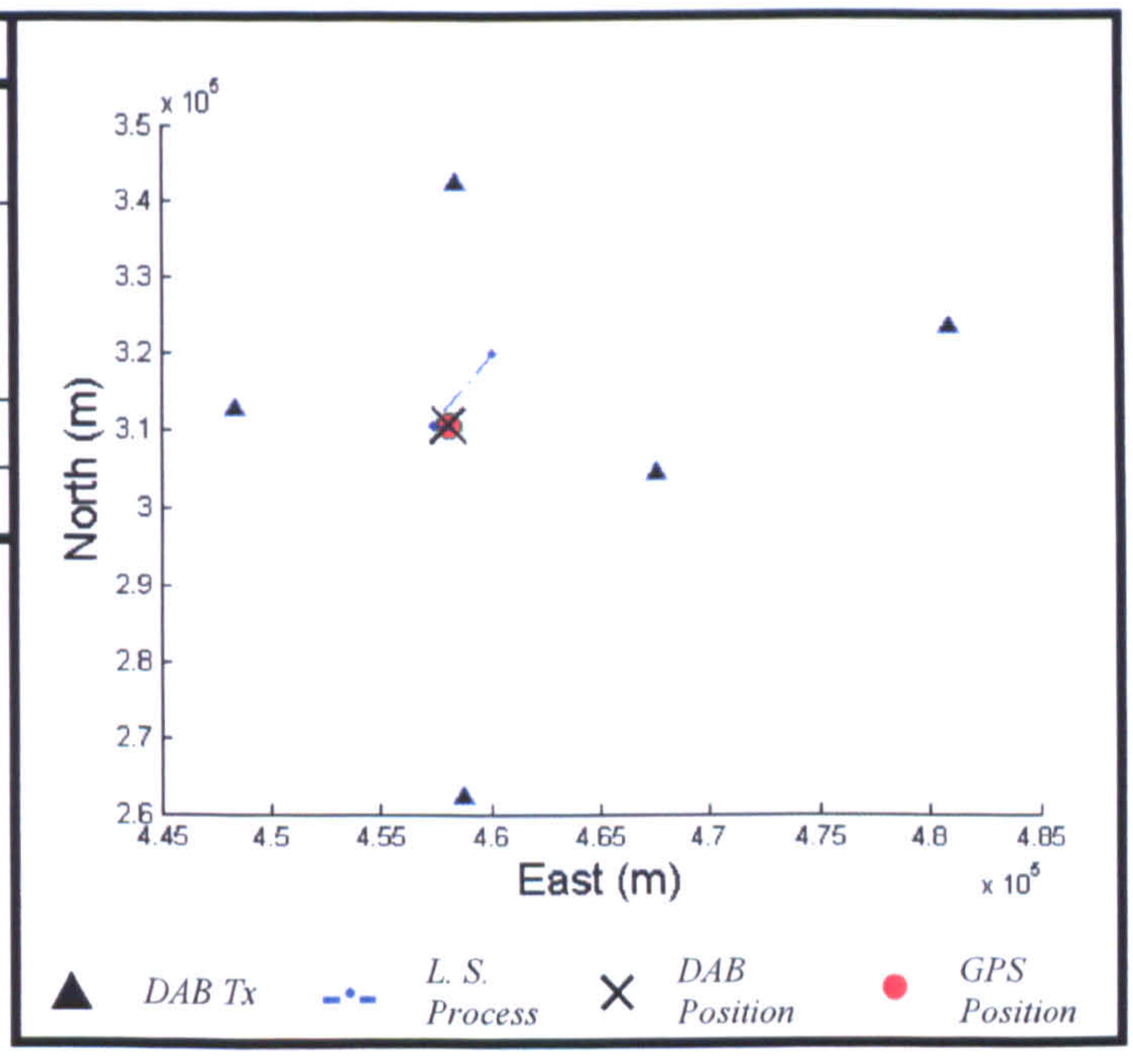

6	DAB Block													
	11B		11C		11D		12A		12B		12C		12D	
TII (Region/Tx)	65 65	21 17							65	16	65	16		
TDOA (T)	4													

Positioning Results		
	East (m)	North (m)
GPS	459110	312164
DAB		
Offset		
HDOP		
Height	60m	

Insufficient Information for standalone DAB position estimation

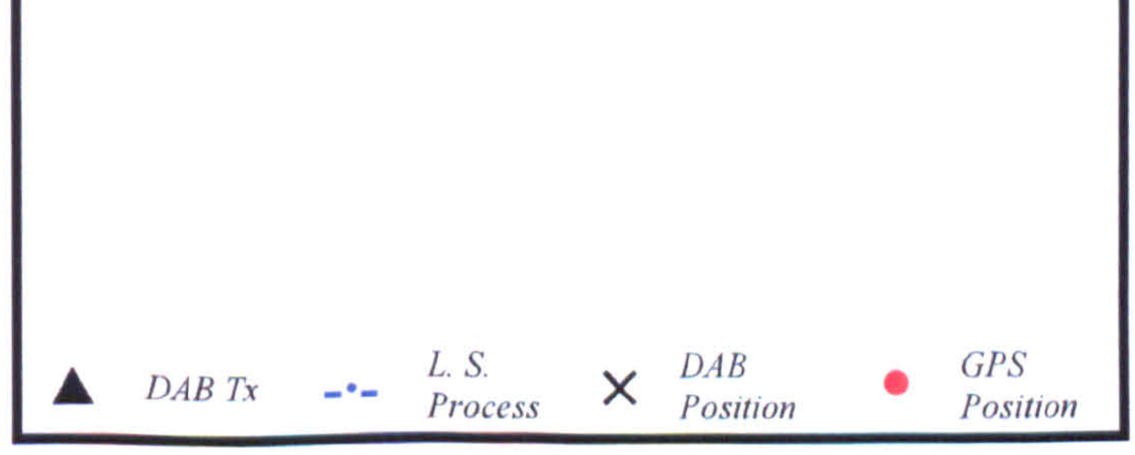

7	DAB Block											
	11B		11C		11D		12A		12B		12C		12D	
TII (Region/Tx)	65 65	17 21			65 65 24	17 21 18			24 24	18 15				
TDOA (T)	62				9									

Positioning Results		
	East (m)	North (m)
GPS	456001	321123
DAB	455857	320771
Offset	144	352
HDOP	1.9686	
Height	50m	

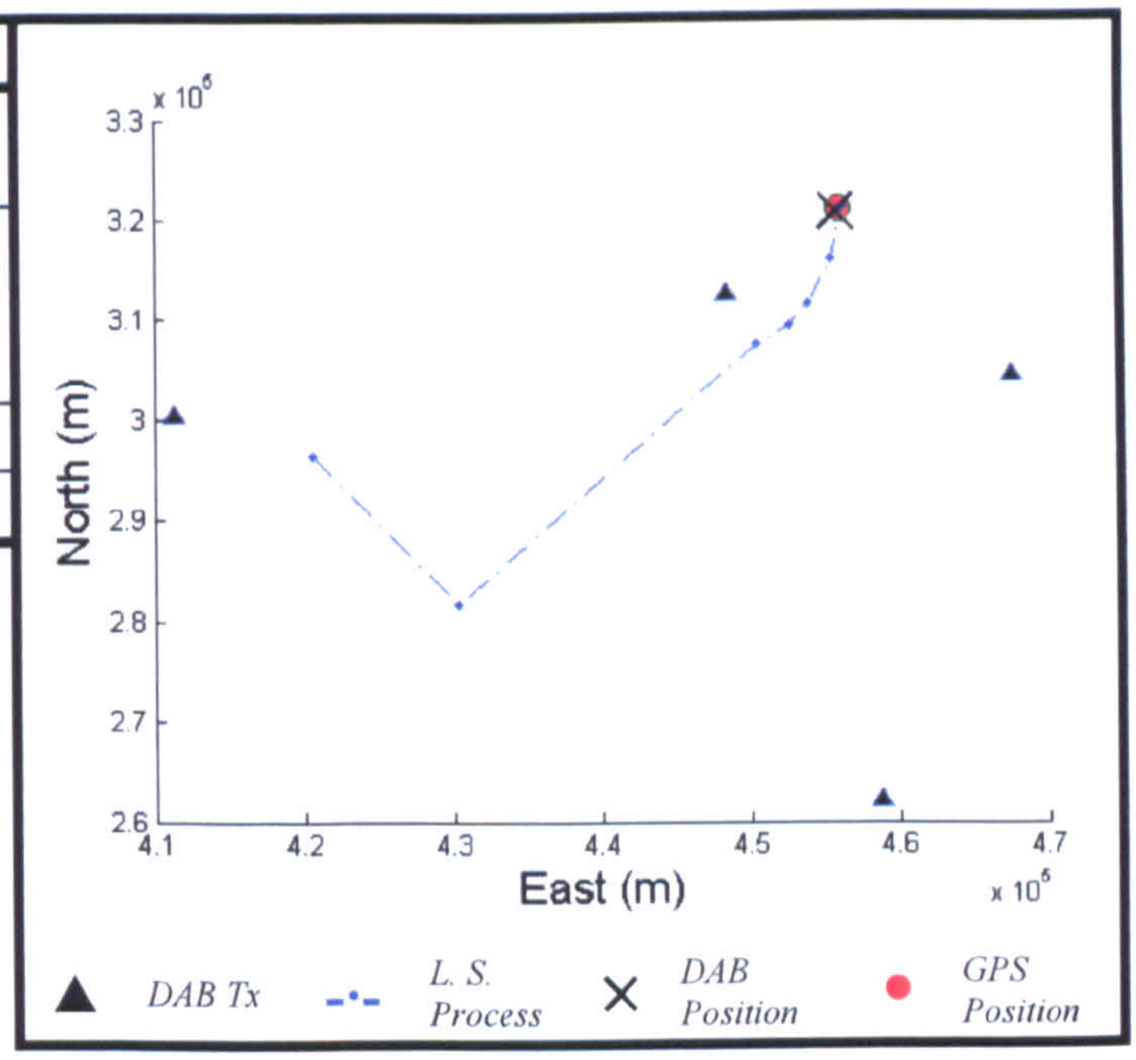

8	DAB Block											
	11B		11C		11D		12A		12B		12C		12D	
TII (Region/Tx)					65 65 24	16 8 18			65 65 24	16 8 18	65 65	16 8		
TDOA (T)					98 218				99 222		95			

Positioning Results		
	East (m)	North (m)
GPS	458237	332018
DAB	458170	332241
Offset	67	223
HDOP	0.5995	
Height	44m	

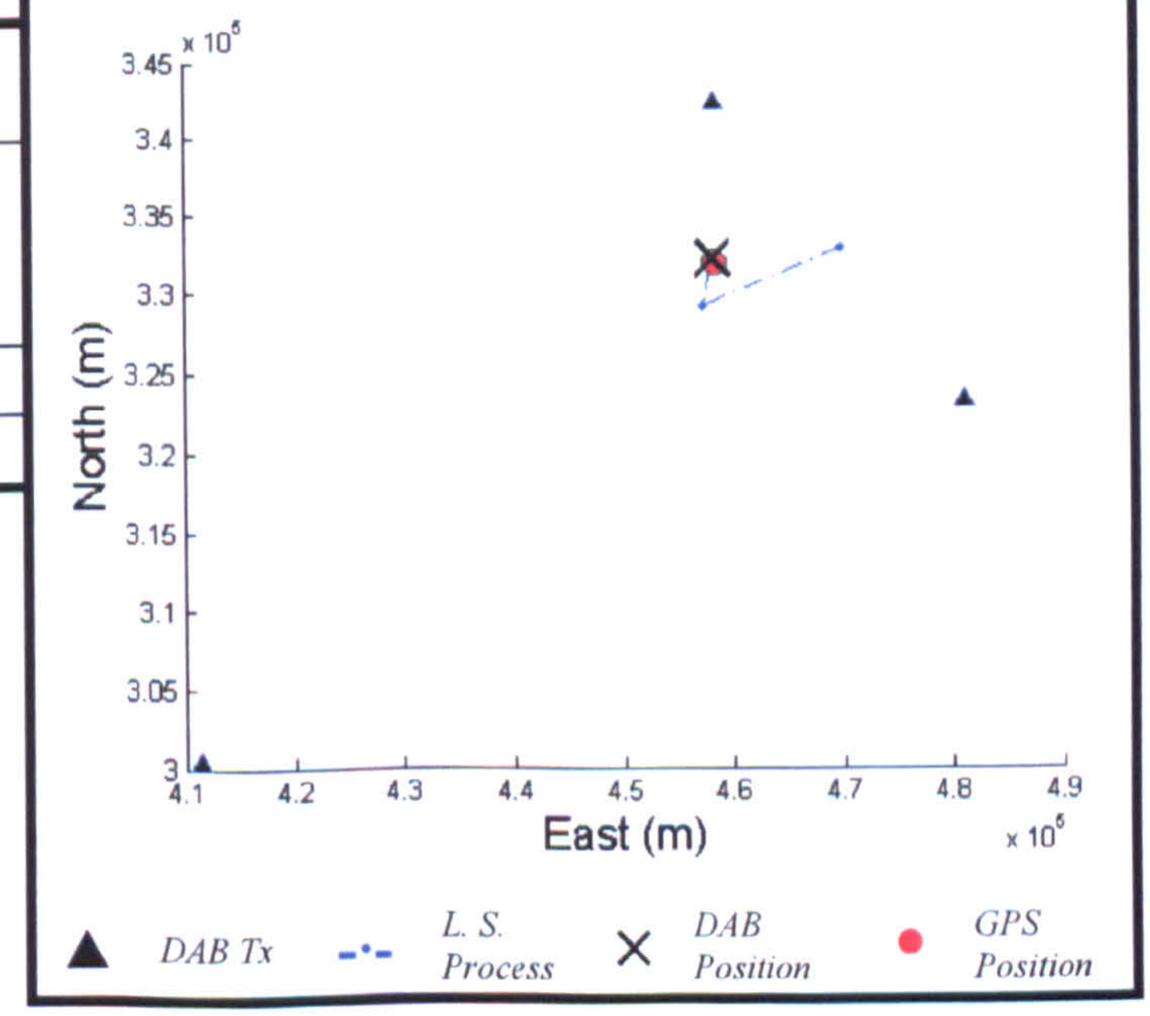

9	DAB Block						
	11B	11C	11D	12A	12B	12C	12D
TII (Region/Tx)			65 16 65 8 24 18		65 16 65 8 24 18	65 16 65 8	
TDOA (T)			170 307		173 311	167	

Positioning Results		
	East (m)	North (m)
GPS	450417	337680
DAB	450368	338117
Offset	49	437
HDOP	0.8861	
Height	64m	

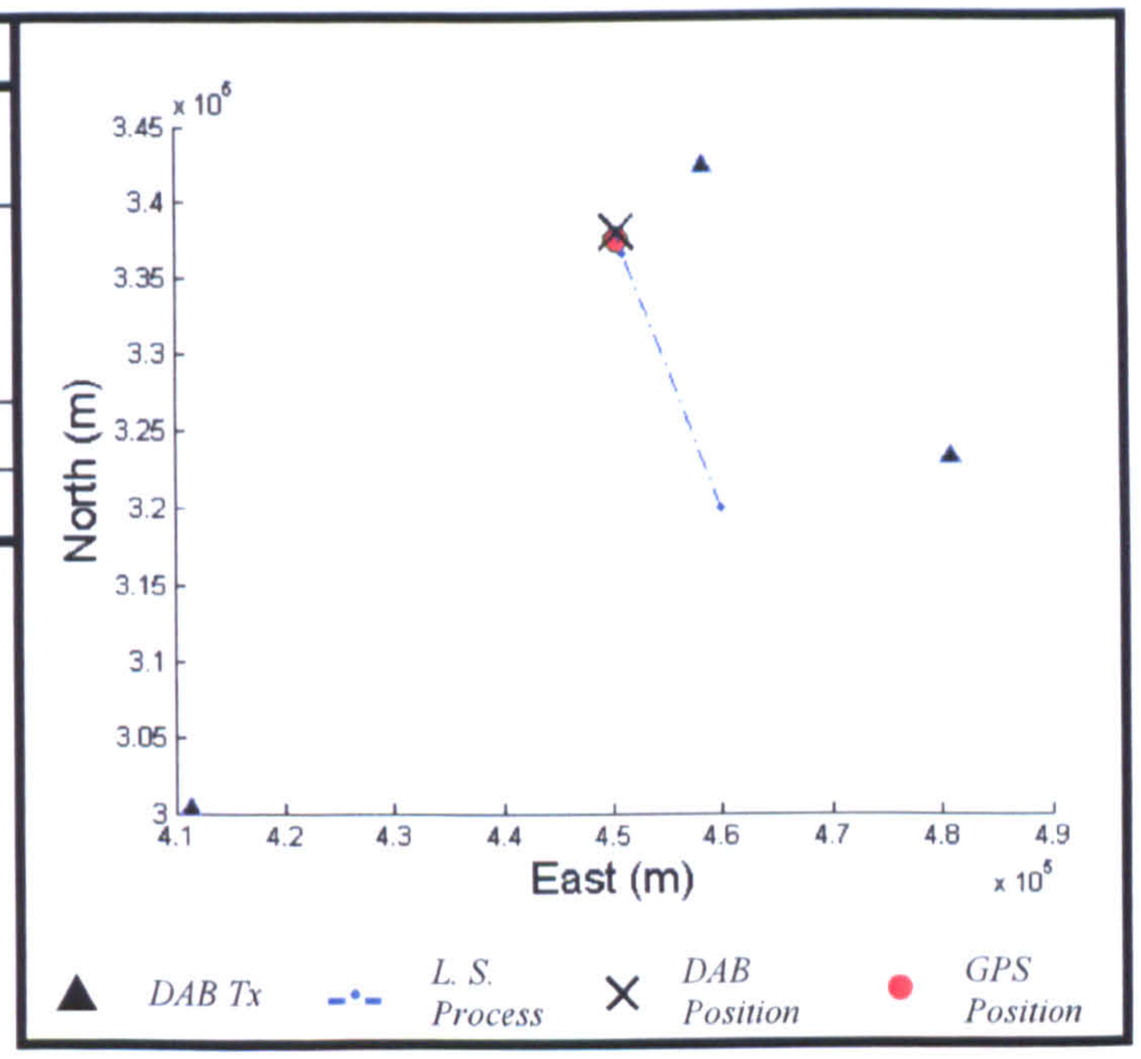

10	DAB Block						
	11B	11C	11D	12A	12B	12C	12D
TII (Region/Tx)	65 17 65 21				65 8 65 16 18 2	65 16 65 8	
TDOA (T)	106				159 408	155	

Positioning Results		
	East (m)	North (m)
GPS	444805	335067
DAB	444744	335659
Offset	61	592
HDOP	1.7817	
Height	69m	

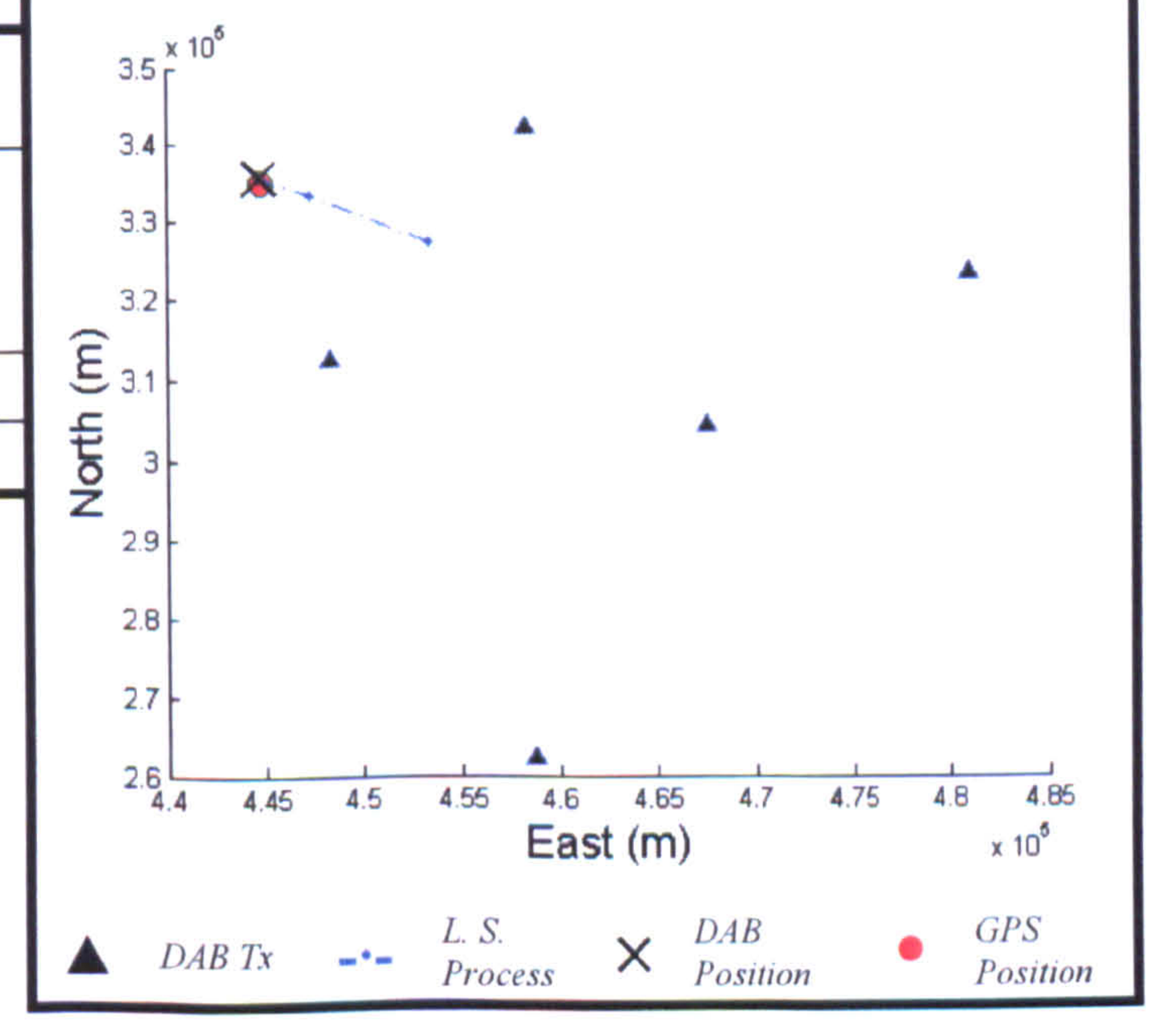

11	DAB Block						
	11B	11C	11D	12A	12B	12C	12D
TII (Region/Tx)					24 18 24 15 24 9		
TDOA (T)					120 230		

Positioning Results		
	East (m)	North (m)
GPS	436522	339267
DAB	429398	333069
Offset	7124	6198
HDOP	27.7327	
Height	59m	

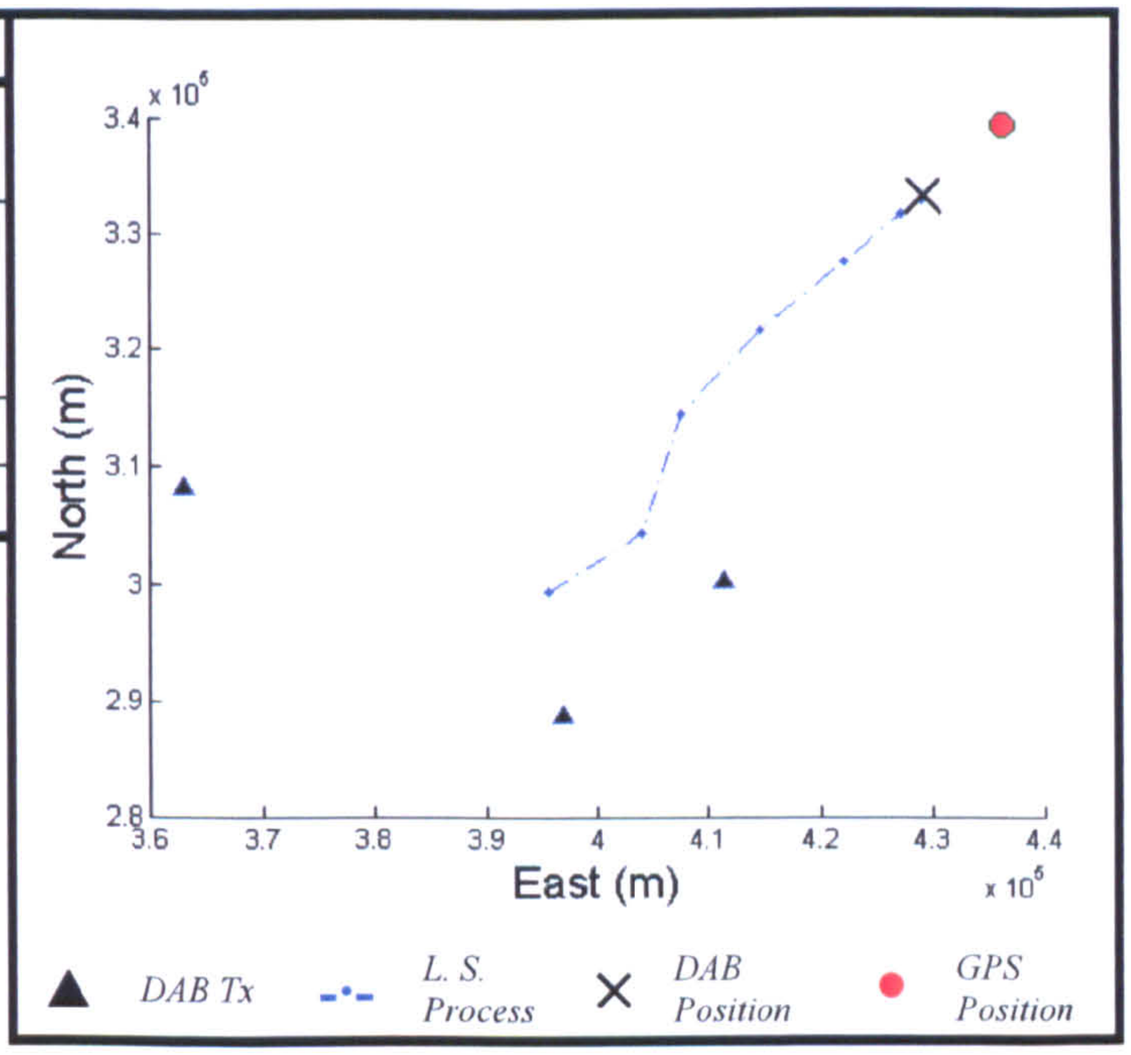

12	DAB Block						
	11B	11C	11D	12A	12B	12C	12D
TII (Region/Tx)	65 17 65 21		65 16 65 17 65 8 65 10		65 16 65 8 24 18	65 16 65 8 65 10	
TDOA (T)	111		101 186 187		38 183	158	

Positioning Results		
	East (m)	North (m)
GPS	439795	342367
DAB	439919	342187
Offset	124	180
HDOP	0.8782	
Height	136m	

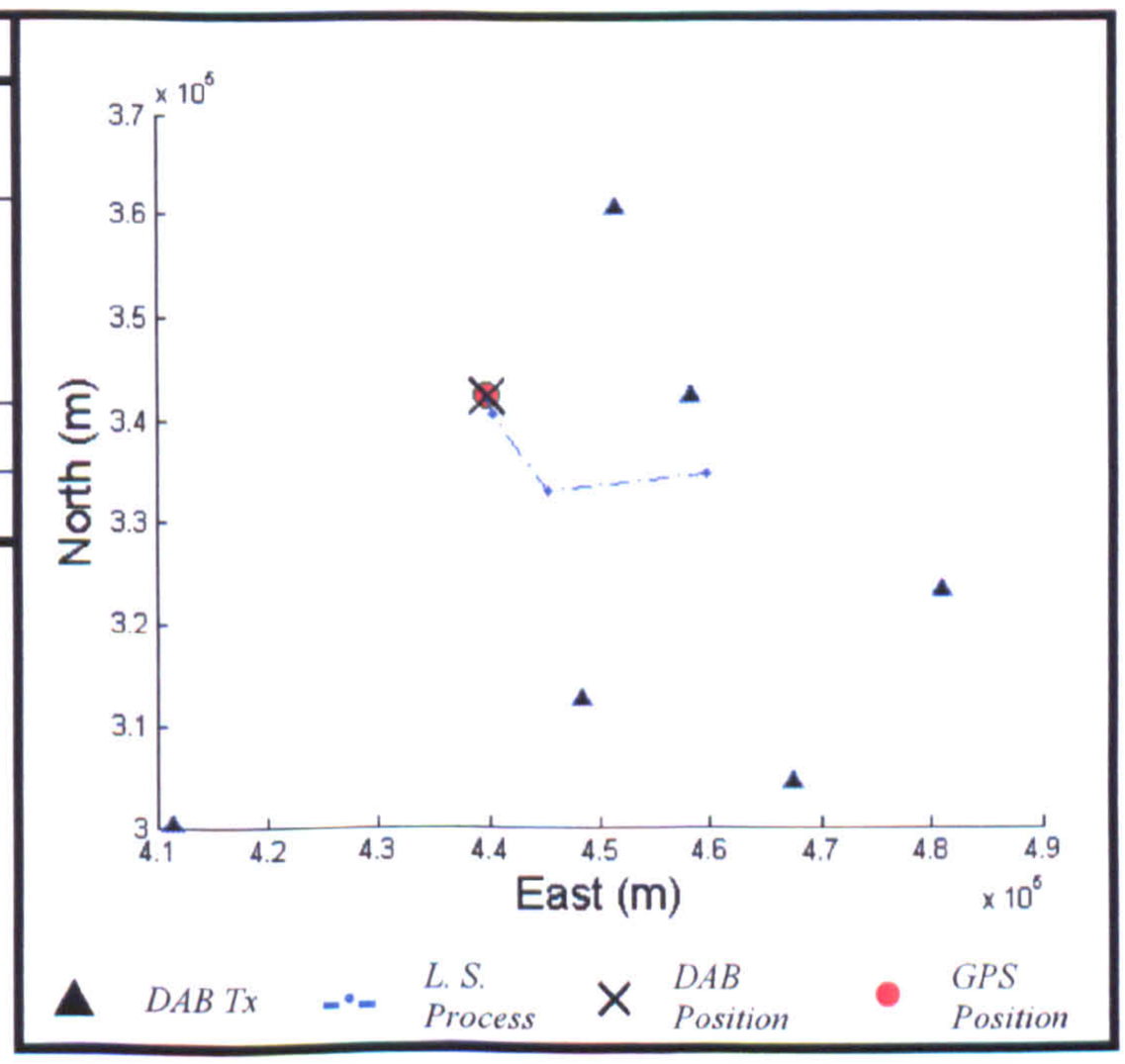

13	DAB Block											
	11B		11C		11D		12A		12B		12C		12D	
TII (Region/Tx)	65 65	17 21			65 65 65	8 16 17			65 65	8 16	65 65	8 16		
TDOA (T)	86				185 127				186		182			

Positioning Results		
	East (m)	North (m)
GPS	449529	340160
DAB	448900	340871
Offset	629	711
HDOP	1.7482	
Height	84m	

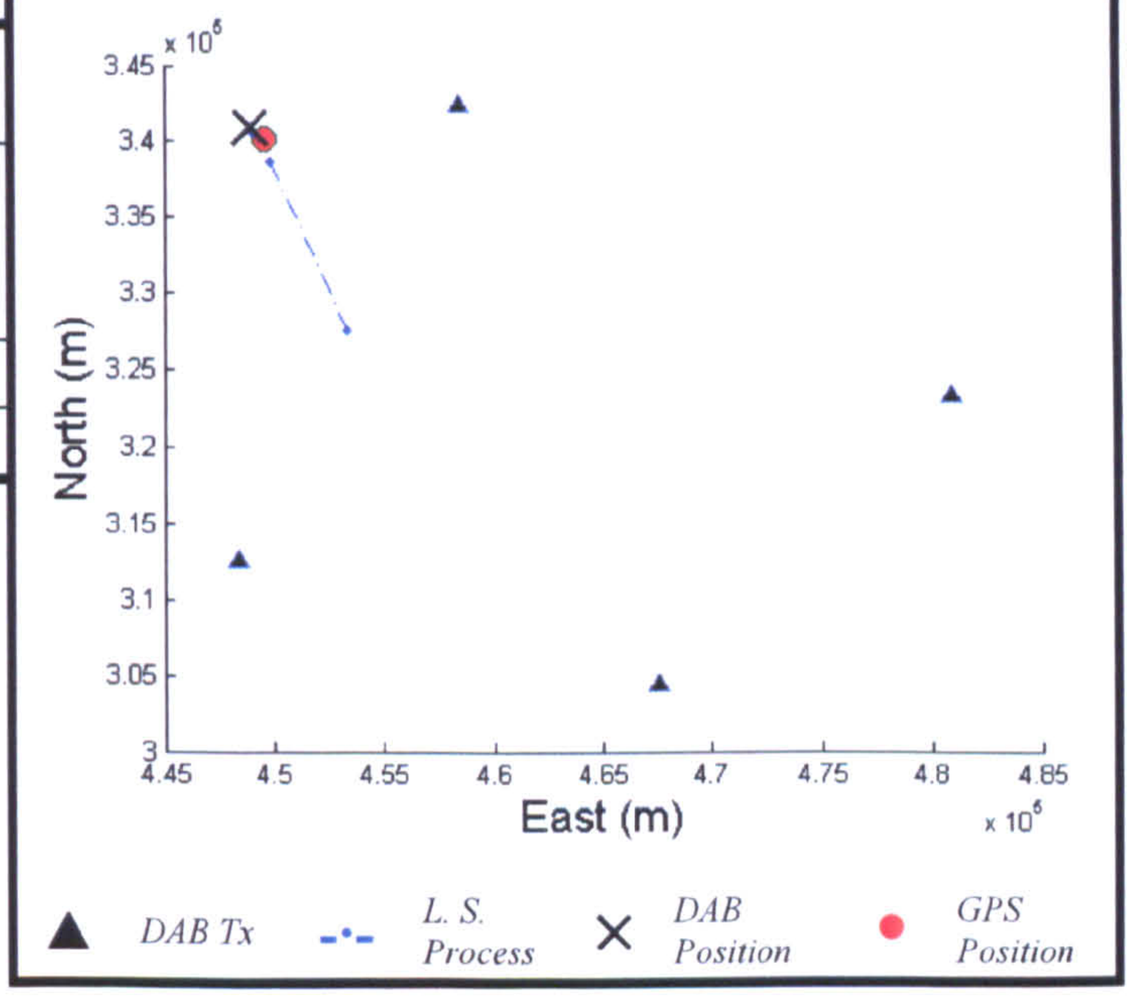

8.8.3 Discussion and analysis of results

The results from this experiment have shown that whilst DAB standalone positions were not attainable at all locations, 11 of the 13 captures provided a position estimation, although the quality of these positions did vary according to the transmitters available. Capture 4, whilst attaining a position of sorts, must also be ruled out as the resultant location calculation lies far outside the transmitters receivable radius (and entirely off of the National Grid).

Figure 8-28 shows a chart of the offset values between GPS and DAB measurements at each capture location. Each capture is shown divided into three values; the differences in the East, North and linear components. Captures 3, 4 and 6 are the captures where insufficient/poor information was collected via DAB and are absent.

It is immediately obvious that it is the quality of the Northings measurement where the major positional error is found in the majority of captures. This is caused by the

layout of the receivable transmitters for each case as the capture positions used in this experiment are not spaced as far apart as the latter trials.

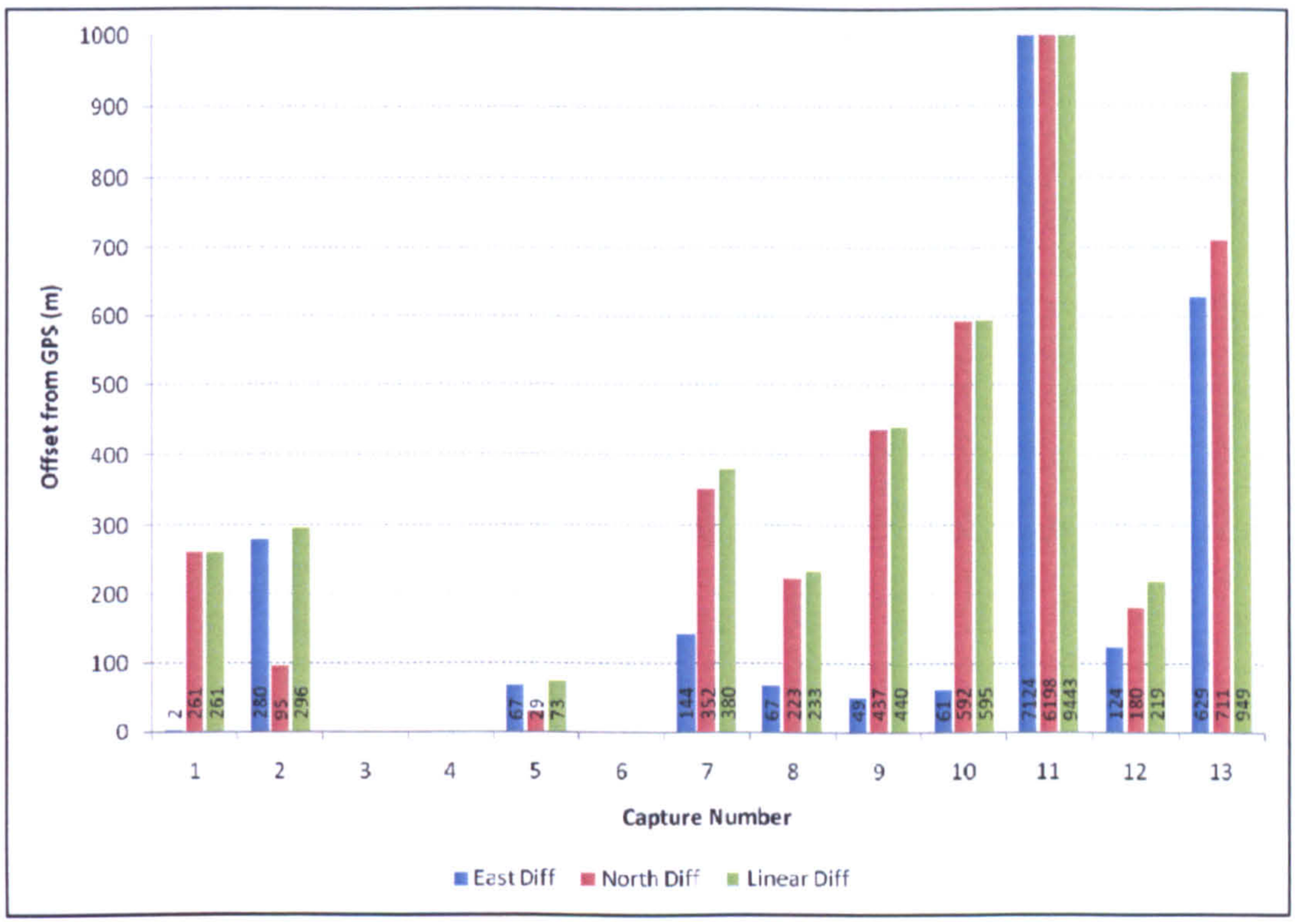

Figure 8-28: Offset from GPS (m) at each capture

Chart divided to show difference in East, North and Linear offsets

The quality of the observations can be seen by viewing Figure 8-29 where all results, with the exception of capture 11, have HDOP values of less than 2. This would appear to be a surprising result when examining capture 13 with a linear offset of almost a kilometre. The problem in this capture appears to be the TDOA measurements passed to the least squares process. Blocks 11D and 12B have the measurements of 185T and 186T respectively from the same transmitters, while block 12C has a measurement of 182T. A difference of up to ±2T is expected due to capture resolution and even broadcast antenna position at the transmitter site, however, a difference of 4T causes the error in position in this case. As the DAB positioning system does not know which value is correct, all three have to be used in the final least squares process.

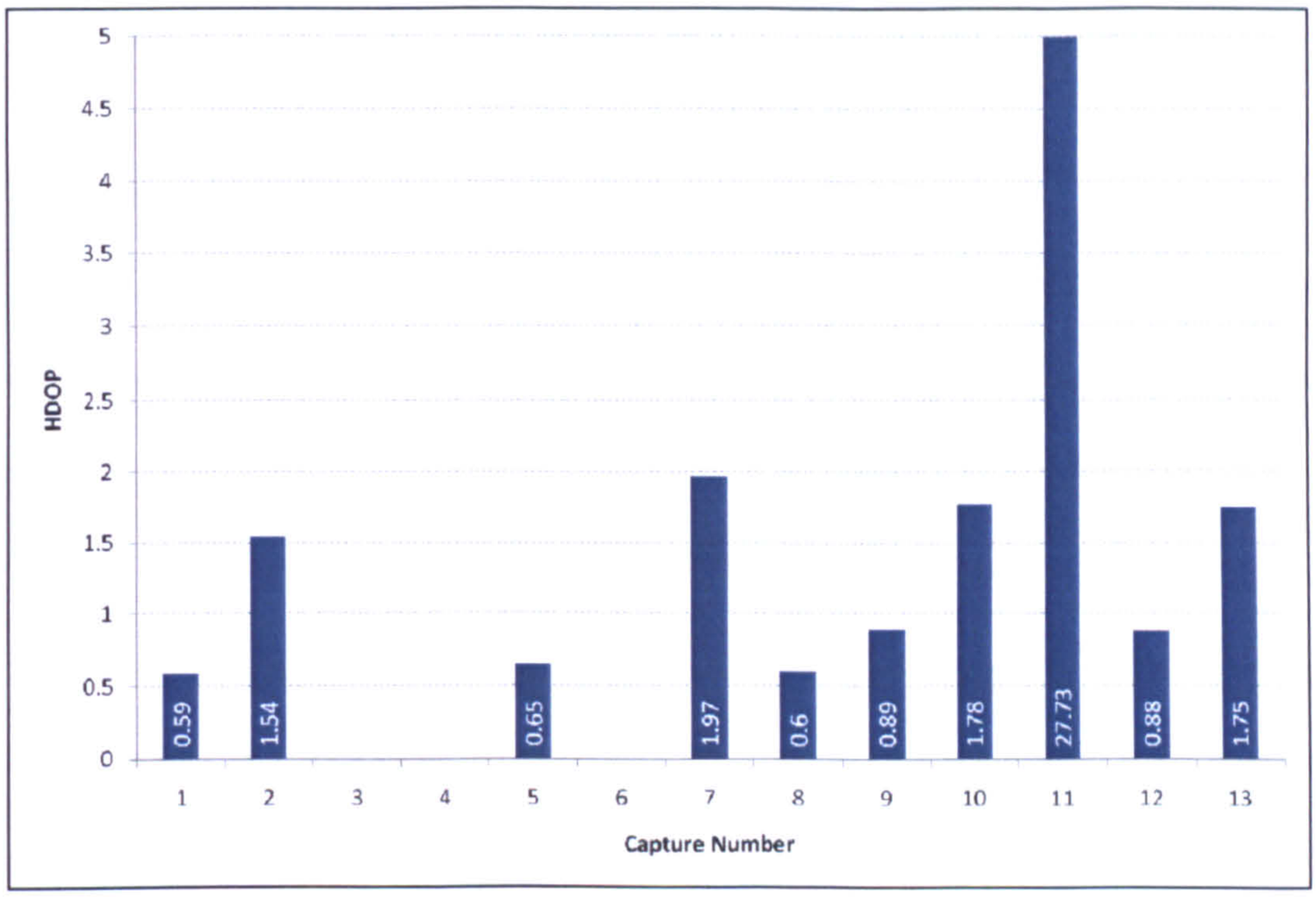

Figure 8-29: HDOP values for DAB position at each capture location

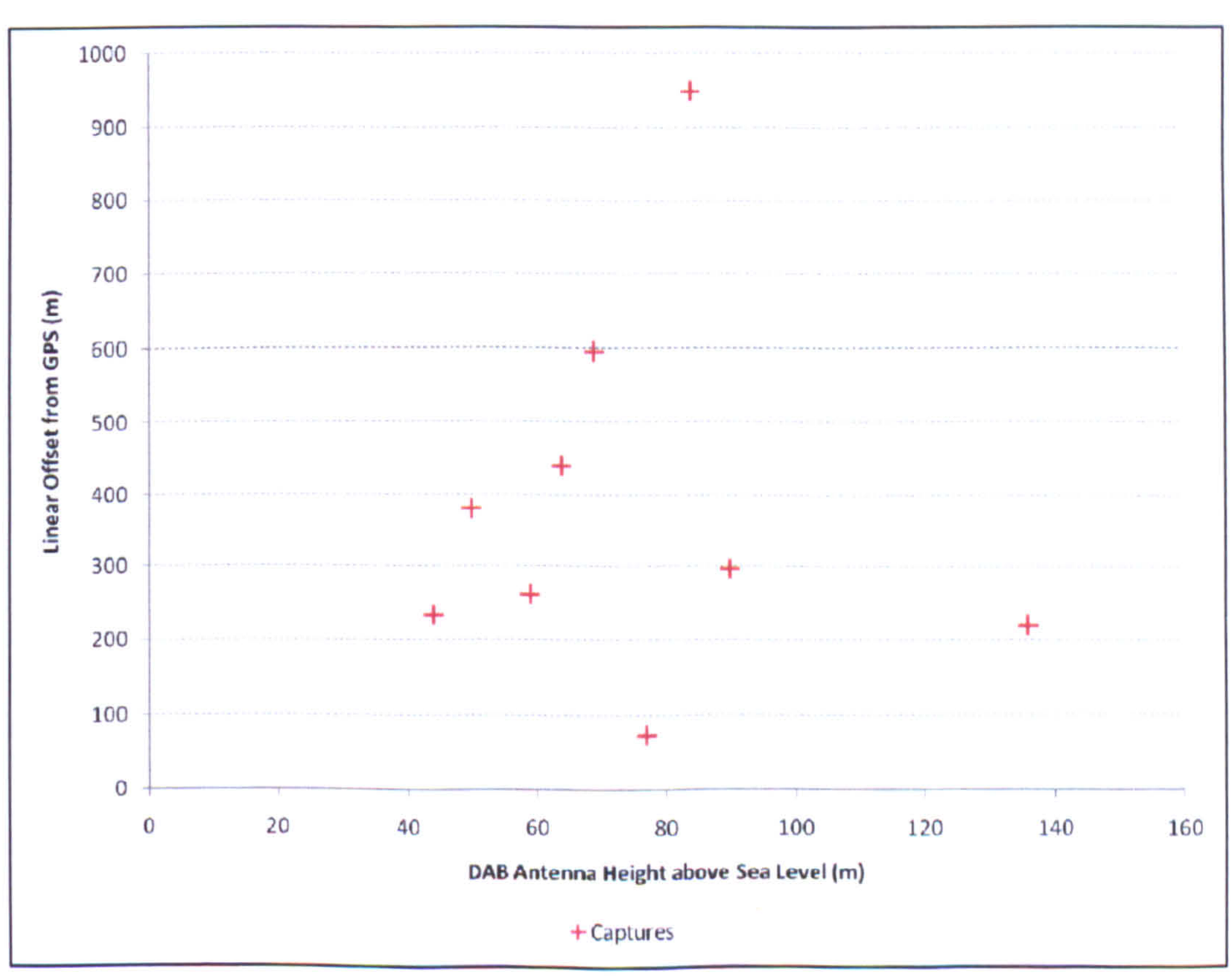

Figure 8-30: Chart showing capture elevation against linear offset

8.9 STATIC TEST – BIRMINGHAM (URBAN/SUBURBAN)

8.9.1 Introduction

The aim of this experiment was to evaluate how the DAB positioning system compared with GPS when used in an urban area. The equipment set-up for this was the same as in previous experiments, with each DAB capture location logged to a GPS position in order to compare the two when post-processed.

The vehicle containing the test equipment travelled from Nottingham to Birmingham via one route and returning via another. This allowed the equipment to be used in areas ranging from open rural land, to suburban areas and into dense urban landscape. Seventeen different transmitters were received during this experiment in total, though at different times. These may be seen in Figure 8-31, with the route taken highlighted in red.

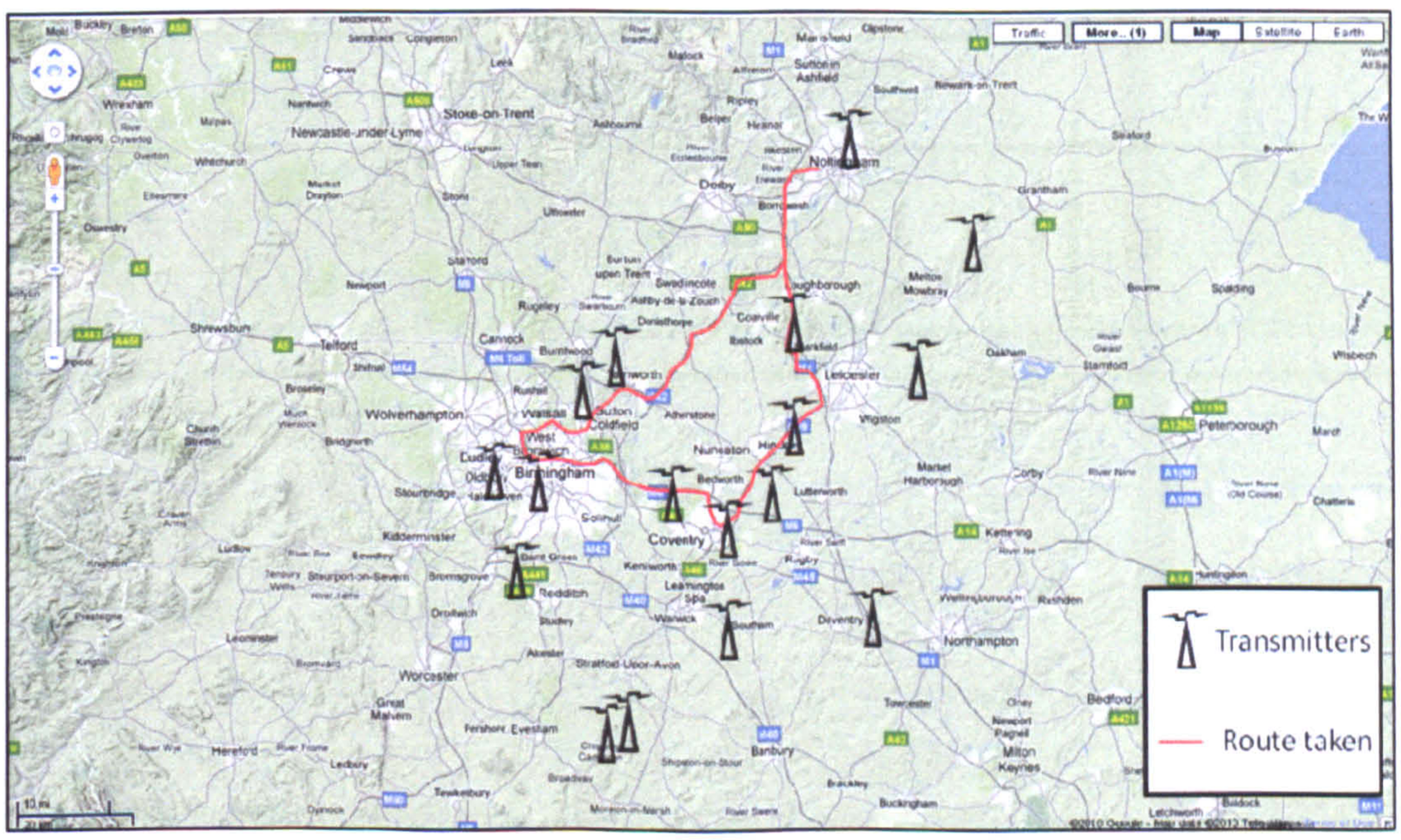

Figure 8-31: Transmitters received during Birmingham trial

(Image courtesy of Google Maps UK)

8.9.2 Results

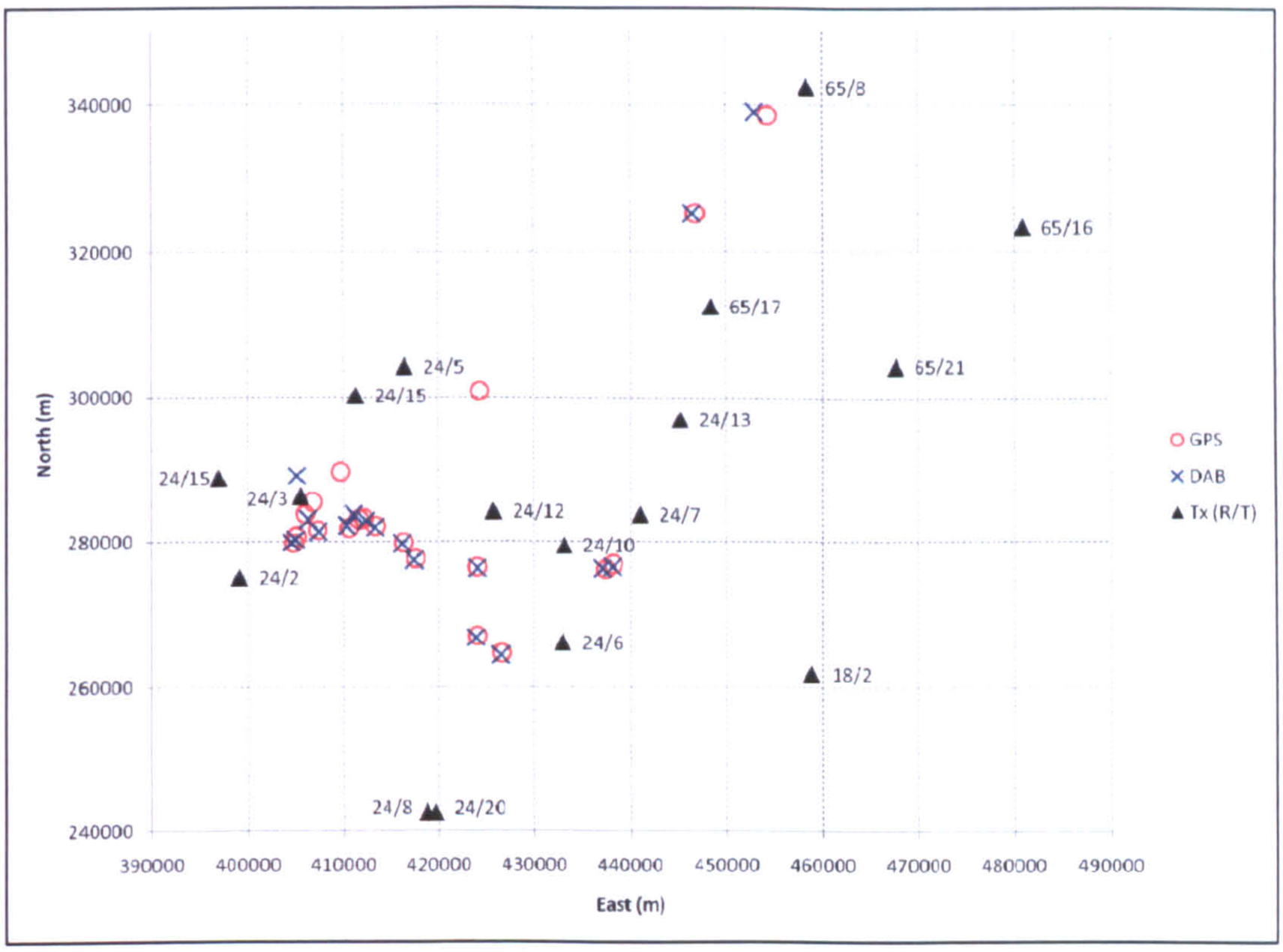

Figure 8-32: Test Results Overview

1	DAB Block						
	11B	11C	11D	12A	12B	12C	12D
TII (Region/Tx)			65 8 65 16 65 21		65 8 65 16	65 8 65 16	
TDOA (T)			175 212		176	174	

Positioning Results		
	East (m)	North (m)
GPS	454275	338484
DAB	452966	338943
Offset	1309	459
HDOP	2.6405	
Height		

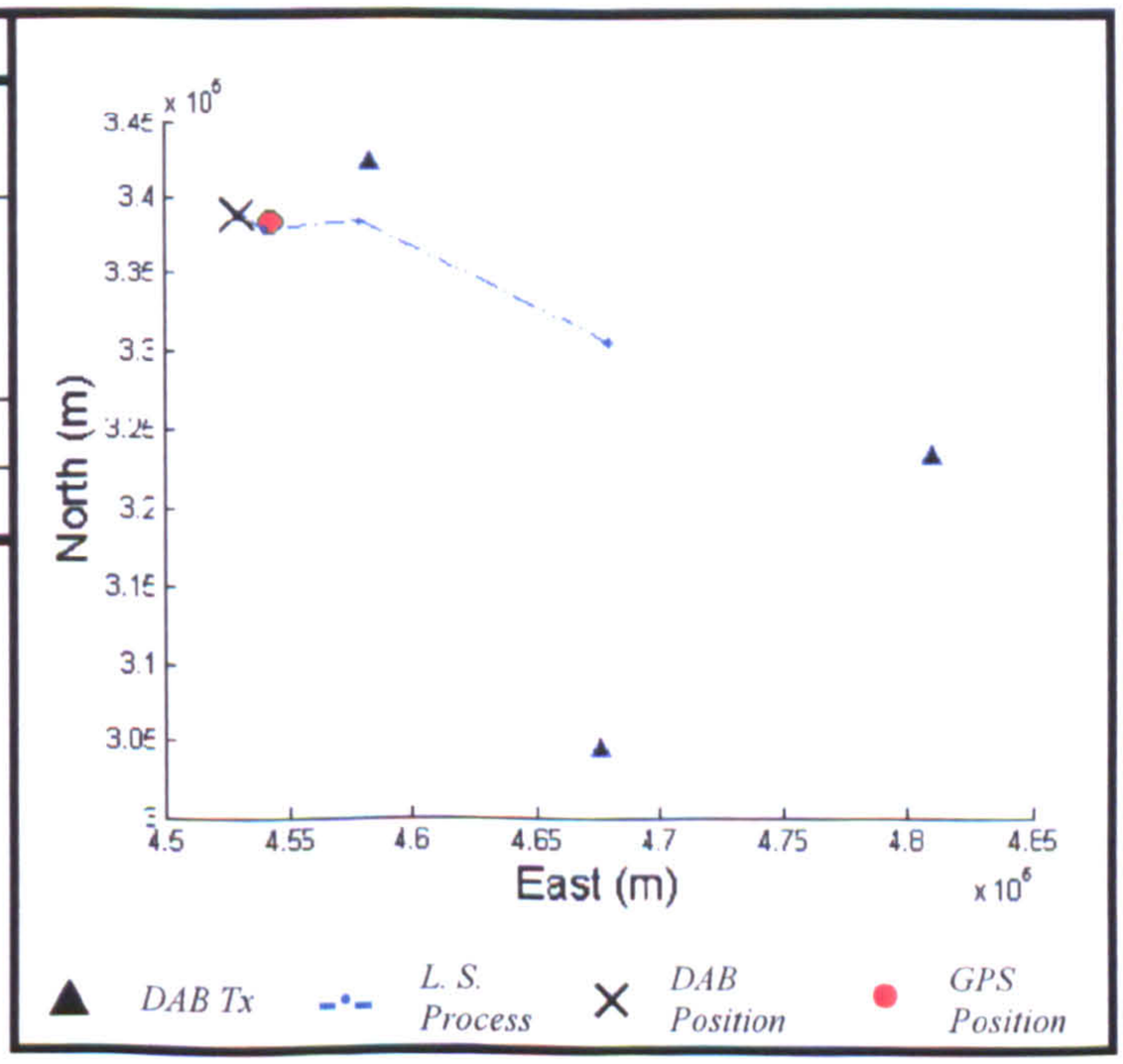

2	DAB Block													
	11B		11C		11D		12A		12B		12C		12D	
TII (Region/Tx)	65 65	17 21			24 24	10 18	24 24	7 10	65 65	8 16			24 24	10 12
TDOA (T)	21				209		13		50				60	

Positioning Results		
	East (m)	North (m)
GPS	438253	276932
DAB	438128	276602
Offset	125	330
HDOP	2.0814	
Height	84m	

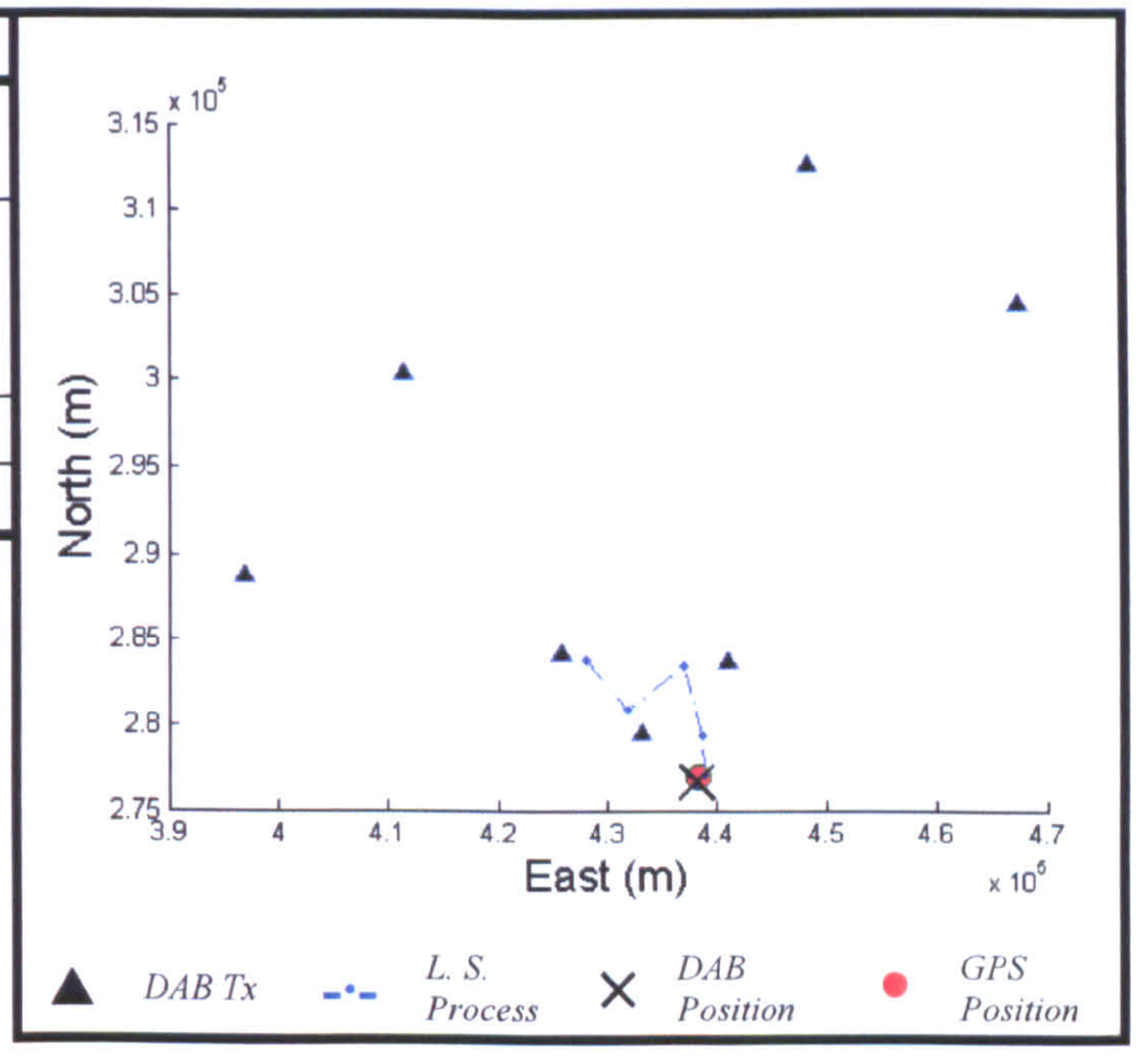

3	DAB Block													
	11B		11C		11D		12A		12B		12C		12D	
TII (Region/Tx)	65 65	17 21			18 24	2 10	24 18 24	7 2 20	18 24	2 8			24 24 24	10 12 6
TDOA (T)	22				143		120 203		83				60 38	

Positioning Results		
	East (m)	North (m)
GPS	437424	276263
DAB	437060	276352
Offset	364	89
HDOP	0.5399	
Height	85m	

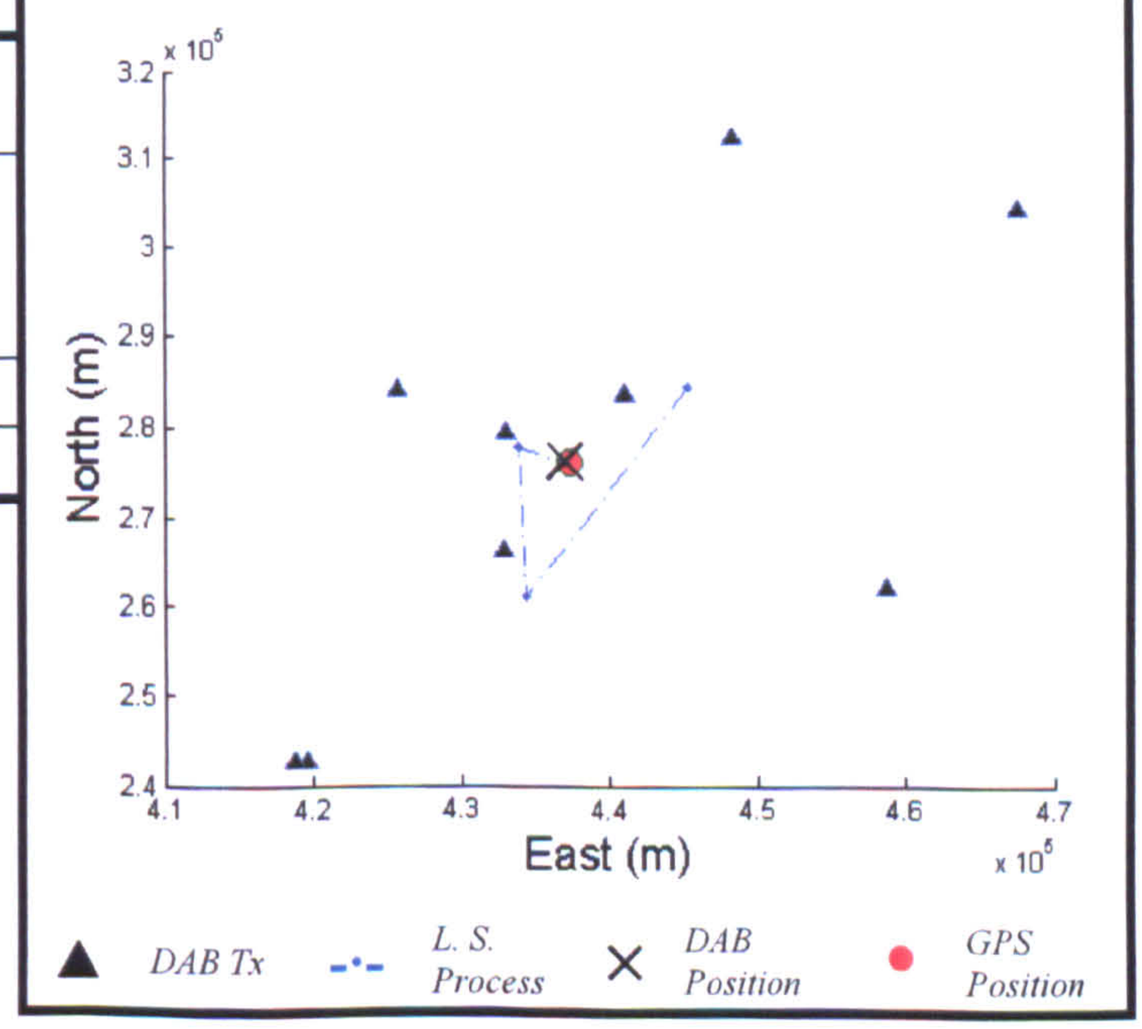

4	DAB Block													
	11B		11C		11D		12A		12B		12C		12D	
TII (Region/Tx)					18 24	2 8	24 18	20 2	18 24	2 8			24 24	6 12
TDOA (T)					63		64		65				89	

Positioning Results		
	East (m)	North (m)
GPS	426602	264656
DAB	426510	264421
Offset	92	235
HDOP	0.9570	
Height	57m	

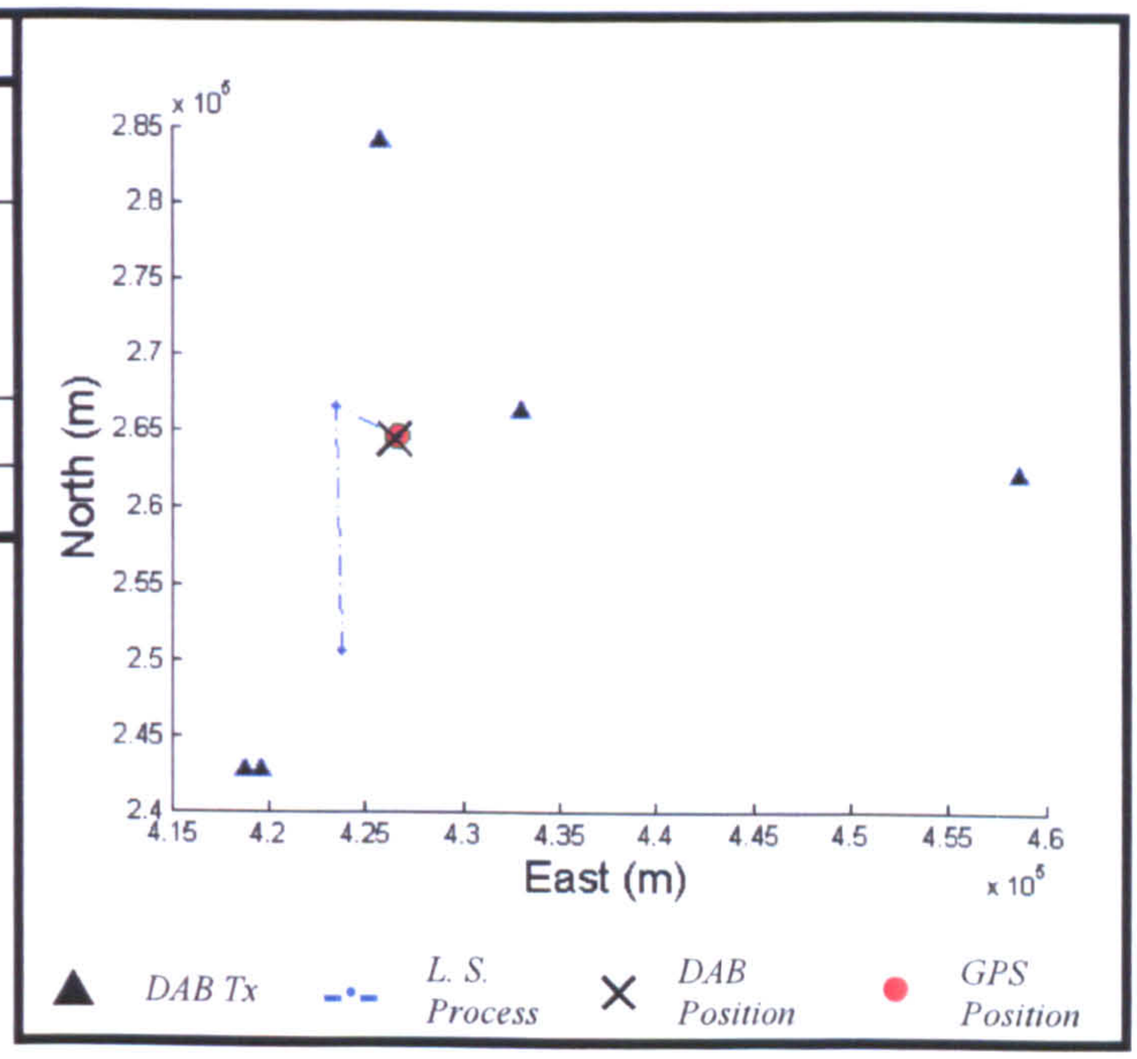

5	DAB Block													
	11B		11C		11D		12A		12B		12C		12D	
TII (Region/Tx)					18 24	2 8	24 18	20 2	24 18	8 2			24 24 24	6 12 10
TDOA (T)					71		72		73				57 45	

Positioning Results		
	East (m)	North (m)
GPS	424094	267049
DAB	423896	266870
Offset	198	179
HDOP	0.7184	
Height	111m	

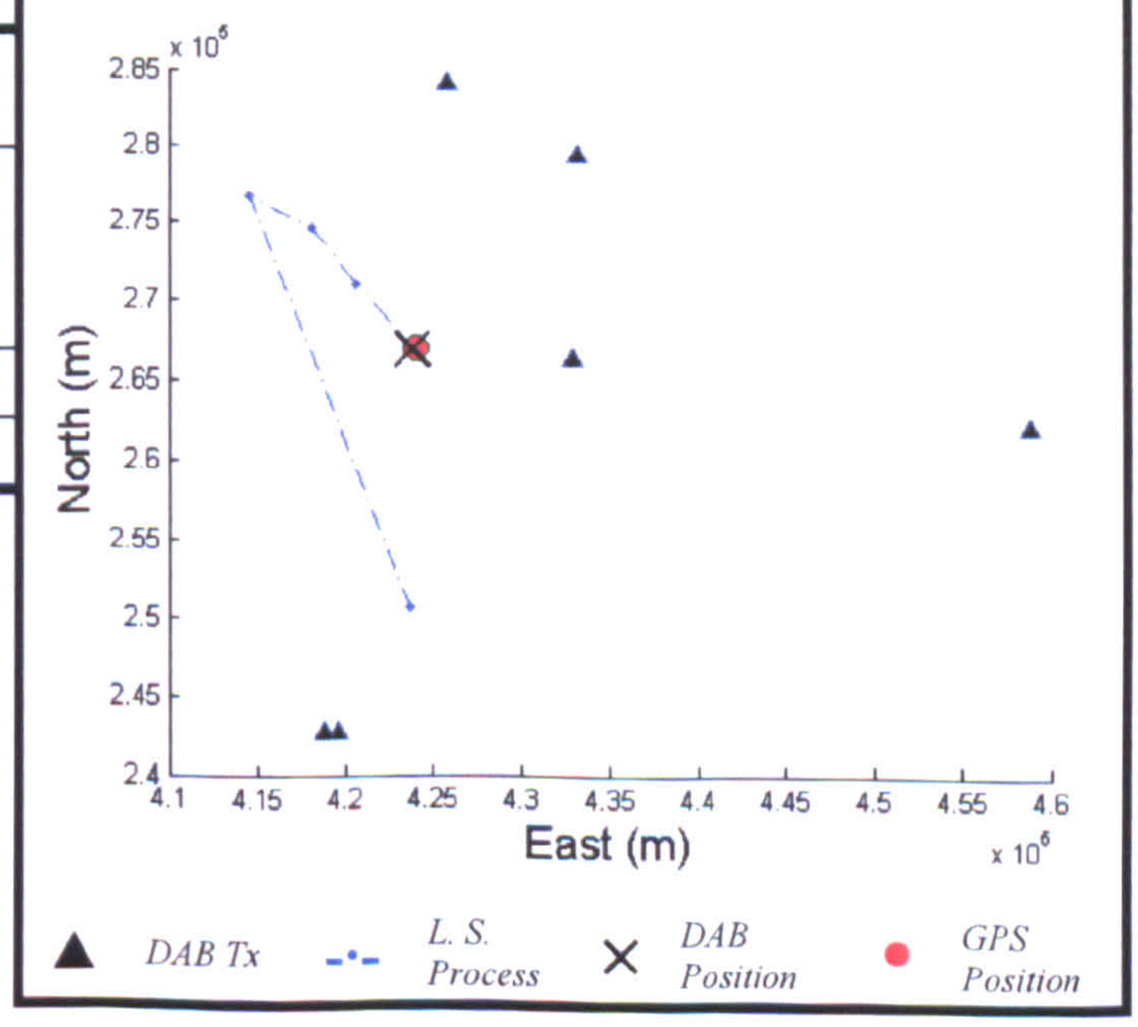

6	DAB Block													
	11B		11C		11D		12A		12B		12C		12D	
TII (Region/Tx)			24 24 24	3 5 15	24 24	18 15	24 24 24	18 20 7	24 24 18 24	18 15 2 8			24 24	12 10
TDOA (T)			57 62		19		29 46		61 19 72				11	

Positioning Results		
	East (m)	North (m)
GPS	424102	276464
DAB	424073	276349
Offset	29	115
HDOP	0.6455	
Height	123m	

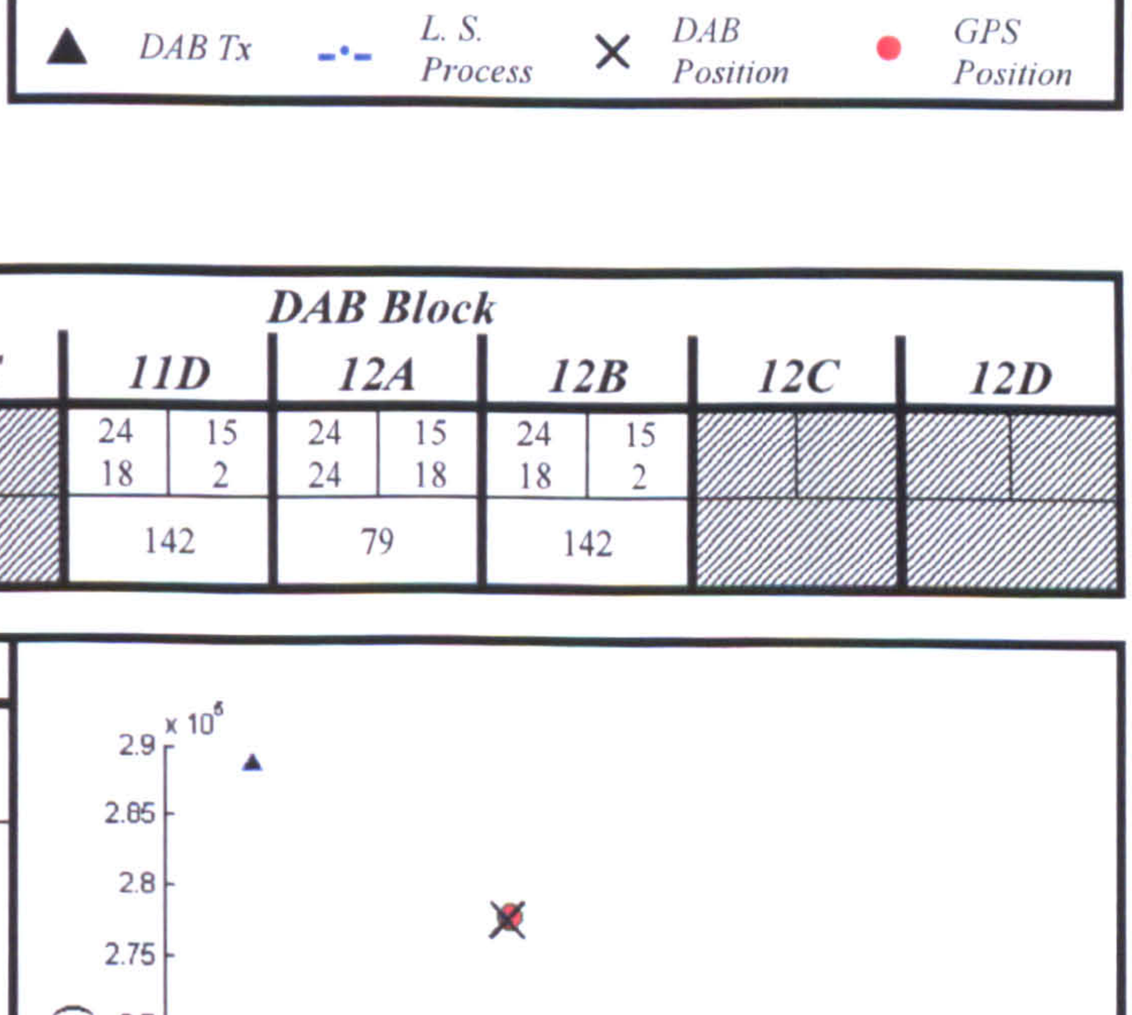

7	DAB Block													
	11B		11C		11D		12A		12B		12C		12D	
TII (Region/Tx)					24 18	15 2	24 24	15 18	24 18	15 2				
TDOA (T)					142		79		142					

Positioning Results		
	East (m)	North (m)
GPS	417526	277688
DAB	417380	277473
Offset	146	215
HDOP	1.2333	
Height	124m	

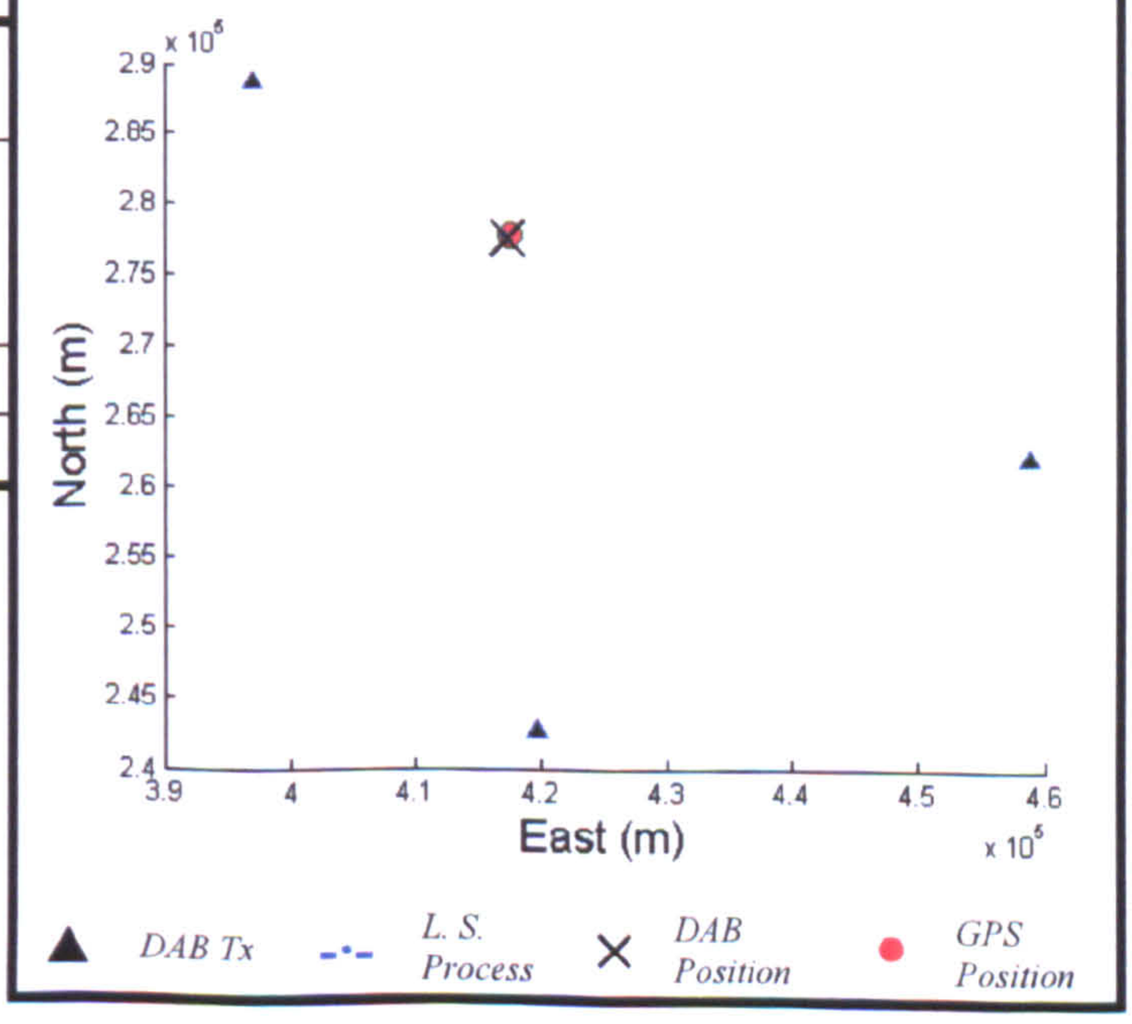

8	DAB Block						
	11B	11C	11D	12A	12B	12C	12D
TII (Region/Tx)			24 18 24 15	24 18 24 15			24 12 24 6
TDOA (T)			171	171			75

Positioning Results		
	East (m)	North (m)
GPS	416300	279894
DAB	416132	279796
Offset	168	98
HDOP	1.4067	
Height	136m	

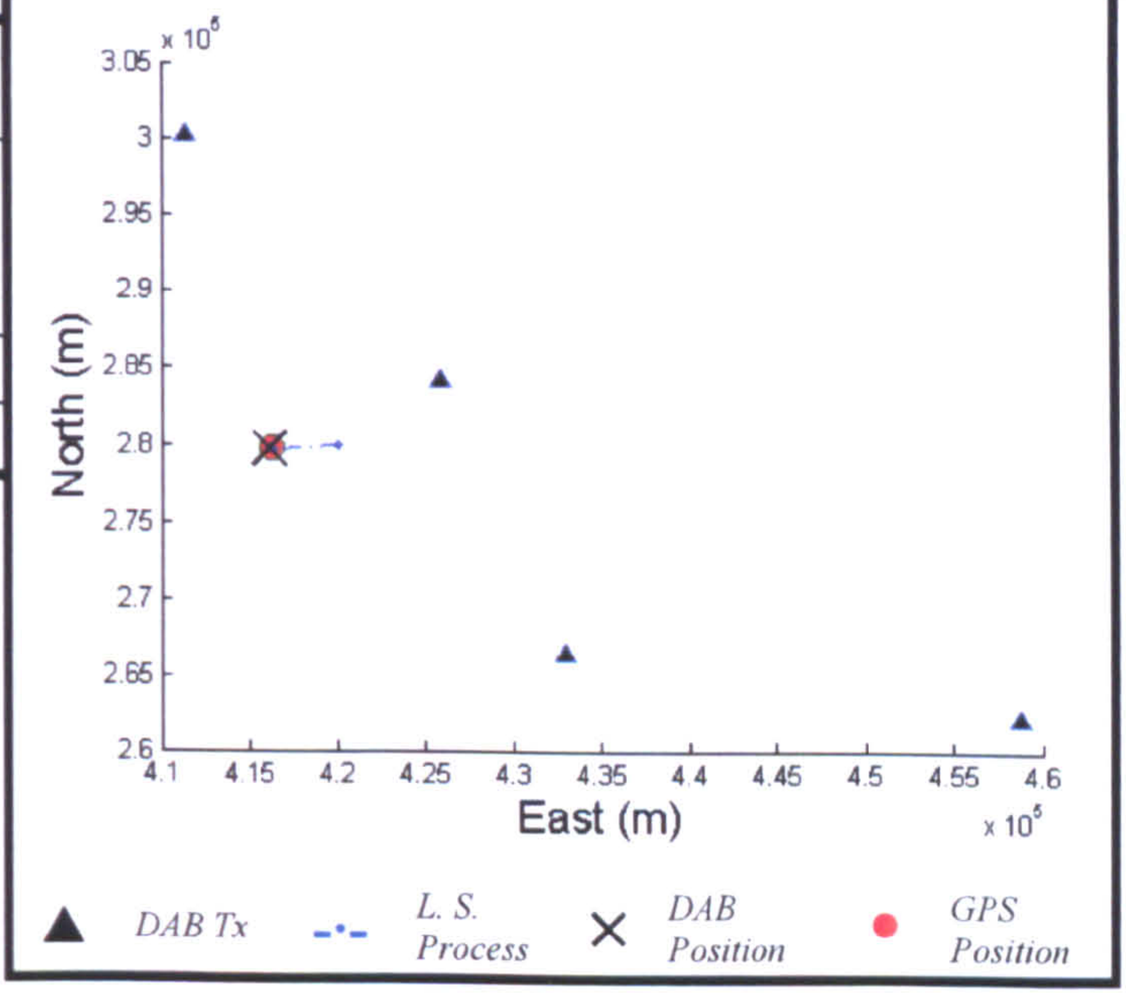

9	DAB Block						
	11B	11C	11D	12A	12B	12C	12D
TII (Region/Tx)			24 18 24 15	24 18 24 15	24 18 24 15 18 2		24 12
TDOA (T)			5	5	5 213		

Positioning Results		
	East (m)	North (m)
GPS	413392	282095
DAB	413316	282032
Offset	76	63
HDOP	0.8078	
Height	125m	

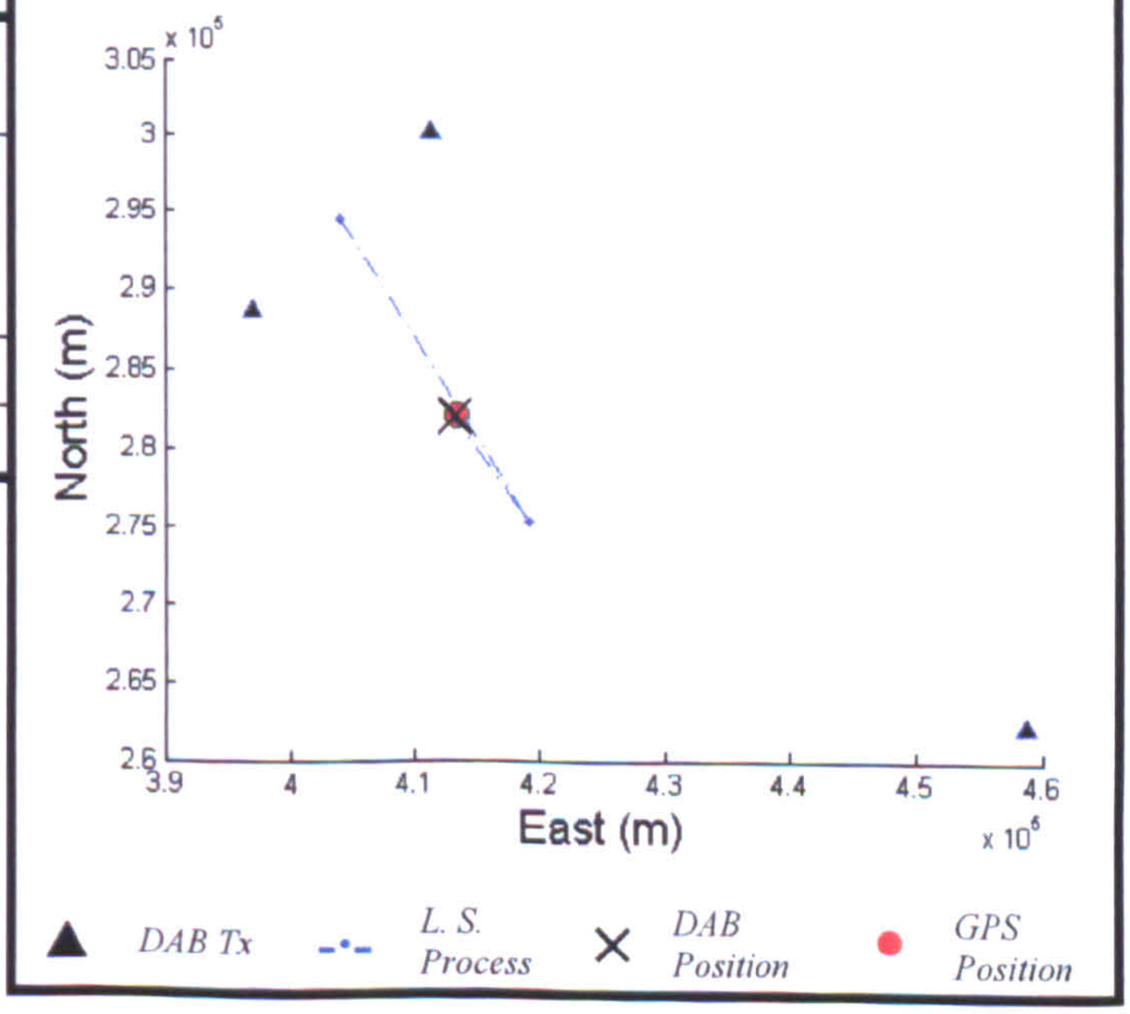

10	DAB Block											
	11B		11C		11D		12A		12B		12C	12D
TII (Region/Tx)	65 65	17 21	24 24 24	3 5 15	24 24 65	15 18 17	24 24	15 18	24 24	15 18		
TDOA (T)	85		100 63		5 199		7		6			

Positioning Results		
	East (m)	North (m)
GPS	412196	283184
DAB	412369	282880
Offset	173	304
HDOP	1.2908	
Height	128m	

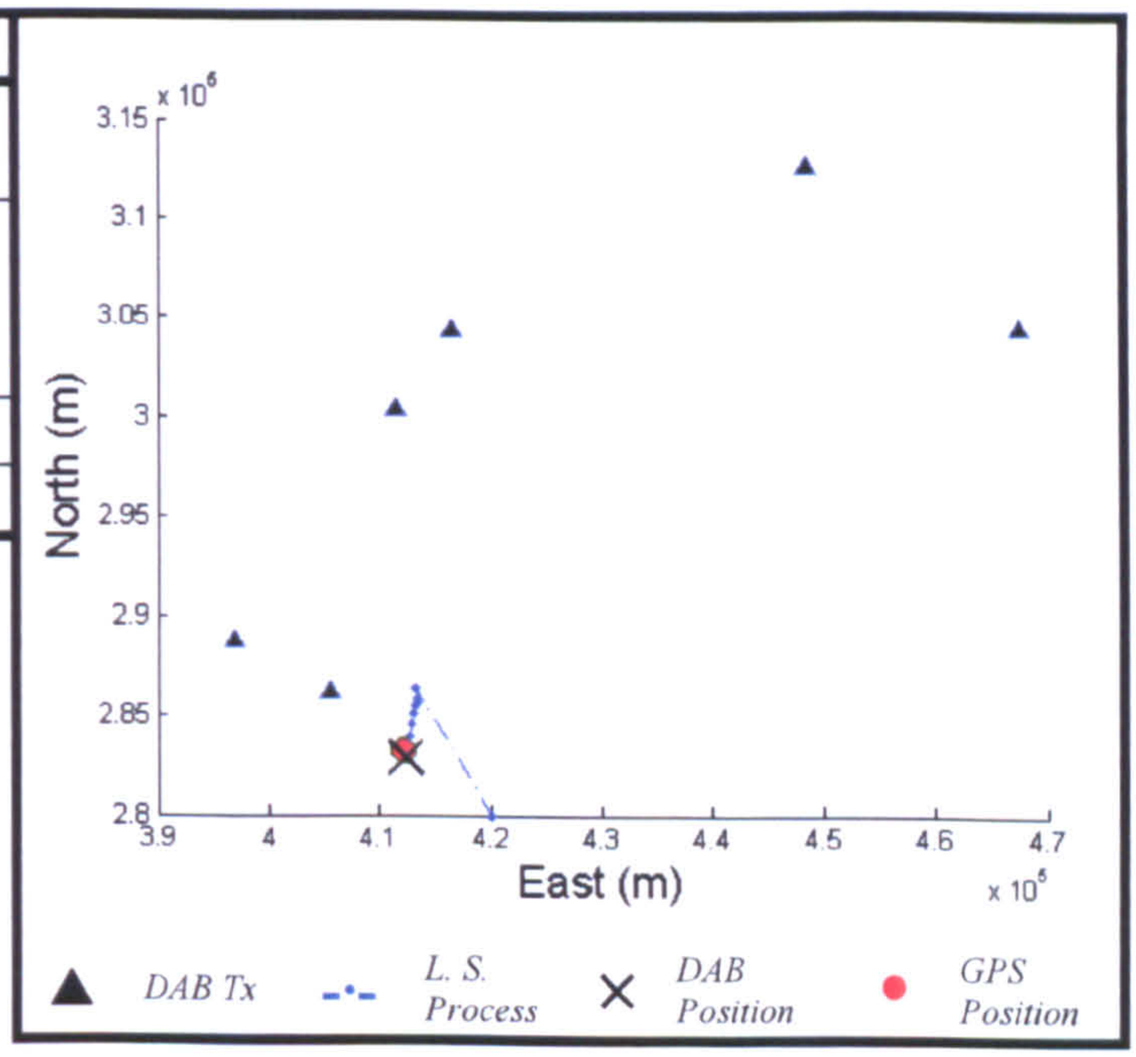

11	DAB Block											
	11B		11C		11D		12A		12B		12C	12D
TII (Region/Tx)			24 24 24	3 15 5	24 24	15 18	24 24	15 18	24 24	15 18		24 24	12 13
TDOA (T)			62 105		11		11		10			151	

Positioning Results		
	East (m)	North (m)
GPS	411662	283082
DAB	411064	283773
Offset	598	691
HDOP	2.7476	
Height	133m	

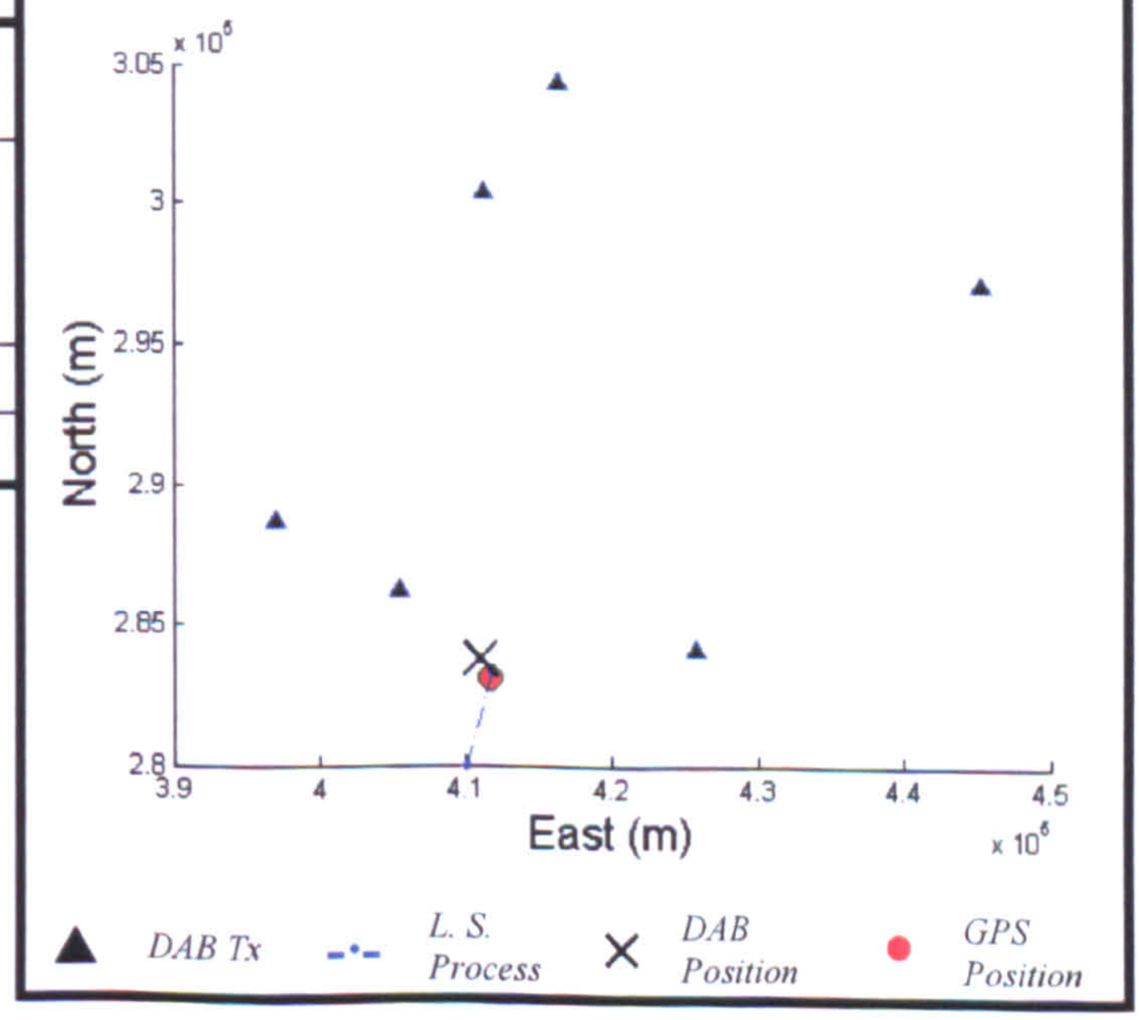

12	DAB Block											
	11B		11C		11D		12A		12B		12C	12D
TII (Region/Tx)					24 24	18 15	24 24	18 15	24 24	18 15		24 24	12 13
TDOA (T)					22		22		22			153	

Positioning Results		
	East (m)	North (m)
GPS	410621	281906
DAB	410361	282258
Offset	260	352
HDOP	3.7753	
Height	135m	

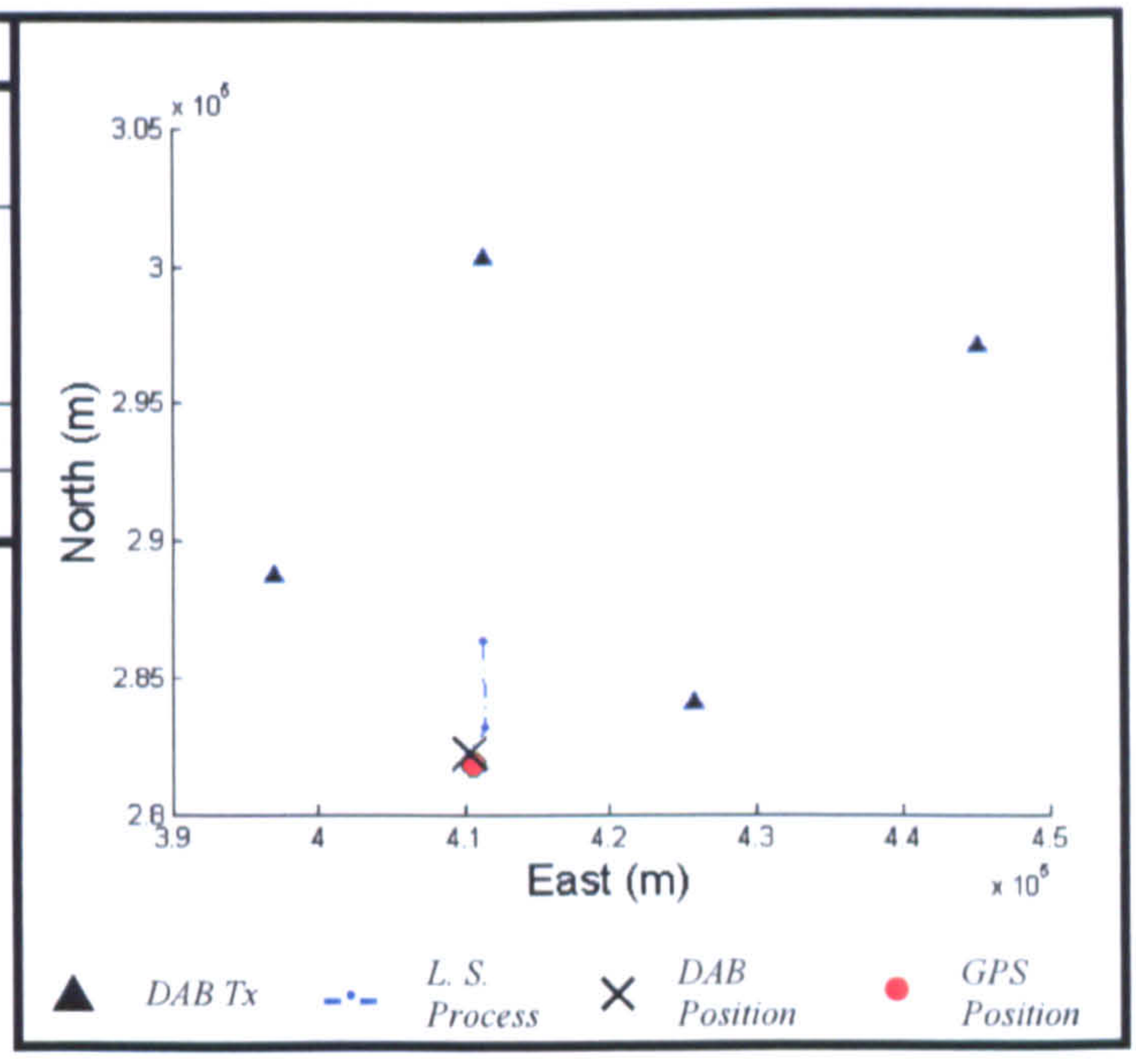

13	DAB Block											
	11B		11C		11D		12A		12B		12C	12D
TII (Region/Tx)					24 24 24	15 18 8	24 24 24	15 18 20	24 24 24	15 18 8			
TDOA (T)					45 189		45 191		44 186				

Positioning Results		
	East (m)	North (m)
GPS	407365	281586
DAB	407437	281416
Offset	72	170
HDOP	0.6266	
Height	160m	

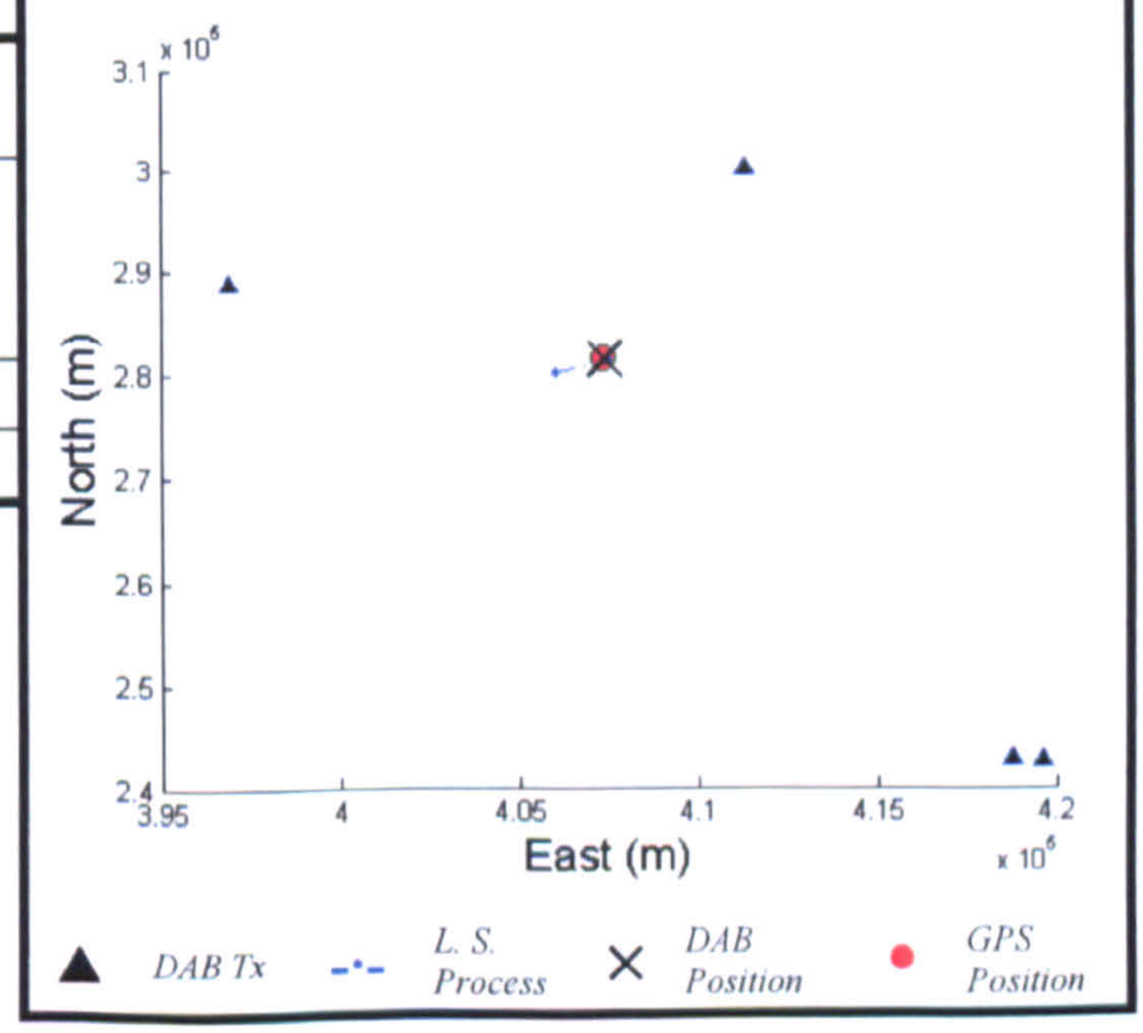

14	***DAB Block***												
	11B		***11C***		***11D***		***12A***		***12B***		***12C***		***12D***
TII (Region/Tx)			24 24 24	3 5 2	24 24	15 18	24 24	15 18	24 24	15 18			
TDOA (T)			144 5		67		67		66				

Positioning Results		
	East (m)	***North (m)***
GPS	404820	279807
DAB	404561	279933
Offset	259	126
HDOP	1.0105	
Height	160m	

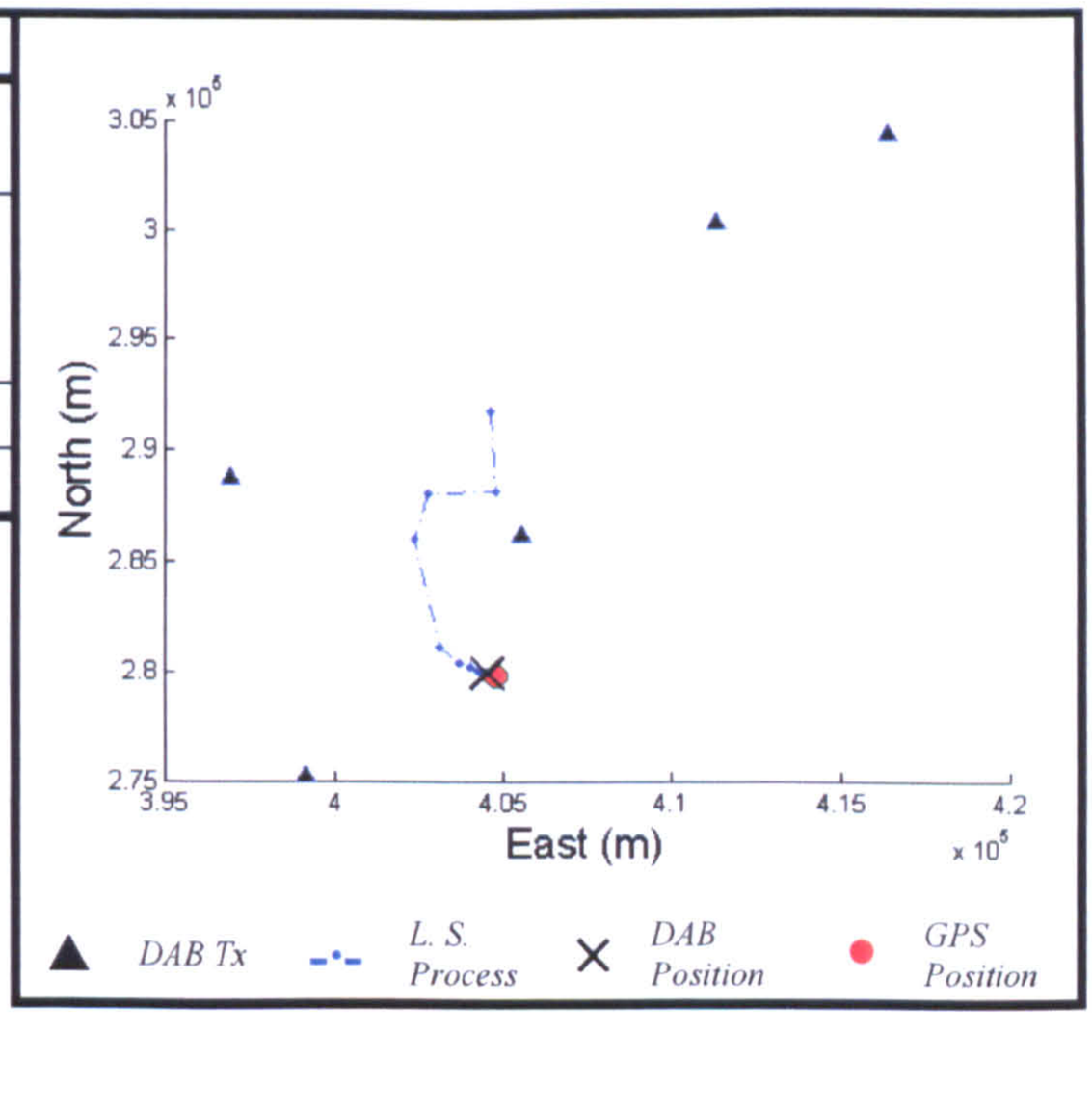

15	***DAB Block***												
	11B		***11C***		***11D***		***12A***		***12B***		***12C***		***12D***
TII (Region/Tx)			24 24 24	3 5 2	24 24	15 18	24 24	15 18	24 24	15 18			
TDOA (T)			144 12		63		64		63				

Positioning Results		
	East (m)	***North (m)***
GPS	405085	280672
DAB	405026	280319
Offset	59	353
HDOP	0.9957	
Height	143m	

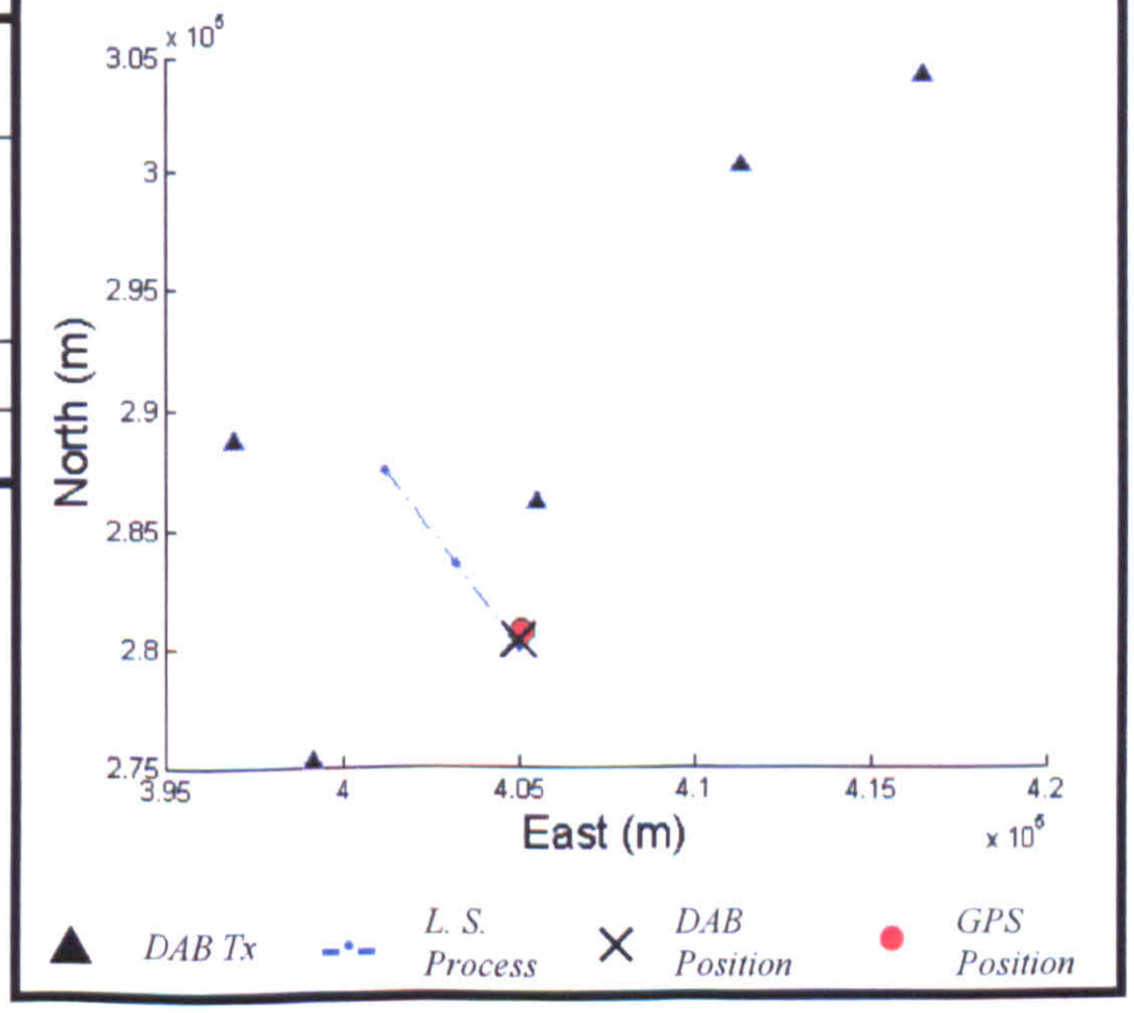

16	DAB Block												
	11B		11C		11D		12A		12B		12C		12D
TII (Region/Tx)			24 24	3 2	24 24	15 18	24 24	15 18	24 24	15 18			
TDOA (T)			50		49		48		48				

Positioning Results		
	East (m)	North (m)
GPS	406036	283722
DAB	406293	283065
Offset	257	657
HDOP	0.9100	
Height	121m	

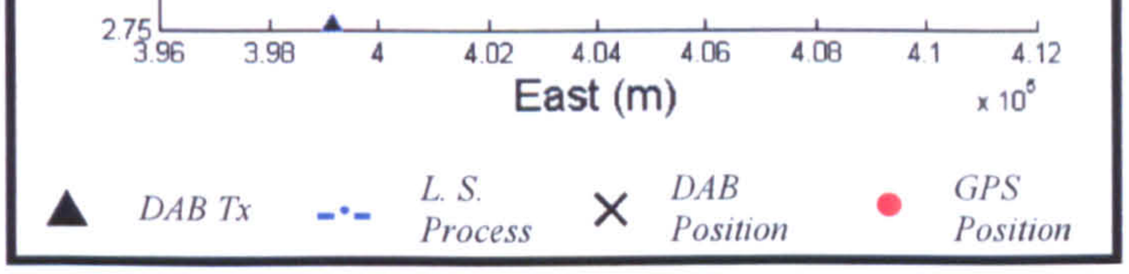

17	DAB Block												
	11B		11C		11D		12A		12B		12C		12D
TII (Region/Tx)			24 24	3 5			24 24	18 15	24 24	18 15			
TDOA (T)			139				36		35				

Positioning Results		
	East (m)	North (m)
GPS	406788	285424
DAB	405154	289003
Offset	1634	3579
HDOP	4.9002	
Height	118m	

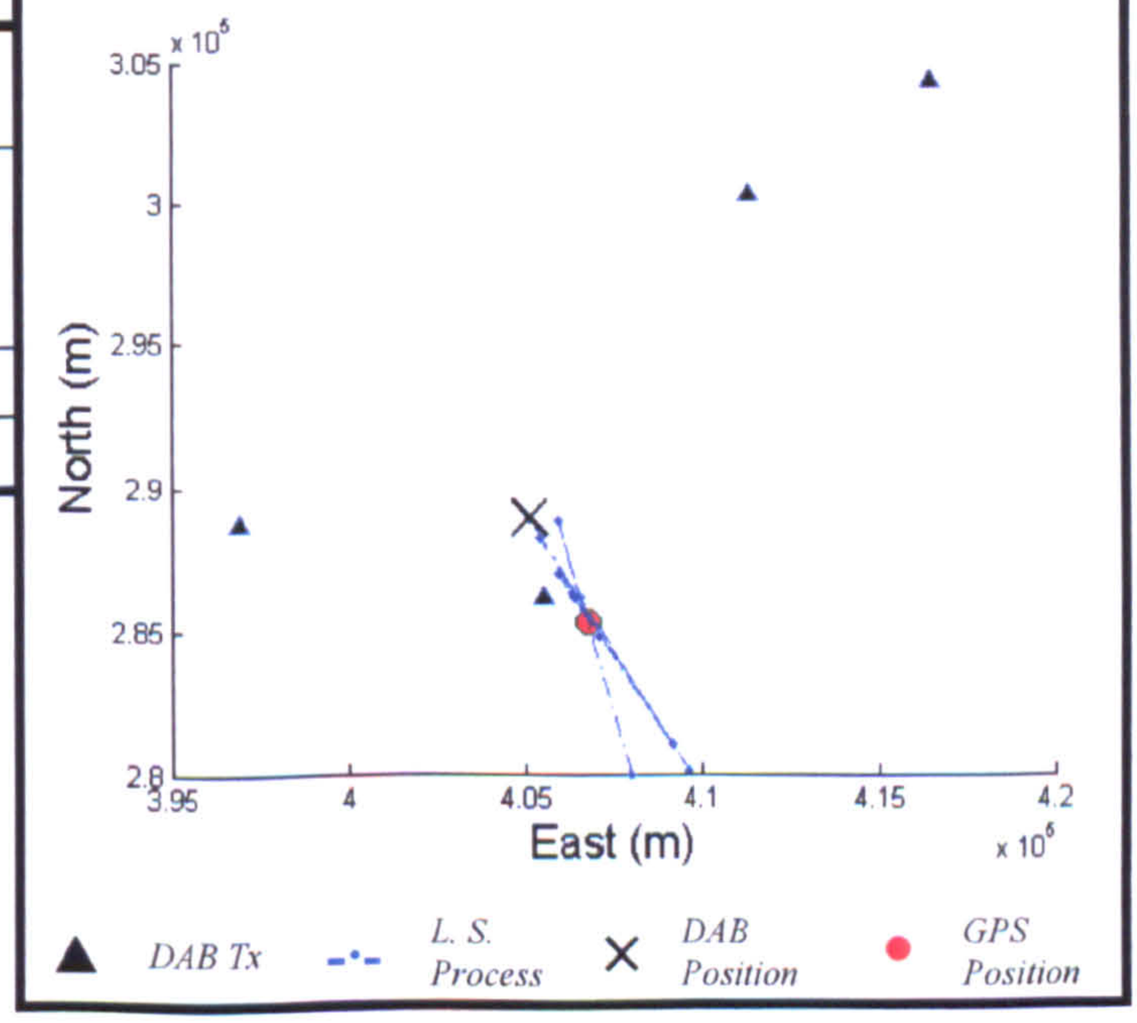

18	DAB Block						
	11B	11C	11D	12A	12B	12C	12D
TII (Region/Tx)			24 15 24 18		24 15 24 18		
TDOA (T)			9		10		

Positioning Results		
	East (m)	North (m)
GPS	409788	289560
DAB Offset		
HDOP		
Height	94m	

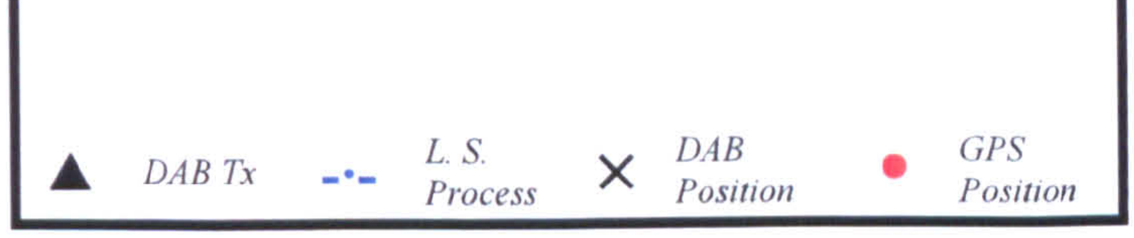

19	DAB Block						
	11B	11C	11D	12A	12B	12C	12D
TII (Region/Tx)			24 15 24 18		24 15 24 18		
TDOA (T)			116		116		

Positioning Results		
	East (m)	North (m)
GPS	424326	300802
DAB Offset		
HDOP		
Height	95m	

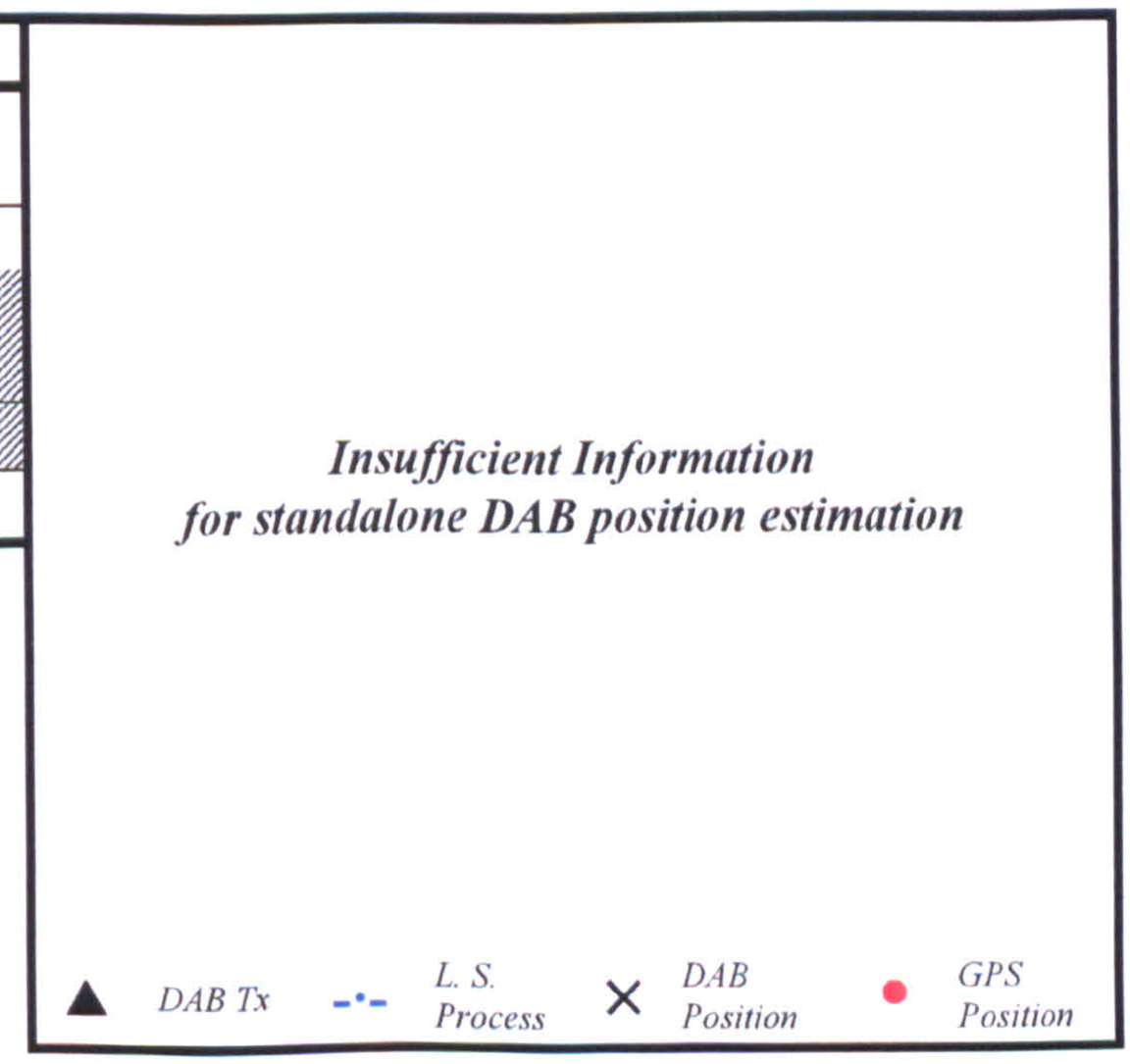

20	***DAB Block***													
	11B		***11C***		***11D***		***12A***		***12B***		***12C***		***12D***	
TII (Region/Tx)	65 65	17 21			65 65	16 17			65 65 65	16 8 10	65 65 65	16 8 10		
TDOA (T)	115				150				96 7		92 10			

Positioning Results		
	East (m)	***North (m)***
GPS	446776	325234
DAB	446401	325233
Offset	375	1
HDOP	0.8333	
Height	87m	

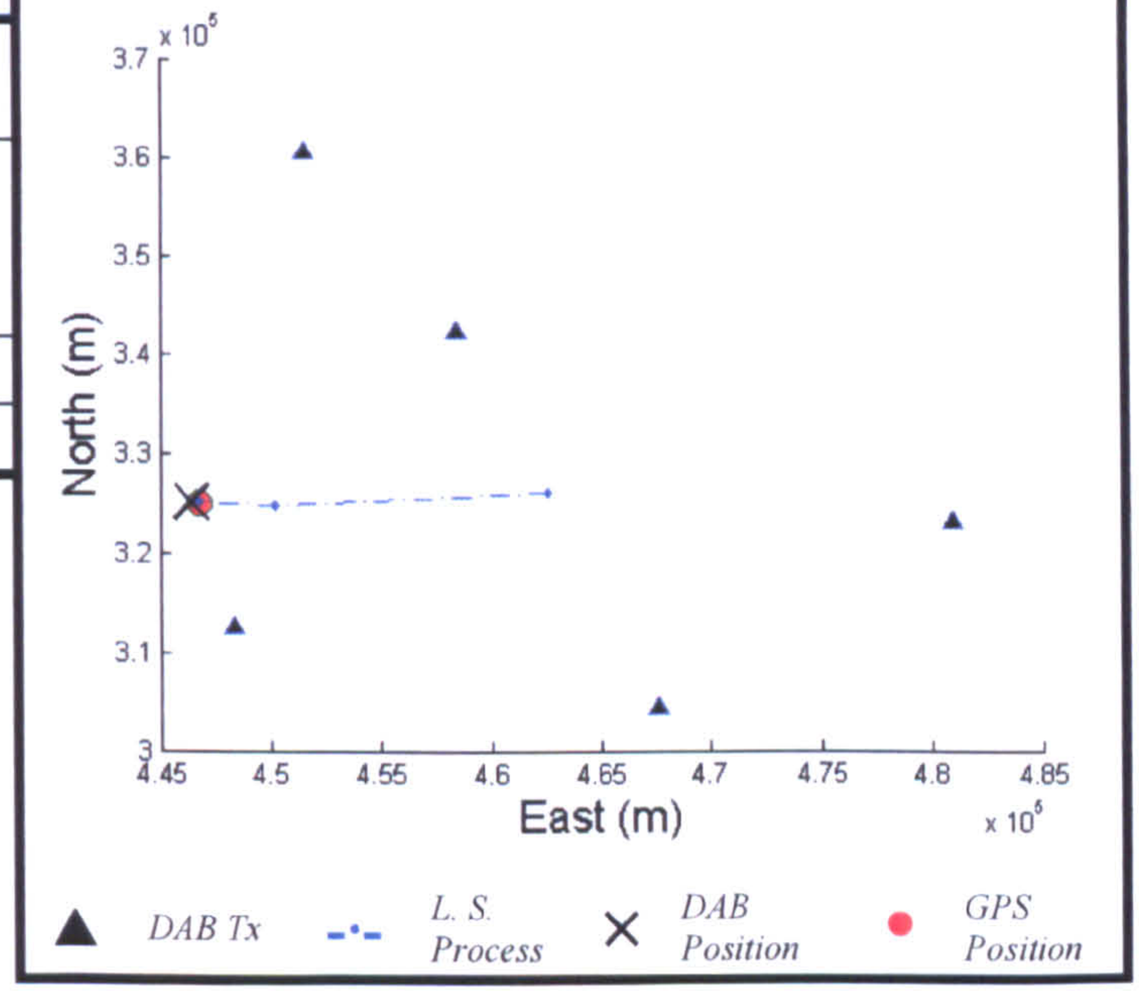

8.9.3 Discussion

As has been shown in the results, the majority of DAB data captures have resulted in a position fix. The offset of all DAB positions from their actual GPS positions can be seen in Figure 8-33. As before, the offset has been divided into the difference in Easting, difference in Northing and total linear offset. The captures taken at locations 18 and 19 do not yield a result and by examining the individual result table for these captures it can be seen that this is due to a lack of TDOA measurements. In both cases, two measurements are extracted from different blocks, but these are from the same transmitters meaning only one can be used.

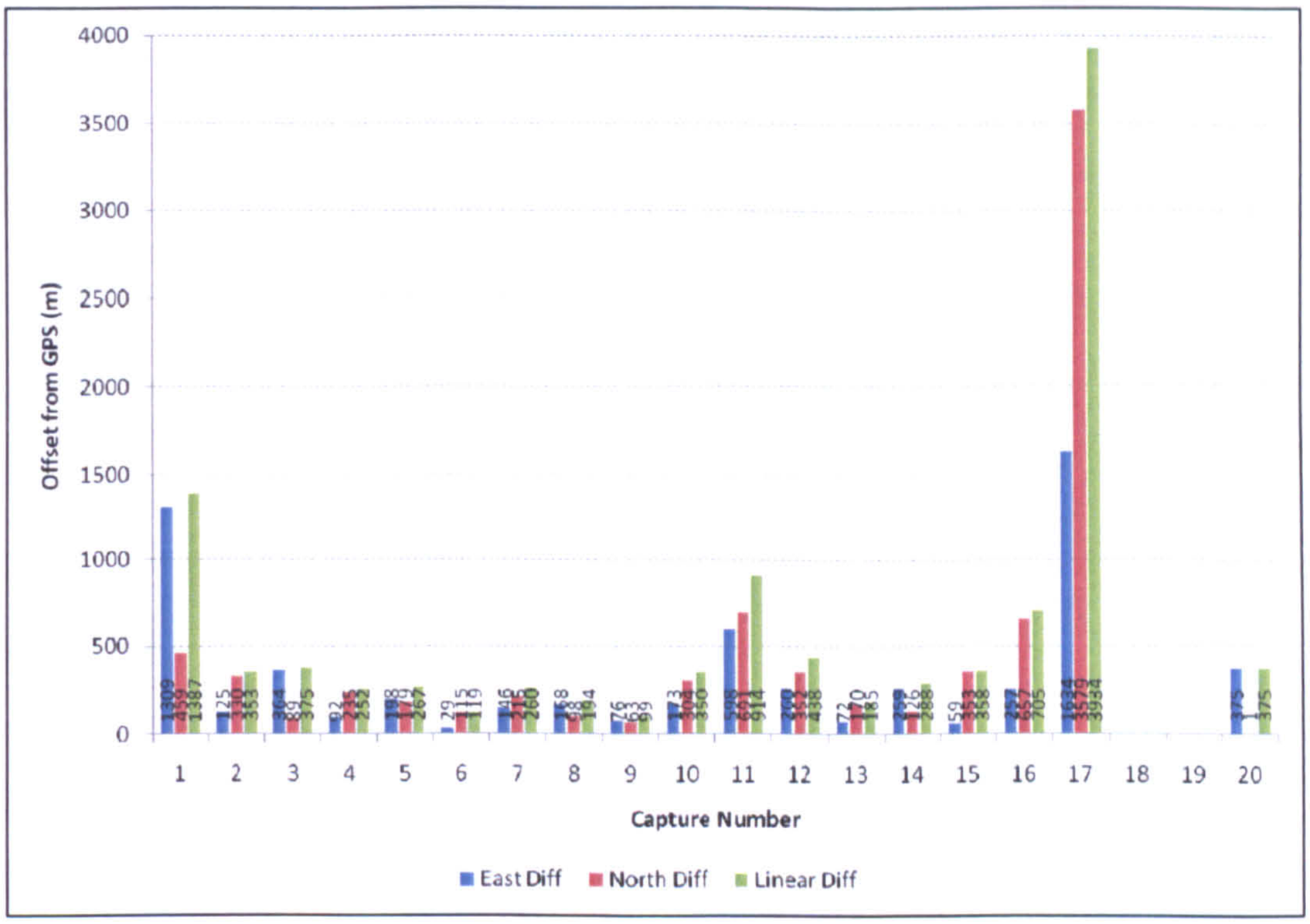

Figure 8-33: Offset from GPS (m) at each capture

Chart divided to show difference in East, North and Linear offsets

Capture 17 shows a very large offset from its true position (almost 4km). Examining the individual result shows that the linear least squares positioning process appears to jump around erratically before eventually settling on a position. Four transmitters are used in this capture to provide two TDOA pairs (there are actually three measurements but two of these involve the same transmitters). The final HDOP value for this capture (see Figure 8-34) shows an uncertainty value of almost 5, proving that the calculated position in this case is poor.

Most other captures during this test show total offsets from the true position of better than 500 metres. The most accurate capture at position 9 shows a linear offset of 99 metres, which also corresponds to a low HDOP value of 0.81.

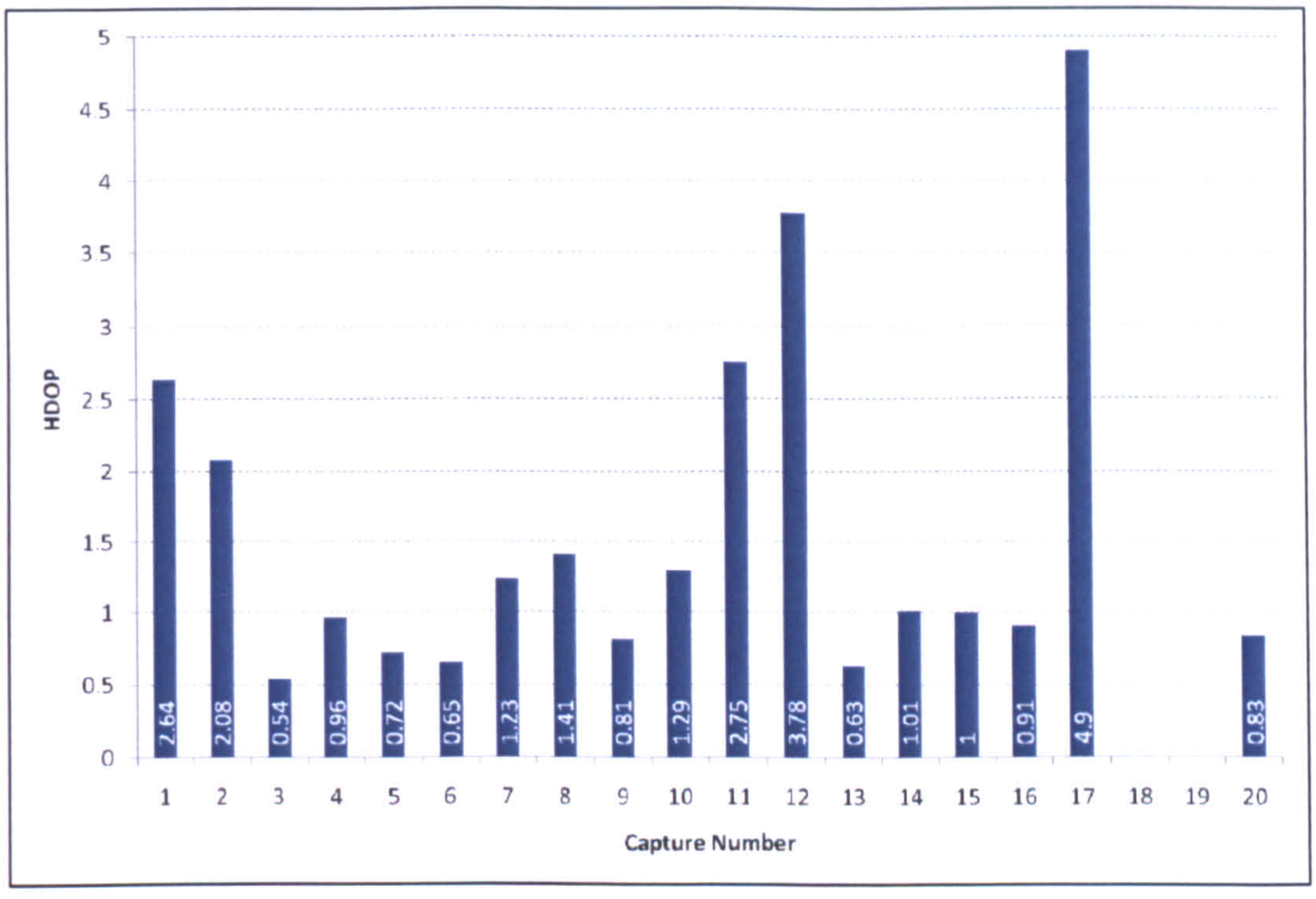

Figure 8-34: HDOP values for DAB position at each capture location

As previously, the linear offset from the GPS and DAB positions can be plotted against the elevation the vehicle was at when the data was collected, which may be seen in Figure 8-35. The general trend again shows that the captures taken on higher ground provide a higher accuracy than those on lower ground. A couple of exceptions are noticeable with capture 17 taken at a relatively high location but providing the highest error in this test.

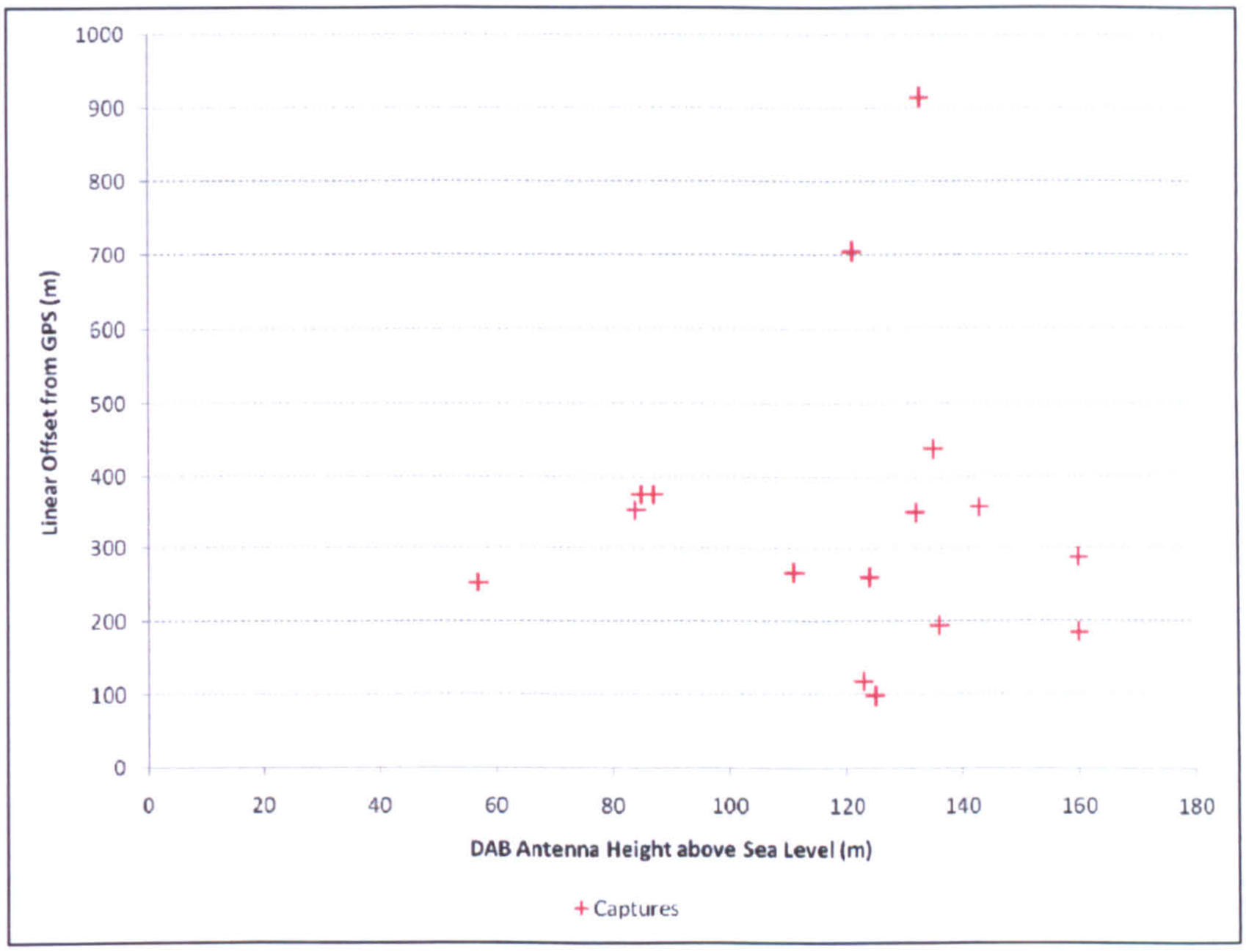

Figure 8-35: Chart showing capture elevation against linear offset

8.10 STATIC TEST: LINCOLNSHIRE (SUBURBAN/RURAL)

8.10.1 Introduction

The final test involving static positioning took place at a number of locations between Nottingham and Lincoln. It was known that there were fewer transmitters in this direction than encountered on the trial towards the urban environment in Birmingham; therefore the general aim was to examine how the system would cope with being in a region of lower transmitter density.

A number of captures were taken starting towards the north of Nottingham, heading east towards Lincoln and then returning back to Nottingham again via an alternative route in order to give as widespread a set of results as possible. This route and the transmitters received during the trial may be seen in Figure 8-36.

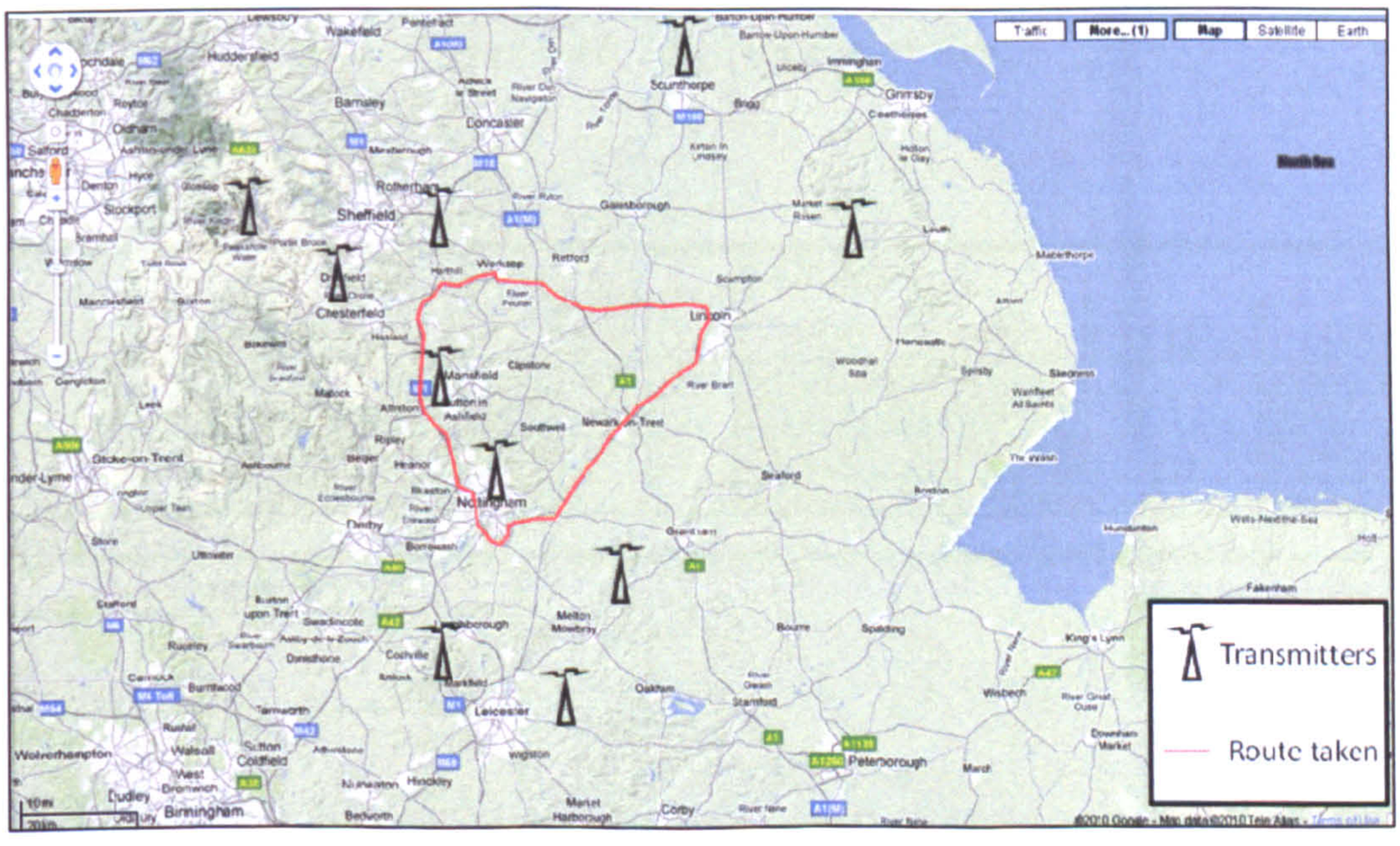

Figure 8-36: Transmitters received during Lincolnshire trial

(Image courtesy of Google Maps UK)

8.10.2 Results

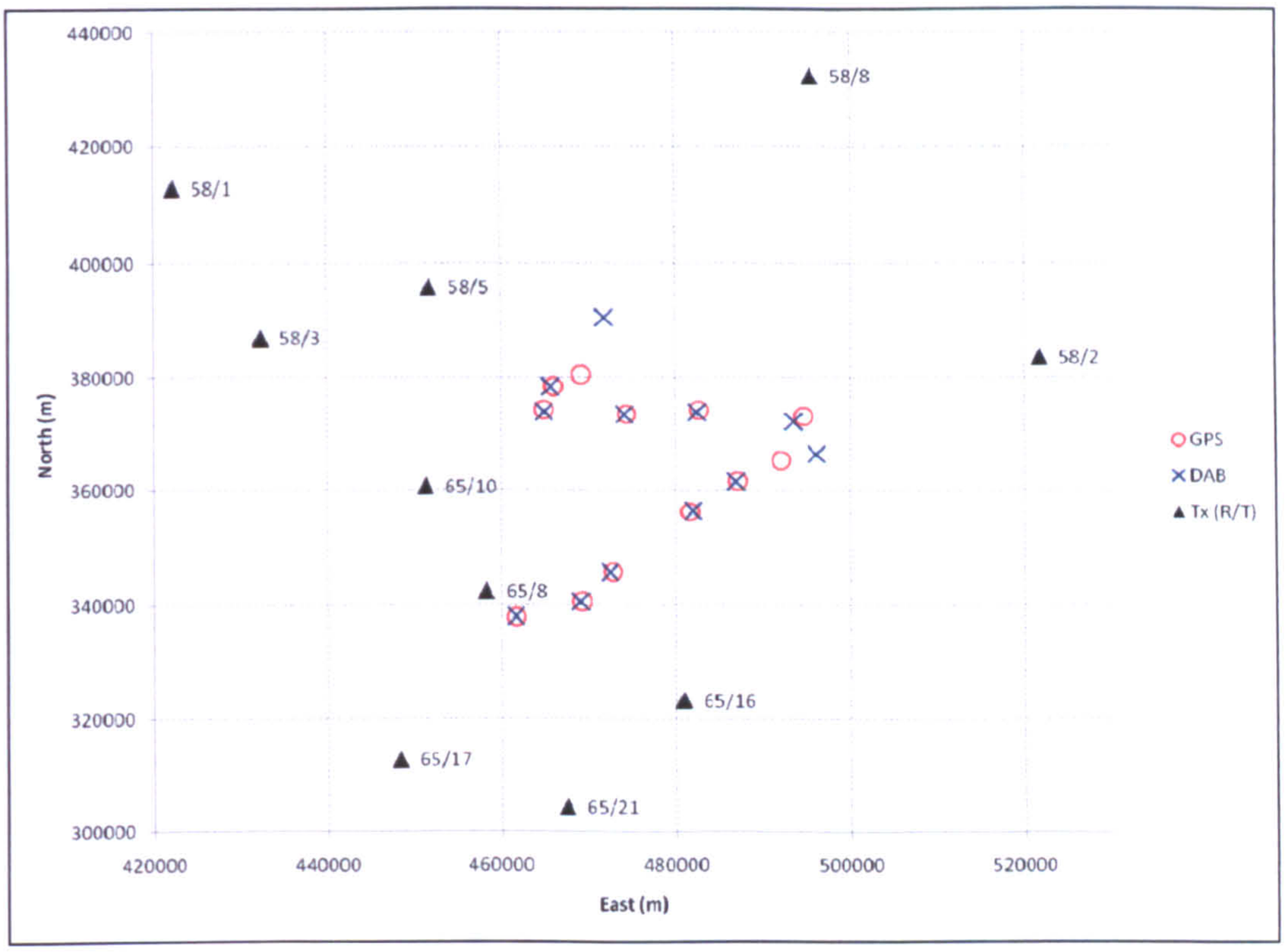

Figure 8-37: Test Results Overview

1	DAB Block						
	11B	11C	11D	12A	12B	12C	12D
TII (Region/Tx)			65 16 58 2			65 16 65 10	
TDOA (T)			31			233	

Positioning Results		
	East (m)	North (m)
GPS	464940	374227
DAB	464990	374028
Offset	50	199
HDOP	1.2842	
Height	49m	

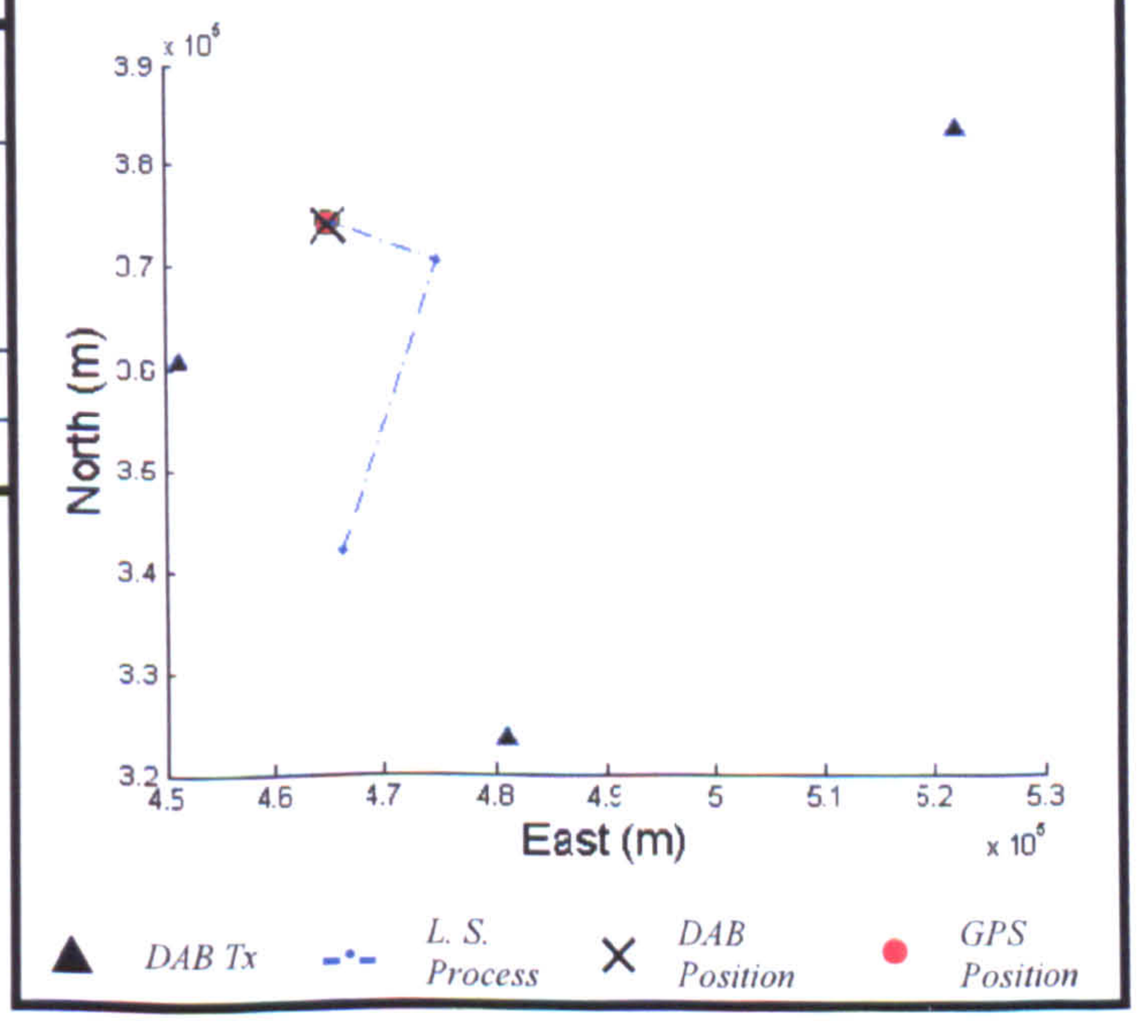

2	DAB Block													
	11B		11C		11D		12A		12B		12C		12D	
TII (Region/Tx)			58 58	5 3	65 58 65 58	10 2 16 3	58 58	3 5	65 58 65	10 2 16	65 65	10 16		
TDOA (T)			83		230 237 83		148		230 237		233			

Positioning Results		
	East (m)	North (m)
GPS	466010	378446
DAB	465732	378420
Offset	278	26
HDOP	0.8292	
Height	34m	

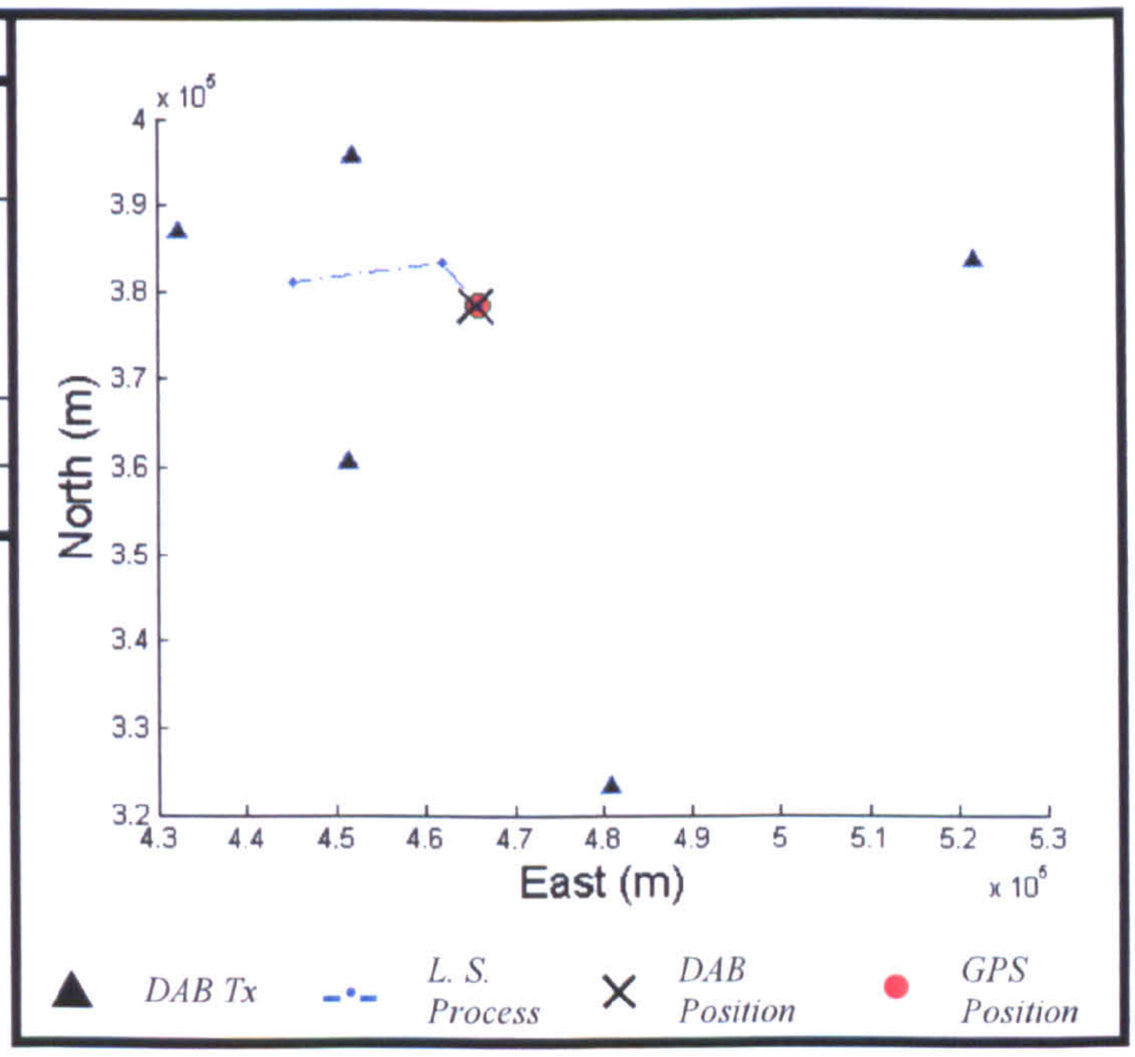

3	DAB Block													
	11B		11C		11D		12A		12B		12C		12D	
TII (Region/Tx)							58 58 58	5 2 1	58 58	5 2				
TDOA (T)							204 230		204					

Positioning Results		
	East (m)	North (m)
GPS	469199	380516
DAB	471814	390614
Offset	2615	10098
HDOP	6.3087	
Height	35m	

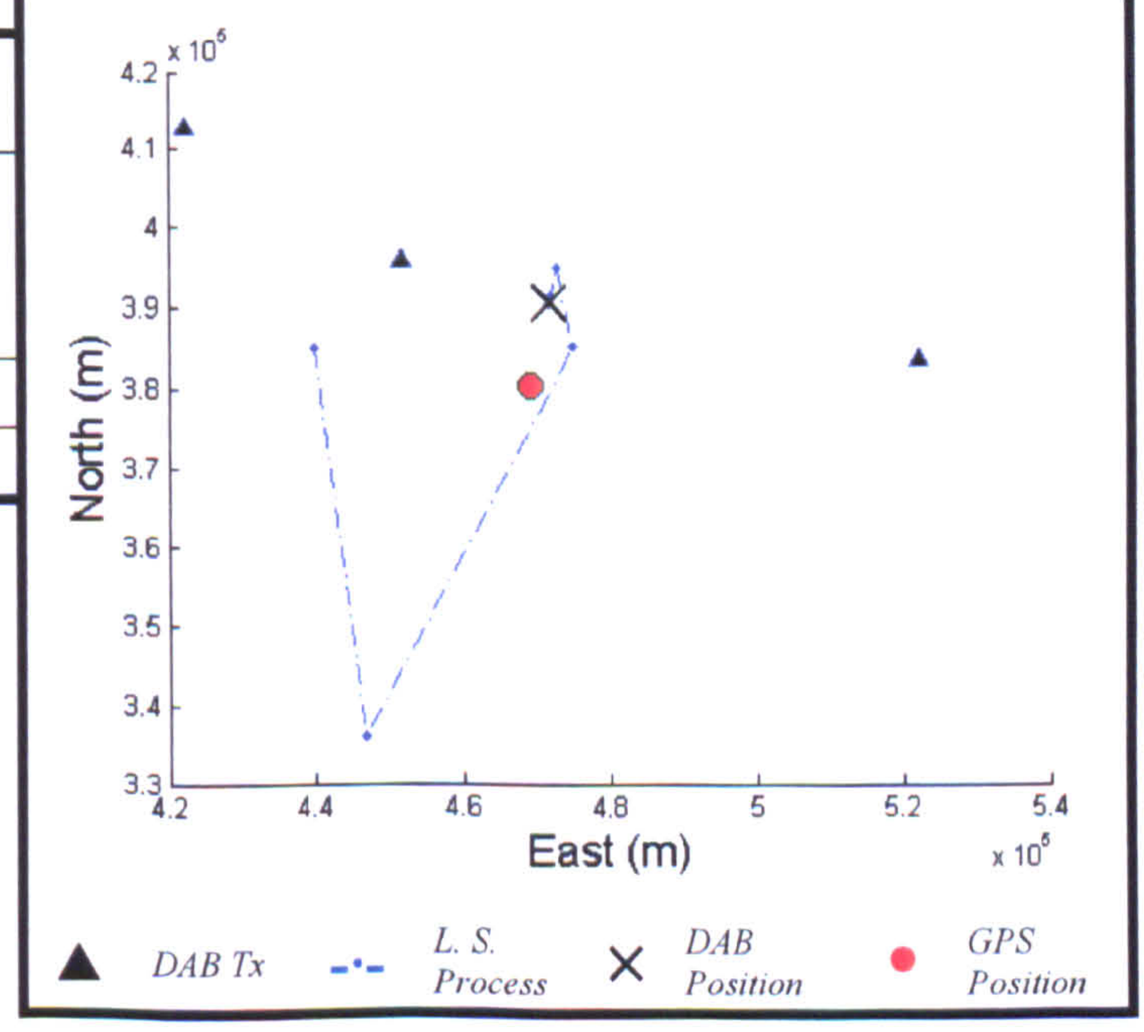

4	DAB Block						
	11B	11C	11D	12A	12B	12C	12D
TII (Region/Tx)			58 2 65 16 65 10			65 16 65 10	
TDOA (T)			14 156			166	

Positioning Results		
	East (m)	North (m)
GPS	474410	373465
DAB	474181	373489
Offset	229	24
HDOP	0.9603	
Height	52m	

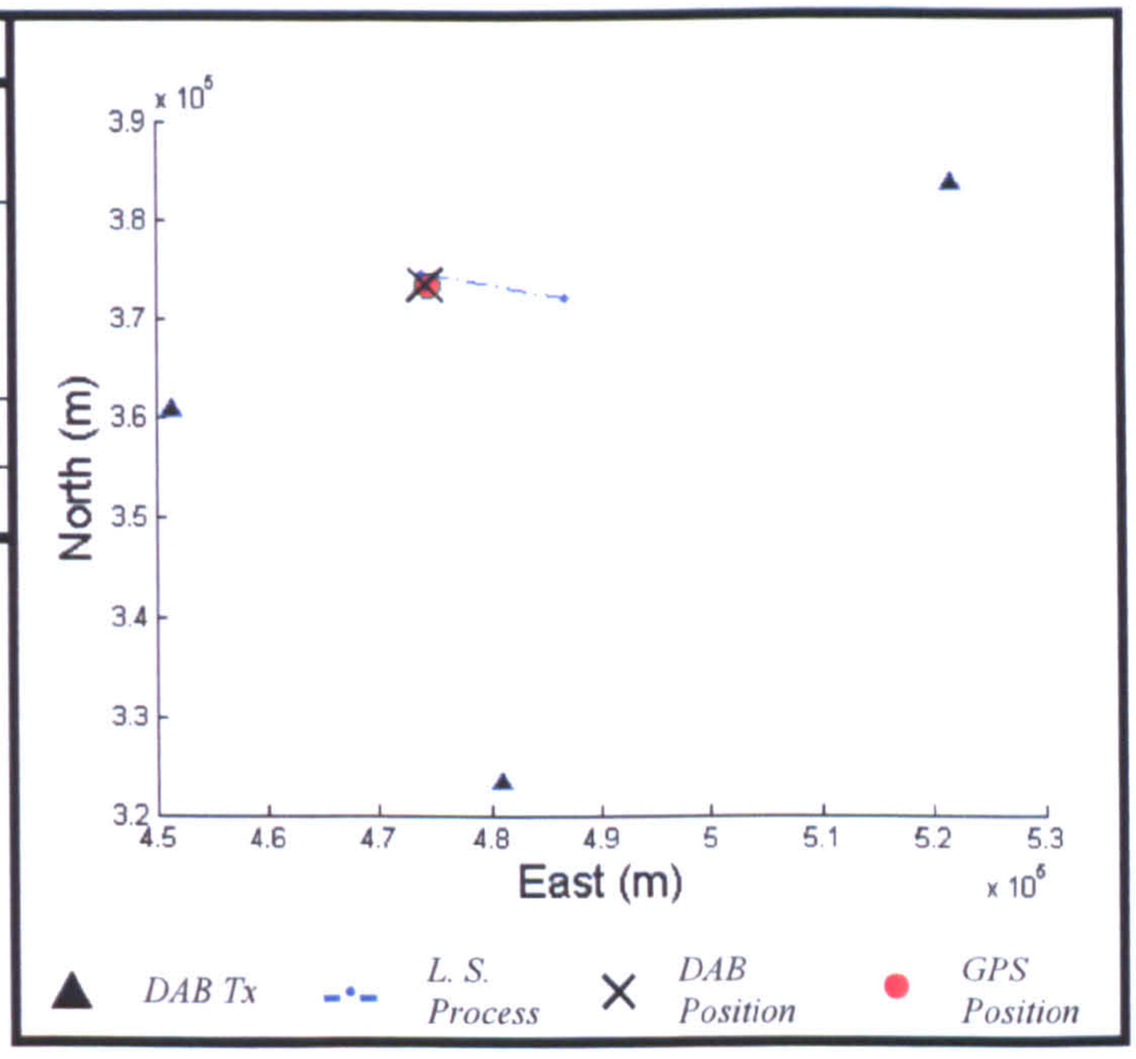

5	DAB Block						
	11B	11C	11D	12A	12B	12C	12D
TII (Region/Tx)		58 5 58 3	65 10 58 2		65 10 58 2 58 5	65 10 65 16	
TDOA (T)		96	47		46 20	115	

Positioning Results		
	East (m)	North (m)
GPS	482652	374236
DAB	482460	373971
Offset	192	265
HDOP	0.9504	
Height	8m	

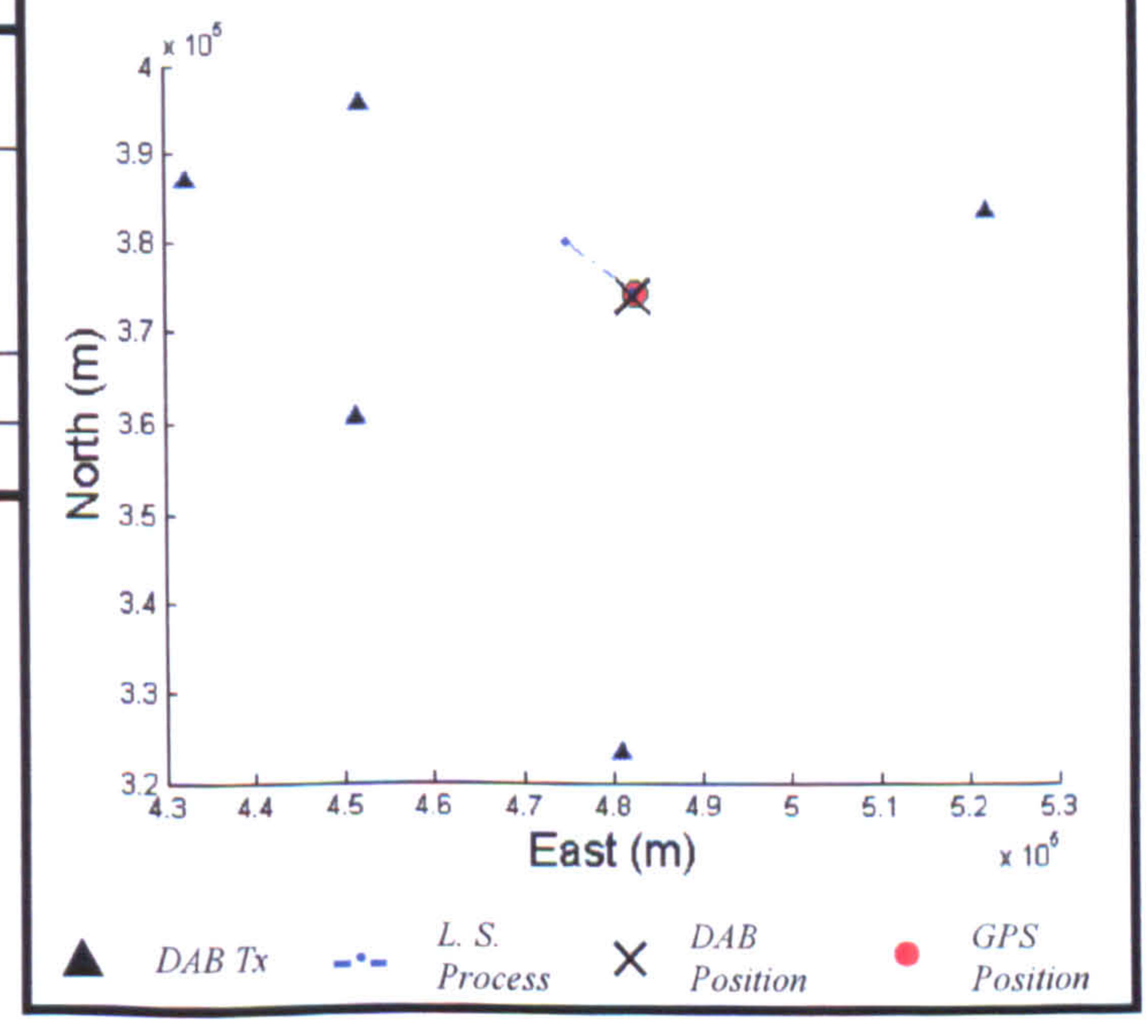

6	DAB Block						
	11B	11C	11D	12A	12B	12C	12D
TII (Region/Tx)			65 10 65 16			65 10 65 16 65 8	
TDOA (T)			49			46 17	

Positioning Results		
	East (m)	North (m)
GPS	494572	373168
DAB	493388	372260
Offset	1184	908
HDOP	7.9803	
Height	6m	

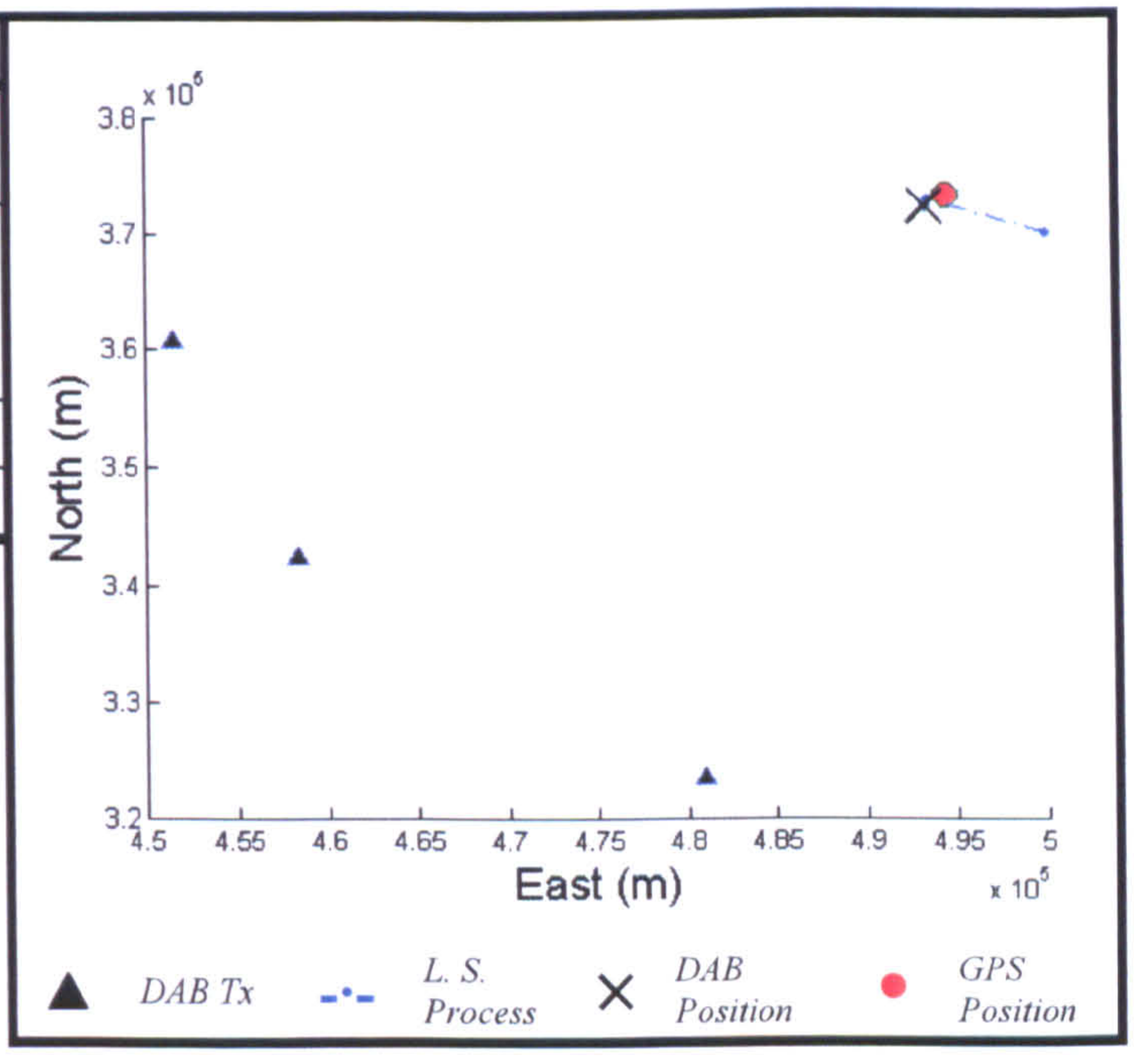

7	DAB Block						
	11B	11C	11D	12A	12B	12C	12D
TII (Region/Tx)			65 16 58 2 65 8		65 16 58 2 65 8	65 16 65 8	
TDOA (T)			57 22		57 23	18	

Positioning Results		
	East (m)	North (m)
GPS	491994	365318
DAB	496036	366416
Offset	4042	1098
HDOP	0.9572	
Height	13m	

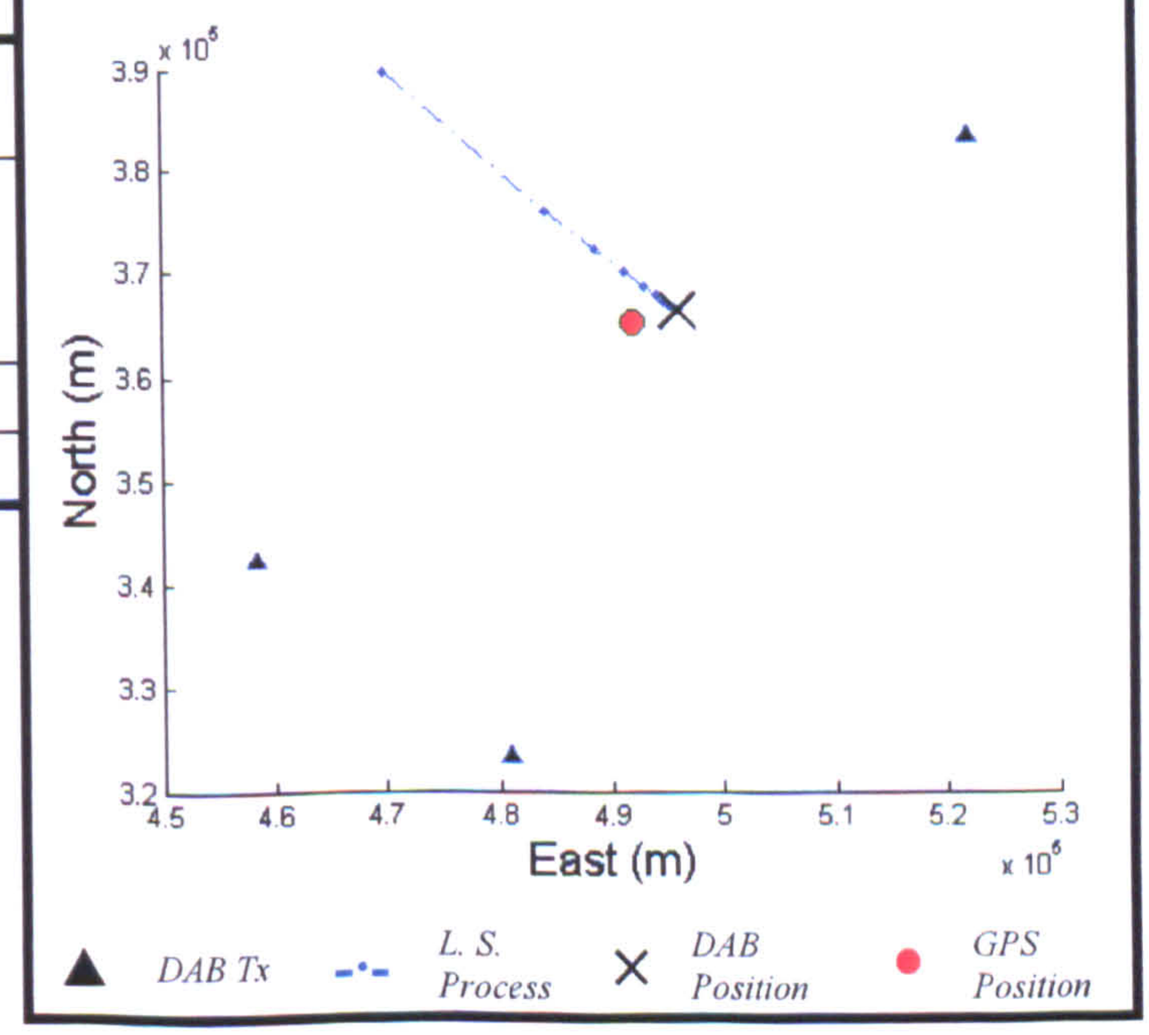

8	DAB Block						
	11B	*11C*	*11D*	*12A*	*12B*	*12C*	*12D*
TII (Region/Tx)			65 10 58 2 65 16	58 2 58 5 58 8		65 10 65 16	
TDOA (T)			41 17	54 205		21	

Positioning Results		
	East (m)	*North (m)*
GPS	487099	361575
DAB	486931	361574
Offset	168	1
HDOP	0.6363	
Height	27m	

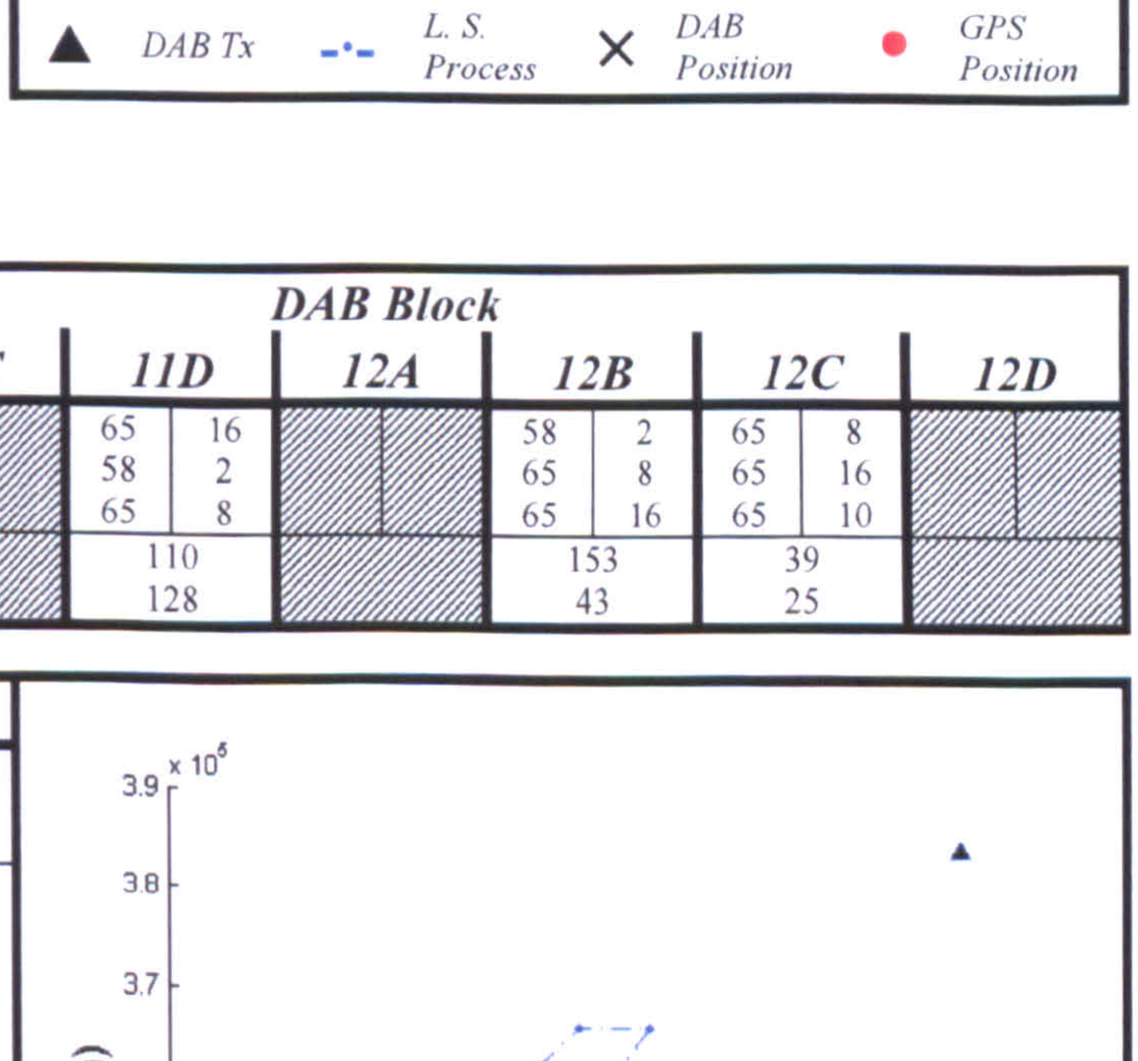

9	DAB Block						
	11B	*11C*	*11D*	*12A*	*12B*	*12C*	*12D*
TII (Region/Tx)			65 16 58 2 65 8		58 2 65 8 65 16	65 8 65 16 65 10	
TDOA (T)			110 128		153 43	39 25	

Positioning Results		
	East (m)	*North (m)*
GPS	481670	356051
DAB	481989	356297
Offset	319	246
HDOP	0.6961	
Height	19m	

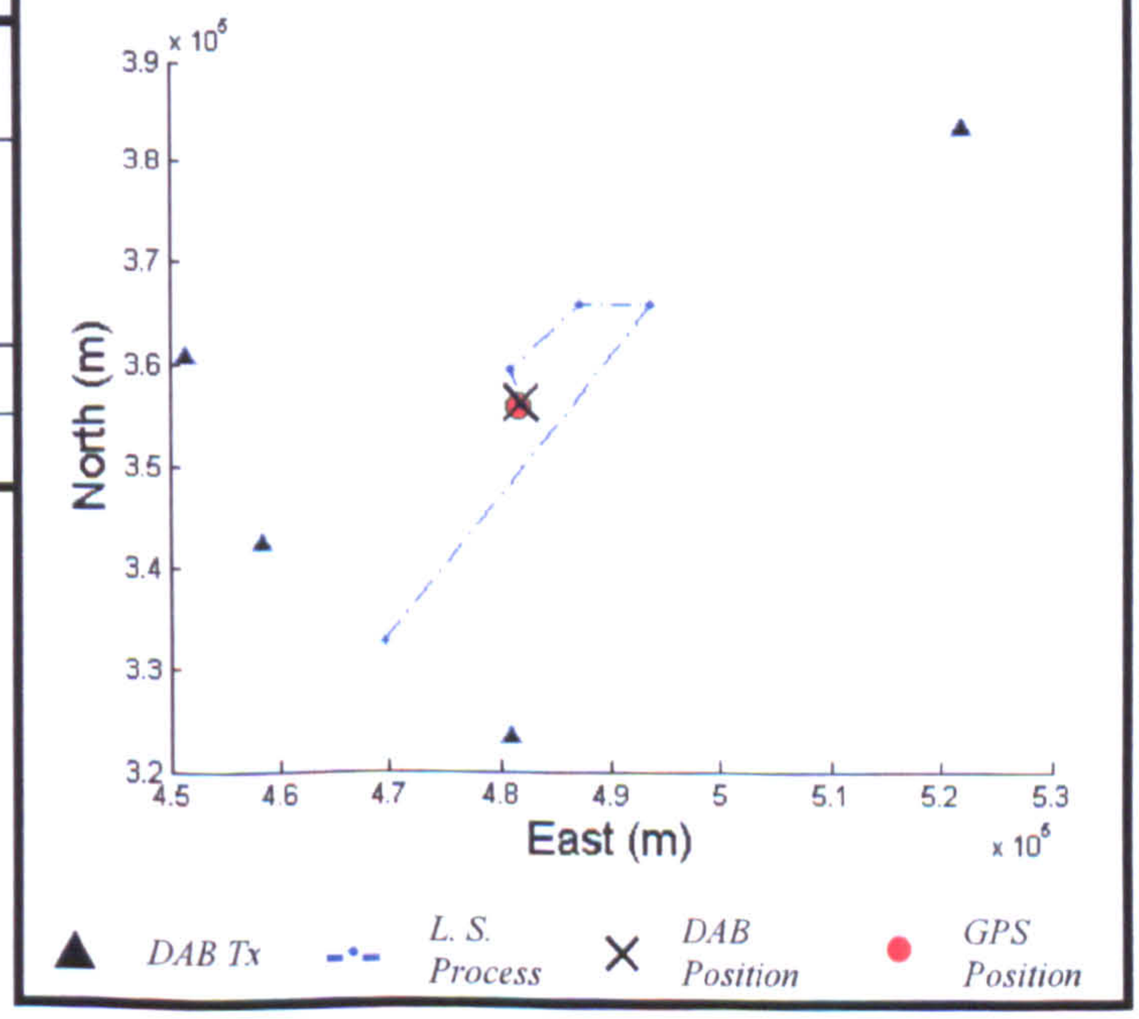

10	***DAB Block***						
	11B	***11C***	***11D***	***12A***	***12B***	***12C***	***12D***
TII (Region/Tx)			65 16 65 8 65 10		65 16 65 8 65 10	65 16 65 8 65 10	
TDOA (T)			65 12		66 12	62 15	

Positioning Results		
	East (m)	***North (m)***
GPS	472784	345646
DAB	472463	345686
Offset	321	40
HDOP	1.1897	
Height	40m	

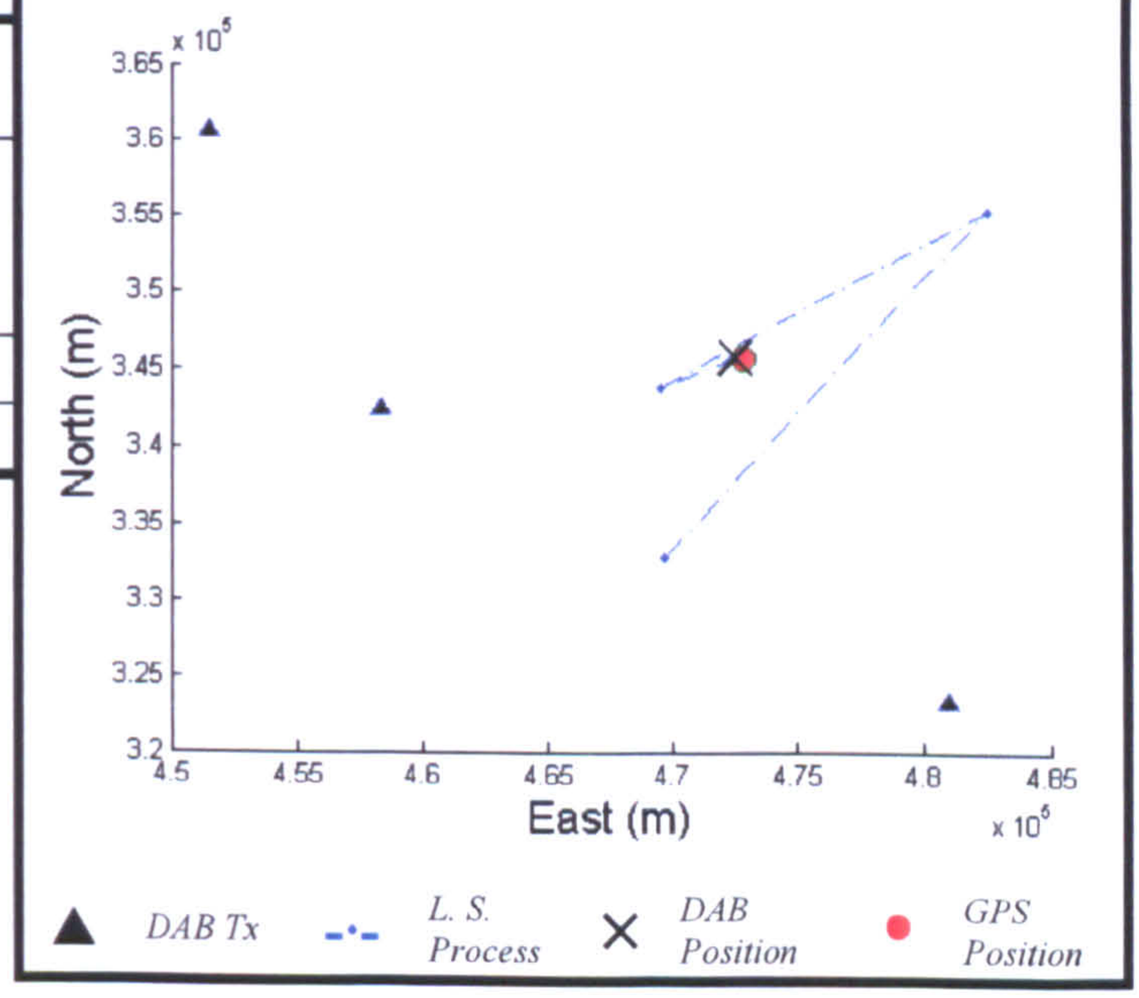

11	***DAB Block***						
	11B	***11C***	***11D***	***12A***	***12B***	***12C***	***12D***
TII (Region/Tx)					65 16 58 2 65 8	65 16 65 8	
TDOA (T)					323 69	66	

Positioning Results		
	East (m)	***North (m)***
GPS	469321	340495
DAB	469140	340519
Offset	181	24
HDOP	0.8587	
Height	27m	

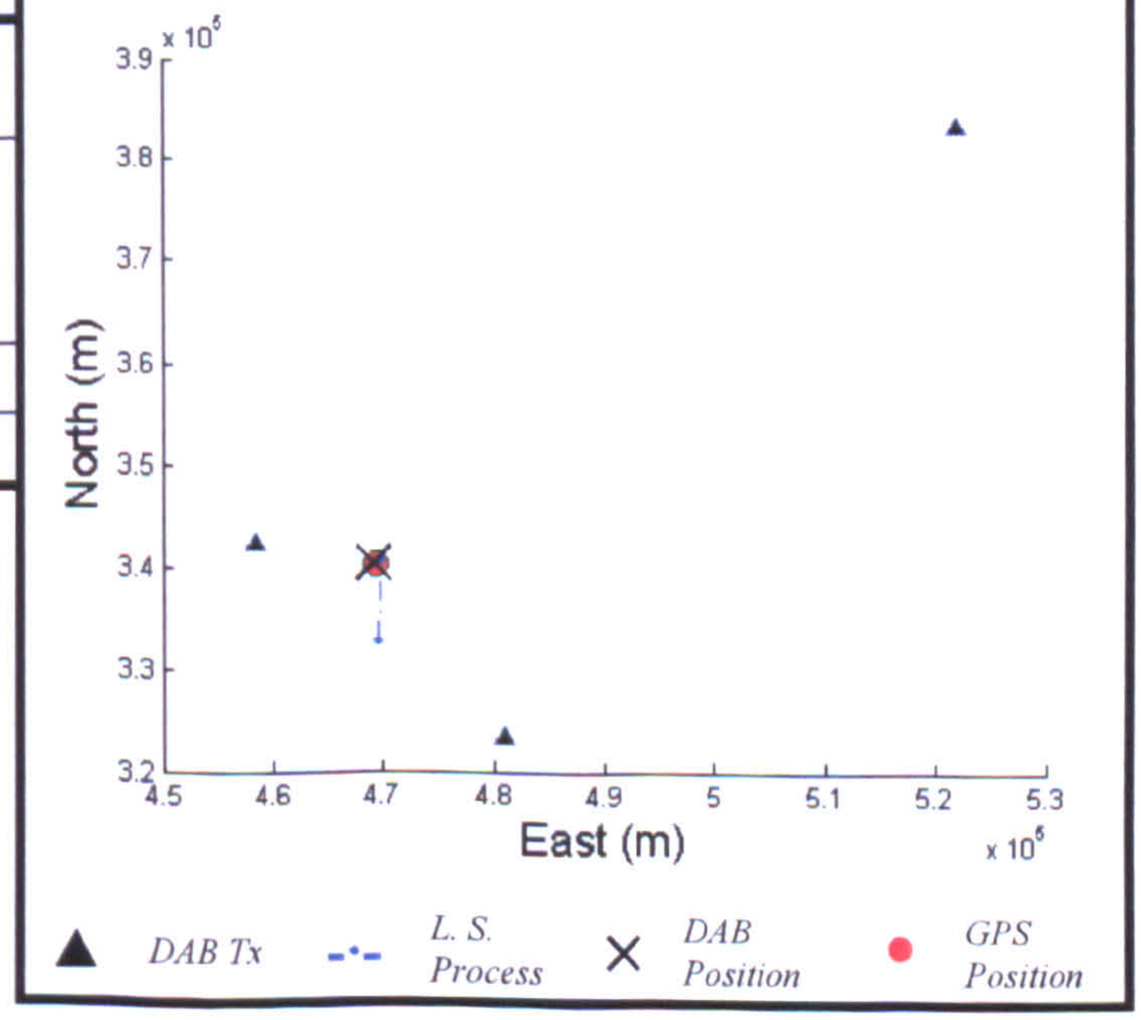

12	DAB Block						
	11B	11C	11D	12A	12B	12C	12D
TII (Region/Tx)			65 8 65 16 18 2		65 8 65 16	65 8 65 16	
TDOA (T)			128 481		129	126	

Positioning Results		
	East (m)	North (m)
GPS	461707	337831
DAB	461678	338023
Offset	29	192
HDOP	1.3128	
Height	25m	

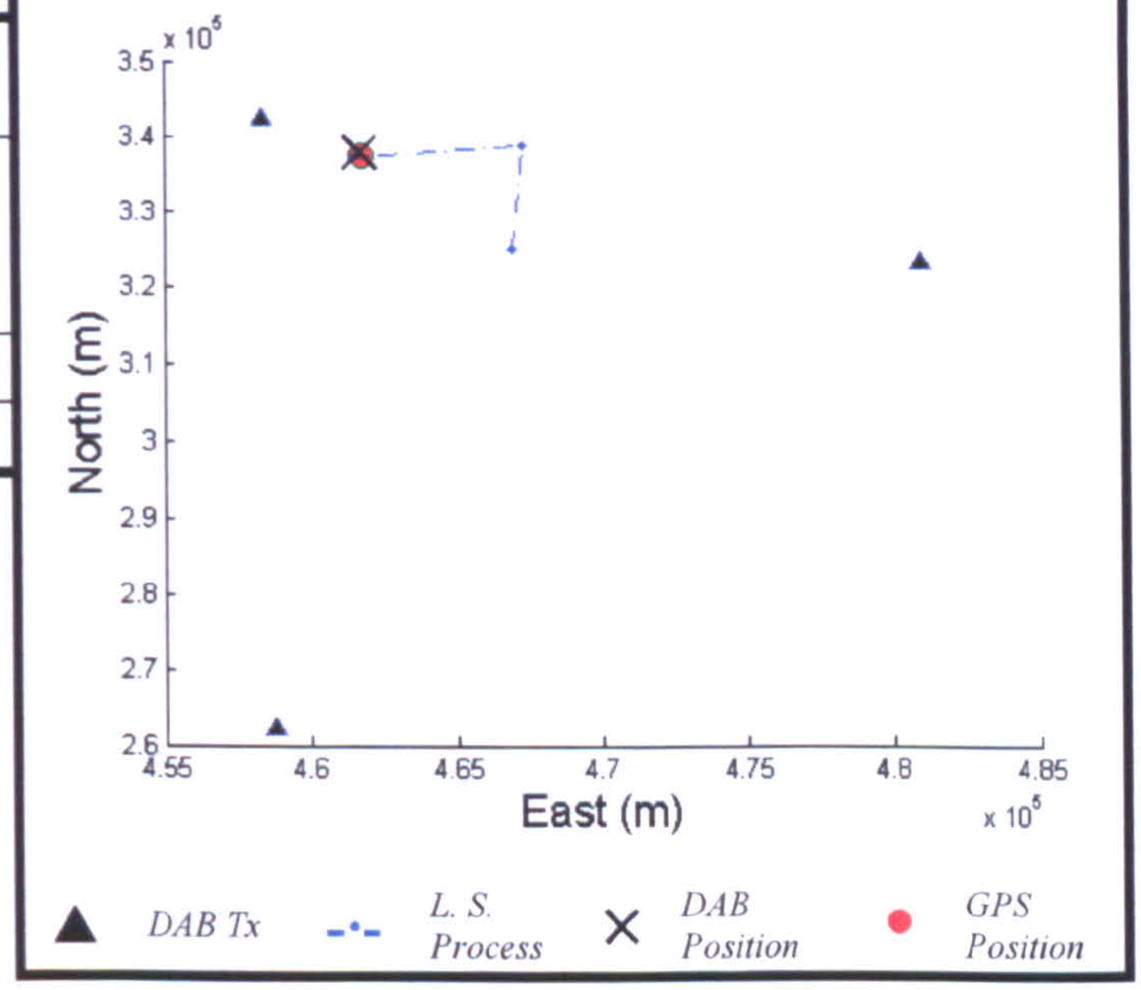

8.10.3 Discussion

As mentioned in the introduction to this section, this final static positioning test was undertaken to examine the positioning performance of the DAB system in regions where there are fewer transmitters present. It was expected that there would be captures taken where insufficient information would be extracted in order to establish a fix, however, this was the only static test where every capture yielded a result.

This region had an elevation generally lower than that of other tests which could have provided poor transmitter view. However, due to the relatively flat nature of the topography in the region, this did not prove to be problematic.

A number of the results do show very poor positional errors, which will be examined in turn. Evidently the capture with the greatest error was taken at location 3 where an offset of over 10km was calculated.

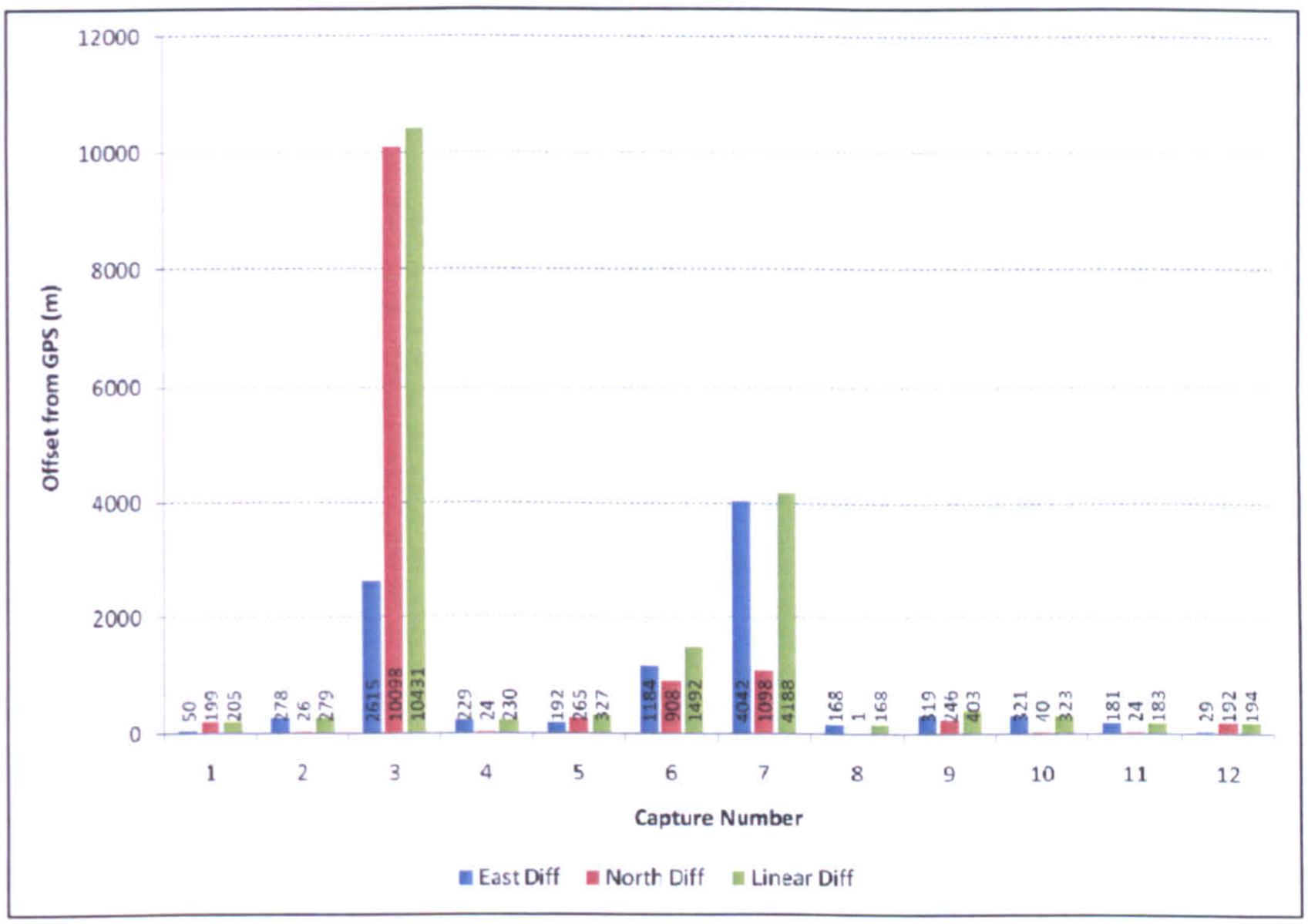

Figure 8-38: Offset from GPS (m) at each capture

Chart divided to show difference in East, North and Linear offsets

Position 7 shows an error of over 4km, again in reality an un-usable result. Examining the individual result more closely it can be seen that while it is using three transmitters and has calculated four TDOA measurements (two of which are unique), the three TDOA measurements using the same transmitters all have different values. It would be expected that measured values may lie up to ±2T of the true value due to the intersecting points on the T-grid, however in this case the TDOA from block 12C is 4-5T adrift of the same measurements on blocks 11D and 12B. As the DAB receiver has no knowledge of which measurement to use in a real-life situation, all three must be used in the least squares process. This creates the ambiguity that is seen in this result.

Position 6 is the last of the position estimates to have a linear error over 1km. This is caused by a similar issue seen in position 7 but on a smaller magnitude. TDOA measurements on blocks 11D and 12C show an ambiguity of 3T which causes the inaccuracy in range in this case.

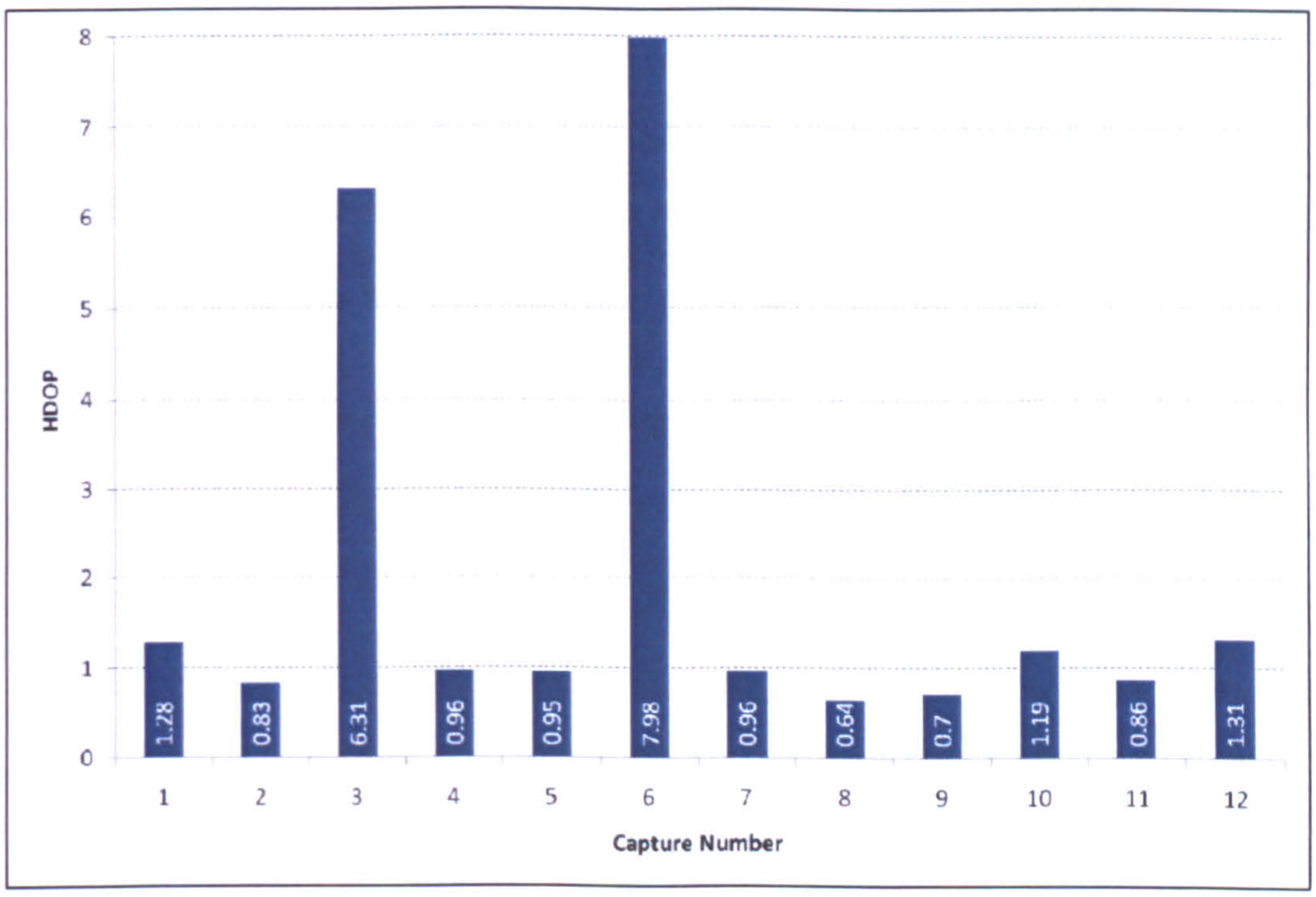

Figure 8-39: HDOP values for DAB position at each capture location

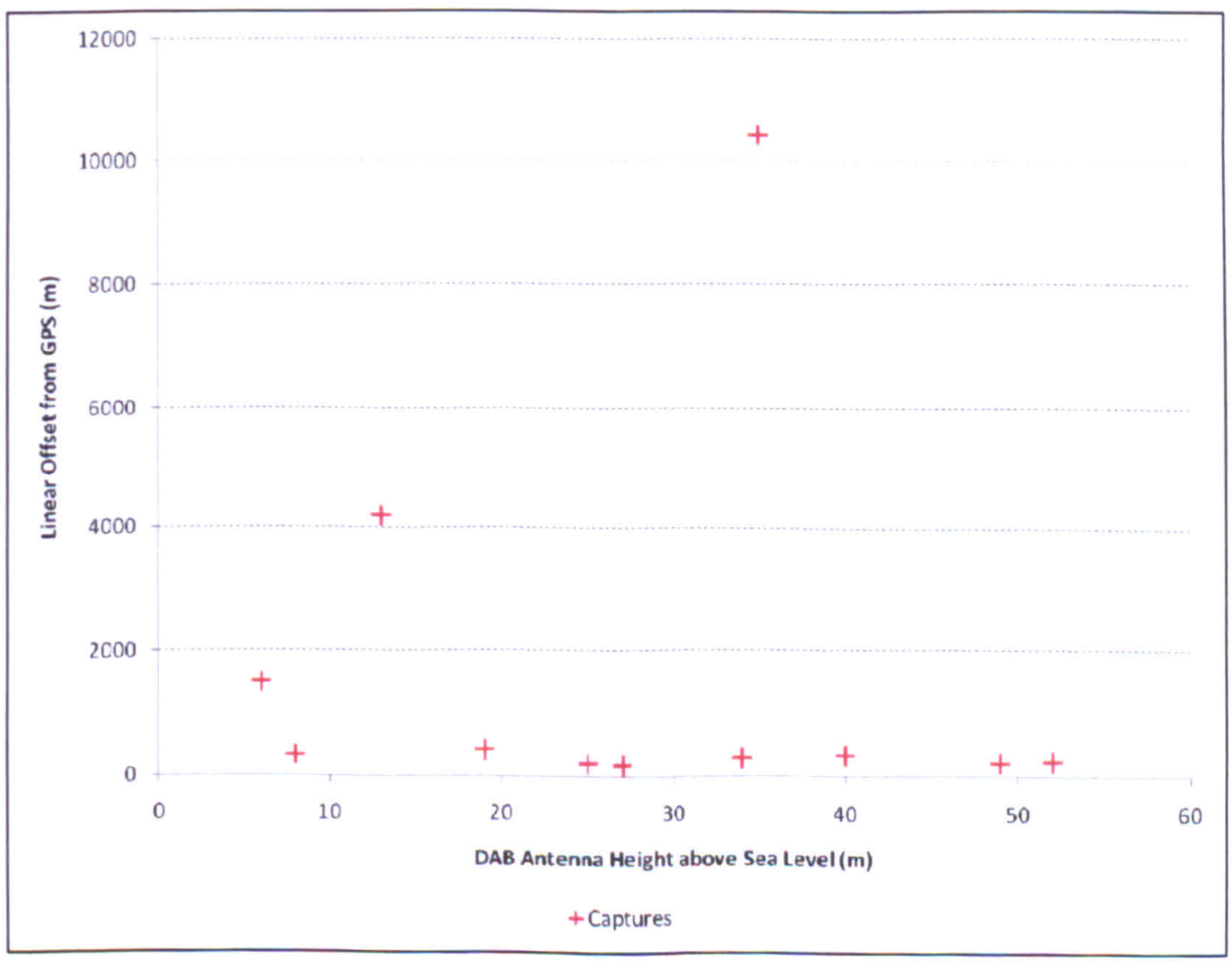

Figure 8-40: Chart showing capture elevation against linear offset

With the exception of these results with large offsets, the DAB positioning system appears to have made standalone results with a mean value of ≈ 250 metres. Depending on the transmitters available to each capture, this is the sort of accuracy that would be expected when taking the "T-grid" into consideration.

Finally, examining the overall capture height vs. linear offset in Figure 8-40, it can be seen once again that the trend-line of the data plotted shows that the more accurate results are captured at lower elevation overall. The three anomalous results represent captures 6, 7 and 3 respectively (left to right), though it has been explained how these results occurred.

8.11 DYNAMIC TESTING

8.11.1 Introduction

The purpose of this test was to examine the effect on the positioning system if the hardware is moving. One important difference in the processing of this data is that the result cannot be averaged over a number of frames as can be done when performing static testing.

This immediately puts the testing process at a disadvantage as the TDOA must be processed every frame (10Hz) and the TII every other frame (5Hz). Therefore for the purpose of this test, the approach was taken to firstly identify a frame containing TII information and then process every second frame from that point onwards.

The process performed previously was run in order to show the shift in correlation spikes over distance. Firstly, the transmitters received must be identified using the TII information. A plot of this information over 500 DAB frames (~50 seconds) can be seen in Figure 8-41.

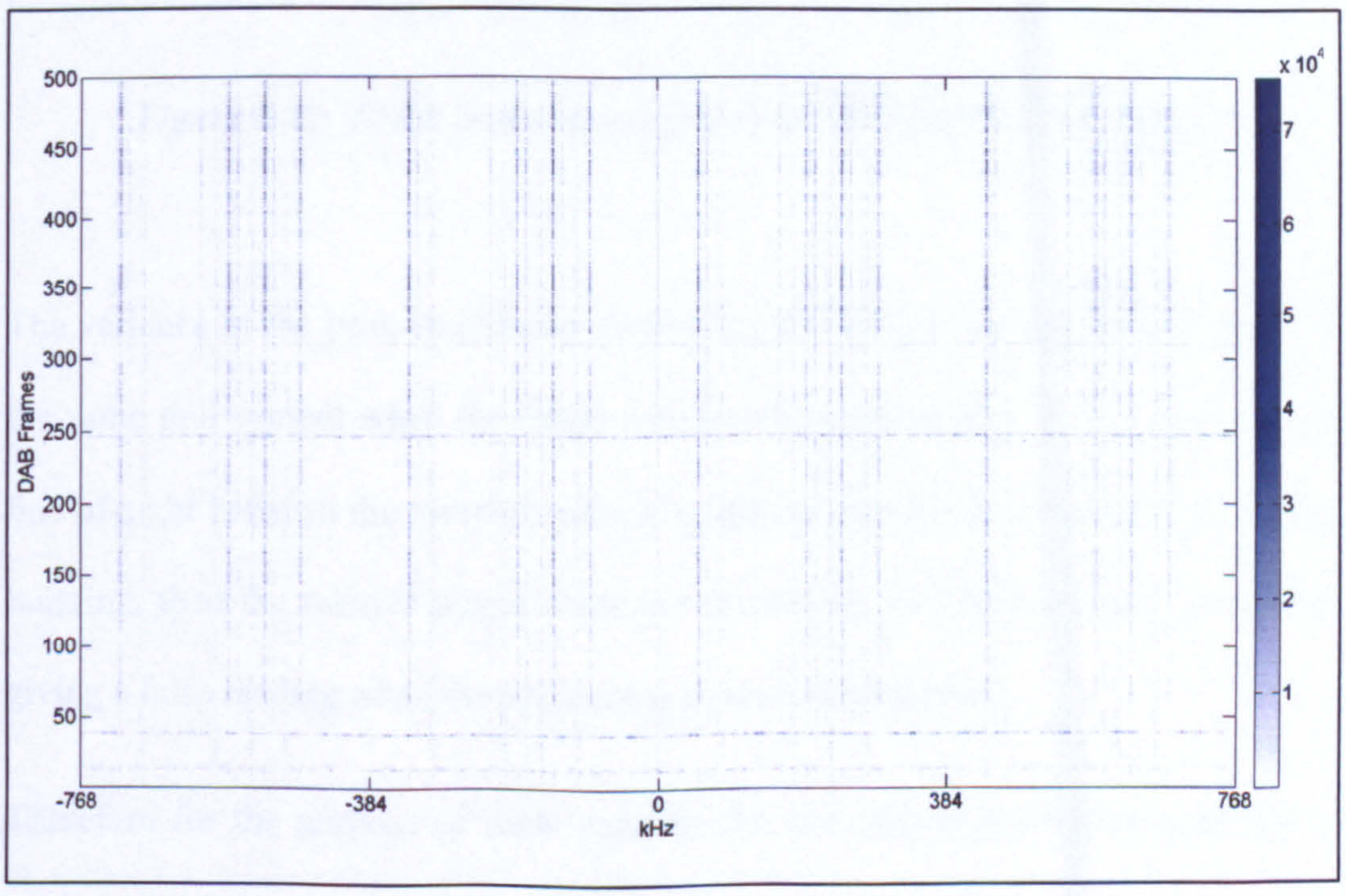

Figure 8-41: TII symbol over 500 dynamic DAB frames

As would be expected over this time period, the transmitters received are going to change minimally, if at all. Therefore it can be seen that the codes remained largely unchanged. By plotting the cross-correlation of each TFPR symbol over this same period (see Figure 8-42), a definite change in the TDOA values relative to the primary signal can be seen (situated in this instance at around 2050T). A number of peaks of varying amplitudes can be clearly seen separating or converging.

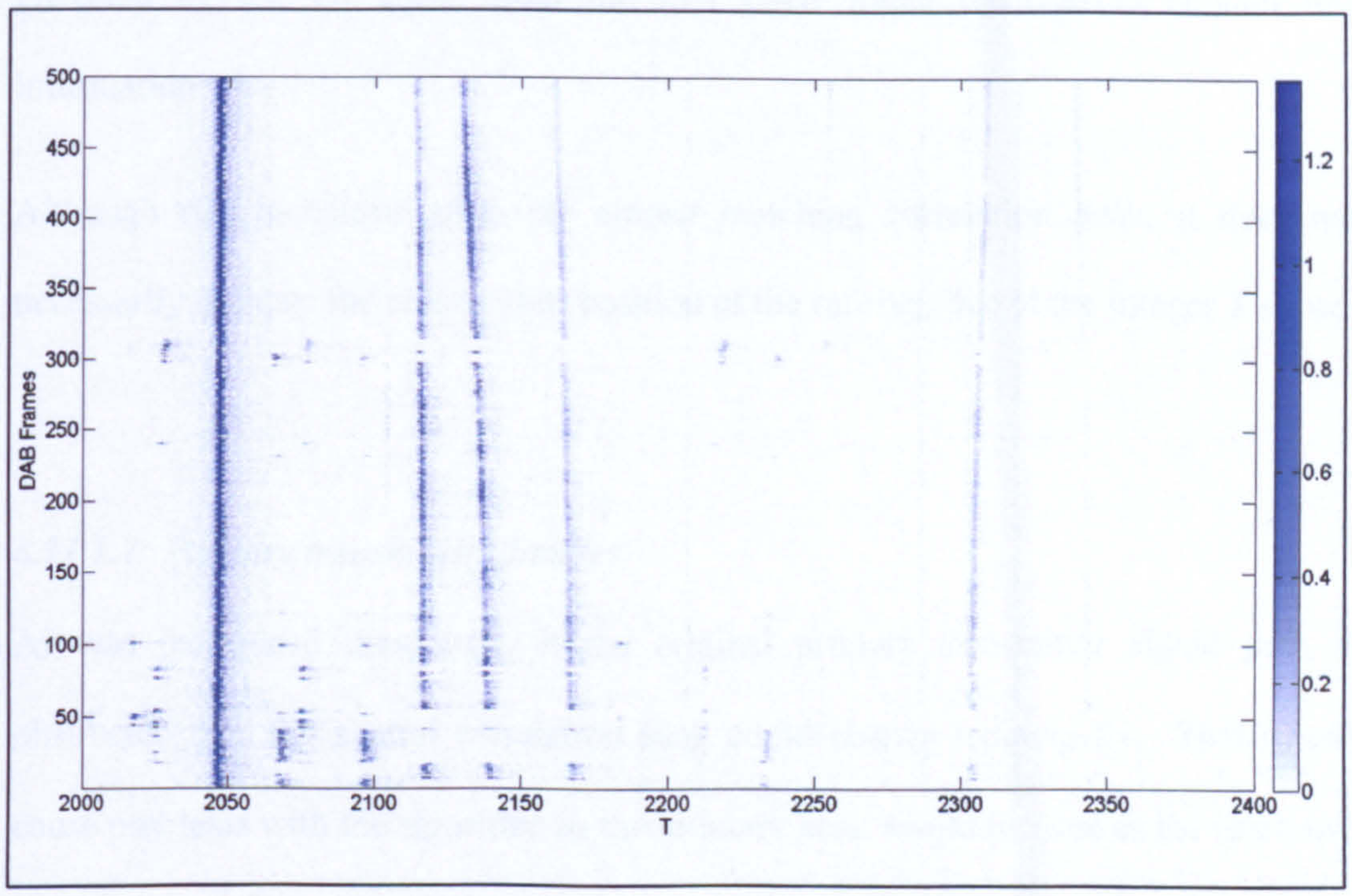

Figure 8-42: TFPR cross-correlation over 500 dynamic DAB frames

The variance of the peak amplitudes means that the system will not always "lock" to the same null symbol when the initial null search is undertaken. If for example, the line-of-sight between the receiver and transmitter is temporarily obstructed by a large building, then the relative power from this transmitter is seen to reduce, potentially giving a false reading when the positioning process is performed.

Therefore for the purpose of these experiments, the following alterations had to be made to the post-processing algorithms.

8.11.1.1 Initial position known

As the vehicle does not begin from a stationary position, this provides an environment where the received signal cannot be averaged over time, as was done for the static positioning. Therefore for the purposes of this test, it is assumed that the vehicle initial start position is known (from GPS in this case), allowing the correlation peaks to be matched by searching around the expected regions on the cross-correlation plot, provided by the TII codes from the first DAB frame received to contain this information.

Although this technique gives the closest matching correlation peak, it does not necessarily indicate the precise start position of the receiver due to the integer T value.

8.11.1.2 Primary transmitter changes

As was mentioned previously, if the original primary transmitter signal path is obstructed then the central correlation peak could change temporarily. This would cause problems with the algorithm as this primary peak would be used as the reference point to measure the TDOA values from. Therefore, this problem can be overcome by monitoring the null position within the total DAB frame found in the early processing. If a receiver is static, this position should not change by more than 1T (which only occurs due to the under-sampling of the original signal). If a receiver is moving, then the position of the null will change over distance depending on the direction of travel and the geometry of the transmitters received.

As the system is limited to measuring the time differences in integer values of T, the position is expected to change erratically, by shifting between the grid points as each measurement is taken.

8.11.2 Results

The results presented over the following pages show the GPS tracking of each dynamic run in addition to the calculated DAB positions. Each chart indicates the start and finish points for both positioning systems, and also includes a plot of the varying HDOP values for each DAB epoch.

8.11.2.1 Dynamic Test 1

This test was performed in the West Midlands region, using DAB signals broadcasting on Block 11D (national commercial), allowing the use of multiple regional transmitters if detectable. The transmitters decoded within the first TII symbol detected show that three transmitters were available at this position. These are listed in the table below.

Transmitter Name	*Region Code*	*Transmitter Code*	*East (metres)*	*North (metres)*
Sutton Coldfield	24	18	411350	300326
Daventry	18	02	458750	262150
Turner's Hill	24	15	396950	288750

Three transmitters provide sufficient information for a two-dimensional position using standalone DAB, the results of which can be seen in Figure 8-43. It can clearly be seen in these results that the DAB positions map to the "***T*** grid" structure mentioned previously. As the road used in this test did not lie along one of the TDOA hyperbolae (which will be the majority of cases), the DAB positions jump from either side of the vehicle path, as would be expected. The quality of the measurements in this instance (with the exception of the DAB start position) show that the closest hyperbolic intersect was found and used to establish each position.

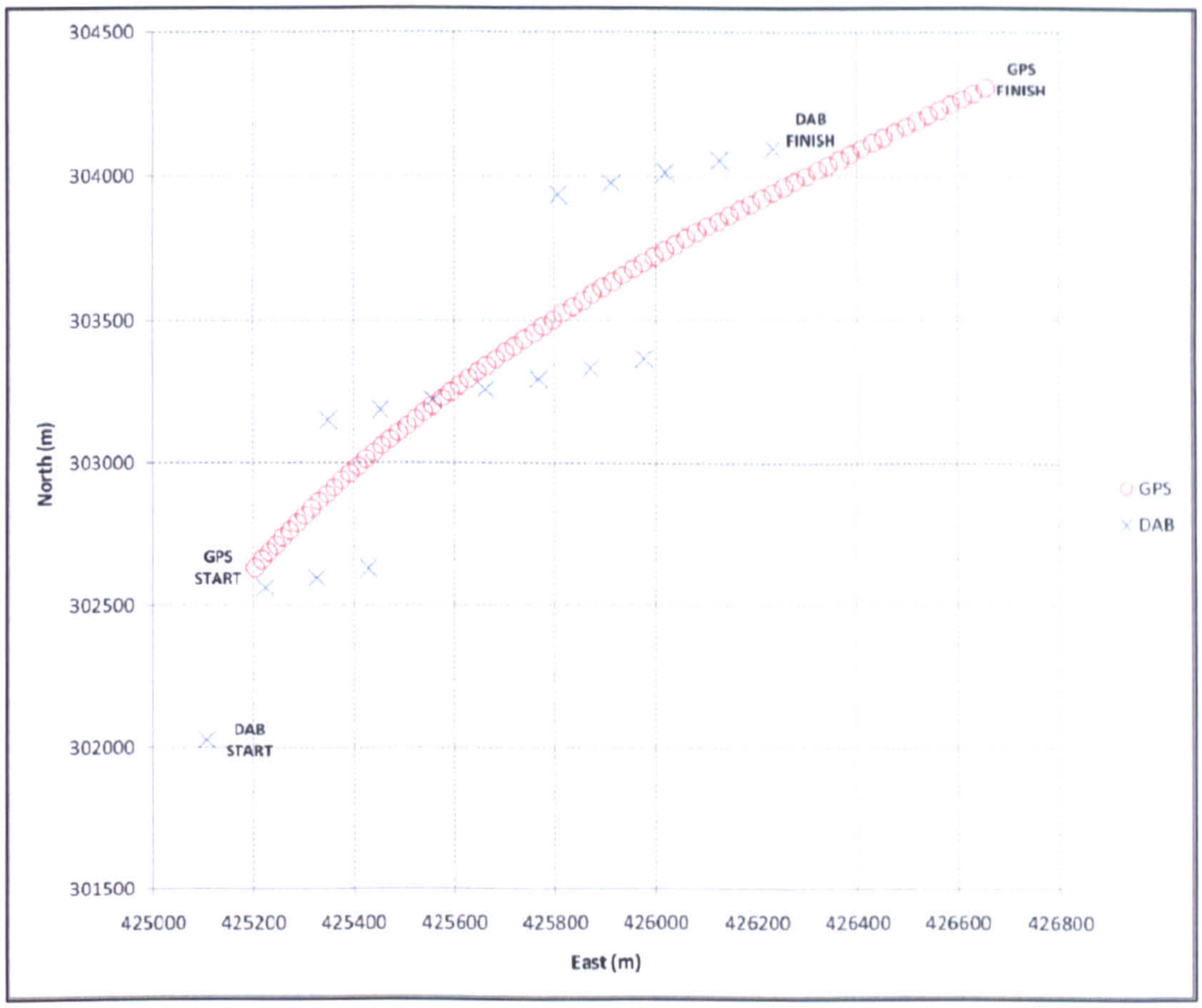

Figure 8-43: Dynamic Test 1 – GPS vs. DAB

The quality of the position measurements are shown as a series of HDOP measurements in Figure 8-44. These fluctuate between certain key values, which coincide with the limited number of DAB positions shown in the positional plot in Figure 8-43. It is at these points where the result "jumps" between values, giving a change in position of around 150 metres, as opposed to the true change which would be one or two metres.

The HDOP values shown are considerably higher than would be expected when viewing the accuracy of the positioning results, meaning that the geometry of the transmitters used was far from ideal in this scenario.

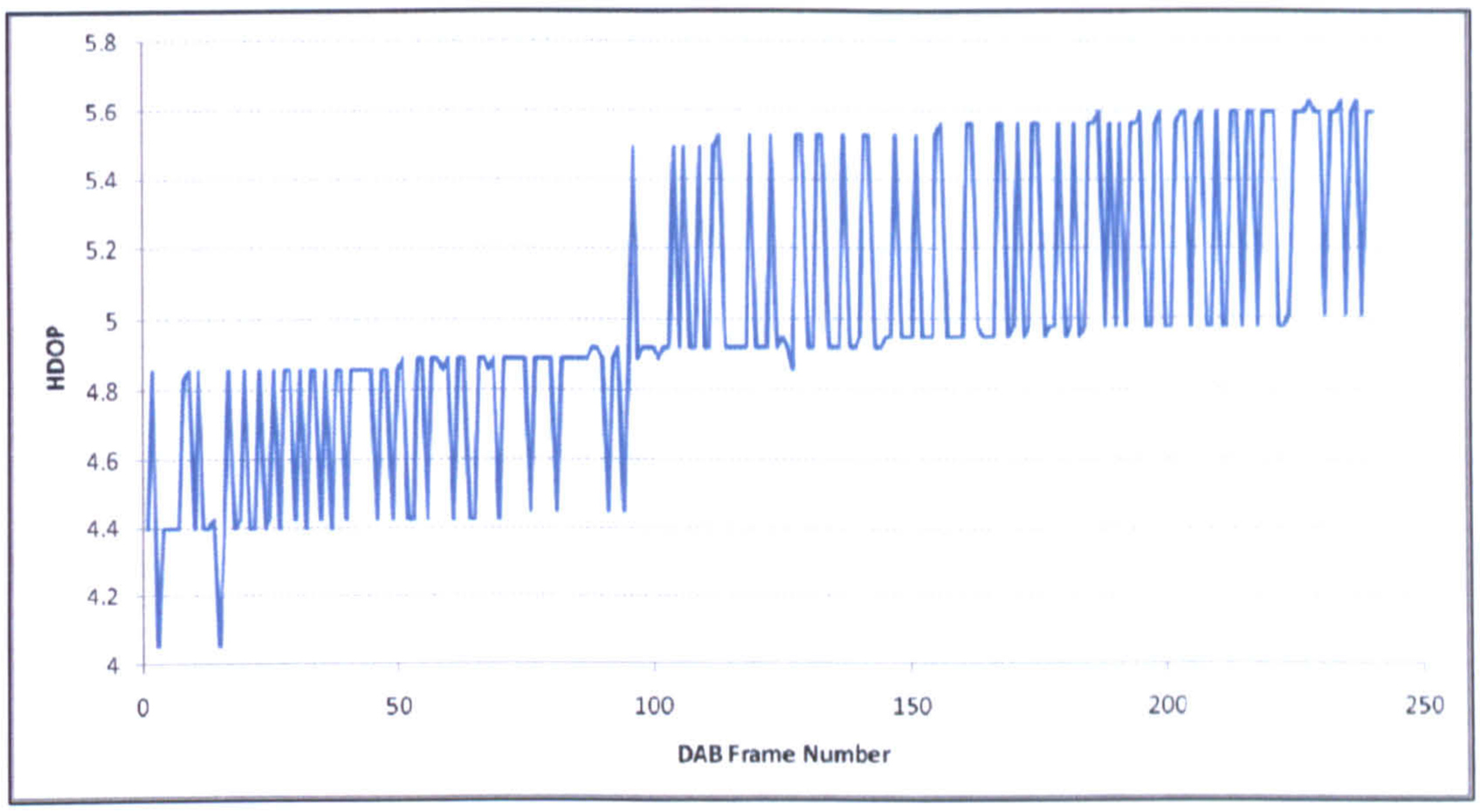

Figure 8-44: Dynamic Test 1 – DAB HDOP values

8.11.2.2 Dynamic test 2

The second dynamic test was performed in the central midlands region using the commercial national DAB block 11D. The initial analysis of the first available TII symbol allowed the software to decode the following five transmitters within range of the vehicle (see table below).

Transmitter Name	*Region Code*	*Transmitter Code*	*East (metres)*	*North (metres)*
Sutton Coldfield	24	18	393350	367650
Waltham	65	16	480950	323350
Mapperley Ridge	65	08	458350	342450
Copt Oak	65	17	448350	312650
Mansfield (Fishpond Hill)	65	10	451450	360650

Five transmitters is more than adequate for a two-dimensional positional fix giving four TDOA measurements to use in the least squares process. It would be expected therefore that precise tracking would be possible for the duration of this trial, however, the positioning plot shown in Figure 8-45 indicates extremely poor DAB signal tracking. It can be seen that the GPS matched initial start position is over a kilometre

away from the true start position in this case, which is where the problems are caused (the start location also has the highest HDOP as can be seen in Figure 8-46, however, as it is less than 1 the confidence in this measurement is high). This means that the peak searching algorithm cannot find the expected correlation peaks for the transmitters in the area.

As the algorithms are searching at each epoch for the correlation peaks, it appears that strong multipath has affected the smaller, and thus more difficult to track signals. This causes the closely clustered measurements near the start of the DAB capture. Towards the middle of the trial, the DAB position is realigned with the true position (indicated by the dip in HDOP values and circled in Figure 8-45); although again as with the beginning the strong multipath makes the signals harder to track causing larger fluctuations in position.

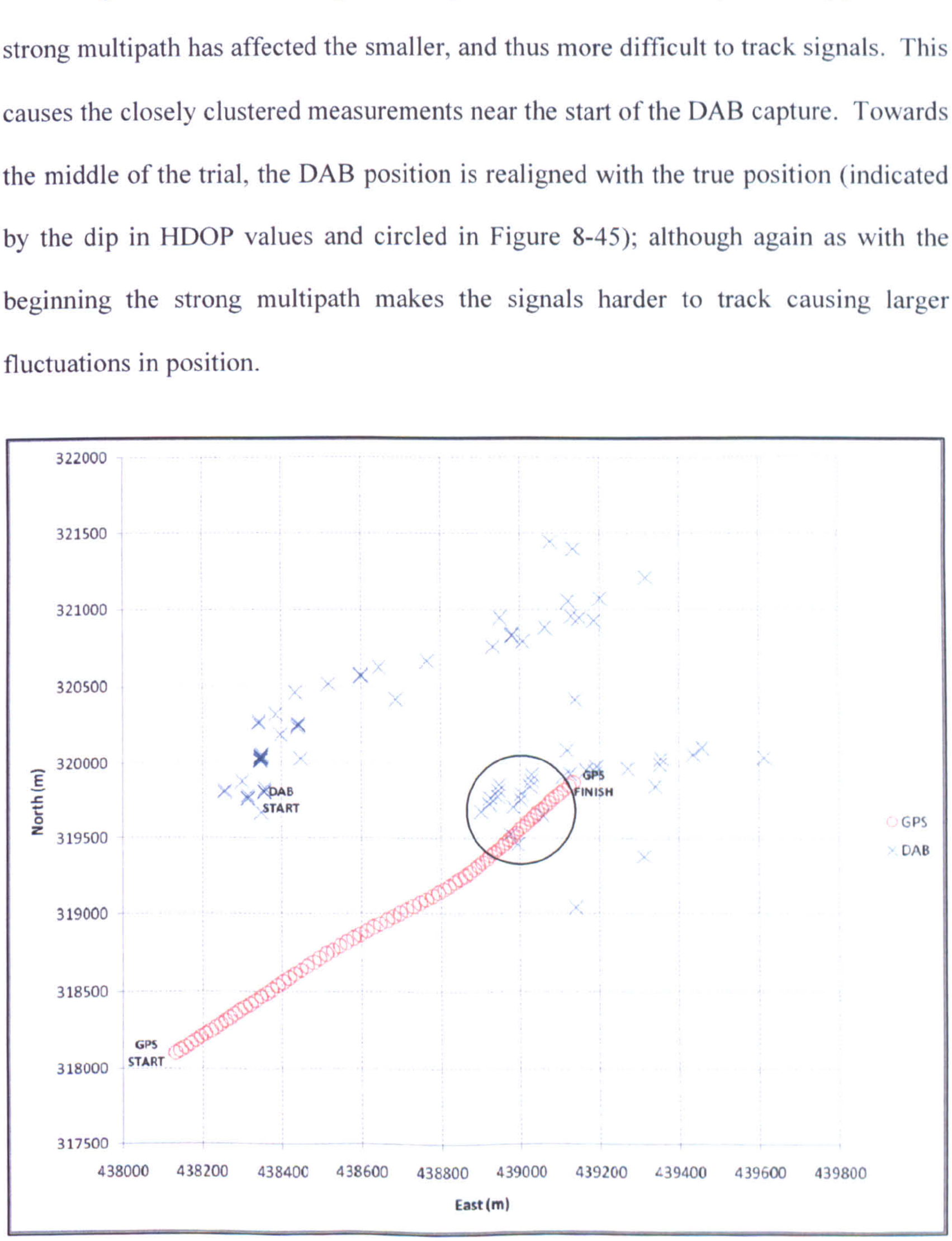

Figure 8-45: Dynamic Test 2 – GPS vs. DAB

This trial run can be evaluated further by viewing the position of the tracked null symbol throughout the capture. It can be seen in Figure 8-47 that the position of the detected null symbol shifts significantly during the same frame where the HDOP value increases. This is due to the algorithm used to find the null symbol tracking a different primary signal to that used at the beginning of the capture. This can be caused by the vehicle moving through a location where the Fresnel zone between the initial primary transmitter and receiver is obstructed (partially or totally) by an object of high density, such as a hill or a large building.

At this point (frame 72 in this instance) the algorithm automatically locks on to the most powerful secondary signal (which then becomes the primary signal) and begins to track this instead, with all measurements being made relative to this signal. Naturally, when moving through an area where multiple such obstructions are present, the detected null symbol will 'jump' as the primary source changes. Such jumps are in addition to the gradual decline/incline of the tracked null depending on whether the vehicle is moving towards or away from the transmitter.

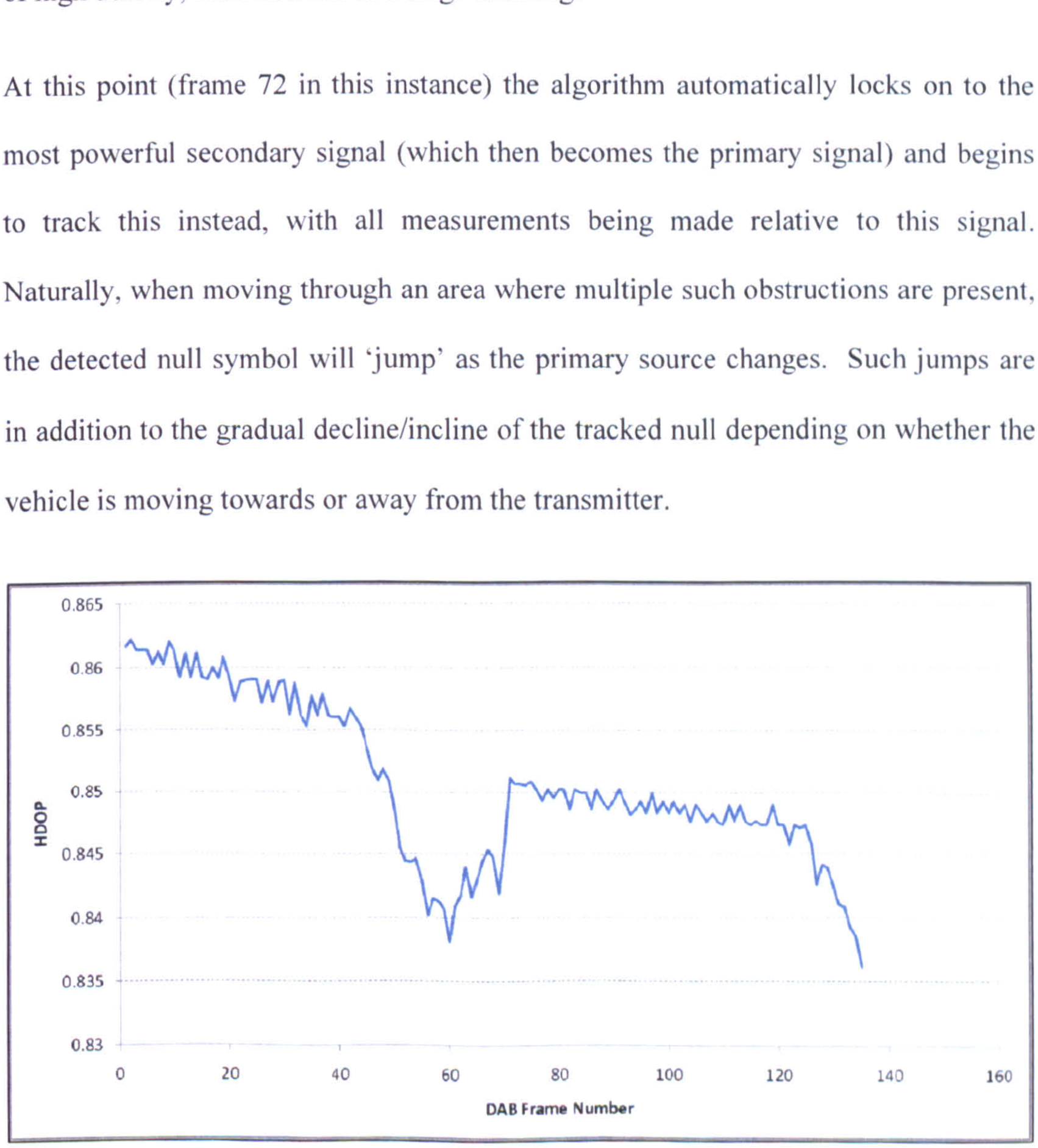

Figure 8-46: Dynamic Test 2 – DAB HDOP values

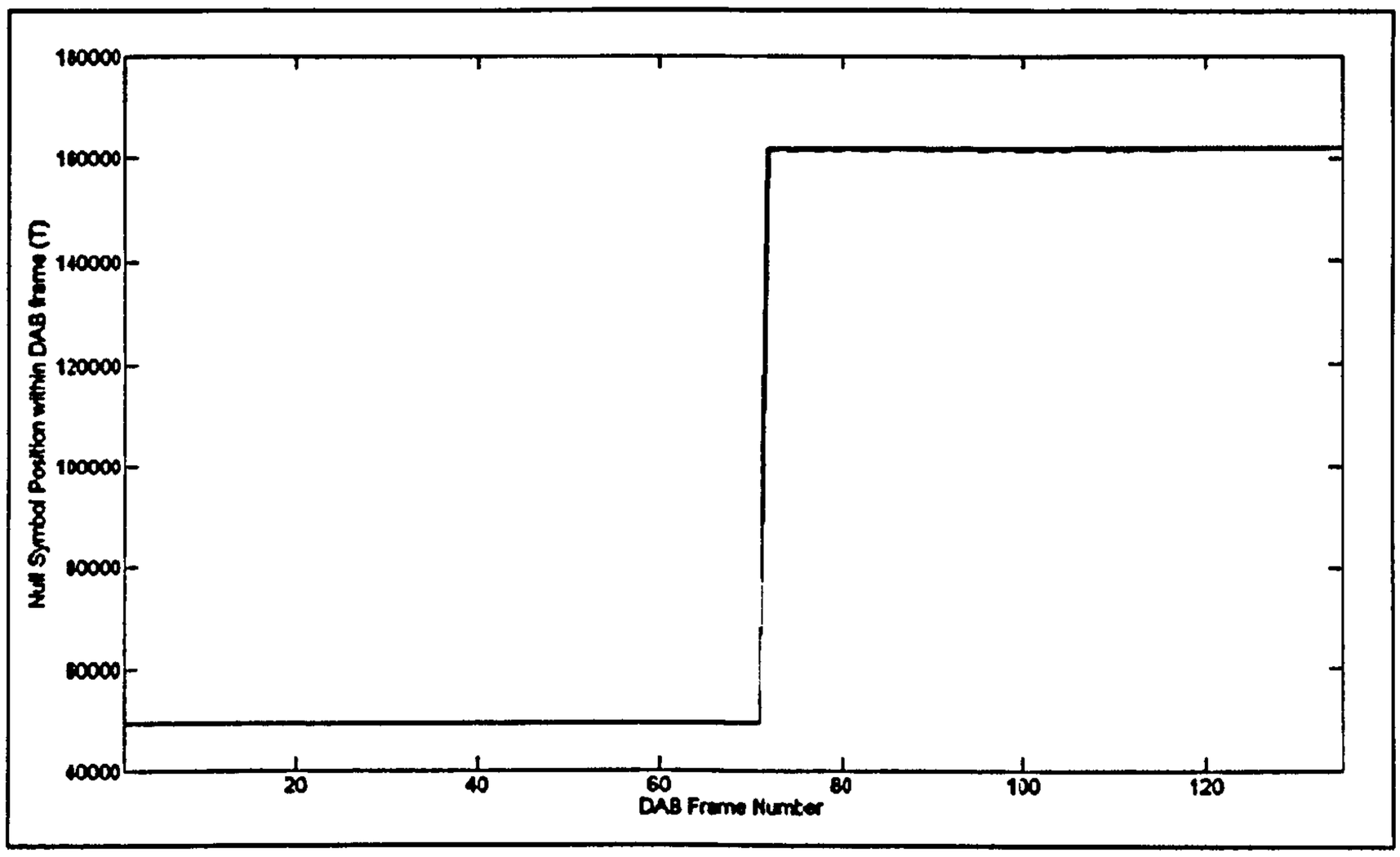

Figure 8-47: Dynamic Test 2 – Null symbol position shift

8.11.2.3 Dynamic Test 3

Dynamic test 3 was undertaken on the Nottinghamshire/Derbyshire border using the BBC national DAB block 12B. Four transmitters were initially available (see below) giving sufficient information for a position fix.

Transmitter Name	*Region Code*	*Transmitter Code*	*East (metres)*	*North (metres)*
Waltham	65	16	480950	323350
Mapperley Ridge	65	08	458350	342450
Sutton Coldfield	24	18	393350	367650
Daventry	18	02	458750	262150

These test results highlight the limitation in the dynamic tracking algorithm, as can be seen in Figure 8-48. The initial position calculated by the DAB signal is roughly 400 metres from the truth, this is acceptable as a start location, and each epoch for the first 500m are clustered around the same area meaning that the correct correlation peaks are being tracked. Beyond this point however, the weakest of the four signals is lost completely for several epochs, meaning that the tracking loop snaps to the closest peak

in its expected position. This means that false readings are now being fed into the least squares solution, which accounts for the perpendicular drift away from the true path. This result can also be seen in the HDOP plot (Figure 8-49) at the point where the values suddenly increase in magnitude between 70 and 80 frames.

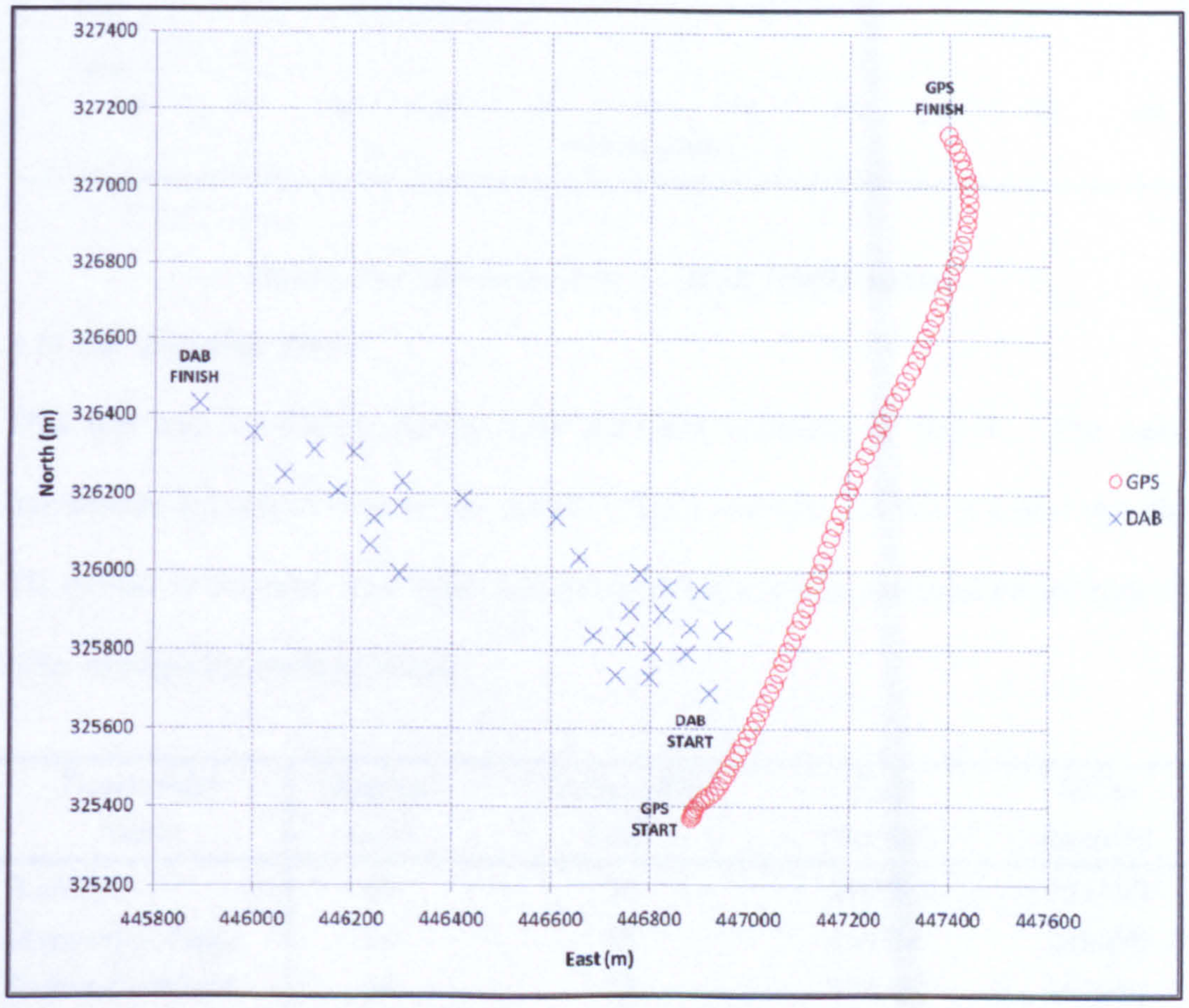

Figure 8-48: Dynamic Test 3 – GPS vs. DAB

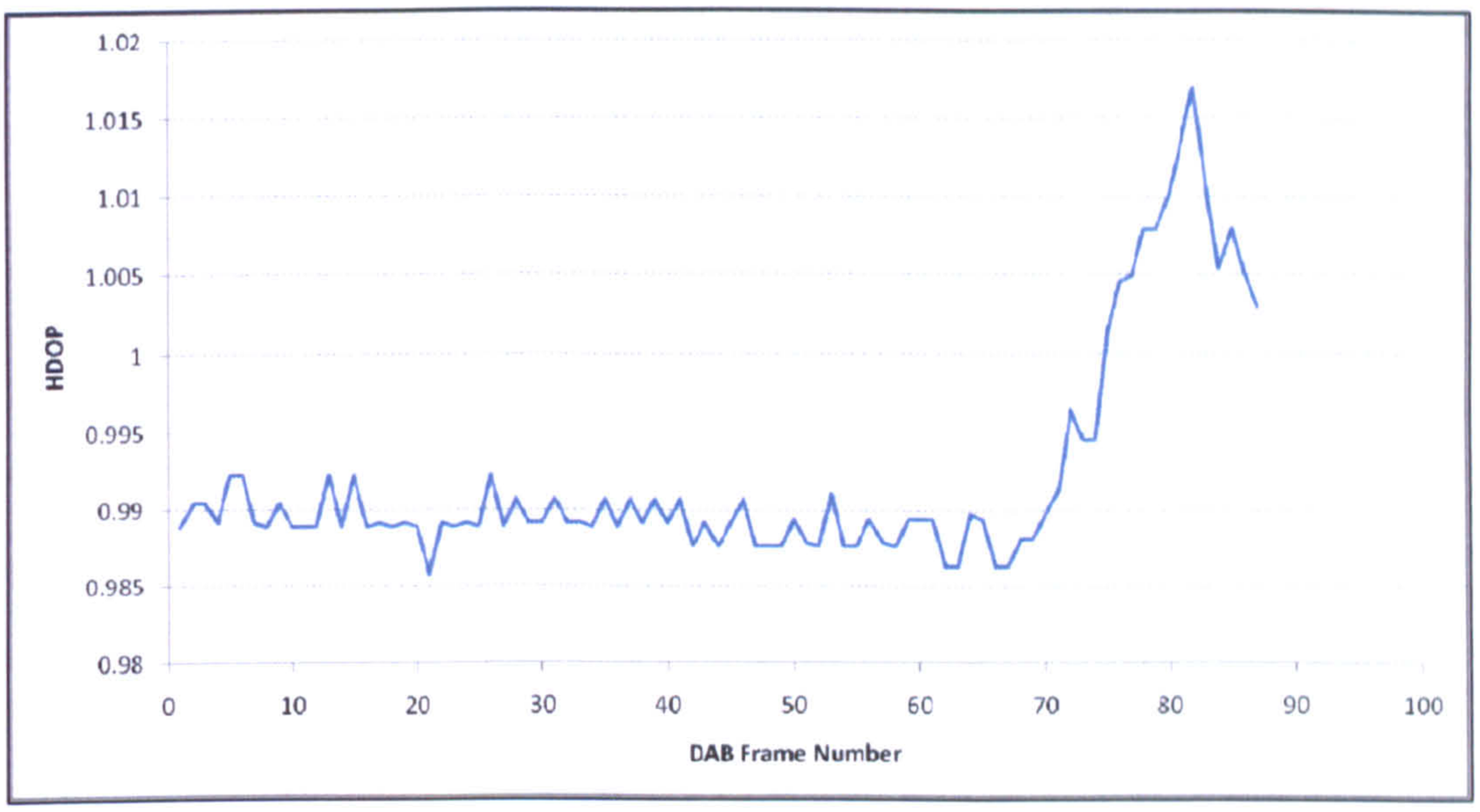

Figure 8-49: Dynamic Test 3 – DAB HDOP values

8.11.2.4 Dynamic Test 4

This test was conducted shortly after the data collected in test 3. The same transmitters are still in view of the vehicle's DAB antenna. As this is a new test, the TII symbol is decoded once again and the correlation peaks assigned accordingly in order to begin the tracking loops.

Transmitter Name	*Region Code*	*Transmitter Code*	*East (metres)*	*North (metres)*
Waltham	65	16	480950	323350
Mapperley Ridge	65	08	458350	342450
Sutton Coldfield	24	18	393350	367650
Daventry	18	02	458750	262150

As can be seen in Figure 8-50, the DAB tracking, whilst performing better than that in test 3, can be seen to fluctuate to the north of the true result. It can be seen by referring to the cross-correlation of the received TFPR symbols over time (Figure 8-51 on page 199) that the system is tracking the four signals as would be expected. The two strongest signals, located at roughly 400 and 500T respectively, show evidence of strong multipath signals each lying at approximately 10T to the right of each. As the frame count surpasses forty, it can be seen that the peak-tracking starts to fail. This

can be due to the vehicle moving through an area of lowered elevation meaning that transmitters can lose line-of-sight from one or more directions. This can be verified by viewing the HDOP plot (Figure 8-52 on page 199), where a leap in HDOP values occurs around the same period.

In situations such as these where DAB fails to provide a position due to transmitters falling below the line-of-sight, where GPS updating would provide the mitigating factor.

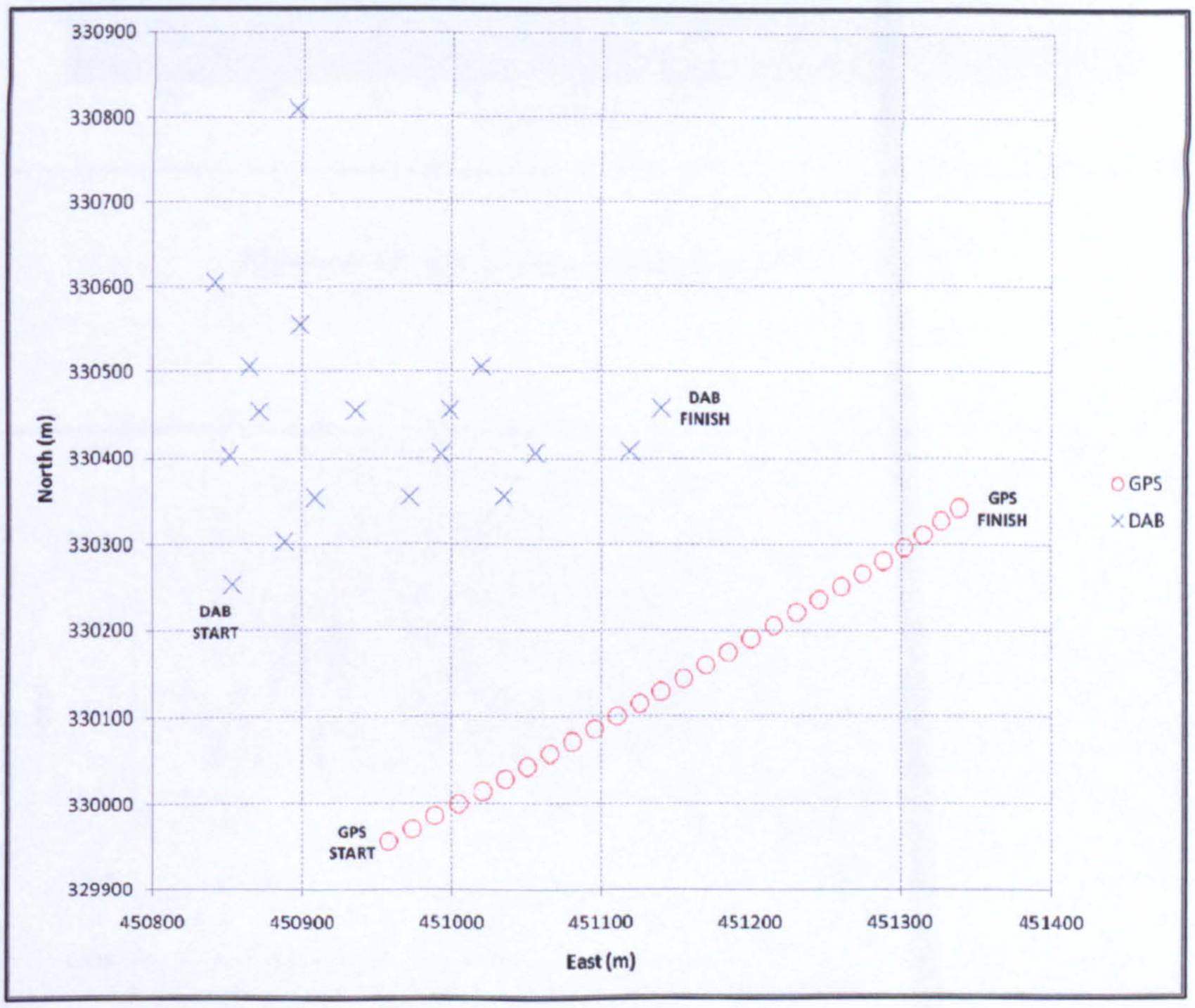

Figure 8-50: Dynamic Test 4 – GPS vs. DAB

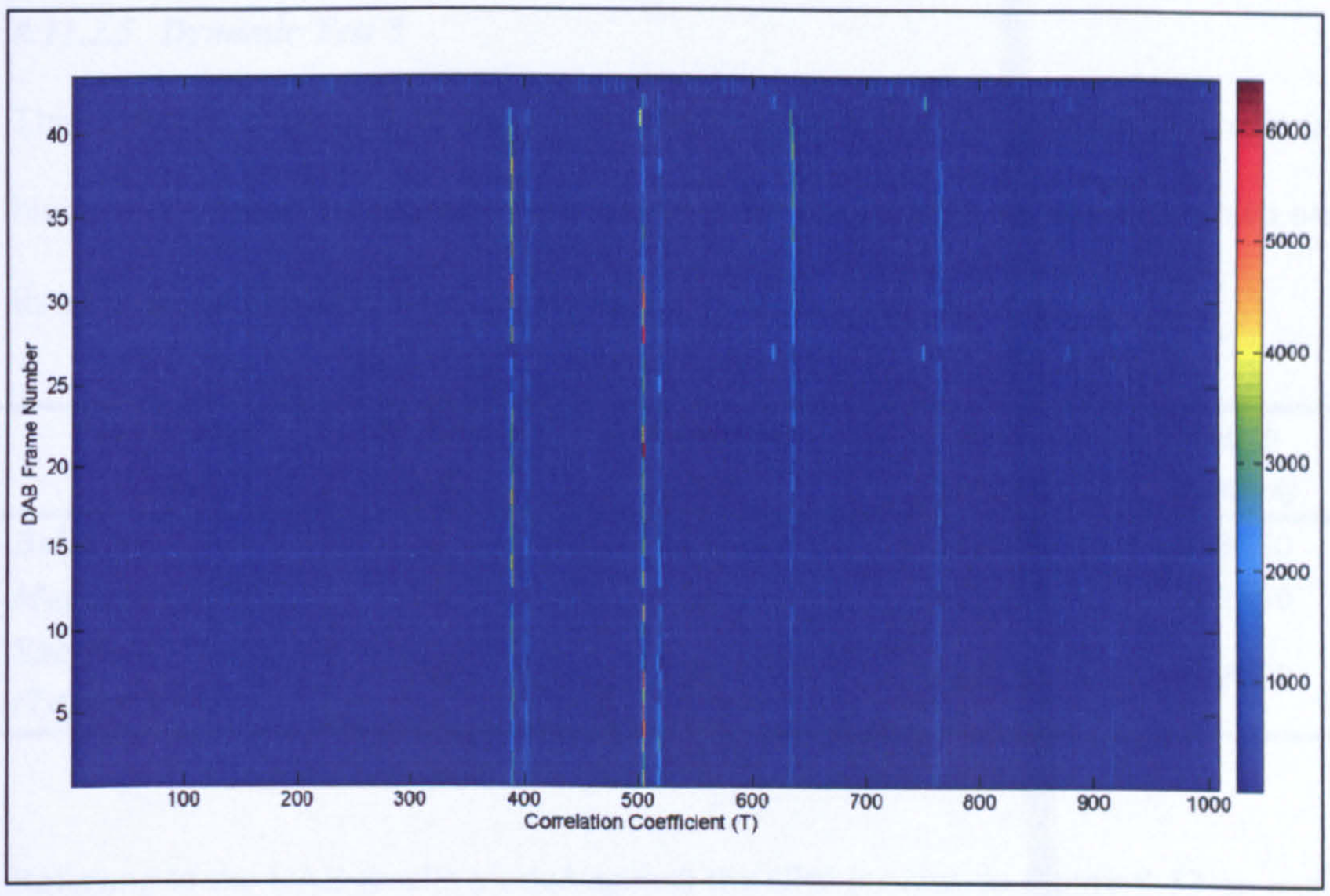

Figure 8-51: Cross-correlation of each DAB frame

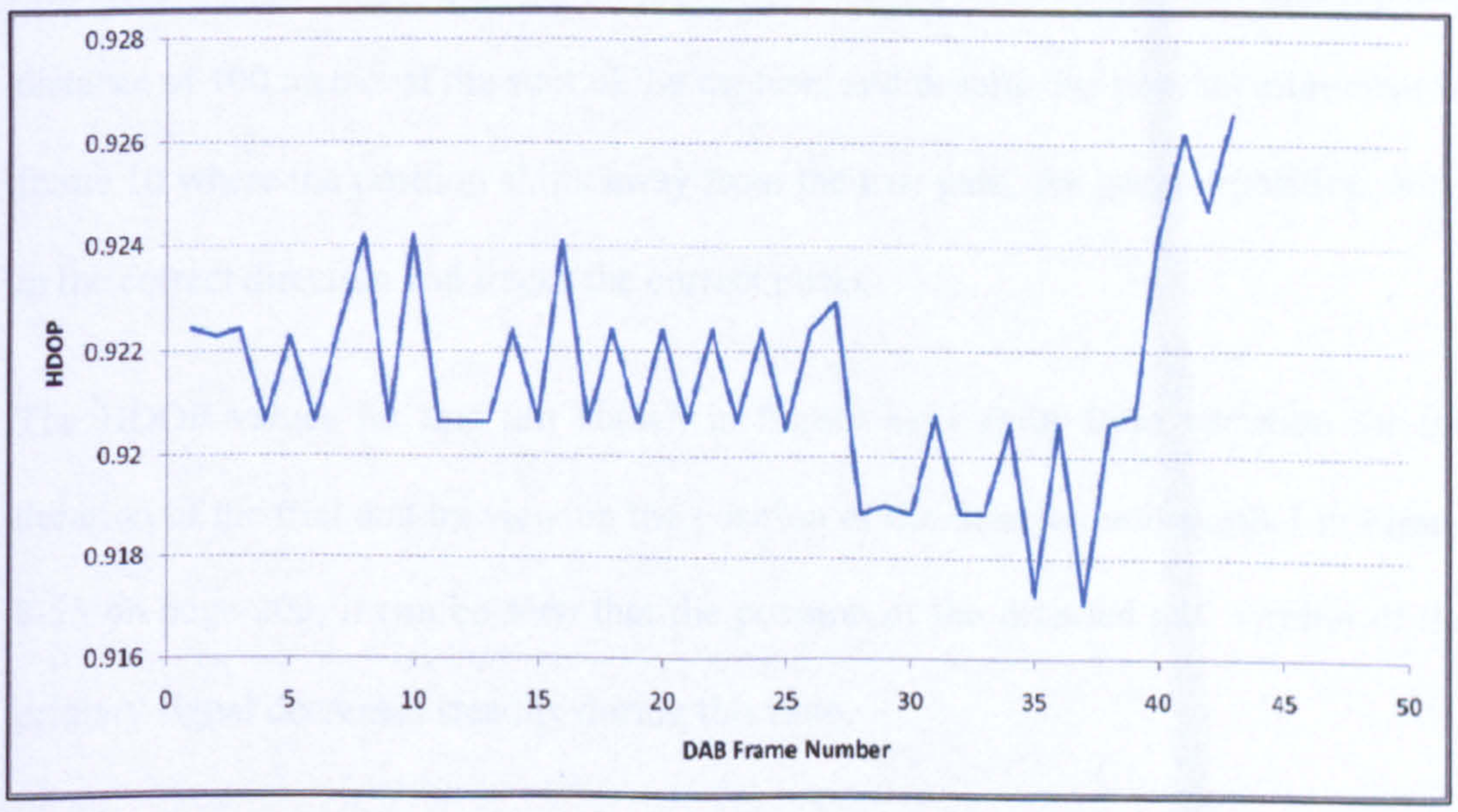

Figure 8-52: Dynamic Test 4 – DAB HDOP values

8.11.2.5 Dynamic Test 5

This test was conducted in the Lincolnshire region using the commercial national block 11D. Three transmitters were viewable for the duration of this trial which are listed in the table below.

Transmitter Name	*Region Code*	*Transmitter Code*	*East (metres)*	*North (metres)*
Belmont	58	02	521850	383650
Mapperley Ridge	65	16	458350	342450
Sheffield (Tapton Hill)	58	03	432450	387050

Referring to the DAB results plotted against the GPS position in Figure 8-53 on page 201, it can be seen that this trial showed very successfully that the DAB tracking module works providing the secondary signal strengths remain at an adequate level relative to the primary signal. The plot shows the DAB position at an approximate distance of 100 metres at the start of the capture, and despite one poor measurement in frame 10 where the position shifts away from the true path, the general position shifts in the correct direction and tracks the correct peaks.

The HDOP values for this test shown in Figure 8-54 show little variation for the duration of the trial and by viewing the position of the detected null symbol in Figure 8-55 on page 202, it can be seen that the position of the detected null symbol of the primary signal decreases steadily during this time.

If the receiver remained at a static location, it can be seen that this value will remain stable with potential fluctuation between two values due to the USRP's front-end under-sampling the signals.

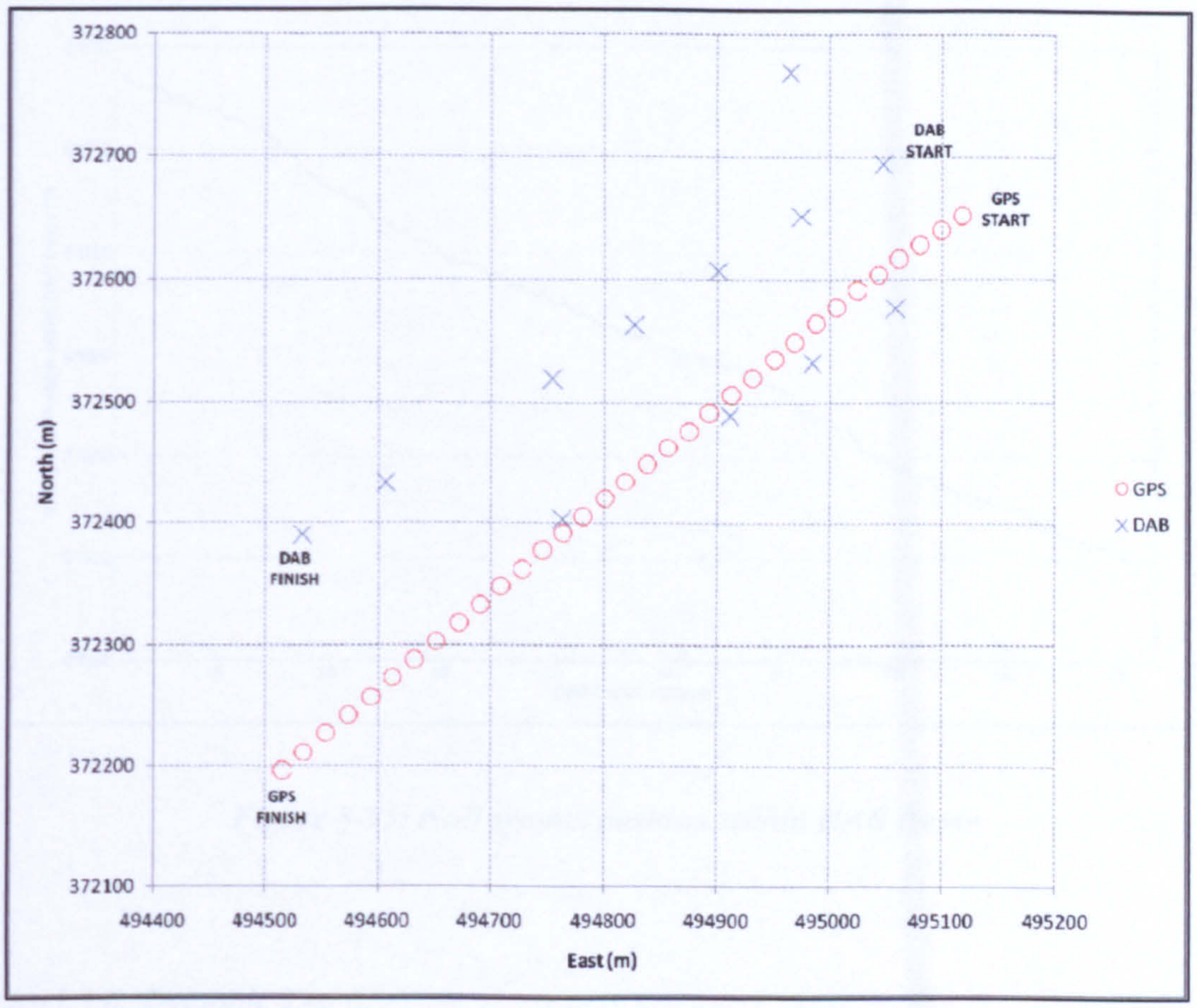

Figure 8-53: Dynamic Test 5 – GPS vs. DAB

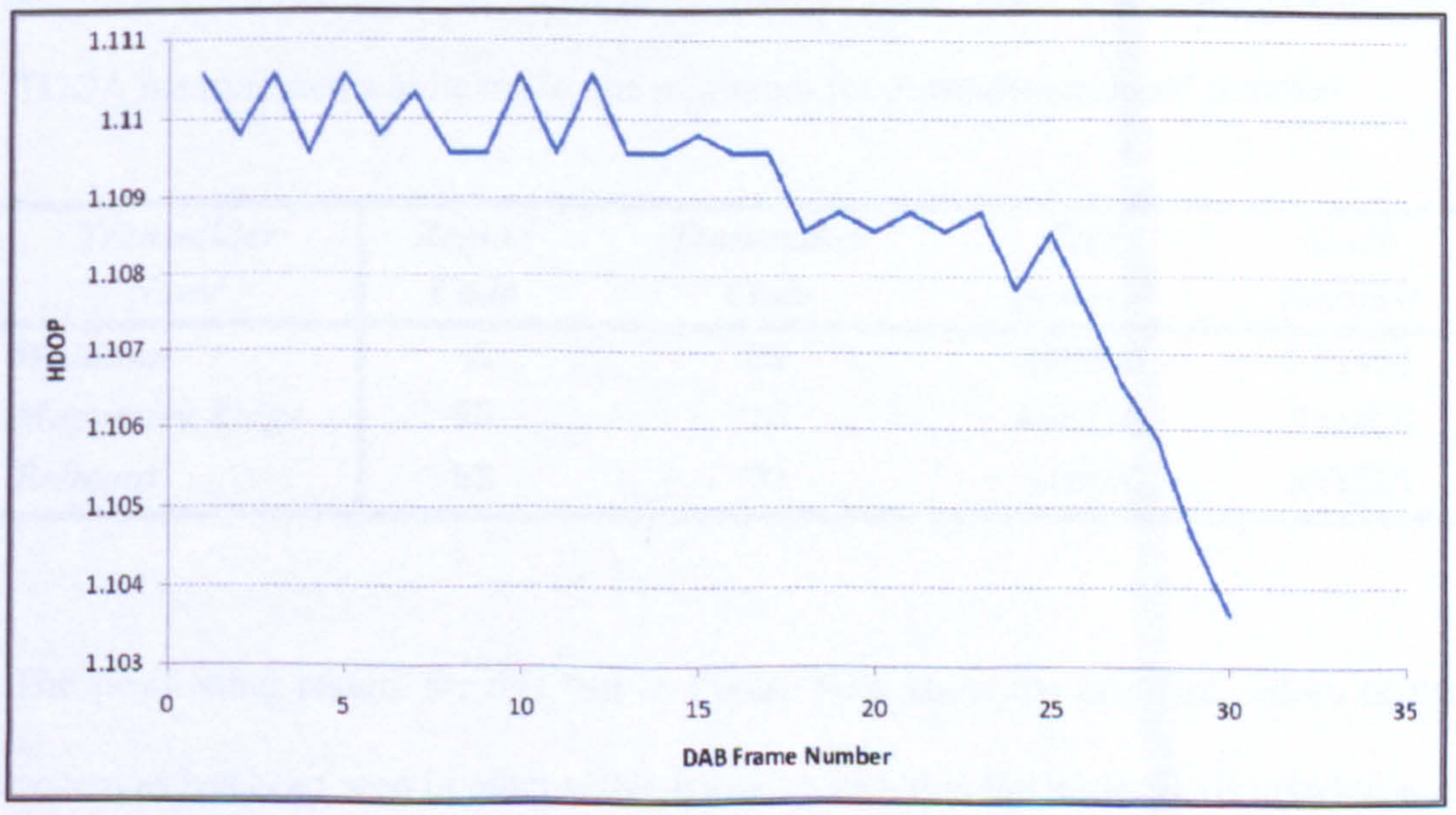

Figure 8-54: Test 5 – DAB HDOP values

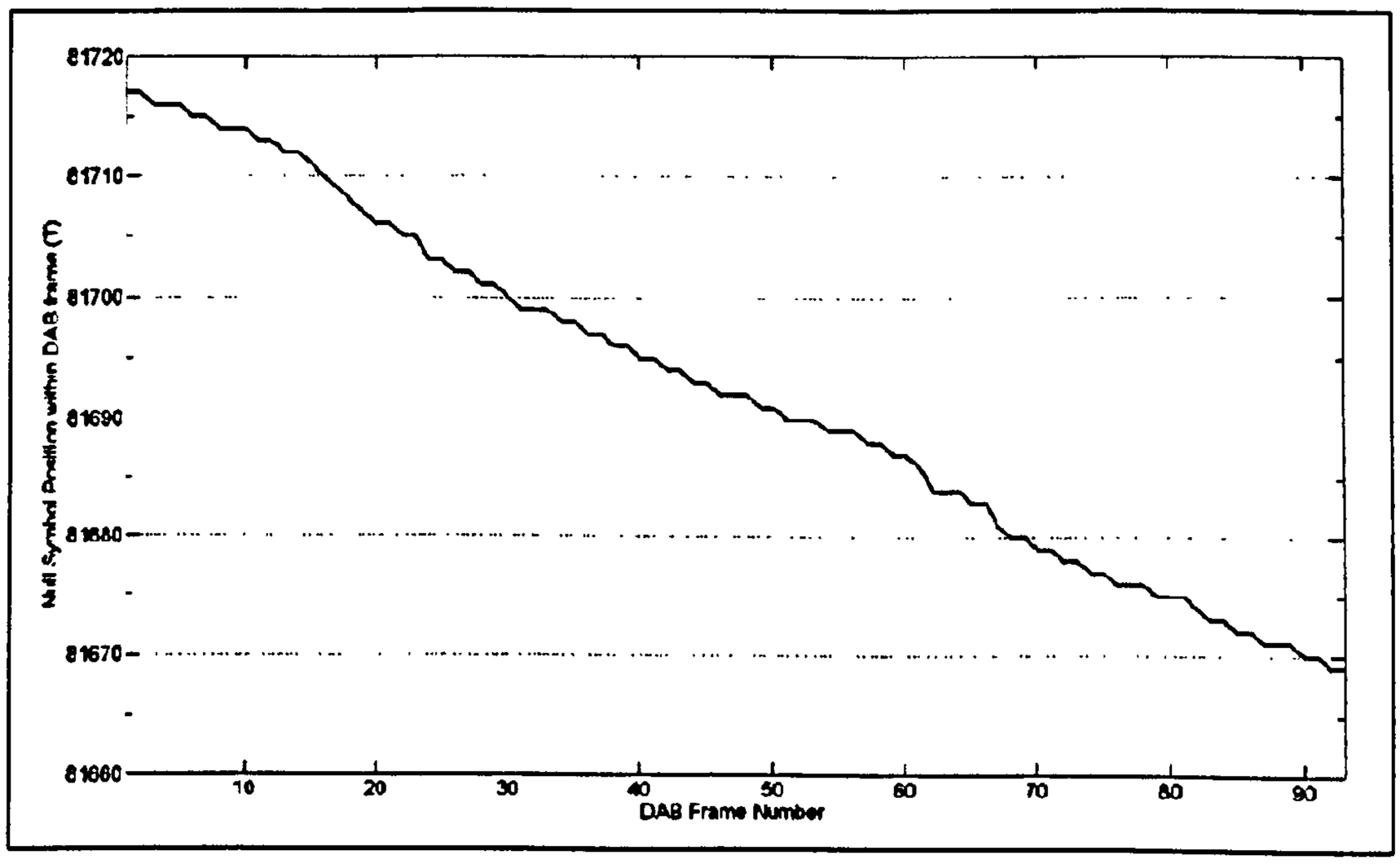

Figure 8-55: Null symbol position within DAB frame

8.11.2.6 Dynamic Test 6

The final dynamic test was conducted towards the east of Nottingham using the 11D national commercial signal on block 11D. Three transmitters were tracked for the duration of the trial, shown in the table below. These transmitters allowed for two TDOA measurements to be made, the minimum for a two-dimensional position.

Transmitter Name	*Region Code*	*Transmitter Code*	*East (metres)*	*North (metres)*
Waltham	65	08	480950	323350
Mapperley Ridge	65	16	458350	342450
Belmont	58	02	521850	383650

The positioning results for this test in Figure 8-56 show the grid-like nature of the system as has been seen in other tests. It can be seen that the initial DAB position was roughly 300 metres from the start of the GPS tracking. At this point, the tracking begins to drift away from the GPS path but is then reacquired to bring the DAB result

within 50 metres. This process is then repeated with the tracking drifting away from the truth but once again being reacquired as the trial finishes.

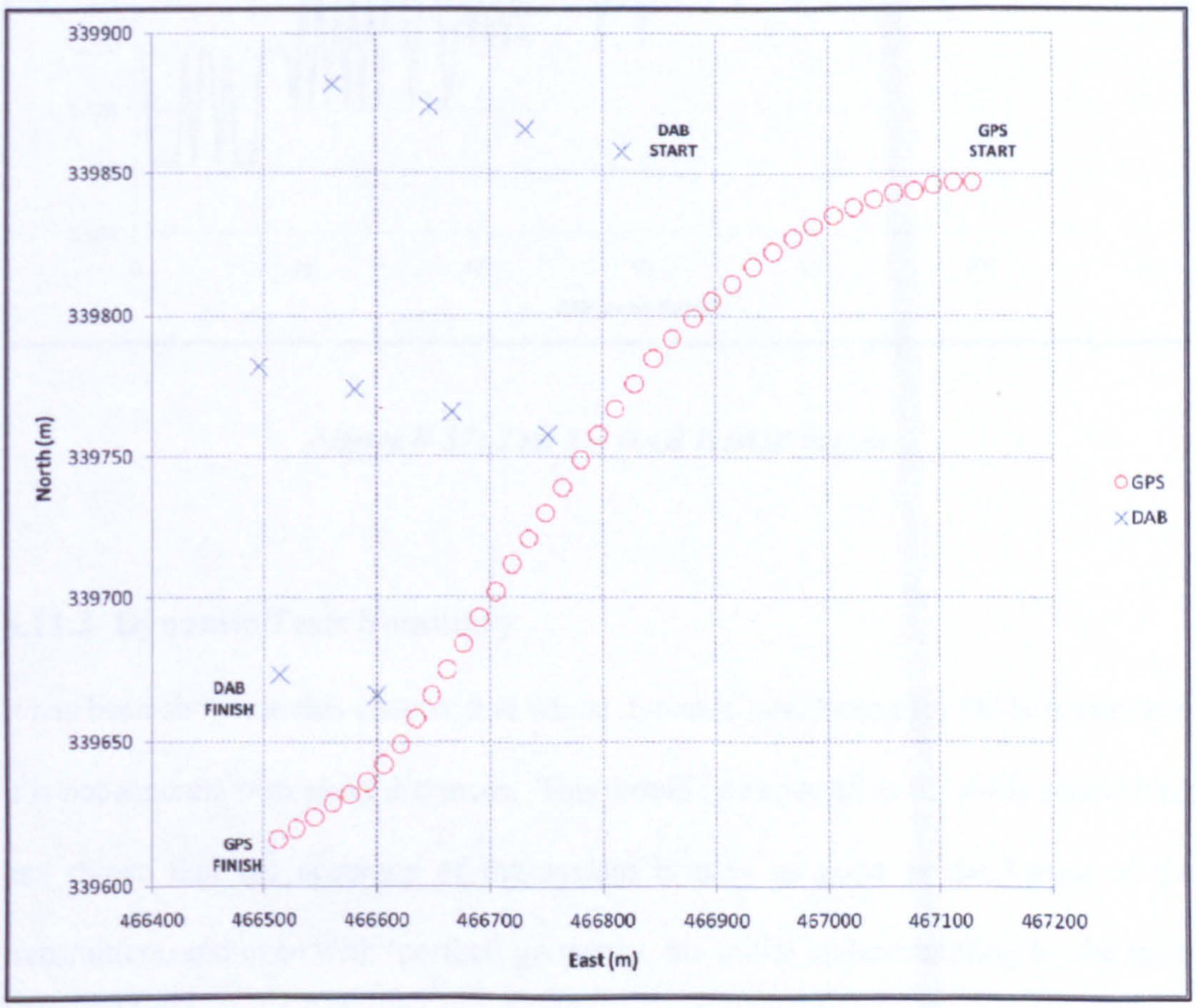

Figure 8-56: Dynamic Test 6 – GPS vs. DAB

The HDOP plot in Figure 8-57 shows the step-like change in values as has been seen previously, though in this instance the precision is deteriorating slightly. This pattern appears to be synonymous with the DAB tracking over the grid system. In such cases, the same transmitters are tracked for the duration of the trial, and while null symbol detection slips may occur, the software can detect and account for these by reallocating the primary transmitter using the next available TII information.

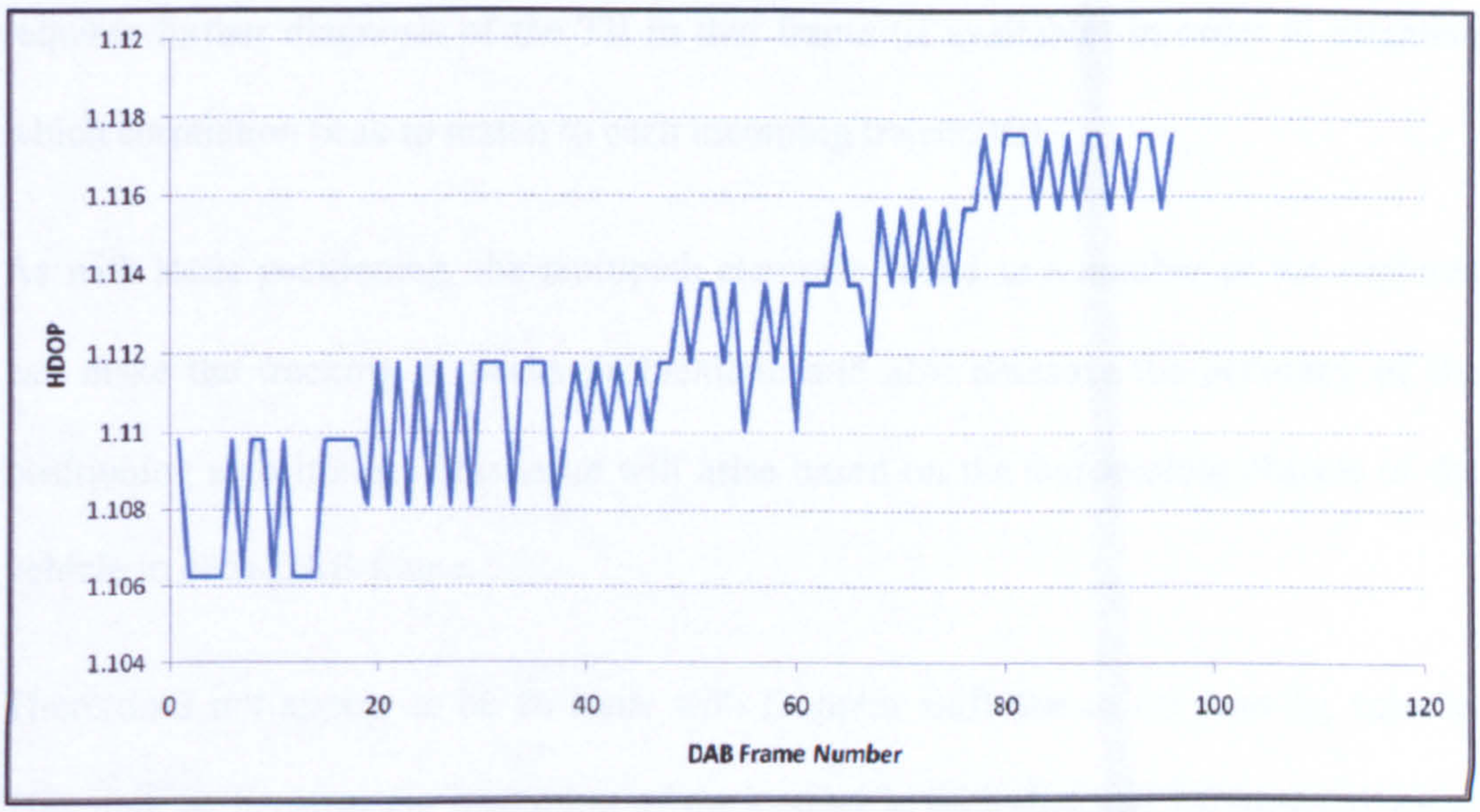

Figure 8-57: Test 5 – DAB HDOP values

8.11.3 Dynamic Tests Summary

It has been shown in this chapter that whilst dynamic positioning for DAB is possible, it is not accurate over short distances. This would be expected as the static positioning has shown that the accuracy of the system is only as good as the layout of the transmitters, and even with 'perfect' geometry, the initial under-sampling by the radio front-end in this project does limit the resolution of the system.

The testing has shown that dynamic positioning requires a modified approach to the algorithms that have been developed for static positioning. Complexities arise as transmitters leave the view of the antenna while others come into view. This means that whilst the initial locations were provided by GPS in these scenarios, the constant monitoring and cross-referencing of the TII symbol with the correlation properties of the received TFPR symbol is critical over longer periods.

In addition to these properties of each usable frame, the relative null symbol position within each frame also has to be monitored to enable the system to identify any sudden changes in position. As has been shown, a dramatic positional change ($> \pm 2T$) in these values means that the current primary transmitter has changed. This change

requires further diagnosis of the TII in that frame (if available) in order to establish which correlation peak to match to each incoming transmitter.

As with static positioning, the multipath elements found in a number of the captures can make the tracking of peaks problematic and also decrease the accuracy of the positioning algorithms. This issue will arise based on the surrounding objects of the vehicle in each DAB frame.

There does not appear to be an issue with Doppler shift due to the moving vehicle. This may be because the resolution of the system is such that any incremental value may not be detected.

9 SUMMARY AND CONCLUSIONS

The final chapter in this thesis is intended to provide an overview of the work undertaken in order to produce this document. The work will be examined and conclusions drawn, with final recommendations being made as to the continuation of research within this field.

9.1 SUMMARY

The aims of this project were to investigate the use of the Digital Audio Broadcast signal as an alternative positioning source to satellite navigation, and to then develop software capable of positioning a receiver using this signal alone. In order to achieve this, a number of simulations were initially performed using transmitter location data obtained from Ofcom, in order to ascertain the feasibility of the aims. Following these simulations, software was developed throughout the duration of the project using the hardware selected at the outset to detect Time Difference of Arrival measurements from multiple DAB sources.

The tools developed were then subjected to an initial testing phase in order to investigate the effects of a number of criteria to enable further development of the software. Static positioning trials followed this period, with equipment installed inside a vehicle and data captures taken at pre-determined locations in order to

examine different geographical settings. These tests covered terrain from wide open and flat rural land to dense urban situations with the intention to cover a spectrum of geography in the UK. GPS tracking provided the "truth" system against which the DAB positioning was compared.

Finally, the most demanding test involved the development of further algorithms to enable the software to track signals when moving at speed. A number of these trials were performed in different regions again to examine how DAB positioning fared when compared to the GPS tracking.

9.2 CONCLUSIONS

This section will examine the various simulations and testing exercises in turn with the purpose of providing an overall summary into the use of DAB as a standalone/aiding positioning source.

9.2.1 Coverage Simulations

The early research involved the examination of DAB signal coverage, based on publicly available details regarding transmitter sites. Initial tests modelled the locations of these transmitters in the UK, and based on the height of these locations and transmitting antennas, produced contour maps for both signal coverage and horizontal dilution of precision values, assuming perfect reception.

The DAB spectrum was sub-divided into seven widely used frequencies at the time (11B – 11D and 12A – 12D), with several test signals on other frequencies and allowance for further expansion in the future. Information on these available frequencies was freely available for all networks, although the BBC information (provided through their own website) declined to mention the height of transmitting antennas at the time of writing. This meant that the BBC national network had to be excluded from these simulations due to the lack of information. The remaining six blocks had complete information for this purpose. In general, sites were found to be identical to those in the dominant Digital One commercial national network (block 11D) and therefore the lack of BBC information was unlikely to add any coverage advantages.

These simulations indicated that within the country as a whole, coverage was sufficient to attain a position fix using a Time Difference of Arrival (TDOA) measurement approach, coupled with linear least squares positioning methodology. Naturally, as transmitters were spaced not for positioning purposes but for the sole purpose of a DAB receiver being within line-of-sight of a single transmitter, this was

found to be a valuable simulation in proving that DAB positioning could be undertaken at the majority of locations within the UK.

Various models were run to investigate how changes in the receiver antenna height above a spherical earth model would increase/decrease the number of transmitters in view of a receiver, in addition to the effect of the COST Hata path-loss model used to determine line-of-sight signal propagation.

The main conclusions that can be drawn from the simulation exercises performed were:

- The general model used for these simulations indicated excellent coverage from three or more transmitters at any one time, especially in areas of high population.
- The height of the receiving antenna can improve the transmitter availability in all areas.
- The resolution of the system is dependent on the position and quantity of transmitters available to the receiver.

9.2.2 System Testing

During the initial build of the processing software, a number of tests were conducted to investigate how the variation of certain parameters could affect the timing extraction ability of the software. The first of these tests was a time-delay exercise whereby the equipment was automated to perform a capture of one DAB block once per hour over 48 hours to examine if the TDOA measurements altered during this period. Any variations would have suggested transmitter clock drift, which would make standalone positioning of a DAB receiver impossible. The antenna was mounted high on the roof of a university building and left over the course of a weekend to capture the data. However, the results indicated that the clock stability

was excellent, with the testing algorithms reporting the same results over the 48 hour period.

The sampling rate of the TVRX daughterboard front-end inside the USRP sampled the incoming signal at a rate that was slightly lower (2MHz) than the DAB sampling frequency (2.048MHz). This meant that it was necessary to re-sample the received signal to the DAB frequency in order to perform the cross-correlation process and was able to separate multiple signals to one unit of DAB time T (1/2.048MHz ≈ 142 metres). This simplified the system to a grid-like structure whereby the TDOA (measured in integer T) would automatically 'lock' to the intersection of each hyperbolic intersect. It was later shown during a further simulation that these grid areas are defined by the geometry of the transmitters and the HDOP of the system.

The second test involved changing the height of the receiving antenna at the same position on the Earth's surface. This was to confirm that the simulation undertaken earlier in the project proved true, that the higher the antenna is, the more transmitters are within line-of-sight. This proved to be the case, but there were surprising results with the severe multipath component in the experiment conducted on the tallest building in the surrounding area on the university campus. These secondary signals were likely to have been reflected upwards from the large number of flat-roofed buildings in the vicinity of the area. This outcome had not been considered previously as it had been assumed that a very clean signal would have been received.

Testing then progressed to study the comparison between two different DAB specific antennas. These involved the examination of the outdoor mounted dipole antenna and the indoor vehicle mounted active patch antenna. These results were immediately conclusive in showing that during identical test conditions, the dipole antenna showed far more potential than the patch by providing a higher signal-to-noise ratio. Naturally the relative size of the dipole antenna meant that it was much less mobile, but the

purpose of the project was to establish how the signals could be used, and this antenna yielded the better quality results.

The dipole antenna was therefore used in the first round of positioning trials based around the university campus road network to test whether the equipment could repeat a set of positioning measurements if it was removed and returned to the same location within the space of an hour. These tests showed that the repeatability was excellent as expected following the successful testing of the transmitter clock stability.

As the equipment had now been tested in an outdoor environment, it proved interesting to test whether signals adequate for positioning could be received inside a building. Positions were found where the signals would have to travel through multiple walls and also where the same position could be tested on three floors. The results from this test did not present enough information for a standalone positional fix which was due to the lower receiving power of the signals, the lower power transmissions then being lost in the background noise. The multiple signals could be separated within a large structure where GPS reception was not possible. However, the lower power signals were lost in the background noise, meaning that there was insufficient information for a positional fix.

The main conclusions of the system testing stages were as follows:

- As was proven in the simulation exercise, the system provided a resolution good enough for rough positioning in an area with good transmitter coverage (approx 150m), which is only marginally greater than GPS when Selective Availability was switched on (approx 100m).
- The transmitter clocks were stable enough for positioning purposes on the resolution of the DAB system, although the stability would need to be tested in order to calculate fractional values of T if an alternative front-end had the ability to over-sample the signal.

- The dipole antenna out-performed the patch antenna in the comparison trial. Technical development would be required for this type of receiver to be hand-held due to its current size.
- Tests proved that repeatability of the developed system was excellent.
- It was shown that signals could be separated within a large dense building, if the signal-to-noise ratio was high enough. The use of this system within an indoor environment caused issues due to secondary transmissions being lost in the background noise.

9.2.3 Field Testing – Static

The field testing was performed over a number of different test runs during 2009 with the aim to try and capture DAB data in as many diverse locations as possible. The equipment was again installed inside a vehicle with the dipole antenna mounted to the roof. Real-time kinematic GPS tracking was used to establish the true position of each capture in order to compare the DAB position calculation. At every static capture location, the DAB capture was made on all seven of the UK blocks along with the true GPS calculated location.

The first of these test-runs involved a combination of suburban and rural environments between the cities of Nottingham and Leicester. Within this region there were four dominant transmitters forming a simple four-sided test area for the system. This allowed for a number of well-spaced tests to be conducted and a mean system error of approximately 380 metres from the true position. A small minority of the captures either did not yield results, or resulted in unusable measurements due to the geometry of the transmitters.

The second test-run involved a combination of suburban and dense urban environments between the cities of Nottingham, Leicester and Birmingham. Within this region there were significantly more transmitters available to the receiver. The

majority of positions yielded excellent results, with an average position approximately 345 metres from the truth.

The third and final test-run involved a combination of suburban and mainly rural environments between the cities of Nottingham and Lincoln. The number of transmitters available to the receiver was similar in quantity to the first test, and this showed an average offset of 254 metres from the majority of results.

The main conclusions that can be drawn from the static positioning trials are:

- Proof that the earlier simulations were correct, in that the linear offset of the DAB position from the true GPS position was proportional to the height of the antenna relative to the transmitters.
- The structure of the hyperbolic intersections, caused by the hardware sampling rate, created a varying accuracy dependent on the quantity and position of transmitters.
- The transmitter location accuracy could have been improved over the Ofcom database by identifying transmitters from satellite imagery (such as Google Maps) and provide an offset of potentially 10's of metres rather than 100+.
- Standalone DAB Positioning was possible in the vast majority of cases tested and although a small number of positions did not yield a location, this was seen as a very encouraging result from a system not designed for positioning.

9.2.4 Field Testing - Dynamic

The final testing of the system involved the use of both DAB and GPS receivers tracking a moving vehicle over a short distance. These tests required new processing modules to be built to allow the receiver to track correlation peaks over time. The techniques used differed from the static positioning, using GPS to 'seed' the preliminary vehicle location allowing the correlation peaks to be matched immediately.

- Transmitter "shadowing", where one or more transmitters would disappear from line of sight for short periods, and then reappear at a later time at a different correlation coefficient, would be eliminated by further development of the system tracking algorithms.
- The tests performed in this section demonstrated that the calculated DAB position lay within the region of interest and was seen to generally follow the local hyperbolic grid structure.
- Such a system would be usable for longer term position tracking, which may not require a high degree of accuracy. For example, the system may not be suited to tracking a vehicle around a housing estate containing many closely located intersecting roads, but would be better suited to tracking a vehicle between villages, towns and cities.

9.2.5 Concluding Remarks

This thesis has presented the use of Digital Audio Broadcasting, a non-navigation signal, as a potential source of delivering a terrestrial-based complement to satellite navigation. A prototype Software Defined Radio system has been developed from basic principles throughout this work providing an environment within which the necessary signal processing operations may be performed.

The key elements required for TDOA positioning have been shown to be present within the DAB signal proving that static and dynamic tracking are possible, however, more work is required on these tracking algorithms for both processes to make a more robust system. Higher precision positioning should also be possible using an alternative radio frontend to oversample the DAB signal, allowing for a unit of measurement smaller than the clock rate T.

It has been proven that the fundamentals of standalone DAB positioning are possible and with further development could provide a robust backup to GNSS.

9.3 POTENTIAL FUTURE WORK RECOMMENDATIONS

This thesis has presented the use of DAB as a positioning source in a wide range of scenarios and shown that the use of a Software Defined Radio approach has been *sufficient in* the post-processing of such data. Due to time limitations within this project, a number of recommendations can be made for *future research in this area:*

- It would be an interesting study to potentially build a custom built front-end allowing for the capture of multiple signals at a higher sampling rate to overcome the limitations of the USRP sampling rate. The second generation USRP2 has the ability to capture much wider signal bandwidths, allowing for the capture of the entire DAB band using a sampling rate of higher resolution than the transmitter clock frequency (2.048MHz). This approach could allow for the measurement of a "sub-T" TDOA system, allowing for a higher resolution than could be achieved with the hardware within this project.
- As a standalone positioning system, DAB accuracy could currently be compared with an early LORAN-C system (accuracy up to 1km). It would be of interest to combine measurements from a number of different terrestrial based sources (such as DVB, DRM, LORAN, Wi-Fi etc) to investigate how a data fusion approach improves upon the results from standalone DAB. This approach could also be adopted using a limited GNSS constellation (< 3 satellites) and a single TDOA measurement from DAB to potentially mitigate the effect or urban canyon GNSS measurements.
- Differential DAB positioning would be an interesting direction to investigate further. Due to the TVRX daughterboard using a separate oscillator to the USRP motherboard, the synchronisation of this system would not be possible, however, custom-built hardware could have this ability and providing two USRP2 devices could connect via a data-link, this approach could prove to produce interesting results.

10 APPENDIX

k range				
min	max	*k'*	*i*	*n*
-768	-737	-768	0	1
-736	-705	-736	1	2
-704	-673	-704	2	0
-672	-641	-672	3	1
-640	-609	-640	0	3
-608	-577	-608	1	2
-576	-545	-576	2	2
-544	-513	-544	3	3
-512	-481	-512	0	2
-480	-449	-480	1	1
-448	-417	-448	2	2
-413	-385	-416	3	3
-384	-353	-384	0	1
-352	-321	-352	1	2
-320	-289	-320	2	3
-288	-257	-288	3	3
-256	-225	-256	0	2
-224	-193	-224	1	2
-192	-161	-192	2	2
-160	-129	-160	3	1
-128	-97	-128	0	1
-96	-65	-96	1	3
-64	-33	-64	2	1
-32	-1	-32	3	2

k range				
min	max	*k'*	*i*	*n*
1	32	1	0	3
33	64	33	3	1
65	96	65	2	1
97	128	97	1	1
129	160	129	0	2
161	192	161	3	2
193	224	193	2	1
225	256	225	1	0
257	288	257	0	2
289	320	289	3	2
321	352	321	2	3
353	384	353	1	3
385	416	385	0	0
417	448	417	3	2
449	480	449	2	1
481	512	481	1	3
513	544	513	0	3
545	576	545	3	3
577	608	577	2	3
609	640	609	1	0
641	672	641	0	3
673	704	673	3	0
705	736	705	2	1
737	768	737	1	1

Table 12: TFPR Construction – relationship between k, k', i and n

j	0	1	2	3	4	5	6	7	8	9	10	11	12	13	14	15
$h_{0,j}$	0	2	0	0	0	0	1	1	2	0	0	0	2	2	1	1
$h_{1,j}$	0	3	2	3	0	1	3	0	2	1	2	3	2	3	3	0
$h_{2,j}$	0	0	0	2	0	2	1	3	2	2	0	2	2	0	1	3
$h_{3,j}$	0	1	2	1	0	3	3	2	2	3	2	1	2	1	3	2

j	16	17	18	19	20	21	22	23	24	25	26	27	28	29	30	31
$h_{0,j}$	0	2	0	0	0	0	1	1	2	0	0	0	2	2	1	1
$h_{1,j}$	0	3	2	3	0	1	3	0	2	1	2	3	2	3	3	0
$h_{2,j}$	0	0	0	2	0	2	1	3	2	2	0	2	2	0	1	3
$h_{3,j}$	0	1	2	1	0	3	3	2	2	3	2	1	2	1	3	2

Table 13: TFPR Construction – relationship between j and h

p	$a_b(p)$ b=0,1,2,3,4,5,6,7
0	00001111
1	00010111
2	00011011
3	00011101
4	00011110
5	00100111
6	00101011
7	00101101
8	00101110
9	00110011
10	00110101
11	00110110
12	00111001
13	00111010
14	00111100
15	01000111
16	01001011
17	01001101
18	01001110
19	01010011
20	01010101
21	01010110
22	01011001
23	01011010

p	$a_b(p)$ b=0,1,2,3,4,5,6,7
24	01011100
25	01100011
26	01100101
27	01100110
28	01101001
29	01101010
30	01101100
31	01110001
32	01110010
33	01110100
34	01111000
35	10000111
36	10001011
37	10001101
38	10001110
39	10010011
40	10010101
41	10010110
42	10011001
43	10011010
44	10011100
45	10100011
46	10100101
47	10100110

p	$a_b(p)$ b=0,1,2,3,4,5,6,7
48	10101001
49	10101010
50	10101100
51	10110001
52	10110010
53	10110100
54	10111000
55	11000011
56	11000101
57	11000110
58	11001001
59	11001010
60	11001100
61	11010001
62	11010010
63	11010100
64	11011000
65	11100001
66	11100010
67	11100100
68	11101000
69	11110000

Table 14: List of TII region codes p and binary codes $a_b(p)$

11 BIBLIOGRAPHY

ABBOTT, A. (2002) Antijamming and GPS for Critical Military Applications [http://www.aero.org/publications/crosslink/summer2002/06.html] Accessed on 08/09/2007

ABHAYAWARDHANA, V. S., WASSELL, I. J., CROSBY, D., SELLARS, M. P. & BROWN, M. G. (2005) Comparison of empirical propagation path loss models for fixed wireless access systems. *Vehicular Technology Conference, 2005.*

AKIYAMA, T., TERANISHI, Y., OKAMURA, S. & SHIMOJO, S. (2009) A Consideration of the Precision Improvement in WiFi Positioning System. *Complex, Intelligent and Software Intensive Systems (CISIS '09).*

ANDERSON, H. R. (1986) Location Statistics of AM Broadcast Groundwave Signal Amplitudes. *IEEE Transactions on Broadcasting,* BC-32.

ANDERSON, J. B. (1964) Fresnel Zones for Ground-Based Antennas. *IEEE Transactions on Antennas and Propagation,* 12, 417 - 422.

ANON (1997) ETS 300 401: Radio Broadcasting Systems; Digital Audio Broadcasting (DAB) to mobile, portable and fixed receivers. European Broadcasting Union.

ANON (2007) ETSI TS 102 563: Digital Audio Broadcasting (DAB); Transport of Advanced Audio Coding (AAC) Audio. European Broadcasting Union.

ANON (2008) SpectraTime to Supply Atomic Clocks to IRNSS [http://www.insidegnss.com/node/789] Accessed on 02/02/2010

BANKS, K. M. (1991) Datatrak automatic vehicle location system in operational use in the UK. *Vehicle Navigation and Information Systems Conference.*

BASKER, S. (2006) The Case for eLORAN. *Report prepared by Research and Radionavigation, General Lighthouse Authorities of the UK and Ireland*

BBC (2009) BBC - Future of the BBC - Building Public Value Document [http://www.bbc.co.uk/info/policies/text/bpv.html] Accessed on 04/01/2010

BROWN, A. & GEREIN, N. (2001) Test Results of a Digital Beamforming GPS Receiver in a Jamming Environment. *Proceedings of ION GPS 2001.* Salt Lake City, Utah, USA.

CASABONA, M. M. & ROSEN, M. W. (1999) Discussion of GPS Anti-Jam Technology. *GPS Solutions, 2.*

CHOI, H. I. & *WILLIAMS, W. J. (1989)* Improved time-frequency representation of multicomponent signals using exponential kernels. *IEEE Transactions on Acoustics, Speech and Signal Processing,* 37, 862 - 871.

CHOI, J. W. & CHO, N. I. (2001) Narrow-Band Interference Suppression in Direct Sequence Spread Spectrum Systems using a Lattice IIR Notch Filter. *Proceedings IEEE International Conference on Acoustics, Speech and Signal Processing.* Salt Lake City, Utah, USA.

COCHRAN, W. T., COOLEY, J. W., FAVIN, D. L., HELMS, H. D., KAENEL, R. A., LANG, W. W., MALING, G. C., NELSON, D. E., RADER, C. M. & WELCH, P. D. (1967) What is the fast Fourier transform? *Proceedings of the IEEE,* 55, 1664 - 1674.

CONNOR, F. R. (1972) *Signals,* London, Edward Arnold Ltd.

CONNOR, F. R. (1973) *Modulation,* London, Edward Arnold Ltd.

DAMOSSO, E. & CORREIA, L. M. (1999) COST 231 Final Report - Digital Mobile Radio towards Future Generation Systems. European Co-operation in the field of Scientific and Technical Research.

DAUBECHIES, I. (1990) The Wavelet Transform, Time-Frequency Localization and Signal Analysis. *IEEE Transactions on Information Theory,* 36, 961 - 1005.

DURAK, L. & ARIKAN, O. (2003) Short-time Fourier transform: two fundamental properties and an optimal implementation. *IEEE Transactions on Acoustics, Speech and Signal Processing,* 51, 1231 - 1242.

EMERY, R. (2009) UK-DAB.info - Coverage [http://www.uk-dab.info/coverage.php] Accessed on 04/01/2010

ETTUS, M. (2008) Ettus Research LLC [http://www.ettus.com/] Accessed on 25/09/2008

EVANS, R. H. & BAILY, S. T. (1997) On-Air Multiplexed Uplinking Of Eureka-147 DAB To EMS. *Fourth European Conference on Satellite Communications.* Rome, Italy.

GROSSKOPF, R. (1995) A prediction method for DAB in urban areas. *Ninth International Conference on Antennas and Propagation.*

GSA (2010) GSA: Galileo Services [http://www.gsa.europa.eu/go/galileo/services] Accessed on 01/09/2009

GUANGHUA, C., SHIWEI, M., TINGHAO, Q., JIAN, W. & JIALIN, C. (2006) The Wigner-Ville Distribution and the Cross Wigner-Ville Distribution of Noisy Signals. *The 8th International Conference on Signal Processing.*

HALL, T. D. (2004) Radiolocation Using AM Broadcast Signals: The Role of Signal Propagation Irregularities. *Position Location and Navigation Symposium.* Monterey, California, USA.

HALL, T. D. (2002) Radiolocation Using AM Broadcast Signals. *Department of Electrical Engineering and Computer Science.* Massachusetts Institute of Technology.

HALLBERG, J., NILSSON, M. & SYNNES, K. (2003) Positioning with Bluetooth. *10th International Conference on Telecommunications.*

HALLIER, J., LAUTERBACH, T. & UNBEHAUN, M. (1994) Multimedia broadcasting to mobile, portable and fixed receivers using the Eureka 147 Digital Audio Broadcasting System. *5th IEEE International Symposium on*

Personal, Indoor and Mobile Radio Communications. The Hague, Netherlands.

HATA, M. (1980) Empirical Formula for Propagation Loss in Land Mobile Radio Services. *IEEE Transactions on Vehicular Technology,* VT-29.

HEIMILLER, R. C. (1961) Phase shift pulse codes with good periodic correlation properties. *IRE Transactions on Information Theory,* IT7, 254 - 257.

HIDE, C. (2003) Integration of GPS and Low cost INS measurements. *Institute of Engineering Surveying and Space Geodesy.* Nottingham, University of Nottingham.

HOEG, W. & LAUTERBACH, T. (Eds.) (2003) *Digital Audio Broadcasting: Principles and Applications of Digital Radio,* Chichester, John Wiley & Sons Ltd.

HOFMANN-WELLENHOF, B., LICHTENEGGER, H. & COLLINS, J. (2001) *GPS Theory and Practice*, Springer.

INGRAM, S. J., HARMER, D. & QUINLAN, M. (2004) UltraWideBand Indoor Positioning Systems and their Use in Emergencies. *Position Location and Navigation Symposium (PLANS).* Monterey, California, USA.

JIAO, W., JIANG, P., LIU, R., WANG, W. & MA, Y. (2008) Providing Location Service for Mobile WiMAX. *IEEE International Conference on Communications.*

JONES, W. W. & JONES, K. R. (1992) Narrowband Interference Suppression Using Filter-Bank *Analysis/Synthesis* Techniques. *IEEE MILCOM Conference.* San Diego, Ca.

JULG, T. (1996) Evaluation of Multipath error and signal propagation in a complex scenario for GPS multipath identification. *IEEE 4th International Symposium on Spread Spectrum Techniques and Applications,* 2, 872 - 876.

KALMAN, R. E. (1960) A New Approach to Linear Filtering and Prediction Problems. *Transactions of the ASME - Journal of Basic Engineering,* D, 35-45.

KUKRER, O. & HOCANIN, A. (2006) An FIR Notch Filter for Adaptive Filtering of a Sinusoid in Correlated Noise. *EURASIP Journal on Applied Signal Processing,* 2006, 1-10.

KÜPPER, A. (2005) *Location-Based Services: Fundamentals and Operation,* Chichester, John Wiley & Sons Ltd.

LACHAPELLE, G., TOWNSEND, B., GEHUE, H. & CANNON, M. E. (1993) GPS versus LORAN-C for Vehicular Navigation in Urban and Mountainous Areas. *IEEE VNIS93.* Ottawa.

LANG, J.-P. (2010) GNU Radio - Wikistart - gnuradio.org [http://vps.gnuradio.org/redmine/wiki/gnuradio] Accessed on 05/01/2010

LAYER, F., ENGLERT, T., FRIESE, M. & RUF, M. (1998) Locating Mobile Receivers using DAB Single Frequency Networks. *3rd ACTS Mobile Communication Summit.* Rhodes, Greece.

LIEBENOW, U. & ZIMMERMANN, G. (1998) Investigations of Single Frequency Networks for Digital Mobile Radio Systems based on COFDM. *IEEE Vehicular Technology Conference.*

LO, S., HARTNETT, R., WENZEL, R., GUNTHER, G. T., MORRIS, P., MACALUSO, J., CARROLL, K., SKALIOTIS, G. & DIGGLE, D. (2004) Loran's Capability to Mitigate the Impact of a GPS Outage on GPS Position, Navigation and Time Applications. *Prepared for the Federal Aviation Administration Vice President for Technical Operations Navigation Services Directorate*

LORENZO, D. S. D., LO, S. C., COHEN, M., CHANG, J., INAN, U. S. & ENGE, P. K. (2009) A Miniaturized Loran H-field Antenna for Handheld Devices. *International Loran Association 38th Annual Convention and Technical Symposium.* South Portland, ME.

MCELLROY, J. A. (2004) Navigation Using Signals of Opportunity in the AM Transission Band. *Department of Aeronautics and Astronautics.* Air Force Institute of Technology.

MERTINS, A. (1996) *Signal Analysis,* Chichester, John Wiley & Sons Ltd.

MOLDON, N. (2010) Tech Parameters - Ofcom [http://www.ofcom.org.uk/radio/ifi/rbl/engineering/tech_parameters/] Accessed on 14/01/2010

PEDERSEN, F. S. (2009) Global Broadcasting Update: DAB/DAB+/DMB - January 2009. World DMB.

PINKER, A. & SMITH, C. (1999) Vulnerability of the GPS Signal to Jamming. *GPS Solutions,* 3, 19-27.

RABINOWITZ, M. & SPILKER, J. (2005) A New Positioning System Using Television Synchronization Signals. *IEEE Transactions on Broadcasting,* 51.

RAQUET, J. F., MILLER, M. M. & NGUYEN, T. Q. (2007) Issues and Approaches for Navigation Using Signals of Opportunity. *ION NTM 2007.* San Diego, California, USA.

RASH, G. D. (1997) GPS Jamming in A Laboratory Environment. *Institute of Navigation ION GPS-97.* Kansas City, Missouri, USA.

RAU, M. C. (1995) Overview of Digital Audio Broadcasting. *Technologies for Wireless Applications Digest*, 187 - 194.

RODRIGUEZ, J.-A., HEIN, G. W., WALLNER, S., ISSLER, J.-L., RIES, L., LESTARQUIT, L., LATOUR, A. D., GODET, J., BASTIDE, F., PRATT, T. & OWEN, J. (2010) The MBOC Modulation: Inside GNSS [http://www.insidegnss.com/node/174] Accessed on 10/01/2010

ROHAN, P. (1991) *Introduction to Electromagnetic Wave Propagation,* Artech House.

ROONEY, S., CHIPPENDALE, P., CHOONY, R., LE ROUX, C. & HONARY, B. (2000) Accurate vehicular positioning using a DAB-GSM hybrid system. *Vehicular Technology Conference (VTC 2000).* Tokyo.

RUGINI, L. & BANELLI, P. (2005) BER of OFDM systems impaired by carrier frequency offset in multipath fading channels. *IEEE Transactions on Wireless Communications,* 4, 2279 - 2288.

SCHROEDER, J., GALLER, S. & KYAMAKYA, K. (2005) A Low-Cost Experimental Ultra-Wideband Positioning System. *IEEE International Conference on Ultra-Wideband.*

SHELSWELL, P. (1996) The COFDM Modulation System: The heart of Digital Audio Broadcasting. BBC Research and Development.

STEINBUCH, K. & WIDROW, B. (1965) A Critical Comparison of two kinds of Adaptive Classification Networks. *IEEE Transactions on Electronic Computers,* EC-14, 737-740.

VAN DE BEEK, J. J. (1998) Synchronization and Channel Estimation in OFDM Systems. Lulea University of Technology.

VAN DEN BREKEL, B. J. H. & VAN DEE, D. J. R. (1992) GPS Multipath mitigation by antenna movements. *Electronics Letters,* 28, 2286 - 2288.

VARSHAVSKY, A., CHEN, M. Y., DE LARA, E., FROEHLICH, J., HAEHNEL, D., HIGHTOWER, J., LAMARCA, A., POTTER, F., SOHN, T., TANG, K. & SMITH, I. (2005) Are GSM Phones THE Solution for Localization? *Mobile Computing Systems and Applications.*

VINCENT, W. R., ADLER, R. W., MCGILL, P., CLYNCH, J. R., BADGER, G. & PARKER, A. A. (2003) The Hunt for RFI: Unjamming a Coast Harbor. *GPS World.*

WANG, J. (1995) LF/MF Skywave Propagation at Daytime. *IEEE Transactions on Broadcasting,* 41.

WANG, J. & SHEN, Z. (2002) An improved MUSIC TOA estimator for RFID positioning. *RADAR 2002.* Edinburgh, UK.

WARD, A. (2007) In-building Location Systems. *The Institution of Engineering and Technology Seminar on Location Technologies.* London, UK.

ZAKA, I., REHMAN, H. U., AZAM, M. & SHAH, S. I. (2005) Comparison of Jammer Excision Techniques. *INMIC 2005 Multi Topic Conference.* Karachi.

ZHANG, J., ZHANG, K., GRENFELL, R. & DEAKIN, R. (2006) On the Relativistic Doppler Effect for Precise Velocity Determination using GPS. *Journal of Geodesy,* 80, 104 - 110.

ZHAO, L., AMIN, M. G. & LINDSEY, A. R. (2000) Subspace Projection Techniques for Anti-FM Jamming GPS Receivers. *Proceedings of the Tenth IEEE Workshop on Statistical Signal and Array Processing.*

ZHAO, L., AMIN, M. G. & LINDSEY, A. R. (2002) GPS Antijam via Subspace Projection: A Performance Analysis for FM Interference in the C/A Code. *Digital Signal Processing,* 12, 175-192.

ZOLTOWSKI, M. D. & GREEN, A. S. (1995) Advanced Adaptive Null Steering Concepts for GPS. *MILCOM 95.* San Diego, California, USA.